Perivascular adipose tissue and vascular function: the influence of nitric oxide, ageing and atherosclerosis

A thesis submitted to the University of Manchester for the degree of Doctor of Philosophy in the Faculty of Biology, Medicine and Health

2016

Rachel Elizabeth Walker

School of Medicine

Division of Cardiovascular Sciences

Contents

Word count: 80, 474

List of Figures

List of tables

Abstract

Perivascular adipose tissue and vascular function: the influence of nitric oxide, ageing and atherosclerosis

Rachel Elizabeth Walker

PhD Cardiovascular Medicine, The University of Manchester, September 2016

Background: The incidence of coronary heart diseases, including atherosclerosis, increases with ageing. The factors which influence arterial function, and which may be changed with ageing, are multiple but effects of perivascular adipose tissue (PVAT) on large arteries have not previously been considered. A key role for nitric oxide (NO) in mediating the anti-contractile capacity of PVAT has been suggested. Caveolin-1 (Cav-1) modulates the production of NO in vivo by tonic inhibition of eNOS. The influence of aortic PVAT and the contribution of NO to vascular reactivity in ageing C57BL/6 mice, atherosclerotic ApoE knockout mice (ApoE$^{-/-}$), Cav-1 knockout mice (Cav-1$^{-/-}$) and atheroprotected ApoECav-1 double knockout mice (ApoE$^{-/-}$Cav-1$^{-/-}$) is unknown.
Hypothesis: The influence of PVAT on vascular function is modulated by ageing and the development of atherosclerosis via NO bioavailability.
Methods: Male mice were used in this study. C57BL/6 mice were obtained at 4 weeks of age and maintained on a normal rodent diet (ND) for 8, 16 or 26 weeks. ApoE$^{-/-}$ and Cav-1$^{-/-}$ mice were bred from in-house colonies and ApoE$^{-/-}$Cav-1$^{-/-}$ mice were generated by interbreeding ApoE$^{-/-}$ and Cav-1$^{-/-}$ mice. Upon weaning, ApoE$^{-/-}$, Cav-1$^{-/-}$ and ApoE$^{-/-}$Cav-1$^{-/-}$ mice were maintained on either a ND or Western-type diet (WD) for 8, 16 or 26 weeks. Vascular reactivity studies on isolated aortic ring preparations were performed in the presence or absence of PVAT. The contribution of NO to the vascular reactivity of aortic PVAT was determined using pharmacological inhibition of NO synthase. Aortic PVAT was assessed for evidence of morphological and/or compositional changes associated with ageing or a WD.
Results: NO mediated an anti-contractile effect of aortic PVAT in C57BL/6 mice fed a ND up to 16 weeks. The anti-contractile capacity of aortic PVAT was lost after 26 weeks on a ND and preceded endothelial dysfunction. Loss of the PVAT anti-contractile effect was accompanied by alterations in PVAT morphology and composition. Aortic PVAT from ND-fed ApoE$^{-/-}$ mice was dysfunctional and did not exert an anti-contractile effect. Furthermore, a WD did not alter the influence of PVAT on vascular reactivity in ApoE$^{-/-}$ mice and PVAT morphology and composition was unchanged. NOS inhibition did not alter the contractile responses. The aortic PVAT of ND-fed Cav-1$^{-/-}$ mice did not exert an anti-contractile effect and PVAT composition was unchanged with increasing age. However, after 26 weeks on a WD, aortic PVAT from Cav-1$^{-/-}$ mice potentiated contractions to phenylephrine and white adipocyte hypertrophy was observed. NOS inhibition revealed a pro-contractile effect of aortic PVAT from Cav-1$^{-/-}$ mice. Loss of Cav-1$^{-/-}$ conferred significant protection against the development of atherosclerosis in WD-fed ApoE$^{-/-}$Cav-1$^{-/-}$ mice despite a proatherogenic lipid profile. Aortic PVAT from ND-fed ApoE$^{-/-}$Cav-1$^{-/-}$ mice did not exhibit an anti-contractile capacity and PVAT morphology was unchanged with ageing. Additionally, a WD did not influence the effect of PVAT on vascular reactivity in ApoE$^{-/-}$Cav-1$^{-/-}$ mice although white adipocyte hypertrophy was observed after 26 weeks of high fat feeding. NOS inhibition revealed a pro-contractile effect of aortic PVAT in 8-week ND-fed ApoE$^{-/-}$Cav-1$^{-/-}$ mice.
Conclusions: This work has produced novel insights into the influence of aortic PVAT and NO on vascular reactivity and the morphology of aortic PVAT in ageing C57BL/6 mice, atherosclerotic ApoE$^{-/-}$ mice, Cav-1$^{-/-}$ mice and athero-protected ApoE$^{-/-}$Cav-1$^{-/-}$ double knockout mice. Ageing to pre-middle age in C57BL/6 mice results in a loss of the anti-contractile effect of PVAT prior to endothelial dysfunction. This is associated with altered NO bioavailability and changes to the morphology and composition of PVAT. This may reveal potential therapeutic targets to restore the anti-contractile capacity of PVAT if comparable age-related PVAT dysfunction is observed in humans. Aortic PVAT of ApoE$^{-/-}$ mice does not exert an anti-contractile effect which may be attributed to decreased basal eNOS activity. A WD does not alter the vascular reactivity of PVAT. In addition, aortic PVAT from Cav-1$^{-/-}$ mice does not exhibit an anti-contractile capacity yet it exerts a pro-contractile effect after 26 weeks on a WD. The aortic PVAT of ApoE$^{-/-}$Cav-1$^{-/-}$ mice does not modulate vascular reactivity and this is unaltered with feeding of a WD although white adipocyte hypertrophy was observed within the PVAT. The critical role of Cav-1 in the initiation and progression of atherosclerosis is reinforced by the atheroprotected phenotype of the ApoE$^{-/-}$Cav-1$^{-/-}$ mice even though a severely proatherogenic lipid profile is observed in both the ND and WD-fed mice. Therapeutically targeting LDL transcytosis into the arterial wall could potentially prevent or halt the development of atherosclerosis. Aortic PVAT of ND-fed Cav-1$^{-/-}$ and ApoE$^{-/-}$Cav-1$^{-/-}$ mice may not be dysfunctional but unable to modulate vascular reactivity due to attenuated vasoconstrictor responses of PVAT-denuded aortic rings as a result of excess NO, although this requires further investigation.

Declaration

I declare that no portion of the work referred to in the thesis has been submitted in support of an application for another degree or qualification of this or any other university or other institute of learning.

Copyright Statement

i. The author of this thesis (including any appendices and/or schedules to this thesis) owns certain copyright or related rights in it (the “Copyright”) and she has given The University of Manchester certain rights to use such Copyright, including for administrative purposes.

ii. Copies of this thesis, either in full or in extracts and whether in hard or electronic copy, may be made only in accordance with the Copyright, Designs and Patents Act 1988 (as amended) and regulations issued under it or, where appropriate, in accordance with licensing agreements which the University has from time to time. This page must form part of any such copies made.

iii. The ownership of certain Copyright, patents, designs, trademarks, and other intellectual property (the “Intellectual Property”) and any reproductions of copyright works in the thesis, for example graphs and tables (“Reproductions”), which may be described in this thesis, may not be owned by the author and may be owned by third parties. Such Intellectual Property and Reproductions cannot and must not be made available for use without the prior written permission of the owner(s) of the relevant Intellectual Property and/or Reproductions.

iv. Further information on the conditions under which disclosure, publication and commercialisation of this thesis, the Copyright and any Intellectual Property and/or Reproductions described in it may take place is available in the University IP Policy (see http://documents.manchester.ac.uk/DocuInfo.aspx?DocID=487), in any relevant Thesis restriction declarations deposited in the University Library, The University Library’s regulations (see http://www.manchester.ac.uk/library/aboutus/regulations) and in The University’s policy on Presentation of Theses

Statement of work done

Adipokine array: All arrays were carried out by Rachel Walker

Animal procedures: Animal experiments were carried out by Rachel Walker. The animals were looked after by the staff at the BSU, University of Manchester.

En face lesion analysis: All en face analysis was carried out by Rachel Walker

Genotyping: All genotyping was carried out by Rachel Walker

Immunohistochemistry: All immunohistochemistry was carried out by Rachel Walker.

Lipidemic and glycaemic profile analysis: All measured by Yifen Liu of the Lipid Biology Research Group, Manchester University, UK.

Myography: All myography experiments were carried out by Rachel Walker.

Funding: This project was funded by The British Heart Foundation.

Conference proceedings

Oral communications

- R.E. Walker, C. Austin, C.M. Holt. Perivascular adipose tissue and atherosclerosis. Northern Vascular Biology Forum (December 2014, Manchester):

Poster presentations

- R.E. Walker, C. Austin, C.M. Holt. The anti-contractile properties of perivascular adipose tissue are potentiated in atherosclerosis in apolipoprotein e-deficient mice. 83rd European Atherosclerosis Society Congress (Glasgow 2015)

  R.E. Walker, C. Austin, C.M. Holt. Perivascular adipose tissue modulates vascular reactivity in atherosclerosis of Apolipoprotein E-deficient mice. International Symposium on Atherosclerosis (Amsterdam 2015):
- R.E. Walker, C. Austin, C.M. Holt. Vascular reactivity in atherosclerosis: the effects of perivascular adipose tissue during the progression of atherosclerosis in the $ApoE^{-/-}$ mouse. British Society of Cardiovascular Research (Manchester 2015).
- R.E. Walker, C. Austin, C.M. Holt. Changes in Perivascular Adipose Tissue in Ageing and Atherosclerotic Mice. British Society of Cardiovascular Research (Manchester 2016).
- R.E. Walker, C. Austin, C.M. Holt. Aortic perivascular adipose tissue displays an aged phenotype in early and late atherosclerosis in $ApoE^{-/-}$ mice. Frontiers in Cardiovascular Biology conference: (Florence 2016).

Travel Grants and Awards

- Young investigator fellowship from the 83rd European Atherosclerosis Society Congress (2015)
- Travel grant was from the 17th International Symposium on Atherosclerosis (ISA) (2015)
- Travel grant from the European Society of Cardiology (ESC) Council on Basic Cardiovascular Science to attend Frontiers in Cardiovascular Biology conference: (Florence 2016).

Acknowledgements

I have been truly fortunate to have been funded by the British Heart Foundation and would like to thank anyone who has ever donated time or money to them.

I would particularly like to thank my fantastic supervisors, Cathy Holt and Clare Austin, who's feedback, support and occasional dinner parties have kept me going. I couldn't have done this without you.

To everyone in the BSF, University of Manchester, thank you! Without your commitment to care for the mice, my PhD wouldn't have been possible. I am especially grateful to Mike Jackson, who's vast knowledge of animal husbandry has been put to good use over the last four years looking after my troublesome mice.

Thank you to Yifen Liu, of the Lipid Biology Research Group, Manchester University, for analysing my serum samples.

Also, to all my lab friends, working with you every day has been a privilege. I'll never forget the hilarious lab chats, nights out blowing off steam, or the Halloween parties where no one could actually break open the piñata.

Thank you to my wonderful parents, who have always encouraged me to improve and better myself and have given their love and support throughout the last four years of this project and more importantly for the foundation of my life before.

To Tom and Chrissy, thank you for reminding me that life exists outside of the lab and for all your cocktail masterclasses, bad movie nights and BBQ sessions. To James, my oldest and dearest friend, your words of 'encouragement' have kept me going over the years.

Finally, to the love of my life, and my favourite person, Sam. I couldn't have done this without you.

This work is for you.

"I mean to arrive at the truth. The truth, however ugly in itself, is always curious and beautiful to the seeker after it.'

~Hercule Poirot *(Agatha Christie)*~

Abbreviations

ADRF	Adipocyte-derived relaxing factor
ANOVA	Analysis of variance
ApoE$^{-/-}$	Apolipoprotein E knockout (Apoe^{tm1Unc}/J)
ApoE$^{-/-}$Cav-1$^{-/-}$	Apolipoprotein E and Caveolin-1 knockout
ApoE	Apolipoprotein E
BAT	Brown adipose tissue
BH_4	Tetrahydrobiopterin
Cav	Caveolin
Cav-1$^{-/-}$	Caveolin-1 knockout (Cav-1^{tm1Mls}/J
CHD	Coronary heart disease
CRP	C-reactive protein
CVD	Cardiovascular disease
DHE	Dihydroethidium
DMSO	Dimethyl sulfoxide
DPPIV	Dipeptidyl Peptidase IV
EAT	Epicardial adipose tissue
EDHF	Endothelial-derived hyperpolarising factor
EDRF	Endothelial-derived relaxing factor
eNOS	Endothelial nitric oxide synthase
FGF	Fibroblast growth factor
HDL	High-density lipoprotein
IGFBP-6	Insulin-like growth factor binding protein-6
iNOS	Inducible nitric oxide synthase
KPSS	High potassium physiological salt solution
LDL	Low-density lipoprotein
L-NNA	Nω-Nitro-L-arginine
NADPH	Nicotinamide adenine dinucleotide phosphate
ND	Normal diet
nNOS	Neuronal nitric oxide synthase
NO	Nitric oxide
NOS	Nitric oxide synthase
oxLDL	Oxidised low-density lipoprotein
PDRF	PVAT-derived relaxing factors
PSS	Physiological salt solution
PVAT	Perivascular adipose tissue
ROS	Reactive oxygen species
sGC	Soluble guanylyl cyclase
SR	Sarcoplasmic reticulum
TAE	Tris-acetate EDTA solution
TBS	Tris-buffered saline
TNFα	Tumour necrosis factor α
UCP-1	Uncoupling protein-1
VCAM-1	Vascular cell adhesion molecule-1
VLDL	Very low-density lipoproteins
VSMC	Vascular smooth muscle cells
WAT	White adipose tissue
WD	Western-type diet

~ Chapter One ~

Introduction

1.1 The impact of cardiovascular diseases

Cardiovascular disease (CVD) encompasses all the diseases of the heart and circulation including coronary heart disease (CHD), stroke, angina, heart attack and congenital heart disease. CVD is one of the principal causes of morbidity and mortality worldwide and in the UK, CVD is the second most common cause of mortality, accounting for 27% of all deaths in 2014 (Townsend N 2015). The predominant contributors to this statistic were CHD and stroke which accounted for approximately 69 000 and 39 000 deaths, respectively (Chiu et al. 2011; Townsend N 2015). These diseases are associated with behavioural and medical risk factors including: smoking, physical inactivity, diet-induced weight gain, hypercholesterolemia, hypertension and increasing age (Nichols et al. 2012). The burden of these collective morbidities is set to dramatically increase due to the ageing population, a rise in diet-induced weight gain and diabetes which is endemic of CVD (Warboys et al. 2011). Currently in the UK, there are approximately 7 million people living with CVD. However, with survival rates and both a growing and ageing population this number is expected to increase substantially (Townsend N 2015). In addition, the economic impact is extensive. The growing number of CVD cases requiring treatment is adding extra strain to the NHS with £4.3 billion spent in England alone for the period 2013/2014 (Leal et al. 2012b; Townsend N 2015).

1.2 Vascular ageing and cardiovascular disease

Ageing is an inevitable cardiovascular risk factor and results in progressive structural and functional changes within the cardiovascular system including arterial stiffening and thickening and endothelial dysfunction. These alterations can disrupt the normal processes of the vasculature, lead to increased systolic pressure and ultimately the pathogenesis of atherosclerosis, stroke, or hypertension (North et al. 2012). It is therefore imperative that the aetiology of vascular ageing and its resulting pathologies are investigated (Lakatta 2002).

1.2.1 The Pathogenesis of Atherosclerosis

Atherosclerosis has been identified as the primary cause of CHD and is predominantly a disease of the large arteries typified by the gradual accumulation of plaques, composed of fatty and fibrous materials, resulting in a narrowing of the arterial lumen. It is the leading cause of death in the developed world due to the associated risk of plaque rupture and thrombi formation within the artery, the consequence of which may be myocardial infarction, stroke and gangrene (Ross 1993).

Atherosclerosis is initiated by a combination of environmental and genetic factors, including, but not limited to, hypercholesterolemia, haemodynamic changes within the arteries and dysfunction of the vascular components either in conjunction with one another or in isolation, resulting in a pathophysiological state (Getz et al. 2012; Simionescu et al. 2012).

Atherosclerosis is a highly complex inflammatory disease of the vascular wall and once established it is characterised by endothelial dysfunction and the progressive accumulation of

macrophages and fatty deposits (such as modified lipoproteins) within the vessel wall, resulting in vascular remodelling (Figure 1.1) (VanderLaan et al. 2004; Warboys et al. 2011). Despite extensive investigation, much remains unclear about the cell types and underlying mechanisms involved in the initiation and progression of the disease (Ross 1999a). Atherogenesis begins in childhood, and has been proven to be present in foetal aortas, as a fatty lesion/streak, and develops progressively throughout adult life (Strong et al. 1992; Napoli et al. 1997; McGill et al. 2000). An understanding of these processes is essential for the development of new therapeutic targets to produce more successful therapies for atherosclerosis. Key to effective treatment is an understanding of the mechanisms at play in the early stages of the disease.

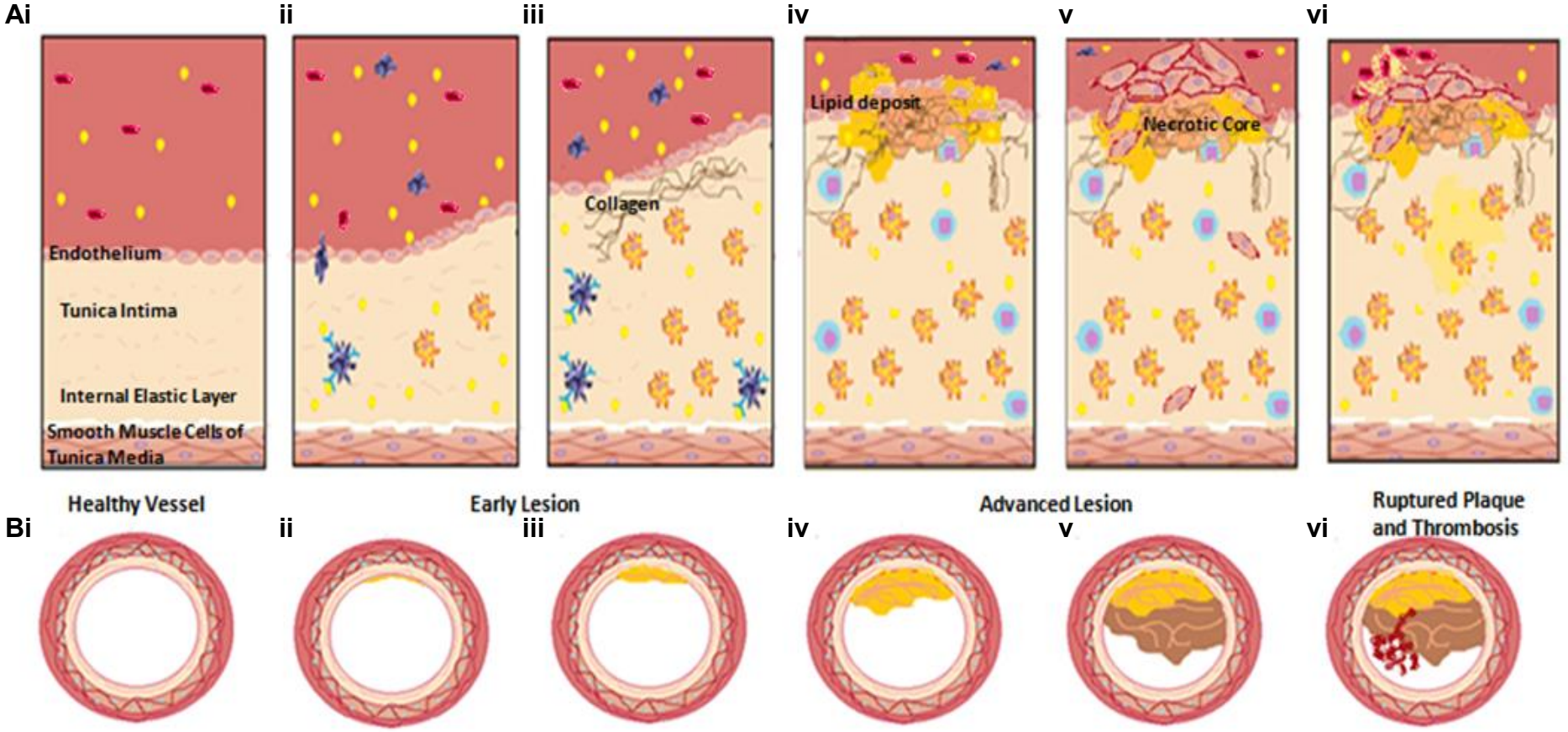

Figure 1.1 The pathogenesis of atherosclerosis

Ai) The artery is initially healthy with no signs of atheroma. ii) Circulating LDL infiltrate the arterial wall. A fatty streak is formed from aggregates of monocyte-derived macrophages and foam cells. iii) In response to inflammation VSMCs migrate from the medial layer and take on a synthetic phenotype and increase secretion of extracellular matrix components. iv) T-lymphocytes are recruited to the lesion. Lesion complexity increases and a fibrous cap is formed. v) A necrotic core develops from apoptotic cells within the atheroma. vi) The plaque ruptures and its components are exposed to the blood stream activating platelets and a coagulation cascade. A thrombus may form which may lead to critical complaints such as ischemia and resulting heart damage. Bi - vi Transverse view of artery. Images adapted from Libby 2001 and Madamanchi et al. 2005.

The formation of an atherosclerotic plaque occurs in a series of stages, the first of which is triggered by an accumulation of lipoproteins in the endothelial layer, this in turn promotes the infiltration of monocytes into the area (Figure 1.1) (Ross 1999b). The infiltration of lipoproteins into the intima is facilitated by low-density lipoprotein (LDL). LDL is essential for the maintenance of cell membranes, but an excess of LDL cholesterol results in hypercholesterolemia, a condition that renders cells unable to remove the lipids from the blood stream (Ross 1999b; Lusis 2000; Pavlides et al. 2012). Upon infiltration into the arterial wall, LDL undergoes modification by reactive oxygen species and forms oxidised LDL (oxLDL). This stimulates inflammation of the endothelial cells due to the expression of surface adhesion molecules such as P-Selectin, E-Selectin and vascular cell adhesion molecule-1 (VCAM-1) (Huo et al. 2001; Blankenberg et al. 2003). These molecules play a key role in the recruitment of monocytes to sites of injury caused by inflammation. Monocytes, in response to inflammation, release inflammatory cytokines and phagocytose a combination of cells and toxic molecules such as oxLDL. Once inside the intima, the monocytes scavenge oxLDL, differentiate into macrophages, with an increased capacity for oxLDL, and further differentiate into foam cells loaded with cholesterol esters, forming a fatty streak (Tacke et al. 2006; Varol et al. 2009). Macrophages also present oxLDL molecules on their surface which stimulates and attracts T-lymphocytes, predominantly $CD4^+$ T-helper cells (Stemme et al. 1995; Nicoletti et al. 1999; Gotsman et al. 2007). This collection of immune cells within the intima amplifies the local inflammatory response due to the secretion of pro-inflammatory cytokines (for example interleukins 1, 6, 12 and 18) and chemokines (including tumour necrosis factor alpha (TNFα), which induce chemotaxis in certain cells) (Ait-Oufella et al. 2011; Vasquez et al. 2012).

As the lesion continues to develop, vascular smooth muscle cells (VSMCs) undergo phenotypic switching from a contractile to a proliferative phenotype, which in turn could potentially lead to dysfunction in vessel contraction and increased turbulence of blood flow (Owens et al. 2004; Gomez et al. 2012). Phenotypic switching allows the VSMCs to migrate towards the intima and alters the extracellular matrix composition due to their increased synthesis of collagen, elastin and proteoglycans (Libby et al. 2011). The macrophages and T-cells within the plaque continue to secrete various molecules such as growth factors and cytokines that further promote the migration of proliferative VSMCs (Owens et al. 2004).

Inside the plaque, macrophages and VSMCs undergo apoptosis throughout the different stages of lesion formation. Initially, infiltrating macrophages remove apoptotic cells from the lesion via efferocytosis, but this occurs less frequently in more complex lesions, resulting in a necrotic core within the centre of the plaque (Pavlides et al. 2012). Developed atheromas may contain small vessels, which originate from the media, and occasionally haemorrhage (Falk et al. 1995). As the plaque matures, a fibrous cap of VSMCs and extracellular matrix covers the necrotic core, this is the fibrous lesion stage (Falk et al. 1995).

Initially, the vessel wall enlarges in order to protect the arterial lumen from the growing plaque (positive remodelling) but eventually, the outer lumen is unable to prevent the plaque from invading into the lumen (negative remodelling) this can lead to restricted blood flow within the

artery (Seo et al. 1997; Walker et al. 2009; Vasquez et al. 2012). However, the most critical complication arises when an unstable fibrotic cap is disrupted or ruptures. This event forms a thrombus within the lumen and if severe enough, can create an acute occlusion, which is widely accepted as the cause of many acute coronary syndromes including: myocardial infarction, sudden cardiac death, stroke and unstable angina (Fischer et al. 2000; Lusis 2000; Libby et al. 2011; Pavlides et al. 2012).

In short, it is clear that numerous cell types are involved in both the initiation and progression of atherosclerosis, including: monocytes, macrophages, lymphocytes, VSMCs and endothelial cells (Ross 1999a; Libby et al. 2011). The wide variety of cells implicated in the pathogenesis of atherosclerosis demonstrates its multifaceted nature and highlights how problematic the disease can be to treat effectively.

1.2.2 Sites of Lesion Development

Atherosclerotic lesions begin to develop at specific focal points throughout the arterial vasculature and are predominantly found at bifurcations and curved areas of large and medium muscular arteries (Figure 1.2) (VanderLaan et al. 2004; Chiu and Chien 2011). Lesions are predisposed to develop within areas of the artery that experience fluctuations in blood flow (Caro et al. 1969). It is now widely accepted that areas within the artery that experience low shear stress and turbulent flow also incline the site to the development of plaques (VanderLaan et al. 2004; Warboys et al. 2011; Kwak et al. 2014).

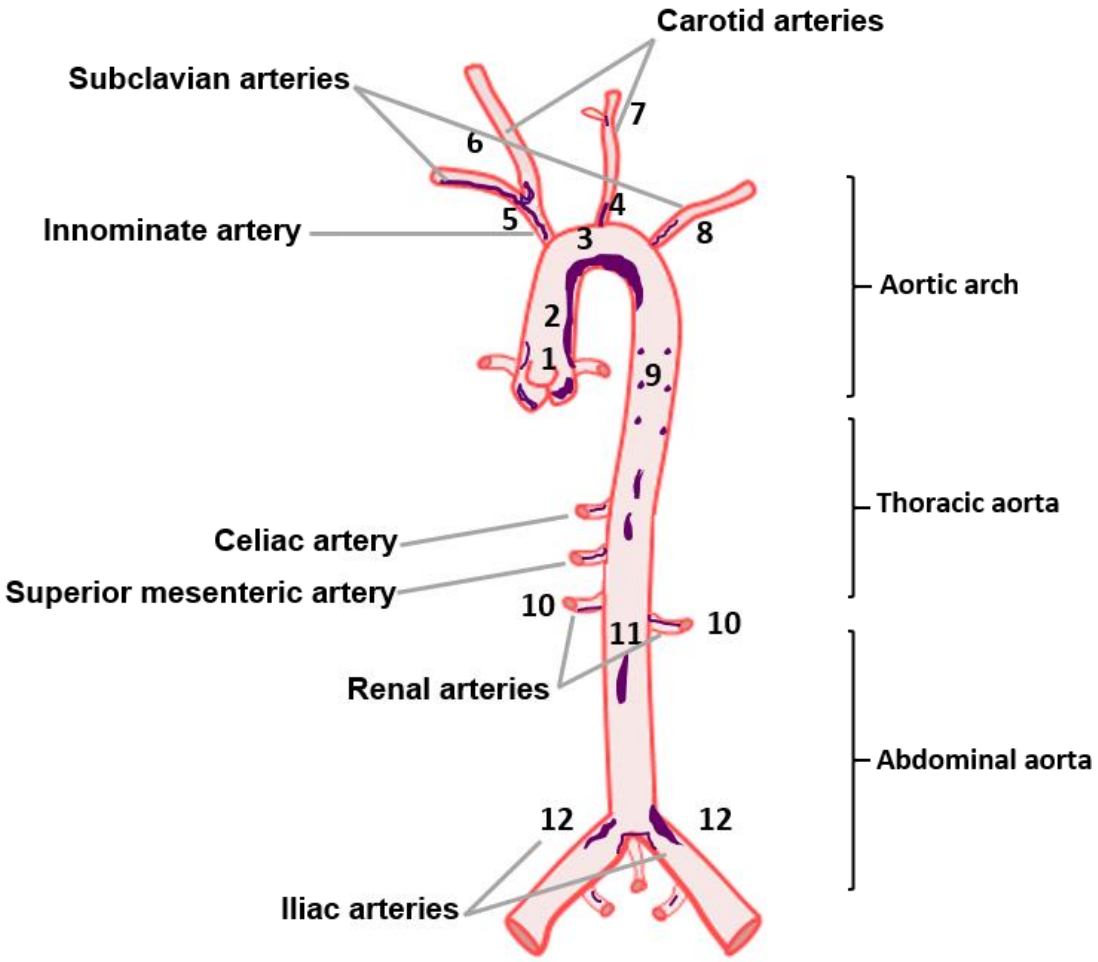

Figure 1.2 Sites of lesion development within the vasculature of high fat fed Apolipoprotein E-deficient mice and low-density lipoprotein receptor-deficient mice
Atherosclerotic lesions predominantly develop in branched areas of muscular arteries. The most common sites of lesion development are highlighted in purple and are: 1) the aortic root/sinus; 2) ascending aorta; 3) lesser curvature of the aortic arch; 4) greater curvature of the arch; 5) innominate artery; 6) right common carotid artery; 7) left common carotid; 8) left subclavian artery; 9) thoracic aorta; 10) renal artery; 11) abdominal aorta, 12) iliac artery. Image adapted from VanderLaan et al. 2004 and Chiu et al. 2011.

Two leading theories have been developed to account for this; the shear stress theory and the mass transport theory (Chiu and Chien 2011). The shear stress theory focuses on the mechanical forces that the endothelial layer is exposed to by circulating blood. At arterial branches, the blood flow undergoes directional changes and shear stress decreases, which could promote the development of atherosclerotic lesions. High shear stress may provide protection from plaques because it is anti-inflammatory, induces cell quiescence and generates an atheroprotective gene expression pattern within the endothelial cells (Malek et al. 1999). In addition, plaque structural stress is observed within the body of the atherosclerotic plaque and is observed as a result of vessel stretch and expansion due to arterial pressure; elevated plaque structural stress may be a mechanism of plaque rupture (Richardson et al. 1989; Brown et al. 2016). The mass transport theory postulates that there is an increased bioavailability of substances, such as LDL, at the

areas where blood flow is disturbed because the endothelial layer is in contact with the blood for a longer period of time (Weinberg 2004; Warboys et al. 2011).

Although it has been established that fluctuations in haemodynamics can facilitate the development of atheroma, there are still numerous mechanisms that underlie the initiation and progression of the disease. Each of these different factors requires consideration in order to further understand atherosclerosis. However, there remains much uncertainty surrounding the detail of atherogenesis.

1.2.3 Ageing, atherosclerosis and the clinical perspective

Due to the progressive nature of atherosclerosis, ageing has a profound effect on the incidence and severity of atherosclerotic disease (Uryga et al. 2016). There is growing evidence that atherosclerotic plaques stimulate an accelerated rate of ageing within the arteries, which does not correspond with their chronological age. These alterations to the normal ageing process are observed not only in advanced plaques but also in the formation of early lesions (Uryga and Bennett 2016). Key features of biological ageing have been identified within atherosclerotic lesions including: damage to nuclear and mitochondrial DNA, VSMC and endothelial cell senescence and telomere shortening of VSMCs and endothelial cells (Ballinger et al. 2002; Martinet et al. 2002; Ogami et al. 2004; Uryga and Bennett 2016). Mitochondrial DNA derangement and damage can lead to an increase in reactive oxygen species (ROS) which subsequently promotes oxidative DNA injury. Strong links exist between the generation of ROS and the development of atherosclerosis and harmful changes to VSMCs such as aberration of cell proliferation and migration (Li et al. 2010).

Ageing is an unavoidable risk factor for the development and progression of diseases, specifically those of the cardiovascular system, such as atherosclerosis. However, vascular ageing in humans is often complicated by the presence of comorbidities which may influence the rate of development of disease hence, it is important to understand how these factors may change with advancing age (Moon et al. 2001; Lakatta 2002; Vazquez-Padron et al. 2004; Ungvari et al. 2010). The use of large artery preparations from rodents in ageing and atherosclerosis research has resulted in significant advancements in our understanding of some of the mechanisms that can trigger vascular ageing and what factors can contribute to its acceleration. However, much remains unknown.

Detection of the early stages of vascular ageing, prior to the development of CVD, and treatment of patients during this period may prove therapeutically beneficial to halt or reverse the pathological changes associated with ageing and thus prevent the subsequent development of CVD.

1.3 Arterial structure and regulation of vascular tone in health

To understand the changes which may occur in the vasculature with ageing, it is important to recognise the different components of the artery and how they contribute to its function.

A healthy and mature arterial wall consists of the endothelium (tunica intima), VSMCs (tunica media), adventitia (tunica externa) and in the majority of cases is surrounded by perivascular

adipose tissue (PVAT). The regulation of arterial tone is dependent on the different constituent cells of the vascular wall, specifically the VSMCs drive contraction of the artery wall, thus altering the diameter of the arterial lumen. However, both the endothelium and PVAT have been demonstrated to modulate contraction or dilation of the VSM by the release of vasoactive substances which will be discussed in further detail below.

1.3.1 Vascular smooth muscle cells

The tunica media is formed from multiple transverse sheets of VSMCs that secrete collagen fibres, proteoglycans and elastin and are held in a matrix of connective tissue. The primary role of VSMCs is the contraction and regulation of arterial tone (Owens et al. 2004). Vascular tone can be modulated in response to vasoconstrictive hormones such as norepinephrine (through α-adrenergic receptors), vasodilatory factors such as catecholamines (through β-adrenergic receptors), mechanical or electrical stimuli. VSMCs contain bundles of myofilaments, organelles, dense plaques and dense bodies (Perrotta 2013). Dense bodies and dense plaques facilitate the transduction of force when actin and myosin contract (Ohashi et al. 1994).

Initiation of contraction of VSMCs is dependent on increases in free intracellular Ca^{2+} (Johns et al. 1987; Somlyo et al. 1993). The free Ca^{2+} binds to calmodulin which subsequently activates the enzyme myosin light chain kinase (MLCK). This activated MLCK, in the presence of ATP, phosphorylates myosin light chains (MLC), the regulatory subunits located on the myosin heads. Upon phosphorylation, MLCs generate cross-bridges between the myosin heads and the actin filaments, found within the cell, thus inducing VSMC contraction (Conti et al. 1981; Sellers et al. 1981; Hashimoto et al. 1990). Conversely, relaxation occurs as a result of reduced phosphorylation of MLC. This is accomplished through several mechanisms mainly, reduction in free $[Ca^{2+}]_i$, MLCK inhibition by increased intracellular cyclic AMP (cAMP) or dephosphorylation of MLCs by myosin light chain phosphatase (MLCP) (Conti and Adelstein 1981; Sellers et al. 1981; Webb 2003).

Elevated $[Ca^{2+}]_i$ within the VSMC can arise through increased influx of Ca^{2+} into the cell via Ca^{2+} channels or by the release of Ca^{2+} from internal stores such as the sarcoplasmic reticulum (SR) (Webb 2003). Extracellular Ca^{2+} influx may occur via numerous Ca^{2+} channels that can be activated in response to a variety of stimuli such as specific agonists or voltage changes. However, the opening of voltage dependent L-type Ca^{2+} channels (LTCC) is the predominant method of extracellular Ca^{2+} entry although, other channels such as the transient receptor potential (TRP) cation channels contribute to Ca^{2+} influx (Reuter 1986; Webb 2003; Le Blanc et al. 2004; Leloup et al. 2015). LTCCs exert the largest influence on global $[Ca^{2+}]_i$ and it is their activity which largely controls the contractile state of VSMCs and consequently artery diameter (Knot et al. 1998). Membrane depolarisation of the VSMC activates voltage-sensitive Ca^{2+} channels resulting in extracellular Ca^{2+} influx and hence VSMC contraction whereas, increases in $[Ca^{2+}]_i$ and alterations in membrane potential an activate K^+ channels, for example the large conductance Ca^{2+}-activated K^+ channel (BK_{Ca}) causing hyperpolarisation (Eichhorn et al. 2007).

Passive stretching of VSM can induce myogenic tone that originates directly from the VSM although this effect is of more importance in small arteries (Fridez et al. 2002; Henrion 2005). Additionally, agonist-stimulated contraction via binding to specific receptors on the VSMC, or

receptors on the adjacent endothelium, can induce contraction and involve various signal transduction pathways which result in increased $[Ca^{2+}]_i$. Agonists may induce contraction through a G-protein-coupled receptor (GPCR)-mediated signalling pathway, mainly Gq, through activation of phospholipase C (PLC) cleave phosphatidylinositol 4,5-bisphosphate (PIP_2) into diacylglycerol (DAG) and inositol 1,4,5-trisphosphate (IP_3) (Putney et al. 2012). IP_3 translocates and binds to its receptor at the SR and Ca^{2+} is released resulting in contraction (Webb 2003; Leloup et al. 2015)

1.3.2 The endothelium

The tunica intima delimits the arterial wall from the lumen and in normal blood vessels is composed of endothelial cells which are in immediate contact with the blood stream (Perrotta 2013). Endothelial cells are organised longitudinally and are connected to one another via a combination of adherens, tight and gap junctions (Wunderlich et al. 2008c). These junctions have different roles such as the control of vascular homeostasis, mediation of adhesion and communication between the cells. Gap junctions directly connect the cytoplasm of adjacent cells enabling the passage of small molecules and ions between them (Lampe et al. 2000; Lampe et al. 2004). Tight junctions regulate permeability whilst adherens junctions are partly responsible for controlling contact inhibition and infiltration of circulating leukocytes in response to damage (Johnson-Leger et al. 2002; Muller 2003; Bazzoni et al. 2004; Shin et al. 2006). A layer of elastic fibres, the internal elastic lamina, surrounds the endothelial monolayer.

Endothelial cells have a relatively slow turnover rate of approximately 3 years (Brandes et al. 2005). Strong links between endothelial dysfunction and the pathogenesis of disease have been recognised (Shaul 2003; Gollasch et al. 2004a; Malinowski et al. 2008; Maenhaut et al. 2011). Damage to the endothelial layer, such as from the development of atherosclerosis, can result in the replacement regenerated endothelial cells exhibiting dysfunctional properties such as morphological changes, increased LDL uptake and decreased nitric oxide production (Fournet-Bourguignon et al. 2000; Brandes et al. 2005; Lee et al. 2007; Vanhoutte 2010; Triggle et al. 2012). Furthermore, although endothelial cell senescence is a normal part of vascular ageing, this process can be augmented by mechanical stress linked to an elevated heart rate, hypertension and atherosclerosis. These challenges can promote further damage via increased oxidative stress and induce a proatherogenic phenotype due to stress-induced senescence and a loss of capacity to repair (Voghel et al. 2007; Thorin 2011; Triggle et al. 2012).

The endothelium has been demonstrated to modulate numerous processes within the vasculature including vascular remodelling, inflammation and platelet aggregation (Feletou 2011; Triggle et al. 2012). Furthermore, the regulation of arterial tone is dependent on a healthy endothelium; the endothelium releases a balance of both vasoconstrictor and vasodilatory factors (Feletou et al. 2006).

1.3.2.1 Modulation of vascular tone: the release of endothelium-derived relaxing and constricting factors

The direct contact between the endothelium and VSMCs enables the endothelial layer to modulate vascular tone via the release of endothelium-derived relaxing factors (EDRF) which can diffuse through to the VSM and mediate relaxation (Triggle et al. 2012). The importance of the endothelium in acetylcholine-mediated relaxation of rabbit aorta was first recognised in 1980 and

subsequently, nitric oxide (NO) was identified as a key EDRF and will be discussed in more detail in Section 1.3.2.2 (Furchgott et al. 1980; Palmer et al. 1987; Furchgott 1996). Furthermore, in large arteries, NO is the main mediator of endothelium-dependent dilation (Martin et al. 1986; Crauwels et al. 2000).

Nevertheless, other EDRFs have been observed to contribute to endothelium-dependent relaxation although this is dependent on the vascular bed and species examined (Triggle et al. 2012). Studies in humans and rodents of flow-mediated vasodilation, identified that prostacyclin plays a role in endothelium-dependent vasodilation (Koller et al. 1993; Duffy et al. 1998). Furthermore, in disease states, when NO bioavailability is diminished, the role of cyclooxygenase-derived factors, such as prostacyclin is more evident and may be part of a compensatory mechanism to improve vasodilation (Corriu et al. 1996; Szerafin et al. 2006). Numerous other EDRFs have been identified including hydrogen peroxide, hydrogen sulphide and carbon monoxide (Triggle et al. 2012).

The endothelium can regulate vascular tone through the activation of endothelium-derived hyperpolarising factor (EDHF) pathways although this mechanism of relaxation is more predominant in resistance arteries than conduit vessels (Tomioka et al. 1999; Brandes et al. 2000). Indeed, it has been demonstrated that the contribution of EDHF-mediated relaxation to endothelium-dependent vasodilation increases as the size of the vessel decreases (Shimokawa et al. 1996; Busse et al. 2002).

In addition, the endothelium can produce constricting factors such as endothelin-1 (Yanagisawa et al. 1988). Additionally, due to the expression of angiotensin converting enzyme and thromboxane synthetase, endothelial cells can release angiotensin II and thromboxane A2, respectively (Barton 2011; Triggle et al. 2012).

1.3.2.2 The importance of endothelial nitric oxide synthase and generation of nitric oxide within the endothelium

Nitric oxide (NO) is a transient gaseous free radical and paracrine mediator that plays many important roles in the physiological and pathophysiological processes of the cardiovascular system (Shaul 2003; Sessa 2005). One such example is the crucial role of NO, as an endogenous vasodilator, in the maintenance of vascular tone (Mulvany et al. 1977; Furchgott and Zawadzki 1980; Ignarro et al. 1988; Fleming et al. 1999). NO is generated by the enzyme nitric oxide synthase (NOS) which exists in three isoforms and can be categorised as constitutive or inducible. Both neuronal NOS (nNOS, type I) and endothelial NOS (eNOS, type III) are constitutively expressed whilst inducible NOS (iNOS, type II) is only activated upon exposure to immunostimulatory cytokines, infection and bacterial products (Aktan 2004; Dudzinski et al. 2007). The NOS isoforms catalyse the oxidation of L-arginine into NO and L-citrulline in the presence of various cofactors such as calmodulin (CaM), flavin mononucleotide, flavin adenine dinucleotide and nicotinamide adenine dinucleotide phosphate (NADPH) (Dudzinski and Michel 2007). eNOS expression is crucial for the normal functioning of the vasculature yet it is not solely expressed in endothelial cells and has been identified in cardiomyocytes, adipocytes, VSMCs and platelets (Buchwalow et al. 2002; Randriamboavonjy et al. 2005; Dudzinski and Michel 2007; Xia et al. 2016).

Vascular endothelial cells continuously produce NO in vivo due to shear stress created by the flow of blood over the vessel surface. Acute activation of eNOS by agonists such as acetylcholine stimulates the activation of soluble guanylyl cyclase (sGC) in VSMCs. sGC generates cyclic guanosine monophosphate (cGMP) which then acts as a second messenger and activates protein kinase G which stimulates the re-uptake of cytosolic Ca^{2+} into the sarcoplasmic reticulum and the opening of Ca^{2+}-activated K^+ channels resulting in relaxation of SM (Furchgott et al. 1989; Carvajal et al. 2000; Derbyshire et al. 2012; Zhao et al. 2015).

Endothelium-derived NO has been demonstrated to mediate a variety of processes including: VSMC proliferation, leukocyte adhesion, platelet aggregation and most crucially, regulation of vascular tone (Shaul 2003; Dudzinski and Michel 2007; Iwabu et al. 2010). The activity of eNOS is modulated by an inhibitory interaction with Caveolin-1 (Cav-1), the main structural component of caveolae, the role of Cav-1 and atherosclerosis will be discussed in more detail in Section 1.6.

In summary, the endothelium can influence VSM and blood vessel function through a series of tightly controlled processes. However, if the regulation of vasoactive agents is perturbed, endothelial dysfunction can occur. Endothelial dysfunction, characterised by an imbalance between vasoconstrictor and vasodilatory factors generated by (or acting upon) the endothelium, disrupts NO signalling resulting in vasoconstriction, vascular inflammation and oxidative stress. A dysfunctional endothelium is considered to be one of the principal factors in the pathogenesis of vascular diseases such as atherosclerosis and is a hallmark of vascular ageing (Taddei et al. 2001; Shaul 2003; Sessa 2005; Forstermann et al. 2006; Malinowski et al. 2008; Seals et al. 2011; Rajendran et al. 2013).

1.3.3 Perivascular adipose tissue is more than structural support

Perivascular adipose tissue (PVAT) surrounds the majority of blood vessels within the body and was, until recently, considered as passive structural support for blood vessels, providing only mechanical protection against contraction of adjacent tissues (Szasz et al. 2012). This understanding was reflected in the preparation of isolated vessels ex vivo with PVAT being dissected away from vessel preparations prior to experimentation. However, in 1991, it was demonstrated that PVAT significantly influenced vascular responsiveness by attenuating the contractility of rat aortic rings to norepinephrine (Soltis et al. 1991). Since this pivotal discovery, PVAT has been proven to regulate vascular tone and exert an anti-contractile effect through interactions with arteries in a wide range of vascular beds, in numerous species and in response to a variety of vasoconstrictors (Lohn et al. 2002; Verlohren et al. 2004; Fesus et al. 2007; Gao et al. 2007b; Greenstein et al. 2009; Ketonen et al. 2010; Rajsheker et al. 2010; Szasz et al. 2013; Victorio et al. 2016; Zaborska et al. 2016). Furthermore, solution transfer protocols (transferring solution from an organ bath with PVAT, adding it to a pre-contracted vessel and measuring vascular response) have demonstrated that the anti-contractile effect of PVAT was induced via a transferable factor released by PVAT and not due to a barrier effect (Lohn et al. 2002; Gao et al. 2005; Malinowski et al. 2008; Greenstein et al. 2009). The influence of PVAT on vascular function will be discussed in more detail in Sections 1.3.3.3-5.

1.3.3.1 Classical definitions of adipose tissue

Adipose tissue is classically divided into white adipose tissue (WAT) or brown adipose tissue (BAT). BAT is more metabolically active and involved in non-shivering thermogenesis (Szasz and Webb 2012). BAT is formed from multiple small fat droplets and is densely packed with mitochondria expressing uncoupling protein-1 (UCP-1) (Fedorenko et al. 2012; Brown et al. 2014). In general, WAT is the less vascularised and exhibits reduced innervation than BAT; BAT is more populated by capillaries and noradrenergic fibres than WAT (Cinti 2005). However, both experience innervation from the sympathetic nervous system whilst the role of parasympathetic innervation is unclear (Berthoud et al. 2006). WAT is composed of a large single fat droplet and is associated with visceral and subcutaneous fat depots, where it is believed to act as a site of lipid storage. A degree of plasticity in the adipose tissue is evident with trans-differentiation of the adipocytes observed in response to β3 adrenergic or peroxisome proliferator-activated receptor-γ (PPARγ) agonist stimulation (Richard et al. 2010). As such, brown adipocytes within WAT, in heterogeneous adipose tissue, have been identified as originating from the progenitors of white adipocytes and not typical BAT progenitors (Cinti 2005; Szasz and Webb 2012).

Beige adipocytes have recently been identified in rodents and humans, whilst expressing UCP-1, these adipocytes express distinctive cell surface markers including CD137 and Tmem26 (Xue et al. 2007; Sharp et al. 2012; Jespersen et al. 2013; Lidell et al. 2013; Park et al. 2014; Lizcano et al. 2016; Min et al. 2016). Interestingly, beige adipocytes appear able to store lipids or produce heat depending on the stimulus (Wu et al. 2012). Furthermore, white and beige adipocytes have been demonstrated to undergo browning and upregulate thermoregulation in response to cold stimulus and exercise-induced irisin which browns the adipocytes via the p38 mitogen-activated protein kinase (p38 MAPK) and extracellular signal–related kinase (ERK) pathways (Bostrom et al. 2012; Ye et al. 2013; Zhang et al. 2014).

These findings demonstrate that fat depots can been classed as an adipose organ which can exert endocrine and paracrine influences within the body and display plastic characteristics in response to changes in temperature or nutritional status.

1.3.3.2 Characteristics of PVAT are determined by anatomical location

PVAT, is different to other fat depots due to its location, surrounding blood vessels (Szasz and Webb 2012). Also, there is no physical barrier between adipocytes within PVAT and the adventitia therefore, any substances secreted by PVAT would be presumed to come into contact with the vascular wall (Rajsheker et al. 2010; Szasz and Webb 2012). The composition of PVAT varies depending on the vascular bed and species examined (Brown et al. 2014). Rodent mesenteric PVAT more closely resembles WAT whilst rodent aortic PVAT is mixed. Aortic PVAT exhibits BAT-like characteristics with multi-locular adipocytes densely packed with mitochondria, expression of UCP-1 and resistance to diet-induced inflammation; in contrast, PVAT of the mesenteric bed is white and less vascularised (Gao 2007; Fitzgibbons et al. 2011). Additionally, PVAT is comprised not just of adipocytes but a wide range of constituents, including: collagen, nerve bundles, mesenchymal stem cells, infiltrating macrophages, T lymphocytes, fibroblasts and, potentially, endothelial cells from structures such as the vasa vasorum (Szasz et al. 2013). The composition of PVAT is variable and alters in response to factors such as the local

environment and age and may become altered in pathophysiological conditions (Miao et al. 2012). The variation in vascularisation, innervation and infiltration of inflammatory cells within the PVAT depends on its anatomical location and may contribute to the differences in function observed (Szasz and Webb 2012).

PVAT is highly specialised and exhibits a substantially different secretory profile than other adipose depots and this is modulated depending on the location of the PVAT (Szasz et al. 2013). Mouse aortic PVAT has been demonstrated to produce less adiponectin, leptin, and resistin and lipid-oxidation genes are substantially downregulated than subcutaneous or visceral adipose tissue and this expression profile is similar to interscapular brown adipose tissue (Chatterjee et al. 2009; Fitzgibbons et al. 2011; Szasz et al. 2013). Furthermore, genetic deletion of PPARγ in SM cells led to a lack of PVAT in mice, impaired intravascular thermoregulation and enhanced atherosclerosis in response to cold stimulus thus, a protective role of PVAT in the development of atherosclerosis was discovered through its thermogenic capacity (Chang et al. 2012a).

The anatomical location of PVAT may influence the pathogenesis of disease. Human studies have demonstrated that the volume of aortic PVAT is correlated with hypertension, diabetes, aortic and coronary calcification (Lehman et al. 2010). In addition, visceral WAT mass has been linked to an increased risk of type 2 diabetes and CVD, due to its inflammatory characteristics in states of metabolic disturbance, whereas subcutaneous mass does not correlate to CVD risk (Xu et al. 2003; Bjorndal et al. 2011; Brown et al. 2014). Moreover, mesenteric white PVAT has been demonstrated to be altered in diabetes and diet-induced weight gain, with an increased inflammatory profile due to greater macrophage infiltration and TNFα expression observed (Fitzgibbons et al. 2011; Aghamohammadzadeh et al. 2013; Brown et al. 2014). However, aortic PVAT from high fat-fed C57BL/6 mice, which is composed mainly of brown adipocytes, was resistant to inflammation and did not exhibit altered inflammation (Fitzgibbons et al. 2011). The highlighted differences may be of relevance in PVAT function and suggest that the characteristics of adipocytes at different anatomical locations may influence the pathogenesis of vascular disease.

1.3.3.3 PVAT-derived relaxing factors contribute to the anti-contractile effect

The recognition that PVAT is an endocrine organ in its own right, with the capacity to secrete a vast array of metabolically active adipokines, chemokines and hormone-like factors led to the investigation of the role of PVAT in health and disease (Gao et al. 2007b; Chatterjee et al. 2009; Ouwens et al. 2010; Rajsheker et al. 2010; Fitzgibbons et al. 2011; Brown et al. 2014). Whilst the study of PVAT in relation to health and diet-induced weight gain has grown in recent years, (predominantly in resistance arteries), the role of PVAT in ageing and atherosclerosis on the modulation of vasoconstriction has been little explored in the murine aortae. As stated previously, atherosclerotic lesions are most prevalent within large arteries and develop at sites of increased blood flow turbulence due to a damaged endothelium thus, alterations in contraction of these arteries, potentially induced by PVAT, could modulate the progression of CVD through an altered adipocyte secretion profile.

Clear evidence exists that PVAT plays an important role in the modulation of vascular tone via the VSM and, potentially, the endothelium (Brown et al. 2014). The presence of PVAT attenuates vascular contractions in response to a range of agonists including norepinephrine, serotonin, angiotensin II and phenylephrine and this has been demonstrated in the various artery preparations from humans, rodents and pigs (Lohn et al. 2002; Gao et al. 2005; Fesus et al. 2007; Greenstein et al. 2009; Bunker et al. 2010; Szasz and Webb 2012). Furthermore, PVAT exerts an anti-contractile effect on veins (Lu et al. 2011b).

Numerous candidates have been suggested to be involved in the modulation of the anti-contractile capacity of PVAT (Table 1.1) and the term PVAT-derived relaxing factor(s) (PDRF) was devised to encompass them all. However, it is probable that no single factor is responsible for the vasodilatory effect of PVAT and that the release of different PDRFs is dependent on the anatomic location of the adipose depot, species investigated and pathophysiological state (Lohn et al. 2002; Brandes 2007; Brown et al. 2014). In human and animal studies, PVAT has been demonstrated to mediate its anti-contractile properties via the release of factors such as hydrogen peroxide, hydrogen sulphide, adiponectin, angiotensin 1-7, prostacyclin and omentin, which mediate an endothelium-dependent relaxation of vessels through the release of NO and subsequent K^+ channel activation (Fesus et al. 2007; Gao et al. 2007b; Chang et al. 2012a; Szasz et al. 2013; Brown et al. 2014; Costa et al. 2016). The role of NO and K+ channel activation as downstream effects of PDRF release were identified via PVAT solution transfer experiments to PVAT-denuded aortic rings which subsequently relaxed upon exposure to a solution incubated with PVAT. Furthermore, the anti-contractile effect of PVAT was attenuated by endothelium-denudation, NOS inhibition, NO scavenging, high extracellular K^+, or blockade of calcium-dependent K^+ channels (Gao et al. 2007b; Brown et al. 2014). An endothelium-independent mechanism of PDRF was also identified as involving hydrogen peroxide (Gao et al. 2007b). PVAT also releases an as yet, unidentified adipocyte-derived relaxing factor (ADRF) which produces endothelium-independent vaso-relaxation via the opening of voltage-dependent Kv and K^+ channels in the plasma membrane of SMCs (Chen et al. 1989; Busse et al. 2002; Gollasch et al. 2004b; Gollasch 2012).

1.3.3.4 Nitric oxide as a mediator of the anti-contractile effect of PVAT

PVAT has recently been demonstrated to contain eNOS and produce NO thus providing the potential to modulate contraction via NO in an endothelium-independent manner (Dashwood et al. 2007; Araujo et al. 2015; Victorio et al. 2016; Xia et al. 2016). NO has been indicated in contributing to the anti-contractile effect of PVAT from the outset of investigations into the influence of PVAT on vascular reactivity. PVAT solution transfer experiments (described in Section 1.3.3) demonstrated that after incubation with a NOS inhibitor or NO scavenger, the anti-contractile effect of PVAT was abolished (Gao et al. 2007b). In addition, after incubation of aortic preparations with a solution containing the PDRF, NO production was observed (Gao et al. 2007b). In further agreement with these findings, studies in the small arteries of humans and mice observed a diminished anti-contractile capacity of PVAT after exposure to a NOS inhibitor (Greenstein et al. 2009; Aghamohammadzadeh et al. 2013; Lynch et al. 2013). Finally, a study on PVAT from the protein kinase G knockout mouse ($PKG^{-/-}$) reported a lack of an effect of PVAT.

Also, this finding was replicated using pharmacological inhibition of PKG and PVAT did not exert an anti-contractile effect on isolated arteries (Withers et al. 2014). PKG is activated downstream of NO thus, this data further enhances the idea that NO contributes to the anti-contractile effect of PVAT (Rapoport et al. 1983).

1.3.3.4 The pro-contractile effects of PVAT

The evidence of PVAT modulating vascular tone through the exertion of an anti-contractile effects is extensive. However, numerous studies have demonstrated that PVAT may release pro-contractile factors that may become upregulated in disease (Table 1.1). With the exception of renin, PVAT contains all the components of the renin–angiotensin system, (Hermenegildo et al. 2005). Vascular reactivity studies on coronary arteries have demonstrated that PVAT diminished endothelial-dependent vasodilation in both canines and swine (Payne et al. 2009; Payne et al. 2010; Owen et al. 2013). Furthermore, a transferrable pro-contractile factor was identified as being released from coronary PVAT of swine and increased contractions in response to high concentration potassium solution and Prostaglandin F2α (Owen et al. 2013). The potential release of PVAT-derived constrictor agents may have implications in the pathogenesis of disease. The balance of pro- and anti-contractile factors released by PVAT may be disrupted in disease states and result in alterations to vascular reactivity and subsequent augmented vascular contractions that may have implications for the development of atherosclerosis, due to the potential for increased turbulence of blood flow, and hypertension.

Table 1.1 Vasoactive compounds demonstrated to be released by perivascular adipose tissue (PVAT)

	Vasoactive effect	Species and location	References
Adipose-derived contracting factor	Vasoconstriction; release of cyclooxygenase (COX)-derived products, probably through antagonising vasodilation	Mouse aorta	(Zhang 2012; Meyer et al. 2013)
Adiponectin	Vasodilator; induces nitric oxide (NO)-mediated endothelium-dependent vasodilation	Rat and mouse aorta	(Xu et al. 2003; Fesus et al. 2007; Boydens et al. 2012; Meijer et al. 2013)
Adipocyte-derived relaxing factor	Vasodilator; opens K_{ATP}, KCNQ or K_{Ca} channels	Mouse and rat mesentery and aorta, human internal thoracic arteries	(Busse et al. 2002; Lohn et al. 2002; Gao et al. 2005; Li et al. 2011)
Angiotensin 1-7	Vasodilator; endothelium-dependent via release of NO	Rat aorta	(Lee et al. 2009)
Chemerin	Vasoconstriction in diet-induced weight gain and diabetes	Rat aorta, superior mesenteric artery and mesenteric resistance arteries and mouse mesentery	(Watts et al. 2013; Neves *in press* 2016)
Hydrogen peroxide	Vasoconstrictor and vasodilator	Mouse mesentery	(Lucchesi et al. 2005)
Hydrogen sulphide	Vasodilator; opening VSM KATP channels.	Rat and mouse aorta	(Bhatia 2005)
Leptin	Vasodilator; activates endothelial nitric oxide synthase (NOS) in aorta, in humans but not mice. Vasoconstriction; activation of the sympathetic nervous system	Human and rat aorta	(Kimura et al. 2000; Lembo et al. 2000; Vecchione et al. 2002)
Nitric oxide	Vasodilator; stimulates soluble guanylate cyclase to generate the second messenger cyclic GMP resulting in relaxation	Rat and mouse aorta and mesentery	(Gao et al. 2007b; Gil-Ortega et al. 2010)
Omentin	Vasodilator; NO-mediated endothelium-dependent dilation	Rat aorta and mesentery	(Yamawaki et al. 2010)
Palmitic acid methyl ester	Vasorelaxation; opening of voltage-dependent K^+ channels in smooth muscle cells	Rat aorta	(Lee et al. 2011)
Prostacyclin	Vasodilator; acts on prostacyclin receptor, resulting in an increase in cyclic AMP and protein kinase A	Human internal thoracic artery, mouse innominate artery	(Egan et al. 2004; Malinowski et al. 2008; Chang et al. 2012a)
Superoxide anion	Vasoconstriction; Ca^{2+} sensitisation	Rat mesentery	(Gao et al. 2006)
Visfatin	Vasodilator; endothelium-dependent relaxation via NO	Rat aorta and mesentery	(Yamawaki et al. 2009)

1.3.3.5 PVAT modulates cell proliferation and migration

PVAT has been implicated in controlling the proliferation and migration of VSM and endothelial cells. PVAT-derived visfatin and TNFα can act as growth factors for VSMCs (Takaoka et al. 2009; Wang et al. 2009). Furthermore, in human studies, the adipokines resistin, leptin and monocyte chemoattractant protein-1 (MCP-1) induced aortic SM cell proliferation via ERK 1/2 or/and NF-kappa B (NFκB) pathways (Calabro et al. 2004; Li et al. 2005; Ozen et al. 2015). However, adiponectin acts as an inhibitor of VSMC proliferation and migration (Zhang et al. 2015). In addition to influencing VSMC proliferation and migration, PVAT-derived factors have been demonstrated to alter endothelial cell proliferation with chemerin and leptin encouraging proliferation (Ferla et al. 2011; Shen et al. 2013; Ozen et al. 2015). Alterations in the release of PVAT-derived factors, such as a shift toward the release or proliferative and/or migratory agents could potentially result in the development of pathophysiological conditions such as atherosclerosis that is closely linked with vascular remodelling.

1.4 Vascular function in pathophysiological conditions

Although the VSM directly controls vascular tone through contraction and relaxation, the endothelium and PVAT are known to modulate vascular reactivity, thus, dysfunction of these components can result in the development of pathophysiological conditions.

1.4.1 Ageing, atherosclerosis and endothelial dysfunction

In health, large arteries, such as the aorta, carotid and femoral, exhibit a high basal production of NO (Martin et al. 1986; Crauwels et al. 2000). The augmented bioavailability of NO is essential within these vessels to prevent the pathogenesis of diseases such as atherosclerosis, through inhibiting the development of inflammation, smooth muscle cell proliferation and thrombosis (Versari et al. 2009). However, if the tight regulation of vasoactive agents is perturbed, endothelial dysfunction can occur resulting in vasoconstriction, vascular inflammation and oxidative stress, which has strong links to the pathogenesis of diseases such as atherosclerosis and hypertension (Rajendran et al. 2013).

Under certain pathophysiological conditions, eNOS can become uncoupled from its cofactors and/or substrates and begin to produce superoxide anion as opposed to NO (Kalinowski et al. 2004; Luo et al. 2014). The predominant mechanism behind eNOS uncoupling is a reduction in the availability of the cofactor tetrahydrobiopterin (BH_4) (Stroes et al. 1998). Furthermore, the production of superoxide promotes vasoconstriction via its reaction with NO, which further depletes NO bioavailability, and results in the generation of hydrogen peroxide and peroxynitrite and subsequent production of pro-contractile prostaglandins (Goodwin et al. 1999; Ardanaz et al. 2006; Ardanaz et al. 2008; Schildknecht et al. 2009). Furthermore, senescent endothelial cells exhibit reduced NO bioavailability and activation of the vasoconstrictor endothelin-1 system. This induces a pro-inflammatory environment and consequently may promote the development of atherosclerosis (Sato et al. 1993; Donato et al. 2009)

Endothelial dysfunction is a hallmark of vascular ageing and is characterised by a reduction in the bioavailability of NO in the large arteries and subsequent deterioration of endothelium-dependent vasodilation (Donato et al. 2009). A dysfunctional endothelium is a well- established risk factor for

CVD and is a key factor in the development of atherosclerosis (Shaul 2003; Dudzinski and Michel 2007). Furthermore, in the absence of overt signs of CVD, endothelial function has been demonstrated to decline in healthy individuals after the fourth decade of life (Celermajer et al. 1994; Taddei et al. 1995; Gerhard et al. 1996; Lyons et al. 1997; Blackwell et al. 2004; Stampfli et al. 2010; Seals et al. 2011). Considerable research is now underway to assess the therapeutic potential of NO donors in the prevention and treatment of atherosclerosis (Herman et al. 2005).

1.4.2 Vascular smooth muscle cell dysregulation with ageing and atherosclerosis

In healthy, young arteries, VSMC is predominantly contractile and blood pressure is tightly regulated (Brozovich et al. 2016). However, in response to environmental cues, such as inflammation, abnormal nutritional status or other factors, the contractile VSMCs are able to reversibly switch to a synthetic (de-differentiated) state (Chamley-Campbell et al. 1979; Owens et al. 2004). This has a protective role in response to vascular injury, with the synthetic VSMCs able to migrate to the site of the insult and stimulate repair (Ross 1999a). Pathological migration occurs when VSMCs fail to revert to the contractile phenotype inducing vascular remodelling and intimal thickening, as observed with ageing and atherosclerosis (Sobue et al. 1999; Wang et al. 2007a; Monk et al. 2015). Alterations to VSMC phenotype have been observed in both large and small arteries. Increased contractility of small resistance arteries, which are key modulators of systemic blood pressure, is known to induce hypertension, whereas altered contraction of large conduit arteries may result in turbulent blood flow which can lead to endothelial injury and may lead to the development of CVD, for example, atherosclerosis (Intengan et al. 2000; Ararat et al. 2009; Chiu and Chien 2011). The effects of ageing on arterial contractility have been demonstrated to depend on both the agonist and vascular bed. Contractile responses evoked by adrenoreceptor agonists have been demonstrated to remain unchanged with ageing, which could indicate that adrenoreceptor-mediated contractions are conserved with advancing age (Matz et al. 2003).

In addition, there is evidence indicating that within ageing and atherosclerotic arteries, VSMCs may become senescent which may also affect vascular reactivity (Wang et al. 2012). Cellular senescence is induced via the shortening of telomeres or stress; senescent cells exhibit permanent growth arrest and altered expression of cell cycle regulators (Wang and Bennett 2012).

In summary, the main processes inducing dysregulation in VSMC leading to atherosclerosis occurs via two main routes: firstly, the switching to a synthetic phenotype and the failure to revert back to a contractile state and secondly, through increasing the turbulence of blood flow (Gomez and Owens 2012).

1.4.3 Perivascular adipose tissue dysfunction in pathophysiological conditions

The emergence of PVAT as an endocrine organ brought with it the consideration that PVAT may influence vascular reactivity in states of disease. Mounting evidence suggests that an imbalance in PVAT-derived adipokines (beneficial and damaging) can influence the development and progression of CVD by augmenting vascular contractility, increasing local inflammatory

environment and promoting VSMC proliferation and/or migration (Mattu et al. 2013; Ozen et al. 2015).

Though the presence of PVAT confers beneficial protective effects in physiological conditions, increased PVAT mass has been demonstrated to exert detrimental effects on the vasculature. Studies in humans and rodents, in a range of vascular beds, have demonstrated a relationship between increased PVAT mass and a decline in the anti-contractile effects of PVAT, although, most of these conditions were associated with diet-induced weight gain (Greenstein et al. 2009; Ketonen et al. 2010; Ma et al. 2010; Meijer et al. 2013). The damaging effects of an overabundance of PVAT is thought to be the result of an imbalance in adipokine secretion and activation of inflammatory and oxidative stress pathways (Szasz et al. 2013).

In states of metabolic disturbance, the anti-contractile effects of PVAT are attenuated in humans, rodents and swine (Gollasch and Dubrovska 2004b; Gao 2007; Greenstein et al. 2009; Ketonen et al. 2010; Maenhaut and Van de Voorde 2011). The loss of the beneficial effects of PVAT in diet-induced weight gain has been suggested to be due to the changes that occur within the PVAT, for example, the loss of the anti-contractile capacity of PVAT has been observed associated with increased macrophage infiltration, inflammation and a reduction in NO bioavailability (Greenstein et al. 2009; Withers et al. 2011). In addition, the adipocytes that form the PVAT become hypertrophic which eventually causes inflammation and oxidative stress leading to a diminished bioavailability of NO (Gollasch and Dubrovska 2004b; Gao 2007; Greenstein et al. 2009). Furthermore, aortic PVAT of obese mice has been demonstrated to release an adipose-derived contracting factor which was attributed to the release of PVAT-derived cyclooxygenase products (Meyer et al. 2013). Also, additional studies reporting PVAT exerting a pro-contractile effect on the vasculature in response to diet-induced weight gain have been recorded (Owen et al. 2013; Watts et al. 2013)

In addition, PVAT has been indicated to play a role in endothelium dysfunction observed in diet-induced weight gain via increased NADPH oxidase-derived oxidative stress and increased production of pro-inflammatory adipokines such as leptin and TNFα (Gil-Ortega et al. 2010; Ketonen et al. 2010; Payne et al. 2010). Studies have suggested a role of increased TNFα expression within obese PVAT of human small arteries contributing to an endothelin-1/NO imbalance which was linked to enhanced expression of endothelin-1 and endothelin receptors. Moreover, this unbalance potentially increased NOS uncoupling and therefore decreased NO bioavailability through NADPH oxidase activation and increased ROS production (Ketonen et al. 2010; Virdis et al. 2013). In addition to this, iNOS, which is induced in response to inflammation, is up-regulated in adipose tissue in diet-induced weight gain as a result of prolonged inflammation (Perreault et al. 2001; Miao and Li 2012). Studies such as this highlight the potential dual role of PVAT. Under physiological conditions PVAT exerts protective vaso-relaxant effects which may be lost and replaced with inflammatory pro-contractile effects (Virdis et al. 2013; Ozen et al. 2015)

A wealth of information is available concerning the effects of diet-induced weight gain on both the phenotype and influence of PVAT on vascular reactivity. However, little is known concerning the effect of ageing on PVAT or its effect on NO signalling within the vasculature (Sverdlov et al. 2014; Melrose et al. 2015). Furthermore, given the importance of NO bioavailability and

inflammation in atherosclerosis, it is highly likely that changes in the perivascular environment may also modulate NO bioavailability in plaque development and progression. This has not previously been investigated.

Until recently, PVAT had not been considered to influence the pathogenesis of atherosclerosis. However, it has now been demonstrated that there is an association between the quantity of PVAT surrounding coronary arteries and atherosclerotic plaque burden in humans (Mahabadi et al. 2010; Verhagen et al. 2011; Verhagen et al. 2012). A link has also been confirmed between PVAT and atherosclerosis in ApoE knockout mice ($ApoE^{-/-}$) using adipose transplantation experiments. Pro-inflammatory visceral WAT was transplanted to an area of the common carotid arteries which generally lack atherosclerotic lesions. After transplantation, atheroma and an elevated inflammatory profile were observed however, no such findings occurred when non-inflammatory subcutaneous WAT was transplanted thus demonstrating that transplanted PVAT was responsible for accelerated atherosclerosis and endothelial dysfunction in recipient mice (Öhman et al. 2011). Furthermore, the influence of PVAT on chronic kidney disease, a condition which enhances the development of atherosclerosis, was evaluated and PVAT was demonstrated to enhance atherosclerosis in the aortae of uninephrectomised $ApoE^{-/-}$ mice due to activation of the renin-angiotensin system within the PVAT (Kawahito et al. 2013).

Taken together, these data suggest that PVAT, through its action on vascular contraction, ROS production and inflammation, likely influences vascular dysfunction associated with ageing and atherosclerosis. However, the interrelationships between ageing and atherosclerosis and PVAT function and morphology has not been well characterised. It remains unclear whether PVAT dysfunction occurs once disease is established or if PVAT itself contributes to disease pathogenesis.

1.4.3.1 Superoxide production attenuates the anti-contractile effect PVAT

PVAT has been reported to express all the enzymatic machinery required to generate ROS (Szasz and Webb 2012; Szasz et al. 2013). Mitochondria are the primary generators of intracellular ROS and are highly expressed within the heterogenous (brown and white adipocytes) aortic PVAT of mice (Kiefer et al. 2012). Elevated superoxide production has been proven to promote an inflammatory environment and cellular senescence, which is a risk factor for CVD (Rizvi 2009; Bailey-Downs et al. 2013; Costa et al. 2016).

Dysfunctional mitochondria have been observed within arteries with ageing and in response to a high fat diet (Ballinger et al. 2002; Trifunovic et al. 2008; Bournat et al. 2010; Payne et al. 2015). Moreover, augmented ROS production within the PVAT of human arteries has been associated with an attenuation of the anti-contractile capacity of PVAT (Greenstein et al. 2009). Also, similar findings have been reported in mice, with superoxide potentiating the contraction of arteries in the presence of PVAT (Gao 2007; Gao et al. 2007b).

1.4.3.2 PVAT modulates the inflammatory environment

Human PVAT has been demonstrated to exert potent chemotactic effects on monocytes, granulocytes, and T lymphocytes and thus contributes to an increased inflammatory profile and recruitment of leukocytes to the interface between PVAT and adventitia of atherosclerotic aortae

(Henrichot et al. 2005; Ozen et al. 2015). An augmented inflammatory activity in the PVAT surrounding vessels prone to the development of atherosclerosis may further promote the development of atherosclerotic lesions. Therefore, in humans, it is possible that aortic PVAT may promote atherosclerosis. Moreover, increased pro-inflammatory adipokine secretion and infiltration of inflammatory cells has been observed in the periaortic PVAT of atherosclerotic ApoE$^{-/-}$ mice (Lohmann et al. 2009). However, the aortic PVAT of high fat fed C57BL/6 mice has been demonstrated to be resistant to increased macrophage infiltration (Fitzgibbons et al. 2011).

1.5 Models of ageing and atherosclerosis

Vascular ageing is a multifaceted process. In humans, the study of normal vascular ageing is often complicated by the presence of cardiovascular risk factors and existing comorbidities, such as atherosclerosis, which is a progressive disease associated with ageing. The C57BL/6 mouse strain is a useful model of healthy vascular ageing because it does not exhibit dyslipidaemia or the spontaneous development of lesions on a normal chow diet thus, the C57BL/6 model allows the study of vascular ageing without unwanted confounding effects (Paigen et al. 1990; Whitman 2004).

The study of atherosclerotic disease in humans, particularly the early stages of atherosclerosis, is hindered by a lack of appropriate tissue samples and a large proportion of these are obtained post-mortem, when atherosclerosis is already established. Although animal models do not exactly mirror human disease they are extremely useful mechanistically and for modelling disease progression.

The most predominant in vivo models of atherosclerosis are genetically engineered mice such as the Apolipoprotein E-deficient mouse (ApoE$^{-/-}$) and the low-density lipoprotein-receptor mouse (Ldlr$^{-/-}$). These mice develop atherosclerotic plaques very quickly and the speed of development can be augmented by the addition of a high fat diet (Jawien et al. 2004). They also have the benefit of being relatively inexpensive to maintain, have short gestation periods, lower ethical burden and can be bred to have identical genetic makeup. However, wild-type mice have an elevated high-density lipoprotein (HDL) to LDL ratio which is the direct opposite of humans (Pendse et al. 2009).

Large animal models are more expensive and difficult to maintain but have certain advantages. Pigs for example, spontaneously develop atherosclerotic lesions which closely resemble those of humans but they are very slow to (Skold et al. 1966). Rabbits fed a cholesterol-rich diet also develop lesions relatively quickly but they are more fatty and inflammatory than the plaques observed in humans (Jawien et al. 2004).

Of the available models, the ApoE$^{-/-}$ mouse is the most extensively used in studies of atherosclerosis (Jawien et al. 2004; Getz and Reardon 2012).

1.5.1 Apolipoprotein E gene and Apolipoprotein E-deficient mice

Apolipoprotein E (ApoE) is a glycoprotein of approximately 34 kDa. It is mainly synthesised in the liver and brain and plays an important role in the metabolism of lipoproteins (Bonomini et al. 2010).

ApoE is a constituent of all lipoproteins (excluding LDL) and acts as a ligand for the chylomicron ApoB and E receptors that remove chylomicrons and very low density lipoproteins (VLDL) (Zhang et al. 1992; Jawien et al. 2004).

In the vasculature, ApoE is synthesised by monocytes and macrophages (Meir et al. 2004). Introduction of macrophage-derived ApoE into ApoE-deficient mice demonstrated that physiologic levels of macrophage-derived ApoE in the artery wall is atheroprotective and slows the progression of atherosclerosis (Fazio et al. 1997; Shi et al. 2000; Fazio et al. 2002). Macrophage-derived ApoE increases the vasodilatory response of resistance arteries, taken from obese humans, to acetylcholine (Yue et al. 2012). Also, work from this same group demonstrated that ApoE and Cav-1 co-localise in adipocytes and ApoE interacts with Cav-1 at the site where eNOS normally binds (Yue et al. 2011). This supports the idea that macrophage-derived ApoE modulates the inhibitory interaction between Cav-1 and eNOS and thus increases NO bioavailability in endothelial cells (Greenstein 2012; Yue et al. 2012).

The ApoE knockout mouse ($ApoE^{-/-}$) was independently generated in two different laboratories in 1992 by targeted gene inactivation (Plump et al. 1992; Zhang et al. 1992). It is a widely-used model of atherosclerosis due to its predisposition to hypercholesterolemia and spontaneous development of lesions within its vessels when fed a normal chow diet (Plump et al. 1992; Zhang et al. 1992; Jawien et al. 2004). The formation of atherosclerotic lesions can be accelerated by feeding the mice a high fat 'Western' diet as in man (Plump et al. 1992). The first signs of atherosclerosis are observed in this model at six to eight weeks old when monocytes attach to endothelial cells. In eight to ten-week-old mice, lesions comprised of foam cells and VSMCs are apparent and by weeks fifteen to twenty, advanced fibrous plaques can be seen within the vasculature (Nakashima et al. 1994; Coleman et al. 2006; Vasquez et al. 2012).

The aortae of $ApoE^{-/-}$ mice develop complex lesions and plaques similar to those observed in humans, including necrotic cores. Plaque rupture, which occurs in humans and can result in stroke or myocardial infarction, has been observed in the brachiocephalic arteries of $ApoE^{-/-}$ mice (Johnson et al. 2001; Meir and Leitersdorf 2004; Coleman et al. 2006; Bond et al. 2011). $ApoE^{-/-}$ mice develop atherosclerotic lesions throughout their macrovasculature including: the aortic root, aortic arch, the left and right common carotid arteries, the thoracic and abdominal aorta and the superior mesenteric artery (Nakashima et al. 1994; VanderLaan et al. 2004; Vasquez et al. 2012). However, these lesions form predominantly in the aortic root and arch rather than in the coronary and carotid arteries as seen in humans, and this has been attributed to the high heart rate of mice (up to 600 beats per minute) (Figure 1.2) (VanderLaan et al. 2004).

Additionally, the $ApoE^{-/-}$ mouse can be used as a model of accelerated ageing. Moreover, there is growing evidence that ApoE can affect the human ageing process (Ang et al. 2008). Indeed, ApoE polymorphisms have been linked with the development of age-related diseases such as dementia and CVD, predominantly due to the substantial role ApoE plays in modulating cholesterol levels (Utermann et al. 1984; Siest et al. 1995; Ang et al. 2008). It has been documented that $ApoE^{-/-}$ mice have a reduced lifespan and similar observations have been made

in humans with ApoE-related disorders (Moghadasian et al. 2001). Populations studies have linked the ApoE4 allele, which is associated with an increased incidence of stroke, coronary artery disease and Alzheimer's disease, to decreased longevity (Smith 2002). Additional reports suggest that in comparison to age-matched C57BL/6 controls, ApoE$^{-/-}$ mice display premature ageing phenotypes such as greying and hair follicle loss at a much earlier age and these characteristics are accelerated in ApoE$^{-/-}$ mice fed a Western-type diet (Ang et al. 2008).

The ApoE$^{-/-}$ mouse displays endothelial dysfunction which is an established pathology in human atherosclerosis. In vitro experiments using rings of thoracic aorta from ApoE$^{-/-}$ mice demonstrated that there is a reduced endothelial-dependent relaxation to acetylcholine linked not only to hypercholesterolaemia but also with lesion development and size within the aorta (Bonthu et al. 1997; Deckert et al. 1999; Crauwels et al. 2003; Johansson et al. 2005; Vasquez et al. 2012; Seto et al. 2013). Whilst endothelial function has been extensively evaluated in ApoE$^{-/-}$ mice, the role of PVAT on vascular reactivity has been largely ignored.

Thus, while no animal model exactly mirrors human conditions, the ApoE$^{-/-}$ mouse is an extremely useful model to study the underlying mechanisms involved in the progression of atherosclerosis. Previous research has indicated that PVAT influences the development and progression of atherosclerosis (Chang et al. 2012a; Szasz and Webb 2012; Brown et al. 2014; Ozen et al. 2015). However, the influence of PVAT on aortic preparations from ApoE$^{-/-}$ mice has not previously been explored. Alterations to the vascular reactivity of the aortae of ApoE$^{-/-}$ mice, as a direct consequence of changes to the PVAT, may contribute to the progression of atherosclerosis. Increased aortic contractions due to an imbalance of NO or the release of vaso-constricting agents from PVAT could, potentially, result in increased turbulence of blood flow and thus, increased atherosclerotic lesion development. Furthermore, the influence of PVAT from ApoE$^{-/-}$ mice on endothelial function has not previously been assessed although, in diet-induced weight gain, PVAT been demonstrated to promote endothelial dysfunction (Ketonen et al. 2010). Taken together, the influence of PVAT on both the VSMCs and endothelium may contribute to the progression of atherosclerosis within the aortae of ApoE$^{-/-}$ mice.

1.6 Caveolae, caveolin-1 and their role in atherosclerotic disease progression

Caveolae are 50-100 nm 'cave-shaped' plasmalemmal invaginations in terminally differentiated cells and are expressed in numerous cell types including the vascular endothelium, VSMCs and adipocytes (Figure 1.3) (Frank et al. 2003; Frank et al. 2004b; Rahman et al. 2009; Frank 2010). Caveolae coat proteins, caveolins -1, 2 and 3 (Cav-1, Cav-2, Cav-3) form the basic components of caveolae and are demonstrated to have different functional roles that can vary by cell type (Chidlow et al. 2010). Cav-1 and -2 are widely expressed throughout the vasculature whilst Cav-3 is preferentially expressed in skeletal, cardiac and smooth muscles (Cohen et al. 2004a).

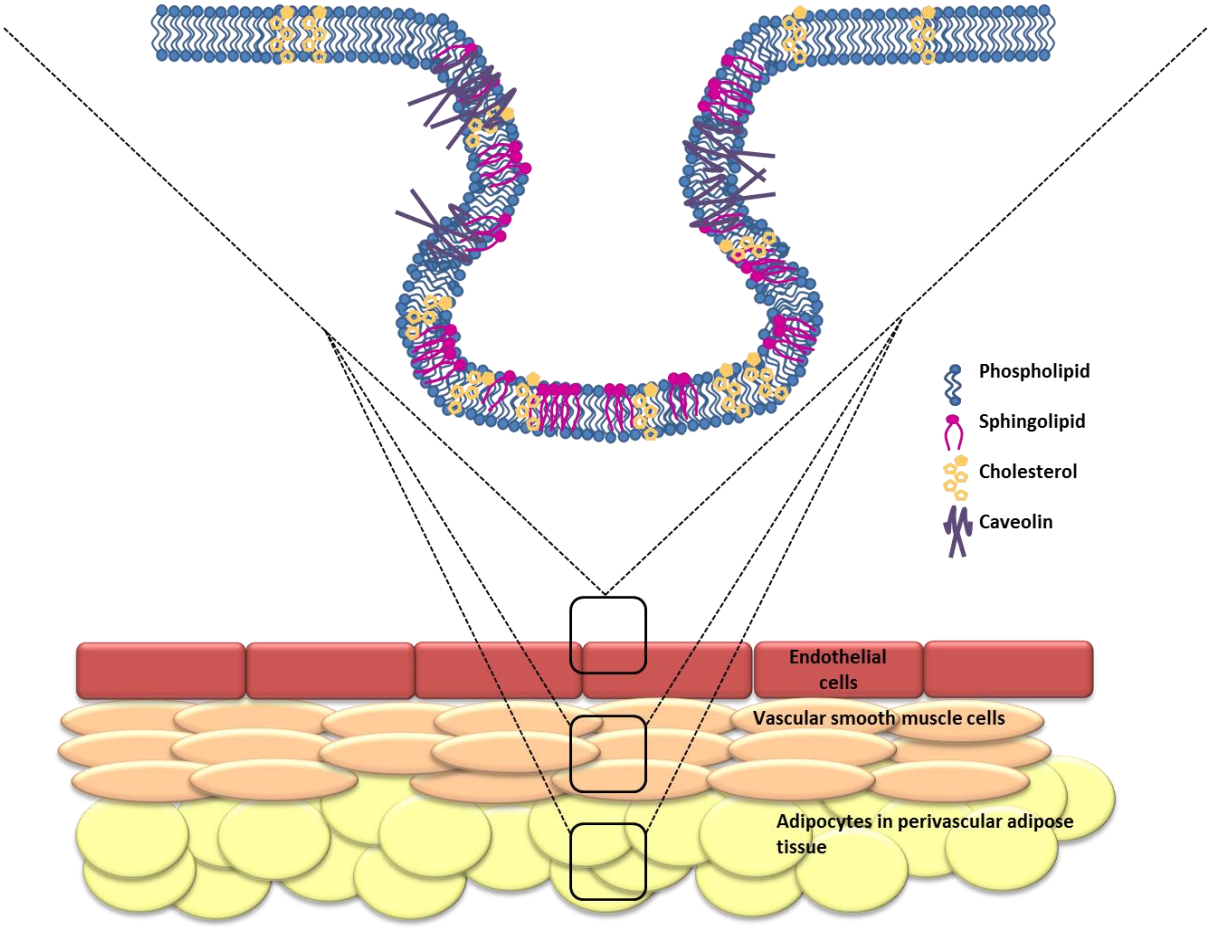

Figure 1.3 Caveolae in endothelial, vascular smooth muscle cells and adipocytes within the vasculature.

Adapted from Rahman, Acta Physiol 195, 231-245 (2009)

Caveolae and Cav-1 have many important functions within the vasculature and one of the most characterised is the inhibitory interaction between eNOS and Cav-1. eNOS is an acetylated membrane protein and is specifically targeted to caveolae through interactions with Cav-1 (Dudzinski and Michel 2007). Dissociation from Cav-1 is essential for eNOS activation and is a calcium-dependent process; the rise in intracellular calcium levels may be triggered via numerous mechanisms for example by shear stress or activation of cell surface receptors (Rizzo et al. 1998; Beny et al. 2008; Mineo et al. 2012). Upon calcium binding to calmodulin, the inhibitory Cav-1-eNOS complex is disrupted leading to eNOS activation and subsequent production of NO. Once intracellular calcium levels become depleted, the inhibitory Cav-1-eNOS interaction is resumed (Dudzinski and Michel 2007).

Due to the relative importance of caveolae structures, the expression of Cav-1 is tightly regulated. Aberrations to Cav-1 levels result in detrimental consequences and over-expression of Cav-1 has been demonstrated to induce cellular senescence in mouse fibroblasts (Volonte et al. 2002). In addition, the modulation of Cav-1 levels within senescent human diploid fibroblasts resulted in recovery of normal growth factor responses and resumption of the cell cycle, leading to the proposal that Cav-1 plays a 'gatekeeper' role in the cellular ageing process (Park et al. 2000; Park 2002; Cho et al. 2005). Cav-1 has also been implicated in the pathogenesis of CVD and is known

to modulate numerous inflammatory pathways, producing conflicting pro- and anti-inflammatory effects (Wang et al. 2006; Briand et al. 2011). Furthermore, NO bioavailability has been demonstrated to be depleted under hypercholesterolaemia conditions due to an increase in the abundance of caveolae, resulting in an increase in inhibitory Cav-1-eNOS complexes (Feron et al. 1999; Grayson et al. 2013). Taken together, these data suggest that variations in caveolae and Cav-1 expression may influence the development of CVD by influencing the morphology and function of arteries with age.

1.6.1 The Cav-1 knockout mouse

The essential requirement for the Cav-1 component of caveolae within the vasculature has been demonstrated through the genetic deletion of Cav-1 in murine models (Cav-1$^{-/-}$), where in the absence of Cav-1, caveolae structures are no longer detected (Razani et al. 2002a; Frank et al. 2003; Shakirova et al. 2006; Hausman et al. 2012).

The simultaneous generation in 2001 of the Cav-1$^{-/-}$ mouse by two independent laboratories allowed for the study of the physiological role of caveolae (Drab et al. 2001; Razani et al. 2001). Due to the ability of Cav-1 and Cav-2 proteins to hetero-oligomerise, the Cav-1$^{-/-}$ mouse could be considered a Cav-1$^{-/-}$Cav-2$^{-/-}$ double knockout because, in the absence of Cav-1$^{-/-}$, Cav-2 is reduced by almost 90% and becomes unstable leading to degradation (Li et al. 1998; Parolini et al. 1999; Cohen et al. 2004a). However, the individual roles of the proteins were teased out by the creation of the Cav-2$^{-/-}$ knockout mouse. The Cav-2$^{-/-}$ mouse retains caveolae structures and does not develop the vascular abnormalities or lipid disorders observed in Cav-1$^{-/-}$ mice (Drab et al. 2001; Razani et al. 2002a; Cohen et al. 2003b). Nevertheless, mice lacking Cav-2 exhibit pulmonary dysfunction, exercise intolerance and endothelial cell hyperproliferation; these disorders are also observed in the Cav-1$^{-/-}$ mice, therefore, these defects are associated with the absence of Cav-2 and not a lack of caveolae (Razani et al. 2002b; Le Lay et al. 2005).

Whilst Cav-1$^{-/-}$ mice are viable and fertile they display a range of abnormalities including significantly reduced lifespans, which add further evidence that Cav-1 is involved in the ageing process (Park et al. 2003; Hausman et al. 2012). In addition, by 2-4 months old, Cav-1$^{-/-}$ mice exhibit cardiovascular disorders, pulmonary hypertension, and hypertriglyceridaemia and begin to show signs of premature neuronal ageing (Drab et al. 2001; Razani et al. 2001; Razani et al. 2002a; Cohen et al. 2003b; Trushina et al. 2006; Head et al. 2010). The observed hypertriglyceridaemia in Cav-1$^{-/-}$ mice suggests that caveolae play a key role in cholesterol homeostasis (Fielding et al. 2000; Frank et al. 2006; Frank et al. 2008; Chidlow and Sessa 2010).

In vitro contractility studies performed on the arteries of Cav-1$^{-/-}$ mice, in the absence of PVAT, have demonstrated that Cav-1$^{-/-}$ negatively regulates the activity of eNOS and therefore modulates NO production. Experiments on isolated aortic rings obtained from Cav-1$^{-/-}$ mice demonstrated attenuated vasoconstrictor responses to the α_1-adrenergic agonist phenylephrine in comparison to wild-type mice. This effect was attributed to increased bioavailability of NO due to significantly increased contraction in the presence of a NOS inhibitor (Razani et al. 2001). However, the influence of PVAT on vascular reactivity in Cav-1$^{-/-}$ mice has not previously been investigated. Given the important role of NO in the mediation of the anti-contractile effect of PVAT,

excess production within the vasculature, specifically PVAT, may confer cardio-protective benefits in the Cav-1$^{-/-}$ mouse. Furthermore, the Cav-1$^{-/-}$ mouse is protected against the development of atherosclerosis and this may in part be a result of the beneficial effects of an overabundance of NO (Frank et al. 2004a; Frank and Lisanti 2004b; Frank et al. 2009).

1.6.2 The ApoECav-1 double knockout mouse

The critical role of Cav-1 in the pathogenesis of atherosclerosis was clearly demonstrated by the generation of the ApoE$^{-/-}$Cav-1$^{-/-}$ double knockout mice (Frank et al. 2004a). In both normal diet and Western-type diet-fed ApoE$^{-/-}$Cav-1$^{-/-}$ mice, the loss of Cav-1 confers significant protection against atherogenesis; ApoE$^{-/-}$Cav-1$^{-/-}$ mice exhibit a significant reduction in atherosclerotic lesion burden ranging between 65-70% less in male and female mice when compared to ApoE$^{-/-}$ mice. This atheroprotective phenotype occurs even though ApoE$^{-/-}$Cav-1$^{-/-}$ mice have a markedly more pro-atherogenic lipoprotein profile in both normal diet and Western-type diet conditions, with an approximate 1.3 – 1.5-fold increase in plasma cholesterol and a 2.3-fold elevation in plasma triglyceride content in comparison to ApoE$^{-/-}$ mice (Frank et al. 2004a). These findings agree with previous studies and firmly suggest that caveolae and Cav-1 are key mediators of transcytosis of lipoproteins into the subendothelial space, a crucial initiating step in the development of atherosclerosis (Vasile et al. 1983; Ghitescu et al. 1986; Kim et al. 1994; Schubert et al. 2001).

Additionally, VCAM-1, an adhesion molecule indicated to play a major role in the development of atherosclerosis was found to be downregulated in the aortae of ApoE$^{-/-}$Cav-1$^{-/-}$ mice by approximately 90% (Huo and Ley 2001; Frank et al. 2004a). A NO-mediated down-regulation of VCAM-1 was proposed due to a combination of previous research demonstrating that absence of Cav-1 increased NO bioavailability in the endothelial cells of ApoE$^{-/-}$Cav-1$^{-/-}$ mice due to the loss of tonic inhibition of eNOS and the finding that chronic overexpression of eNOS was linked to the down-regulation of VCAM-1 in the endothelium of eNOS-transgenic mice (Garcia-Cardena et al. 1996; Kawashima et al. 2001; Fernandez-Hernando et al. 2009)

Whilst the genetic deletion of Cav-1 elicits a beneficial atheroprotective phenotype, the mechanisms by which this occurs are complex and much remains unknown. However, it is clear that in the endothelium, Cav-1 plays a pro-atherogenic role. Endothelial caveolae and Cav-1 were demonstrated to be essential for the transcytosis of LDL into the arterial wall, modulation of NO production and for the subsequent accumulation of macrophages, whilst overexpression of Cav-1 induced an accelerated atherosclerotic disease progression (Fernandez-Hernando et al. 2009) (Fernandez-Hernando et al. 2010). In contrast, the absence of Cav-1 in macrophages is pro-atherogenic and the macrophages are more prone to apoptosis and result in an inflammatory environment (Pavlides et al. 2014). Together, these findings highlight the cell-specific role Cav-1 plays in the pathogenesis of atherosclerosis. Nevertheless, the effects of Cav-1 deletion on the bioavailability of NO within the SM and PVAT remain uncertain.

The vascular reactivity of ApoE$^{-/-}$Cav-1$^{-/-}$ mice has not been explored previously. In addition, no observations of PVAT have been made in these mice. The protective effect of Cav-1 deletion in the ApoE$^{-/-}$ background may be in part due to alterations within the PVAT of the double knockout.

Contractility studies of Cav-1$^{-/-}$ mice demonstrated that the vasculature exhibits an attenuated vasoconstrictor response which is proposed to be the result of increased NO bioavailability due to the loss of tonic inhibition of eNOS (Razani et al. 2001). Recently, eNOS expression was detected within aortic PVAT of rodents therefore, enhanced eNOS activity within the aortic PVAT of the ApoE$^{-/-}$Cav-1$^{-/-}$ may contribute to the atheroprotected phenotype (Araujo et al. 2015; Victorio et al. 2016; Xia et al. 2016).

1.7 Hypothesis and aims

The importance of PVAT in the modulation of vascular tone in health and in pathophysiological states is clear. Much attention has been focused on the role of PVAT in diet-induced weight gain and metabolic disturbance. However, the influence of PVAT and NO on normal vascular ageing has not been explored. The identification of alterations to PVAT function in the early stages of vascular ageing may offer a therapeutic target to inhibit the development of CVD. Furthermore, increasing evidence suggests that PVAT may modulate the development and progression of atherosclerosis. A key role for diminished NO bioavailability within the endothelium and the acceleration of vascular ageing and atherosclerotic disease progression has been identified. However, the presence of NO within aortic PVAT of ApoE$^{-/-}$ mice has not been explored; attenuated NO bioavailability may contribute to alterations in PVAT function and ultimately the development of atherosclerosis.

Cav-1$^{-/-}$ mice exhibit enhanced NO production within their vasculature. NO has been demonstrated to play an important role in mediating the anti-contractile effect of PVAT therefore, Cav-1$^{-/-}$ mice may exhibit a potentiated effect of PVAT-mediated vaso-relaxation. In addition, Cav-1 has been demonstrated to confer protection against the development of atherosclerosis on an ApoE$^{-/-}$ background. This atheroprotected phenotype may in part be due to increased NO within the aortic PVAT of the ApoE$^{-/-}$Cav-1$^{-/-}$ mice. Therefore, the hypothesis of this study is that the influence of PVAT on vascular function is modulated by ageing and the development of atherosclerosis via nitric oxide bioavailability.

To test this hypothesis the following aims will be addressed:

1) Investigate whether NO mediates the anti-contractile effect of aortic PVAT in C57BL/6 mice and determine if ageing modulates this effect.

2) Determine if PVAT modulates the vascular function of aortic rings from ApoE$^{-/-}$ mice and investigate whether this is modified by ageing, NO bioavailability or a Western-type diet and the development of atherosclerosis.

3) Elucidate the effect of PVAT and the contribution of NO to PVAT function in aortic preparations from Cav-1$^{-/-}$ mice and establish whether this is influenced by ageing or a Western-type diet.

4) Investigate the influence of PVAT on the vascular function of aortic rings from ApoE$^{-/-}$Cav-1$^{-/-}$ mice, the role of NO, and establish if PVAT function is altered by ageing or a Western-type diet and atherosclerosis.

~ Chapter Two ~

Materials and Methods

Suppliers of materials and reagents are listed in Appendix 1.1. Recipes for solutions and buffers are listed in Appendix 1.2.

2.1 Animal models

All experiments were conducted in strict accordance with the Animals (Scientific Procedures) Act 1986 under the authority of valid Home Office project and personal licences, PPL 40/3558 and PIL 70/25934, respectively. Mouse colonies were housed under a 12-hour light-dark cycle in the Biological Services Unit of The University of Manchester and provided with food and water ad libitum.

Apoe^{tm1Unc}/J (ApoE$^{-/-}$) mice were originally obtained from Jackson Laboratories. The *ApoE*^{tm1Unc} mutant strain was produced via homologous recombination in embryonic stem cells (129P2/OlaHsd-derived E14Tg2a cell line) (Zhang et al. 1992). The *ApoE*^{tm1Unc} strain was backcrossed to the C57BL/6J strain ten times to produce the *Apoe*^{tm1Unc}/J (ApoE$^{-/-}$) mice.

Cav-1$^{-/-}$ mice (*Cav-1*^{tm1Mls}/J) were kindly donated by Lisanti (University of Manchester) and were previously generated by homologous recombination in embryonic stem cells (WW6 cell line) and backcrossed to the C57BL/6J strain for approximately five generations (Razani et al. 2001)

Control mice, C57BL/6J, were acquired from Envigo (formerly Harlan Laboratories) at 4-weeks of age.

2.1.1 Generation of ApoE$^{-/-}$Cav-1$^{-/-}$ double knockout mice

The ApoE$^{-/-}$Cav-1$^{-/-}$ mice were generated through three stages of interbreeding of Cav-1$^{-/-}$, ApoE$^{-/-}$ mice and their offspring (Figure 2.1), genotypes were determined by PCR (Section 2.1.3). Once the ApoE$^{-/-}$Cav-1$^{-/-}$ double knockout was produced, the colony was maintained under the previously mentioned conditions.

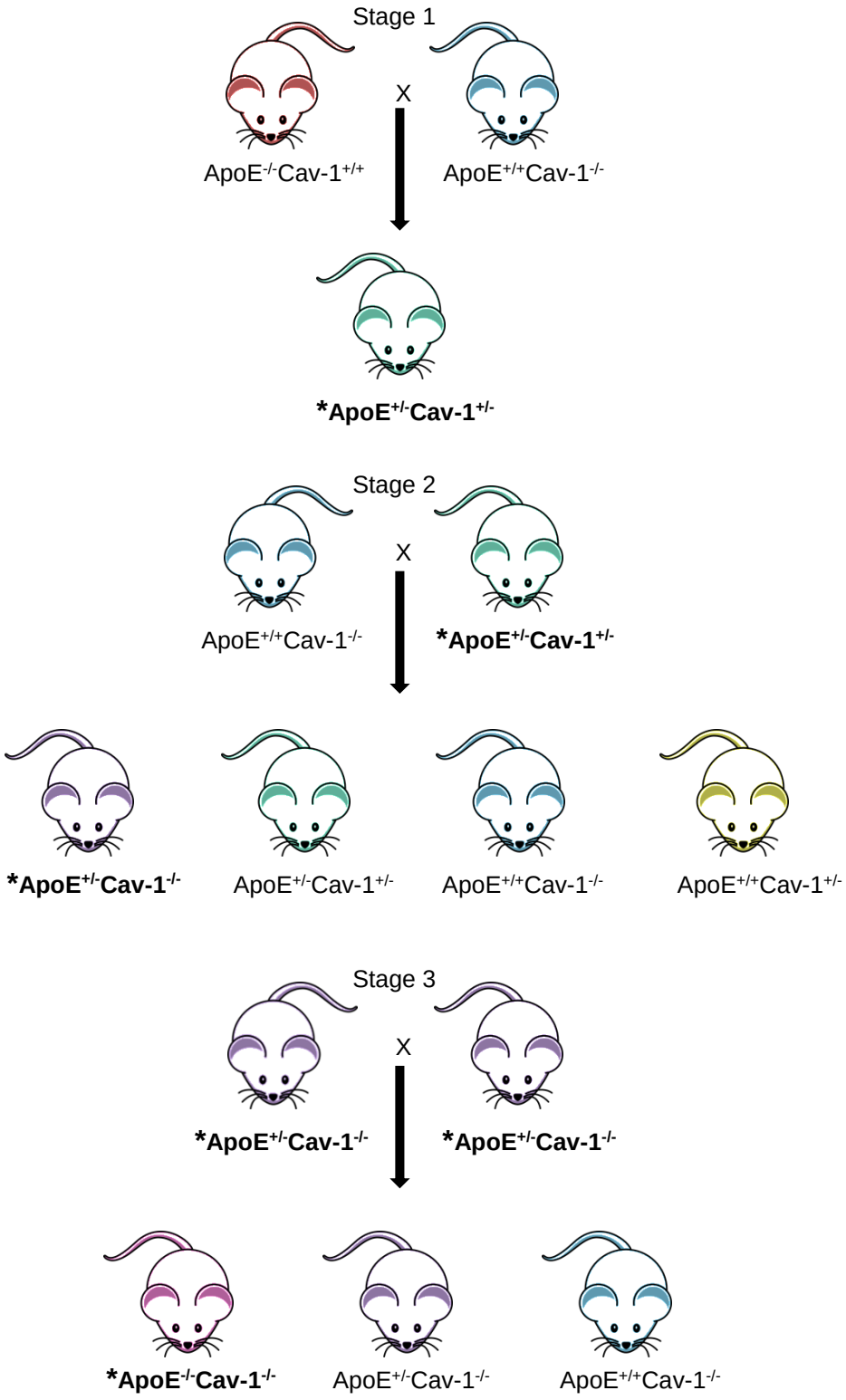

Figure 2.1 Breeding strategy for the generation of the ApoE$^{-/-}$Cav-1$^{-/-}$ double knockout mouse

Stage 1) Female ApoE$^{-/-}$ and male Cav-1$^{-/-}$ mice were interbred to produce heterozygous offspring.

Stage 2) Heterozygous mice were crossed with a homozygous Cav-1 knockout which resulted in a variety of genotypes including the ApoE$^{-/+}$Cav-1$^{-/-}$ phenotype.

Stage 3) ApoE$^{-/+}$Cav-1$^{-/-}$ mice were mated to produce the ApoE$^{-/-}$Cav-1$^{-/-}$ double knockout mouse.

** denotes the sought-after genotype from each stage.*

2.1.2 Diet modulation and generation of experimental groups

Upon weaning, at 3-4 weeks of age, male mice were fed either standard rodent chow (BK001; Special Diets Services, UK) containing 7.52% fat, referred to as normal chow diet (ND) or a high fat 'Western' diet (829100; Special Diets Services) comprising 21% milk fat and 0.15% cholesterol, referred to as Western-type diet (WD). Male mice were used to circumvent the confounding effects of the oestrus cycle (White et al. 2000; Lamping et al. 2001; Shaw et al. 2001). Mice were maintained on either diet for a period of 8 (12 weeks old), 16 (20 weeks old) or 26 weeks (30 weeks old) (Figure 2.2).

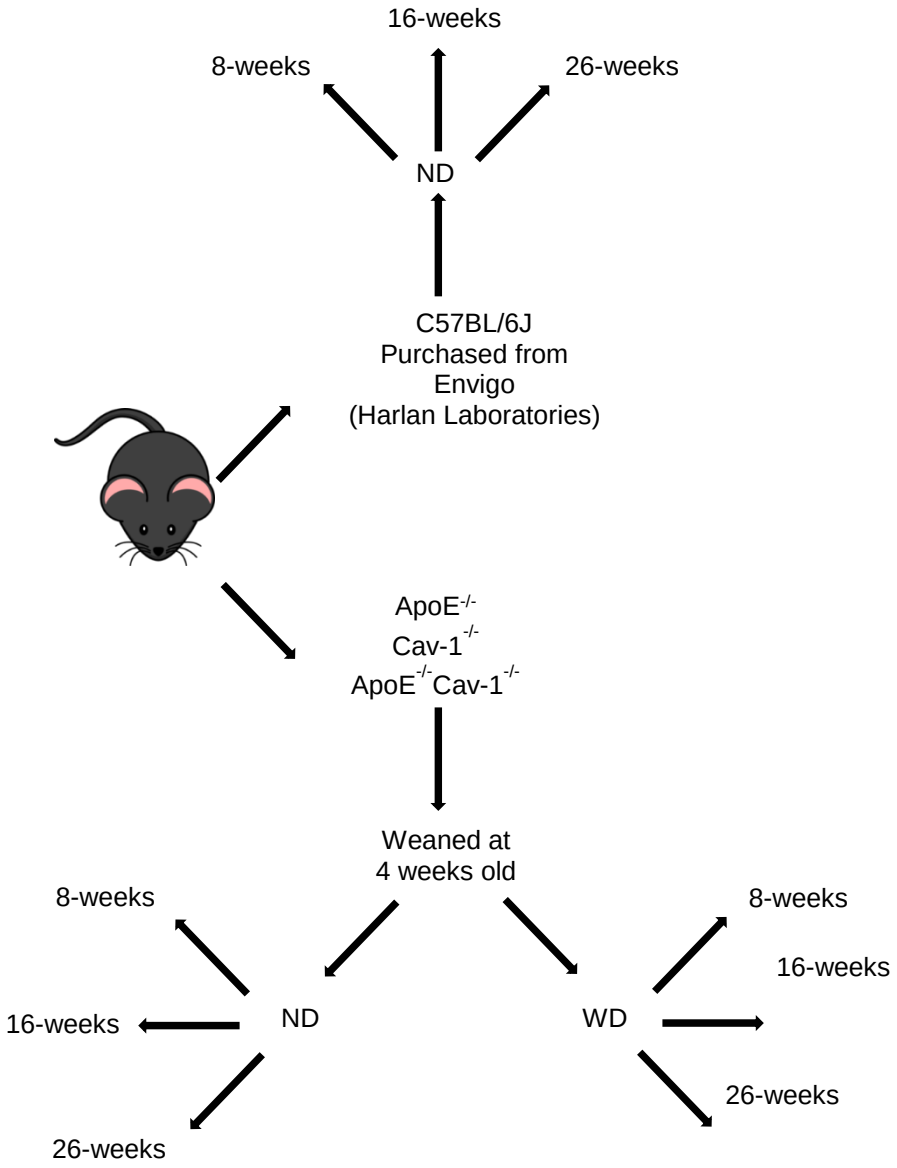

Figure 2.2 Generation of the experimental groups

Post weaning, male mice were fed either a normal chow diet (ND) (7.52% fat) or a Western-type diet (WD) (21% fat) and experimented on after a period of 8, 16 or 26-weeks.

2.1.3 PCR genotyping

Ear snips were obtained from the offspring of the different mouse colonies and stored at -20 °C until required. Genomic DNA was extracted using a REDExtract-N-Amp Tissue PCR Kit (Sigma

Aldrich, UK). A 20 µl PCR reaction was prepared using the following reagents: 10 µl REDExtract-N-Amp PCR Reaction Mix, 5 µl distilled water, 0.33 µl (1.65 µM) per primer of either the ApoE or Cav-1 primer set and 4 µl DNA (or distilled water for the negative control) (Table 2.1).

Reactions were performed in a Thermal Cycler (Applied Biosystems, Veriti 96-well thermal cycler) under the conditions listed in Table 2.1.

Table 2.1 List of primer sequences and PCR conditions for genotyping experiments *Primer sets for ApoE and Cav-1 genotyping are listed. Conditions were followed as detailed by the Jackson Laboratory, 35 cycles were performed (in bold). The expected band sizes resulting from the PCR are detailed in the right-hand column.*

Gene	Primer sequences	Cycling conditions	Expected size, base pairs
ApoE	oIMR0180, common forward GCC TAG CCG AGG GAG AGC CG oIMR0181, wild-type reverse TGT GAC TTG GGA GCT CTG CAG C oIMR0182, knockout reverse GCC GCC CCG ACT GCA TCT	94 °C 3 mins **94 °C 30 secs** **68 °C 40 secs** **72 °C 1 min** 72 °C 2 mins 4 °C hold	Wild-type 155 Knockout 245
Cav-1	oIMR1972, wild-type forward GTG TAT GAC GCG CAC ACC AAG oIMR1973, knockout forward CTA GTG AGA CGT GCT ACT TCC oIMR1974 CTT GAG TTC TGT TAG CCC AG	94 °C 3 mins **94 °C 30 secs** **65 °C 1 min** **72 °C 1 min** 72 °C 2 mins 4 °C hold	Wild-type 690 Knockout 410

Gel electrophoresis was performed in order to separate the PCR products, expected band sizes are listed in Table 2.1. Amplified DNA from the Cav-1 PCR reaction was electrophoresed on a 1.5% agarose gel whilst a higher density of agarose, 3%, was used for the ApoE reaction products. Agarose gels were made in 0.5X TAE buffer from a 50X stock. For gel electrophoresis, 5 µl of 5X loading buffer (Bioline, UK) was added to 20 µl of PCR reaction and 5 µl Hyperladder V DNA 100bp marker (Bioline, UK) was loaded at either end of the gel. The gel was immersed in 0.5 X TAE buffer and samples were loaded into individual wells. Electrophoresis was performed at 100 V for approximately 1 hour. Gels were stained for 40 minutes with Nancy-520, a fluorescent stain specific for double-stranded DNA, (Sigma Aldrich, UK) and visualised using a UV transilluminator on the ChemiDoc MP imaging system (Bio-Rad, UK). Gel images were captured with the same system.

2.2 Tissue and blood collection

At the required time-point, mice were sacrificed by CO_2 asphyxiation and weighed. Animals were pinned out and an incision made along the midline of the abdomen exposing the peritoneum. The peritoneum was cut to expose the internal organs and diaphragm. Once the diaphragm was

pierced, the rib cage was dissected away to expose the thoracic cavity. The right jugular vein was then severed and approximately 0.1 – 0.5 ml of blood was collected and stored on ice. The aorta, encased in PVAT, was excised from the thoracic cavity to the point of the diaphragm, with the heart and lungs left in situ, and placed in ice-cold physiological salt solution (PSS, refer to Appendix 1.2 for recipe). Also, the liver, spleen and epididymal fat pads were removed and their weights recorded.

2.3 Assessment of serum lipidemic and glycaemic profile

Blood was collected from animals as described above, (Section 2.2). Serum was collected after the blood was spun at 1700 g (3000 rpm) for 10 minutes at 4 °C and then stored at -80 °C until further use. Lipidemic profile analysis and glucose measurements were performed by Yifen Liu of the Lipid Biology Research Group, Manchester University, UK. All lipid and glucose measurements were assessed using kits from Randox laboratories and a Cobas Mira analyser (Roche Diagnostics, Switzerland). Blood glucose, total cholesterol and serum triglyceride measurements were determined at a wavelength of 500 nm whilst HDL-cholesterol was measured at a wavelength of 600 nm. All serum measurements are expressed as mmol/L.

2.3.1 Blood glucose measurements

Non-fasted serum glucose levels were determined via an enzymatic colourimetric method. Glucose is oxidised by glucose oxidase and is converted to gluconate and hydrogen peroxide is generated. The hydrogen peroxide reacts with phenol and 4-aminophenazone in the presence of a peroxidase to produce a red-violet quinoneimine dye (Barham et al. 1972). The intensity of colour produced is directly proportional to glucose concentration.

2.3.2 Total cholesterol measurements

Total serum cholesterol levels were measured via the cholesterol oxidase-phenol 4-aminoantipyrine peroxidase (CHOD-PAP) method (Deeg et al. 1983). Cholesterol esters are hydrolysed via cholesterol esterase, which generates free cholesterol, and the reaction products oxidised by cholesterol oxidase to form cholest-4-ene-3-one and hydrogen peroxide. Horseradish peroxidase catalyses the oxidation of 4-aminoantipyrine to produce a quinoneimine indicator. Sample colour intensity is directly proportional to the total cholesterol concentration of the sample.

2.3.3 Assessment of serum triglycerides

Serum triglyceride content was assessed via a colourimetric method using the glycerol phosphate oxidase-phenol 4-aminoantipyrine peroxidase (GPO-PAP) system (Bucolo et al. 1973). In the presence of lipases, triglycerides undergo hydrolysis to produce glycerol and fatty acids. Glycerol-3-phosphate is generated from the transfer of a phosphate from ATP to glycerol which is mediated by glycerol kinase. Glycerol-3 is oxidised and produces hydrogen peroxide which in the presence of peroxidase, reacts with 4-aminophenazone and 4-chlorophenol to form a quinoneimine indicator.

2.3.4 Measurement of HDL-cholesterol

Serum HDL-cholesterol concentrations were measured using an enzymatic direct clearance method (Warnick et al. 2001). The first reaction utilises cholesterol esterase, cholesterol oxidase and catalase to eliminate chylomicrons, VLDL-cholesterol and LDL-cholesterol from the sample.

HDL-cholesterol levels were determined after their release from the serum, by a surfactant, in the presence of cholesterol esterase and cholesterol oxidase. Peroxidation of hydrogen peroxide produces a quinone pigment which is measured at 600 nm.

2.4 En face Oil Red O staining for quantitation of atherosclerotic lesions

Aortae were dissected as described previously (Section 2.2). The surrounding PVAT and adventitia was carefully removed under a dissecting microscope (Figure 2.3). Oil Red O stains lipids, neutral triglycerides, and some lipoproteins. Aortae were cut longitudinally between the intercostal vessels, immersed in 60% (volume/volume) aqueous triethyl phosphate for 10 seconds and incubated in 0.5% Oil Red O solution for 20 minutes on a shaking platform. Aortae were rinsed for ten seconds in 60% triethyl phosphate and washed in distilled water. Aortae were pinned out flat on a black resin block in PSS with the lumen exposed for imaging with an Olympus Camedia-c-7070 wide zoom camera attached to an Olympus SZ61 dissecting microscope. The total aortae area and atherosclerotic lesion areas were measured using Image J 1.46r and the percentage lesion to total vessel area was calculated (Farrell 2008).

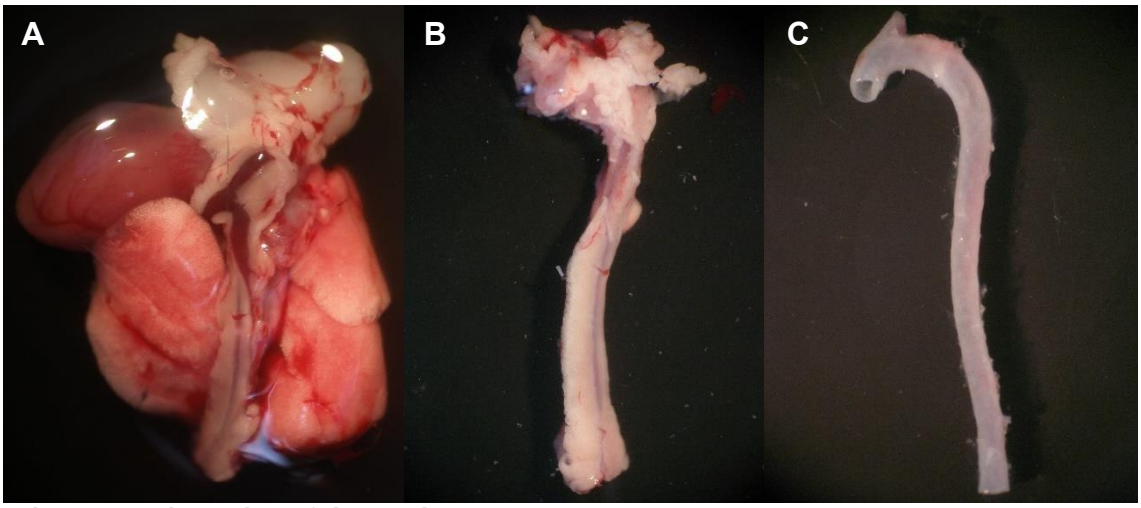

Figure 2.3 Dissection of the murine aorta

A) The aorta was removed from the mouse and placed in a petri-dish containing ice cold PSS. B) The heart, lungs and pulmonary artery were dissected away from the aorta. C) The adventitia and perivascular adipose tissue (PVAT) were carefully removed from the aorta.

2.5 Tissue preparation for histology and immunohistochemistry

The aorta, with PVAT intact, was divided into two sections, thorax I, from the base of heart, including the short ascending aorta, aortic arch and long descending thoracic aorta, and thorax II beginning at the 7th rib and finishing at the diaphragm (Figure 2.4). Thorax I and epididymal fat pads from animals used in myography experiments were fixed in 4% paraformaldehyde (PFA) at 4 °C for 18 hours then stored in phosphate-buffered saline (PBS) until processed for immunohistochemistry.

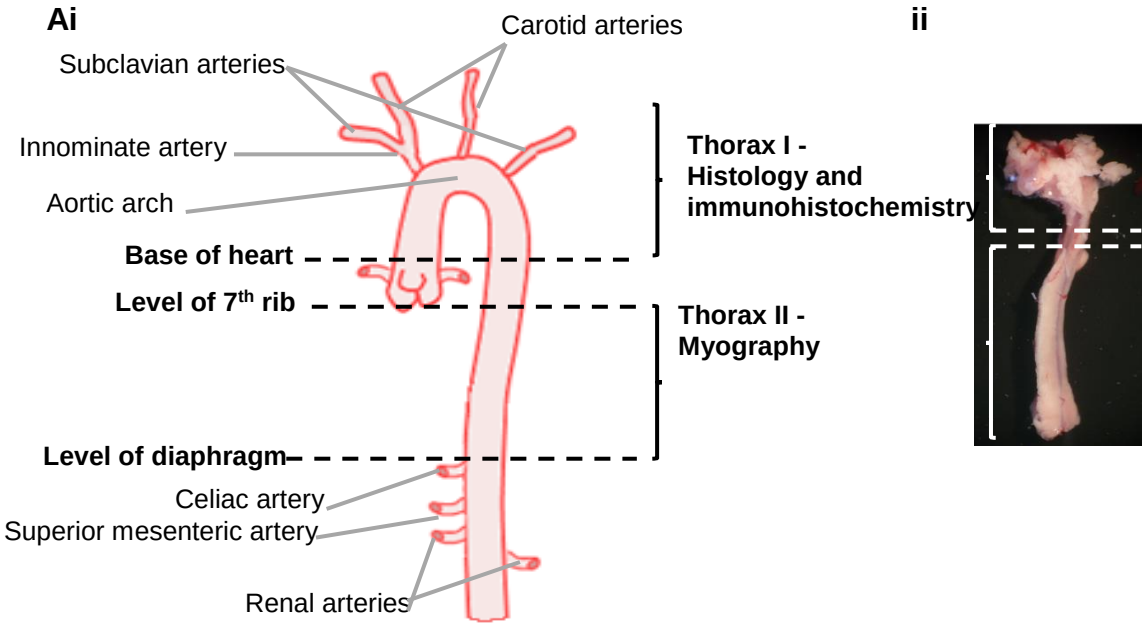

Figure 2.4 Schematic representation of the sections of aorta used for histology, immunohistochemistry and myography.

Ai) The aorta was split into thorax I and thorax II for immunohistochemistry/histology and myography studies, respectively. The dashed lines represent dissection points. ii) an excised aorta surrounded by perivascular adipose tissue (PVAT).

Sections of aorta, with the PVAT left intact, (thorax I, Figure 2.4) and epididymal fat pads were wrapped in thin tissue paper, placed in plastic histology cartridges and suspended in 50% industrial methylated spirits (IMS) until transfer into a Shandon Citadel 2000 tissue processor. Tissue samples were processed in a series of dehydration (in IMS and xylene) and paraffin wax infiltration steps (full processing procedure is outlined in Appendix 1.3). Samples were removed from the tissue paper and embedded in moulds filled with molten paraffin wax before the cassette lid was set into place. Aortic samples were embedded vertically in order for a cross section to be observed after sectioning. The wax blocks were left to set on a cooling plate before removal from the moulds and storage at room temperature.

Prior to sectioning, on a Leica RM2145 microtome, wax blocks were chilled for 30 minutes at -20 °C to facilitate cutting. Ribbons of 5 µm thick sections were floated in a water bath at 45 °C and collected onto poly-L-lysine microscope slides. Slides were dried for 3 hours at 37 °C before baking at 42 °C for a minimum of 48 hours and then stored at room temperature.

2.5.1 Haematoxylin and eosin staining

To visualise the tissue histology of both the PVAT surrounding the descending thoracic aorta (Thorax I, Figure 2.4) and the epididymal fat pads, sections prepared as above, were stained using automated haematoxylin and eosin staining (Varistain 24-4), full processing procedure is outlined in Appendix 1.4. Briefly, sections were de-waxed in xylene and rehydrated through a series of graded alcohols before immersion in deionised water. Gill's haematoxylin No. 2 was applied for 2 minutes followed by a water wash. Slides were briefly exposed to 5% acetic acid and blueing agent before dehydration with graded alcohols. Tissue sections were incubated with an alcoholic eosin Y solution for 2 minutes and immersed in ethanol before clearing in xylene. Stained tissue sections were mounted under glass coverslips using DPX mounting medium (VWR International, UK). Tissue histology was visualised using bright-field microscopy (DM5000, Leica, Germany) at 10 x magnification.

2.5.2 Quantification of epididymal adipocyte area as a marker of diet-induced weight gain

Adipocytes were characterised and quantified using Image J 1.48v software (NIH, USA). Adipocyte area was calculated by manually tracing the adipocyte membrane demarcated by the haematoxylin stain. One hundred consecutive adipocytes were assessed per mouse and a mean area calculated to give n=1, 4 mice were assessed per experimental group (Aghamohammadzadeh et al. 2013).

2.5.3 Assessment of aortic PVAT composition

Aortic PVAT composition was assessed by measuring the total PVAT area followed by tracing the cell membranes of individual white adipocytes within the tissue (Figure 2.5); average white adipocyte size was measured and the percentage area of total aortic PVAT occupied by white adipocytes calculated.

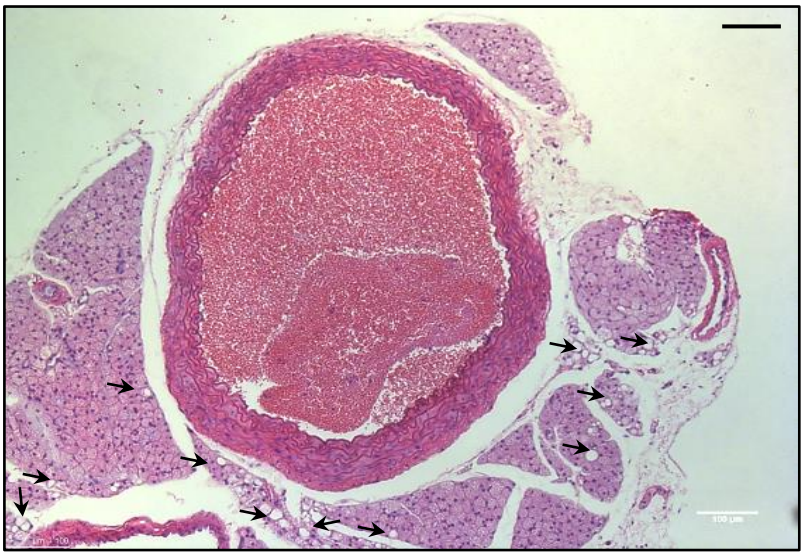

Figure 2.5 Representative haematoxylin and eosin stained thoracic aorta section with perivascular adipose tissue (PVAT)

Thoracic PVAT is mainly comprised of brown adipose tissue with small multi-locular lipid droplets; however, a small population of white adipocytes, highlighted by arrows, was dispersed throughout the PVAT. Scale bar represents 100 µm.

2.5.4 Detection and quantification of superoxide with dihydroethidium

The presence of superoxide anion was assessed via dihydroethidium (DHE) staining of aortic tissue sections. DHE is a fluorochrome which reacts readily with superoxide forming 2-hydroxyethidium (Zielonka et al. 2008; Wojtala et al. 2014) Briefly, paraffin-embedded 5 µm sections of thoracic aorta with intact PVAT (thorax I, Figure 2.4) were dewaxed in xylene, rehydrated through a series of alcohols ending in distilled water. Sections were protected from the light and incubated in a humidity chamber for 30 minutes at 37°C with 2 µM DHE (dissolved in DMSO), washed with tris-buffered KPSS (TBS) and mounted in Vectashield anti-fade mounting media. DHE was omitted and replaced with DMSO as a negative control. Superoxide in the PVAT was visualised using a fluorescent microscope (DM5000, Leica, Germany) at 10 x magnification with excitation and emission wavelengths of 520 and 610 nm, respectively. DHE positive stained nuclei (DHE^+) were sampled using 5 fields of view of 200 µm x 150 µm per aortic PVAT section, and expressed as positive cells per mm^2 (Figure 2.6). A reproducibility study was performed to determine the number of fields of view required to produce a representative population of DHE+ nuclei within the PVAT (Appendix 1.5).

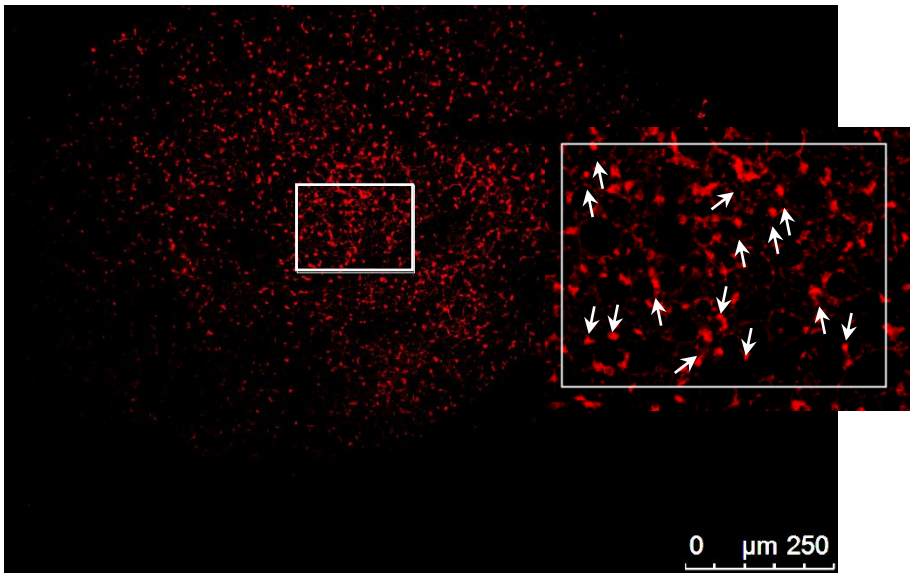

Figure 2.6 Representative dihydroethidium$^+$ staining of aortic perivascular adipose tissue (PVAT) from one field of view

Section of thoracic PVAT incubated with the superoxide indicator DHE which produces red fluorescent staining highlighted by arrows in the magnified image. Scale bar represents 250 µm and the area of the field of view is 200 µm x 150 µm. DHE = dihydroethidium, PVAT = perivascular adipose tissue.

2.5.5 Immunostaining for macrophages with Mac-3

Immunohistochemistry was used to visualise the localisation of macrophages, using a Mac-3 antibody, within a section of tissue. Titrations were performed to optimise staining. Incubations were performed in a humidity chamber.

Sections of thoracic aortae (thorax I, Figure 2.4) were dewaxed in heated xylene prior to rehydration through a series of alcohols and immersion in water. A heat-mediated antigen retrieval step was performed with citrate buffer heated to 95 °C for 15 minutes. Slides were washed in TBS and endogenous peroxidase activity quenched with 3% hydrogen peroxide for 10 minutes. Sections were outlined using a delimiting wax pen. To prevent non-specific binding of immunoglobulins, sections were incubated with 10% horse serum (Invitrogen, UK) in 0.1% BSA for 6 hours at room temperature. Without washing, tissue sections were incubated overnight at 4 °C with the Mac-3 (CD107b Clone M3/84) monoclonal rat anti-mouse antibody (550292, BD Biosciences) at a dilution of 1:200 in TBS (5 µg/ml).

Isotype controls were produced by incubation with rat IgG (559072, BD Biosciences) the same host species as the primary antibody and diluted to the same concentration as the primary (5 µg/ml). Moreover, negative controls were conducted where the primary, secondary or both primary and secondary antibodies were omitted from the diluent (TBS). Furthermore, positive control tissue, a section of aortic arch from a severely atherosclerotic ApoE$^{-/-}$ mouse, was utilised to ensure that specific macrophage staining had occurred.

The following day, slides were washed in TBS-Tween and incubated for 1 hour at room temperature with a rabbit anti-rat, biotin-conjugated secondary antibody (E0468 Dako) at a dilution of 1:1000 (1.5 µg/ml) in TBS. Slides were then washed for a further 15 minutes in TBS-Tween and incubated with Vectastain ABC (avidin-biotin conjugate) (PK-6100, Vector Laboratories, USA) solution for 30 minutes at room temperature. After washing in TBS, a DAB Peroxidase (horse radish peroxidase) detection system (SK-4100 Vector Laboratories) was applied per the manufacturer's instructions. Slides were not counterstained to ensure that Mac-3^{+} staining was not obscured. However, background staining from DAB allowed visualisation of the morphology of the perivascular adipose tissue section. Tissue sections were dehydrated through a series of alcohols, cleared in xylene and mounted with DPX. The slides were left to dry overnight before visualisation under bright-field microscopy (DM5000, Leica, Germany).

2.5.6 Analysis of macrophage infiltration in aortic PVAT

Inflammation of aortic PVAT was assessed via the presence of macrophages (Mac-3 stain). Quantitative analysis of immunostaining was performed using ImageJ (v1.47, NIH, USA). Images were taken at 10x magnification and total PVAT area measured by manually tracing the margins of PVAT. Mac-3^{+} stained cells were counted and data presented as Mac-3^{+} cells per mm^{2} of aortic PVAT (Figure 2.7).

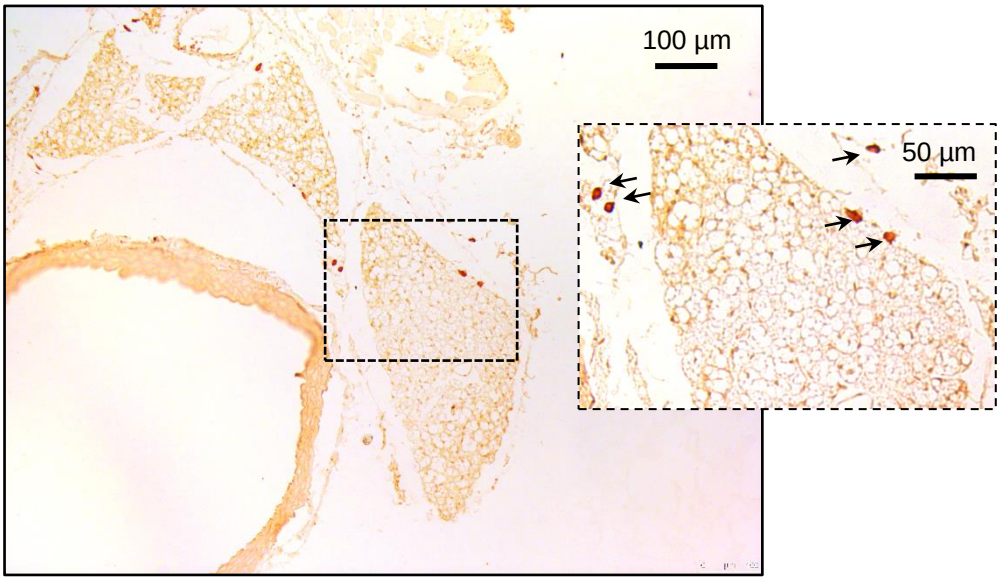

Figure 2.7 Representative Mac-3$^+$ immunostaining of thoracic aorta section in perivascular adipose tissue

Mac-3$^+$ cells stained brown and highlighted by arrows in the magnified image. Scale bar represents 100 µm and 50 µm in the 10 x and 20 x magnified image, respectively.

2.6 Assessment of aortic vascular reactivity using myography

2.6.1 Preparation of mouse thoracic aortae for myography

Aortae were removed as described previously in Section 2.2. The aortae were pinned out on a dissection plate in ice-cold PSS (refer to Appendix 1.2 for recipe) and the aortic arch removed, leaving the thoracic aortae intact (thorax II, Figure 2.4). Four, 2 mm sections, alternating between intact PVAT and PVAT denuded segments, were cut allowing for the examination of the functional effects of PVAT on the thoracic aorta.

2.6.2 Mounting and normalisation of aortic rings

Aortic rings were mounted onto two 200 µm pins in each myograph bath (Danish Myo Technology, Denmark) containing 6 ml of PSS (Figure 2.8) and gassed with 5% CO_2 balanced air. During a 20-minute equilibration period, at 37°C, no tension was applied to the aortic segments. Aortic rings were then gradually exposed to an increase in tension up to 5 mN, over 30 minutes until the tension remained stable at 5 mN, as described previously (Judkins et al. 2006; Xu et al. 2012; Cobb 2013).

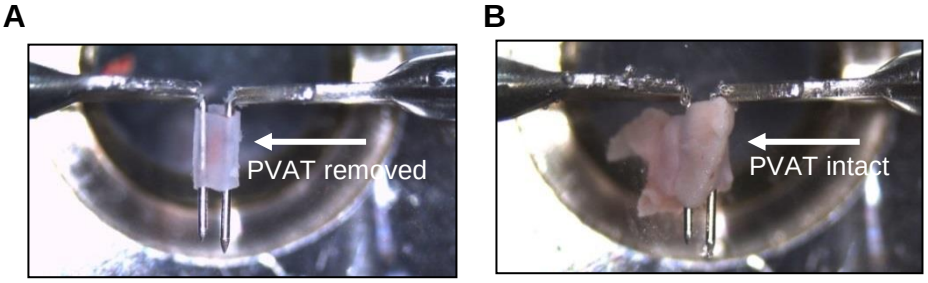

Figure 2.8 Mounted aortic segments in a myography bath*A, Perivascular adipose tissue (PVAT) removed B, PVAT intact.*

2.6.3 Assessment of aortic ring viability and endothelial integrity

Contractile viability was tested with a high potassium physiological salt solution (KPSS, PSS with equimolar substitution of 100 mM potassium chloride for sodium chloride, refer to Appendix 1.2 for recipe). After maintenance of a stable contraction, defined as a plateau of maximal contraction (Figure 2.9), the solution was removed and replaced with PSS, a minimum of three washes with PSS were performed to remove the contractile stimulus and allow the aortic rings to relax back to baseline tension.

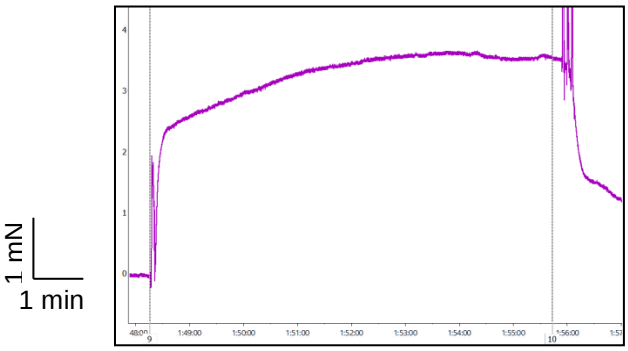

Figure 2.9 Representative sample trace of aortic ring constriction elicited by addition of 100 mM KPSS

X axis represents time in minutes, Y axis represent change in tension mN. Scale bar represents 1 mN (y axis), 1 minute (x axis).

Aortic rings were then pre-constricted with phenylephrine (10 µM) (Sigma-Aldrich, UK) and the functional endothelial integrity of the aortic ring was evaluated by examining relaxation to acetylcholine (10 µM) (Sigma-Aldrich, UK), an endothelium-dependent dilator (Figure 2.10) (Leal et al. 2012a; Cobb 2013; Shahid et al. 2013).

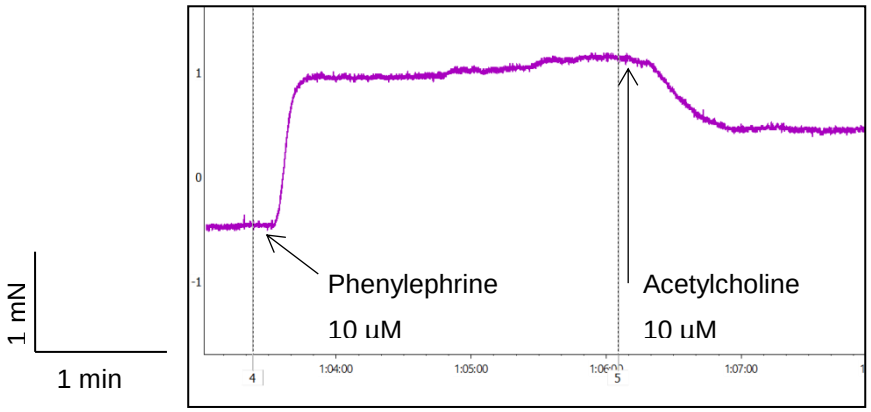

Figure 2.10 Representative trace of endothelium integrity assessment

Aortic rings were pre-constricted with 10 µm phenylephrine and, upon stable constriction, 10 µm acetylcholine was added. X axis represents time in minutes, Y axis represent change in tension in mN. Scale bar represents 1 mN (y axis), 1 minute (x axis).

In some aortic preparations, the endothelium was mechanically removed by introducting air bubbles into the lumen of the aortic ring prior to mounting on the pins (Ko et al. 2010). Endothelium

denudation was considered successful where acetylchline-induced vasorelaxation induced dilation of less than 30%.

This protocol was performed to re-activate the aortic segments and to ensure that the dissection and mounting procedure did not result in any damage or adverse effects on vessel functionality. Exclusion criteria were set in order that any aortic segments that did not maintain a stable contraction when challenged with KPSS of phenylephrine, were excluded from the study; approximately 15% of the aortic rings tested throughout the studies were therefore excluded.

Baths were washed at least three times with PSS and aortic rings were left to relax back to baseline tension. Aortae were constricted for a second time with KPSS until maximal contraction was observed and washed again with PSS until they reached baseline tension.

2.6.4 Cumulative dose responses of aortic rings to phenylephrine

Cumulative concentration-response curves were constructed to the vasoconstrictor phenylephrine (1 x 10^{-10} - 3 x 10^{-5} mol/L) (Figure 2.11).

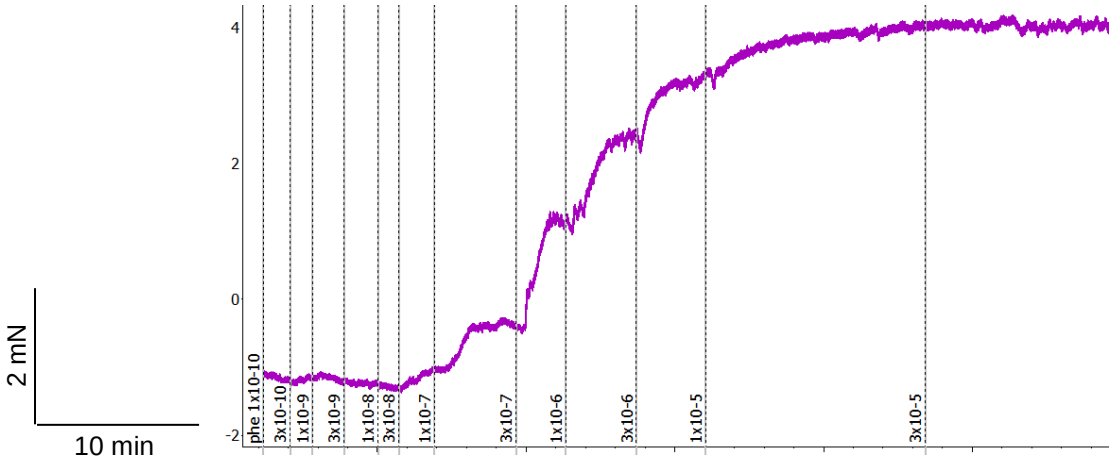

Figure 2.11 Representative trace of a phenylephrine dose response (1 x 10-10 - 3 x 10-5 mol/L)

Aortic rings were exposed to cumulative doses of phenylephrine, represented by dotted lines. X axis is time in minutes, Y axis represent change in tension in mN. Scale bar represents 2 mN (y axis), 10 minute (x axis).

2.6.5 Pharmacological inhibition of nitric oxide synthase with L-NNA

A pharmacological inhibitor of NOS (N_{ω}-Nitro-L-arginine, L-NNA) was used to determine the contribution of NOS to vascular function. Aortic rings were incubated with L-NNA (50 µM) (Sigma-Aldrich, UK) (dissolved in PSS) for 1 hour and time controls performed in parallel with the inhibition experiments (Otter et al. 1999; Schleifenbaum et al. 2010; Cobb 2013). Post incubation, phenylephrine dose responses were performed and after the final dose the arteries were exposed to 10 µM acetylcholine to determine the contribution of NO to the acetylcholine-induced vasodilatory response.

Arteries were washed with PSS and allowed to relax back to baseline tension. Inhibitor-containing solutions were used for all washes post incubation so that L-NNA was present throughout the

remainder of the experiment, with the exclusion of time-controls. Aortic rings were challenged for a final time with KPSS to ensure that contractile responses were unaffected after the pharmacological intervention.

2.6.6 Assessment of endothelium-independent relaxation

After a final series of washes with PSS, aortic rings were pre-constricted with phenylephrine (10 µM) and endothelial-independent dilation assessed by examining relaxation to sodium nitroprusside (10 µM) (Sigma-Aldrich, UK), a potent nitric oxide donor.

2.7 Adipokine secretion from phenylephrine-stimulated PVAT

To investigate adipokine secretion from aortic PVAT, a mouse obesity adipokine array was used. PVAT was collected from the entire thoracic aortae, placed in 600 µl PSS and stimulated with phenylephrine (3×10^{-5} mol/L) for 45 minutes at 37 °C (to mimic the conditions of a myography protocol). The solution surrounding the PVAT (supernatant) was removed and stored at -80 °C prior to analysis. A Proteome Profiler Adipokine array (R&D systems, USA) was used to detect a range of 38 mouse adipokines, spotted in duplicate on nitrocellulose membranes, per the manufacturer's protocol. The list of adipokines present and the layout of the array membrane is presented in Appendix 1.6.

The adipokine supernatant was collected from three mice per experimental group and pooled, mixed with the biotinylated detection antibodies and incubated overnight with the array membrane at 4 °C on a rocking platform shaker. Membranes were visualised, following application of streptavidin-HRP and chemiluminescent detection reagents, using a ChemiDoc MP imaging system (Bio-Rad, USA). Pixel densities were used as a measure of protein present and normalised to positive control reference spots using Image Lab software (v5.0 Bio-Rad, USA). Intensities from subsequent arrays were normalised to positive control reference spots from the original array. The pooled adipokine profile of aortic PVAT from 26-week ND-fed C57BL/6 mice was assessed by using the pooled PVAT secretome from 8-week ND-fed C57BL/6 mice as the control; adipokine expression of the 8-week ND fed C57BL/6 mice were assigned a value of 1. Changes in adipokine secretion from the 26-week C57BL/6 mice were compared to the 8-week group and any observed alterations in adipokine profile were expressed as percentage change from the 8-week ND-fed group.

The reliability of the assay was validated by repeating array experiments for C57BL/6 26 week ND-fed mice using the same pooled samples (Appendix 1.7).

2.8 Data analysis and statistics

Mouse body and organ weights, en face lesion analysis, adipocyte area, histology, immunohistochemical quantification and serum glucose and lipids measurements data are presented as mean ± standard error of the mean (SEM) for all measurements. Differences between experimental groups were analysed using a one-way analysis of variance (ANOVA) with a post-hoc Tukey's multiple comparison test for C57BL/6 mice and two-way ANOVA with Bonferroni's post hoc tests for the $ApoE^{-/-}$, $Cav\text{-}1^{-/-}$ and $ApoE^{-/-}Cav\text{-}1^{-/-}$ strains.

For assessment of vascular contractility, all data were recorded using LabChart (Version 7; AD Instruments, Oxford, UK). Reported measurements were from the maximum stable contraction and maximal relaxation. Maximal contractions to all agonists are presented as actual changes in tension (mN); relaxations are expressed as a percentage reduction in tension from maximal contraction prior to addition of the agonist (% relaxation). Dose responses to phenylephrine were analysed using a two-way ANOVA followed by a Bonferroni post hoc test at each dose response point**.** Maximal contractions and relaxations were analysed using either one-way ANOVA for comparisons of the effect of ageing on contraction and relaxation in C57BL/6 mice whilst Two-way ANOVA was performed to compare ND versus WD responses. Data are presented as mean ± SEM.

The adipokine secretome profile data are expressed as percentage change from the absolute values of the young 8-week ND-fed C57BL/6 mice.

For the purposes of this study, comparisons were drawn between ND-fed mice of similar genetic backgrounds to tease out the effects of the different genotypes therefore, the following comparisons were made:

- $ApoE^{-/-}$ mice versus C57BL/6
- $Cav\text{-}1^{-/-}$ versus C57BL/6
- $ApoE^{-/-}Cav\text{-}1^{-/-}$ versus $ApoE^{-/-}$
- $ApoE^{-/-}Cav\text{-}1^{-/-}$ versus $Cav\text{-}1^{-/-}$

Analyses were performed with GraphPad Prism (version 7.01, GraphPad Software, USA). Probability values < 0.05 were considered significant.

An overview of the different methods used to perform the studies in this thesis is depicted in Figure 2.12.

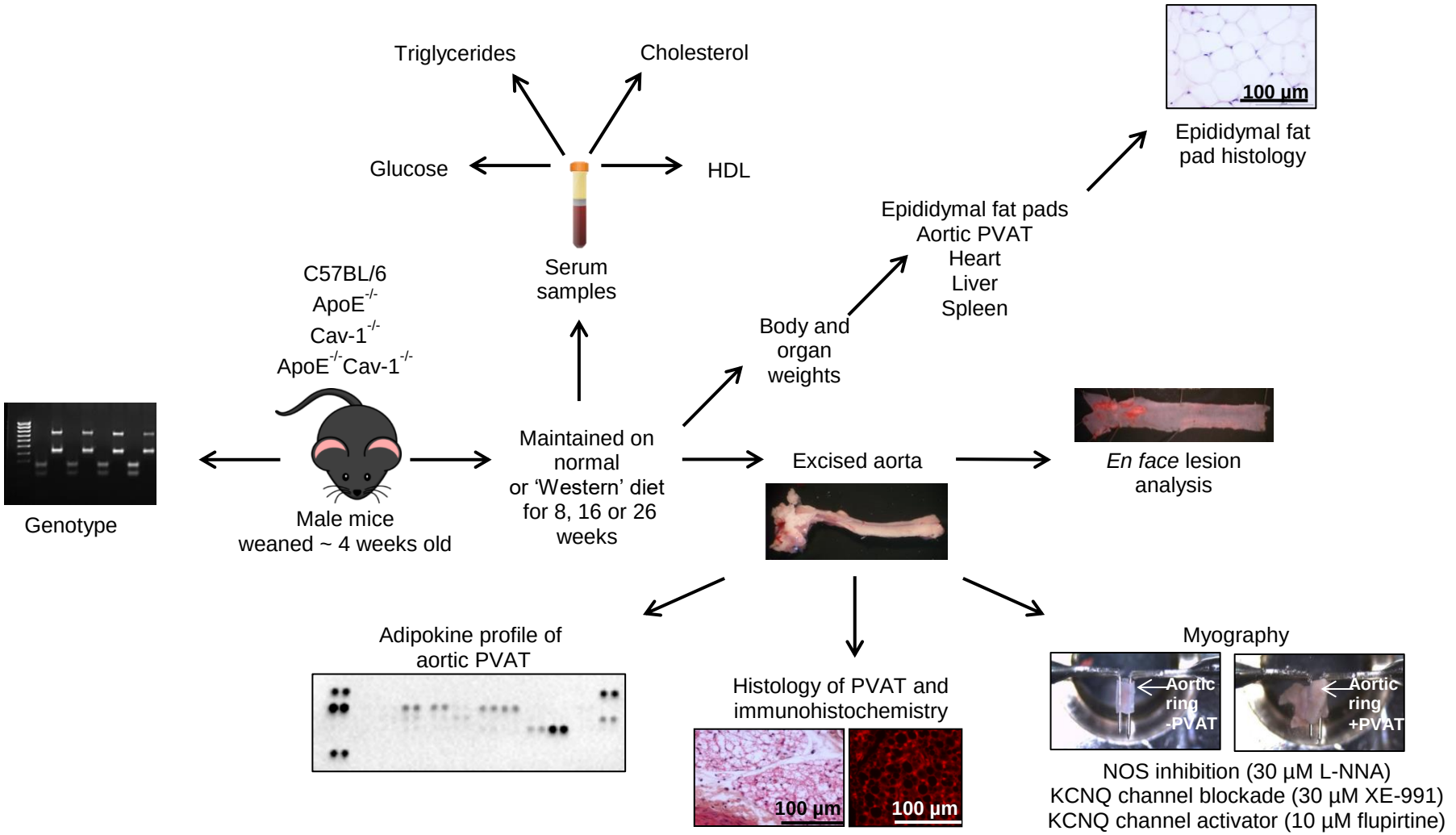

Figure 2.12 Summary of methods

~ Chapter Three ~

Characterisation of normal vascular ageing in C57BL/6 mice: vascular reactivity and morphology of aortic perivascular adipose tissue

Abstract

Background: With increasing age, the vasculature experiences an accumulation of structural, cellular and molecular changes, including changes to nitric oxide (NO) bioavailability. The continuous production of NO, an endogenous vasodilator, is essential for maintenance of vascular tone and is of significant importance within large arteries, such as the aorta, where endothelium-dependent vasorelaxation is primarily mediated through NO. Endothelial dysfunction is known to precede the development of diseases such as atherosclerosis. The influence of perivascular adipose tissue (PVAT) on vascular reactivity and the contribution of NO to the anti-contractile effect of PVAT with ageing has not been well characterised. Potentially, if age-induced changes in the PVAT are identified at an early stage they could be reversed and prevent PVAT dysfunction and subsequent development of cardiovascular disease (CVD).

Purpose: The following experiments were conducted in order to characterise ageing to pre-middle age in normal diet-fed C57BL/6 mice and to determine the influence of aortic PVAT on isolated arterial contractility and investigate the morphology/composition of aortic PVAT in ageing mice.

Methods: At 4 weeks of age, male C57BL/6 mice were fed a normal chow diet (normal diet, ND) for a period of 8, 16 or 26-weeks. Contractility studies were performed on isolated rings of thoracic aortae with or without PVAT. In addition, the contribution of NO to the anti-contractile effect of aortic PVAT was investigated using a nitric oxide synthase (NOS) inhibitor (L-NNA). Alterations in the aortic PVAT environment were examined using histology and immunostaining.

Results: PVAT exerted an anti-contractile effect on aortic rings derived from C57BL/6 mice fed a ND for 8 or 16-weeks (both $P < 0.0001$). However, the anti-contractile effect of aortic PVAT was abolished in the oldest mice, fed a ND for 26 weeks; PVAT dysfunction preceded any alterations to endothelial function. Inhibition of NOS with 50 μM L-NNA attenuated the anti-contractile capacity of PVAT in the 8 and 16-week ND-fed groups. NOS inhibition had no effect on PVAT-intact or PVAT-denuded aortic rings from the 26-week ND-fed mice, which may be indicative of a potential decrease in PVAT-derived NO. Ageing led to a series of alterations to the aortic PVAT composition including: increased weight of PVAT surrounding the aortae, white adipocyte hypertrophy, increased production of superoxide ($P < 0.05$ each) and an altered adipokine profile.

Conclusions: Ageing induces a series of structural and functional changes in the aortic PVAT of C57BL/6 mice. Alterations to the normal functioning of PVAT, as opposed to endothelial function, could potentially be used as an earlier indicator of CVD. These data reveal adipocyte hypertrophy, superoxide production and NOS, particularly eNOS, as potential targets for the treatment of age-associated PVAT dysfunction.

3.1 Introduction

Population ageing, is rapidly becoming a global issue. An ageing population is defined by both an increase in the median age and the proportion of older people within a population. Within the UK in 2015, around 17.8% of the population (11.6 million) were aged 65 years old and over, an increase of 21% compared to 2005 (Office for National Statistics 2015).

Ageing is an established risk factor for CVD. With increasing age, the vasculature experiences an accumulation of structural, cellular and molecular changes such as arterial stiffening and thickening and endothelial dysfunction all of which can contribute to the development of CVD such as atherosclerosis (North and Sinclair 2012). Endothelial dysfunction has been observed in man as early as the fourth decade (Celermajer et al. 1994; Seals et al. 2011). However, other changes within the artery may have preceded and even contributed to the damaged endothelium.

The production of NO, an endogenous vasodilator, is essential for maintenance of vascular tone and within large arteries, such as the aorta, relaxation is predominantly mediated through NO (Martin et al. 1986; Crauwels et al. 2000). In addition, the continuous production of NO promotes endothelial regeneration and offers protection against leukocyte adhesion and prevention of platelet aggregation. Crucially, diminished bioavailability of NO within the arteries may result in a shift towards the release of vasoconstrictor agents, increased inflammation and thrombosis, each of these pathologies is associated with CVDs (Versari et al. 2009).

A key role for NO in the exertion of the anti-contractile effect of PVAT on arteries has been identified. Furthermore, the recent discovery of eNOS expression, the primary generator of NO within the vasculature, provides more evidence in support of NO-mediating the anti-contractile PVAT effect. In states of metabolic disturbance, the anti-contractile effects of PVAT are attenuated (Szasz and Webb 2012). These effects have been attributed to changes within the PVAT including increased macrophage infiltration, altered adipokine expression, elevated superoxide production, adipocyte hypertrophy and a reduction in NO bioavailability (Gollasch and Dubrovska 2004b; Gao et al. 2005; Greenstein et al. 2009; Ketonen et al. 2010; Withers et al. 2011; Meyer et al. 2013).

Alterations to PVAT composition and function have been well characterised in conditions such as obesity. However, relatively little information exists surrounding the effect of ageing on the influence of aortic PVAT on vascular reactivity and the contribution of NO to this process (Sverdlov et al. 2014; Melrose et al. 2015). Furthermore, the effects of ageing on PVAT composition, such as adipocyte size, adipokine secretion, superoxide production and macrophage infiltration has not been assessed.

This study aimed to identify if any early age-associated changes occurred within the aortae of C57BL/6 mice, specifically within the PVAT. Alterations to aortic PVAT could potentially precede endothelial dysfunction and contribute to the development of CVD through increased aortic contractility.

Whilst ageing is inevitable and a risk factor for CVD, unmasking early age-related changes within large arteries in humans, prior to the development of overt CVD, and treatment of patients during this period may confer a therapeutic benefit. Modifying the speed at which the vasculature ages

or maintaining/restoring a healthy PVAT environment so that its anti-contractile effects are retained could potentially lower cardiovascular risk and incidence of CVD.

3.2 Aim and objectives

The specific aim of this chapter is to investigate whether NO mediates the anti-contractile effect of aortic PVAT in C57BL/6 mice and determine if ageing modulates this effect. The objectives of this chapter are as follows:

- Characterise ageing in C57BL/6 mice by examining lipid profiles, body and organ weights and determine if atherosclerosis develops within the aortae during these time-frames.
- Determine if endothelial-dependent relaxation is altered by ageing or the presence of PVAT in C57BL/6 mice using aortic preparations and the ex vivo technique of myography.
- Investigate if ageing modulates the anti-contractile effect of PVAT using cumulative dose responses to the vasoconstrictor, phenylephrine.
- Elucidate the contribution of NO to the anti-contractile effect of aortic PVAT using pharmacological inhibition of NOS.
- Characterise aortic PVAT from ageing C57BL/6 mice using histology, immunohistochemistry and adipokine arrays.

3.3 Methods

In order to study the vascular effects of normal ageing C57BL/6 mice was used in this study. Rough equivalencies to human ageing have previously been calculated (Flurkey et al. 2007). Three time-points were selected: young adult mice approximately 12 weeks old (maintained on a ND for 8 weeks) equated to early 20s in humans; mature adult mice approximately 20 weeks old (fed a ND for 16 weeks) which roughly approximates to late 20s to early 30s in humans and, a third group, ageing mice, around 30 weeks old (fed a ND for 26 weeks), equated to pre-middle age in humans. This time-frame was chosen because it would be therapeutically beneficial to treat patients at this age whilst the pathological changes associated with ageing are in the initial stages and can potentially be reversed.

At 4 weeks of age, male C57BL/6 mice were maintained on a ND for a period of 8, 16 or 26 weeks. Ageing was characterised by evaluating lipid and glucose profiles and by measuring body and organ weights. Endothelial function was assessed in each group. Contractility studies were performed on rings of thoracic aortae with or without PVAT to determine whether PVAT modulated vascular function and if this was maintained with increasing age of the mice. Additional functional studies to determine the contribution of NO to the anti-contractile effect of PVAT were performed in the presence or absence of the NOS inhibitor L-NNA (50 µM). The sensitivity of aortic rings to NO was assessed through application of an exogenous NO source, sodium nitroprusside to pre-constricted aortic rings. Alterations in the aortic PVAT environment were examined using histology, the superoxide indicator dihydroethidium to assess superoxide and immunostaining was performed to detect macrophage infiltration within the aortic PVAT of C57BL/6 mice. The adipokine secretome of 26-week ND-fed mice was assessed using an adipokine obesity array and compared to the 8-week ND-fed group. Methods are described in detail in Chapter 2.

3.4 Results

3.4.1 Characteristics of ageing on lipid, body and organ weights in C57BL/6 mice

Ageing did not induce any significant alterations in the examined lipidemic or glycaemic profiles of the C57BL/6 mice (Table 3.1).

Table 3.1 Lipidemic and glycaemic profiles were unaltered in ageing C57BL/6J mice

	8-weeks ND	16-weeks ND	26-weeks ND	P
Total cholesterol	2.87 ± 0.51	2.81 ± 0.29	3.06 ± 0.25	NS 0.91
HDL-cholesterol	1.60 ± 0.28	1.71 ± 0.17	2.02 ± 0.18	NS 0.46
Triglycerides	2.43 ± 0.38	1.74 ± 0.10	1.19 ± 0.63	NS 0.42
Glucose	20.55 ± 0.78	17.01 ± 3.51	20.22 ± 2.60	NS 0.53

Serum derived from blood obtained at time of sacrifice (mice were weaned at 4 weeks of age then maintained on a normal chow diet (ND) for the appropriate length of time, 8, 16 or 26 weeks). Data are expressed as mean ± S.E.M and measurements are shown in mmol/L. Statistical analysis was carried out by One-way ANOVA with Tukey's multiple comparison post-hoc tests, n=3-4 mice per group.

Heart weight, heart weight: body weight ratio, liver and spleen weights remained unchanged with increasing age (Table 3.2).

Table 3.2 Organ weights did not change with ageing in C57BL/6 mice

	8-weeks ND	16-weeks ND	26-weeks ND	P
Heart (mg)	160.6 ± 9.0	149.4 ± 6.0	168.2 ± 4.2	NS 0.20
HW: BW (mg/g)	5.5 ± 0.3	5.0 ± 0.1	4.8 ± 0.2	NS 0.07
Liver (g)	1.97 ± 0.06	1.89 ± 0.08	2.01 ± 0.06	NS 0.42
Spleen (mg)	102.5 ± 12.1	89.49 ± 7.5	79.8 ± 4.4	NS 0.24

Data are expressed as mean ± S.E.M. HW:BW = heart weight: body weight ratio. Statistical analysis was carried out by One-way ANOVA with Tukey's multiple comparison post-hoc tests, n=4-6 mice per group.

Ageing of C57BL/6 mice led to a significant gain in body weight in the oldest cohort, mice fed a ND for 26-weeks post weaning, when compared to the younger 8 and 16-week ND-fed mice (8-weeks ND versus 26-weeks ND: P = 0.002; 16-weeks ND versus 26-weeks ND: P = 0.005, n = 5-6 mice per group, Figure 3.1A). However, the body weights of the 8 and 16-week groups were similar (P = NS, n= 6 mice per group).

Weight gain was attributed to significant increases in abdominal fat deposition which was associated with an increase in epididymal fat pad weight after 26-weeks on a ND (8-weeks ND versus 26-weeks ND: P < 0.0001; 16-weeks ND versus 26-weeks ND: P = 0.003, n = 5-6 mice per group, Figure 3.1B) and adipocyte hypertrophy was observed with advancing age (8-weeks ND versus 26-weeks ND: P = 0.0012, n = 4 mice per group, 100 adipocytes per mouse, Figure 3.1C and D). Although epididymal fat pad weight did not differ significantly between the 8 and 16-week ND-fed groups (8-weeks ND versus 16-weeks ND: P = NS, n = 6 mice in each group), substantial adipocyte hypertrophy was apparent in the epididymal fat pads of the mice after 16 weeks on the ND (8-weeks ND versus 16-weeks ND: P = 0.002, n = 4 mice per group, 100 adipocytes measured per mouse, Figure 3.1C). This enlargement was sustained and no further

increases in adipocyte size were observed in the epididymal fat pads of 26-week ND-fed mice (16-weeks ND versus 26-weeks ND: P = NS, n = 4 mice per group, 100 adipocytes measured per mouse, Figure 3.1C).

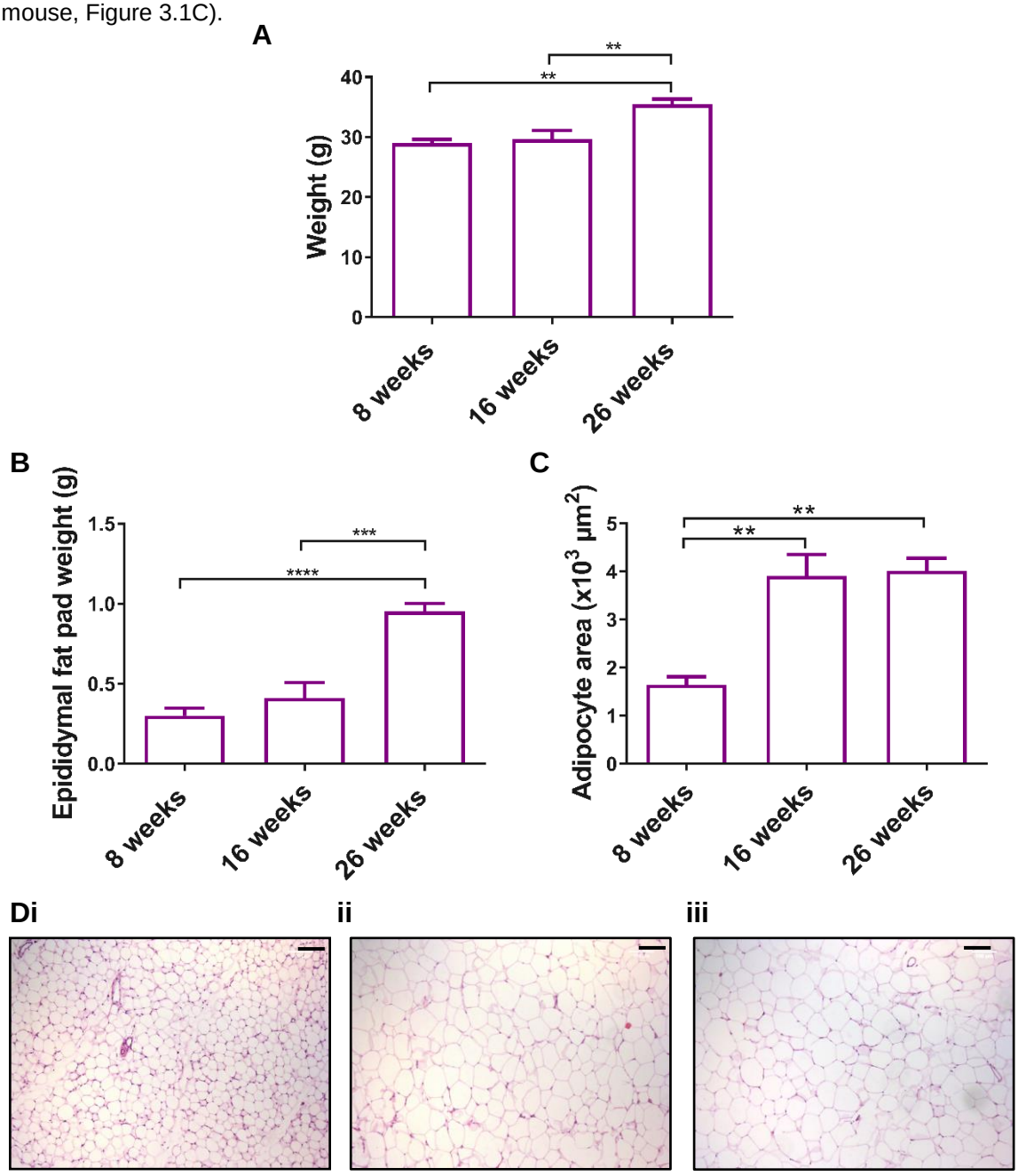

Figure 3.1 Ageing of C57BL6 mice causes an increase in body weight which is associated with increased abdominal fat deposition and adipocyte hypertrophy

*A) Body weight increased with ageing of C57BL/6 mice. B) Epididymal fat pad weight was significantly increased with increasing age C) Ageing led to significant adipocyte hypertrophy within the epididymal fat pads of the C57BL/6 mice. D) Epididymal fat pads from mice fed a ND for i) 8, ii) 16 and iii) 26 weeks post weaning were stained with haematoxylin and eosin to determine adipocyte area. Representative images obtained at 10x magnification and scale bars represent 100 µm. Data are presented as mean ± S.E.M, n = 5-6 mice per group for body and epididymal fat pad weight, ND =normal diet n = 4 mice per group, 100 adipocytes measured per mouse to calculate adipocyte area, ** P < 0.01, *** P < 0.001, **** P < 0.0001, one-way ANOVA with Tukey's post hoc tests.*

3.4.2 Atherosclerotic lesions do not develop within the aortae of C57BL/6 mice

C57BL/6 mice were fed a ND diet for 26 weeks post weaning (n = 3) and en face Oil Red O staining was performed; it was determined that atherosclerotic lesions did not develop within the aortae of this mouse strain during this time frame on a ND (Figure 3.2).

Figure 3.2 En face Oil Red O-stained aortic preparations of 26 week normal diet-fed C57BL/6 mice

Lipid lesions were not detected along the luminal surface of the aortae of the C57BL/6 mice. Representative image. Scale bar represents 1 mm.

3.4.3 The presence of PVAT does not alter aortic contractile responses to a depolarising stimulus in C57BL/6

The constriction responses of PVAT-denuded and PVAT-intact aortic rings to 100 mM KPSS, a depolarising stimulus, was similar in each age group (P = NS; n = 5-8 mice per group Figure 3.3).

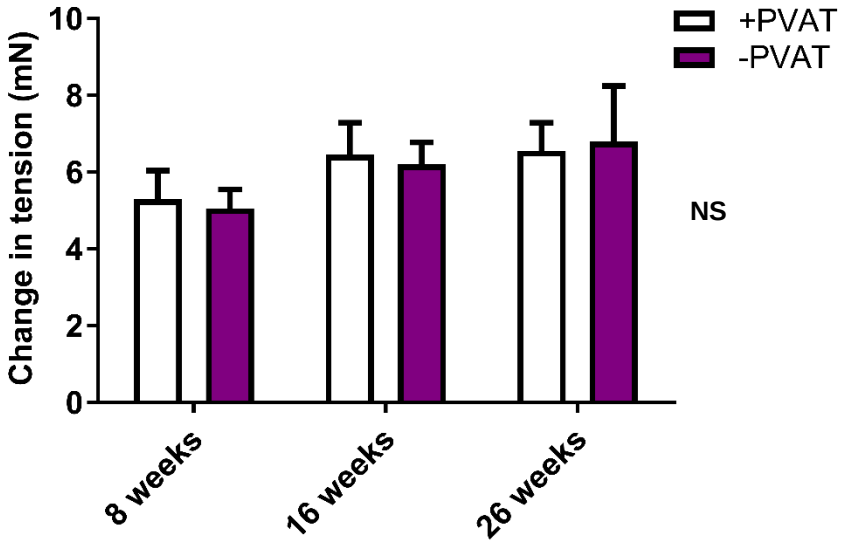

Figure 3.3 Ageing and the presence of PVAT has no effect on the contractile responses of aortic rings to KPSS

A, Contractions to 100 mM KPSS were similar in PVAT-denuded and PVAT-intact aortic rings in each age group of C57BL/6 mice. Data are presented as mean ± S.E.M, n = 5-8 mice per group, two-way ANOVA with post hoc Bonferroni's multiple comparisons test.

3.4.4 The anti-contractile effect of aortic PVAT is attenuated with ageing in C57BL/6 mice and this precedes endothelial dysfunction

The presence of PVAT had no significant effect on the vasodilatory responses of aortic rings to 10 µM acetylcholine, an endothelium-dependent relaxant (P = NS; n = 5-8 mice per group, Figure 3.4SA); endothelial function was maintained in mice fed a ND for 26 weeks post weaning (P = NS; n = 5-8 mice per group Figure 3.4A).

The presence of PVAT on aortic rings, significantly decreased vasoconstrictor responses to the α1-adrenoreceptor agonist phenylephrine in the 8-week (+PVAT versus -PVAT: P < 0.0001; n = 6 mice per group, Figure 3.4B) and 16-week ND-fed C57BL/6 mice (+PVAT versus -PVAT: P < 0.0001; n = 6 mice per group, Figure 3.4C). The anti-contractile effect of PVAT was abolished in the oldest, 26-week ND-fed, C57BL/6 group (+PVAT versus -PVAT: P = NS, n = 8 mice per group, Figure 3.4D).

The contractility of PVAT-denuded aortic rings was unchanged with increasing age (Figure 3.4E). However, in the presence of PVAT, the constriction of aortic rings from mice fed a ND for 26 weeks were significantly augmented (8-weeks ND versus 26-weeks ND: P < 0.0001; 16-weeks ND versus 26-weeks ND: P < 0.0001, n = 6-8 mice per time-point, Figure 3.4F). Additionally, the anti-contractile effect of PVAT was endothelium-independent in 8-week ND-fed C57BL/6 mice (Appendix 2.1).

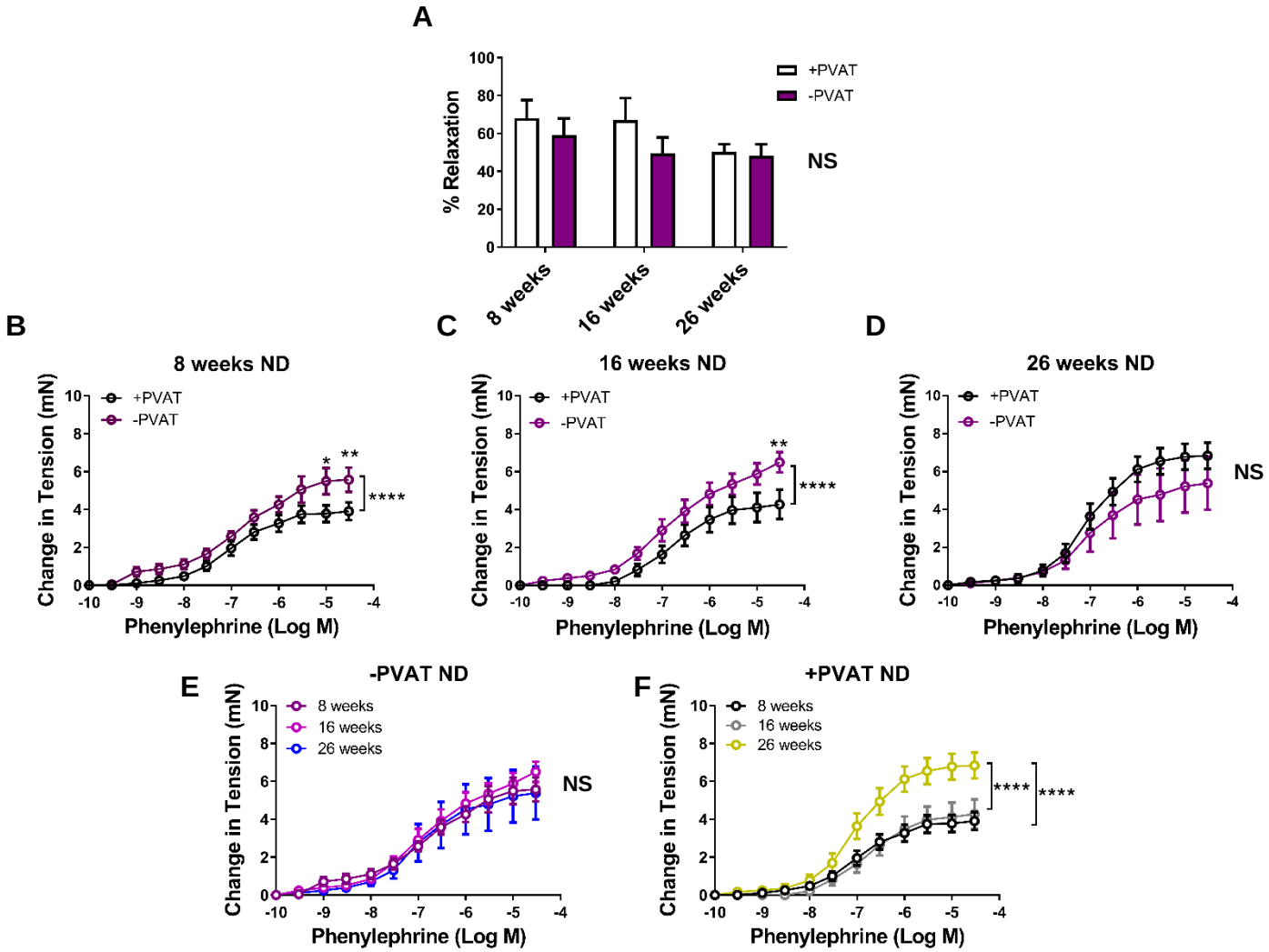

Figure 3.4 Endothelial function is maintained whilst PVAT dysfunction occurs after 26 weeks on a ND in C57BL/6 mice

*A) Phenylephrine pre-constricted aortic rings did not relax significantly differently, to 10 µM acetylcholine, with ageing. B) PVAT reduced constriction to phenylephrine in aortic rings from mice fed a ND for B) 8, and C) 16-weeks post weaning. D) PVAT dysfunction was observed in mice fed a ND for 26 weeks post weaning. E) Contractility of PVAT-denuded aortic rings did not change with increasing age. F) Contraction of PVAT-intact rings was significantly increased in the oldest group of mice. Data are expressed as mean ± S.E.M., ND = normal diet, n = 6-8 mice per group, * P <0.05, ** P < 0.01, **** P < 0.0001, two-way ANOVA with Bonferroni's post hoc tests.*

3.4.5 PVAT-derived nitric oxide mediates the anti-contractile effect in C57BL/6 mice fed a ND up to 16 weeks

Incubation with the NOS inhibitor, L-NNA (50 μM) attenuated the anti-contractile effect of PVAT in both the 8-week (+PVAT + L-NNA versus -PVAT + L-NNA: P = NS; n = 5-6 mice per group, Figure 3.5A) and 16-week ND-fed C57BL/6 mice (+PVAT + L-NNA versus -PVAT + L-NNA: P = NS; n = 5 mice per group, Figure 3.5B). Furthermore, NOS inhibition had no effect on aortic rings from the oldest mice, fed a ND for 26 weeks post weaning (+PVAT + L-NNA versus –PVAT + L-NNA: P = NS; n = 8 mice, Figure 3.5C) in which the anti-contractile effect of PVAT had already been lost.

NOS inhibition did not significantly alter the contractions of PVAT-denuded aortic rings at any of the experimental time-points (-PVAT versus -PVAT +L-NNA: P = NS for each time group, n = 5-6 mice per group, Figure 3.5A- C). Nevertheless, the contraction of PVAT-intact aortic rings was significantly augmented by the presence of L-NNA in the 8 and 16-week ND-fed groups (+PVAT versus +PVAT +L-NNA: 8-weeks ND P = 0.005; 16-weeks ND P < 0.0001, n = 5-6 mice per group, Figure 3.5A and B) but no effect was observed in the 26-week ND-fed mice (+PVAT versus +PVAT +L-NNA: P = NS, n = 8 mice per group, Figure 3.5C).

These data suggest that PVAT-derived NO contributes to the anti-contractile effect of PVAT in the younger, 8 and 16-week ND-fed C57BL/6 mice. NOS inhibition with L-NNA did not alter the contraction of aortic rings, in the presence or absence of PVAT, of 26-week ND-fed mice, which in combination with the lack of an anti-contractile effect of aortic PVAT, suggests a reduction in PVAT-derived NO.

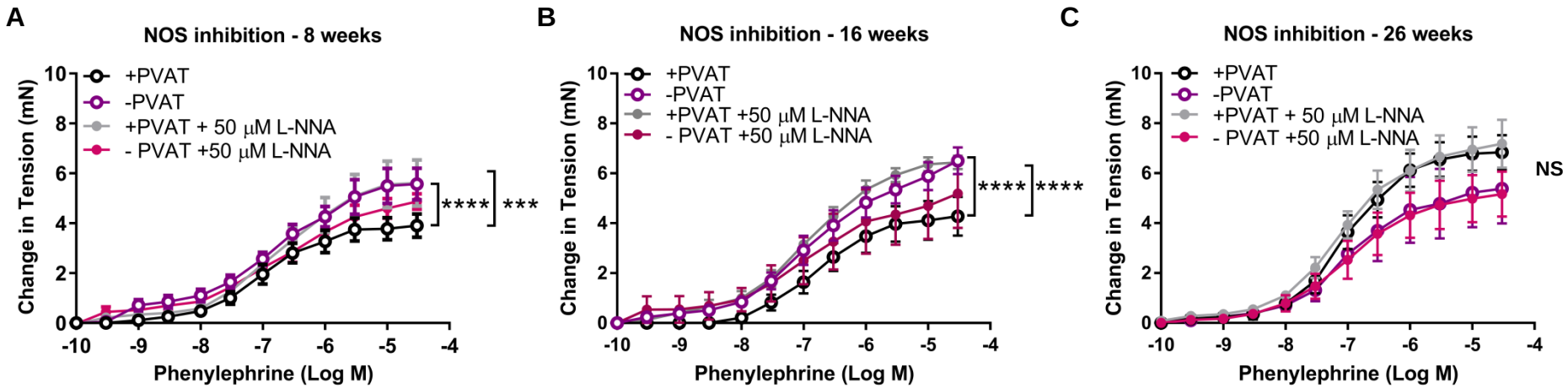

Figure 3.5 Nitric oxide synthase (NOS) inhibition attenuates the anti-contractile effect of aortic PVAT in C57BL/6 mice.

*NOS inhibition with LNNA (50 μM) abolished the anti-contractile effect of PVAT and increased vasoconstrictor responses to phenylephrine in aortic rings with PVAT in C57BL/6 mice fed a ND for A) 8 or B) 16weeks post weaning. C) NOS inhibition had no effect on aortic rings from mice fed a ND for 26 weeks. Data are expressed as mean ± S.E.M., ND = normal diet, n = 5-6 mice per group, *** P < 0.001, **** P < 0.0001, two-way ANOVA with Bonferroni's post hoc test.*

3.4.6 Nitric oxide is the main contributor to acetylcholine-induced vasodilation in the aorta of C57BL/6 mice

Incubation with L-NNA produced a significant decline in the capacity of PVAT-intact aortic rings to relax in the 8-week ND-fed group (+PVAT control: 54.84 ± 5.41% versus L-NNA: 10.69 ± 8.51%, P = 0.0099, n = 5 mice per group, Figure 3.6A) whilst a decline in relaxation was observed in PVAT-denuded aortic rings this was not statistcally significant when compared to relaxations in the absence of L-NNA (-PVAT control: 45.27 ± 6.0% versus L-NNA: 12.50 ± 11.64%, P = 0.076; n = 5 mice per group, Figure 3.6A). Similar findings were observed in mice fed a ND for 16 weeks, with a significant reduction in the vasodilation of L-NNA-incubated PVAT-intact aortic rings (+PVAT control: 48.86 ± 8.86% versus L-NNA: 0.22 ± 0.19%, P = 0.003 and -PVAT control: 45.29 ± 9.77% versus L-NNA: 18.13 ± 7.25%, P = NS; n = 5-6 mice per group, Figure 3.6B).

A signiifcant reduction in relaxation was observed in both PVAT-intact and PVAT-denuded aortic rings after NOS inhibition, in the 26-week ND-fed C57BL/6 mice (+PVAT control: 49.87 ± 8.54% versus L-NNA: 1.16 ± 0.47%, P = 0.0001 and -PVAT control: 68.63 ± 10.06% versus L-NNA: 4.83 ± 3.06%, P < 0.0001; n = 8 mice per group, Figure 3.6C).

Taken together, these data suggest that PVAT does not influence acetylcholine-induced relaxation and NO is the main contributor to acetylcholine-induced vasodilation in the aorta of C57BL/6 mice.

3.4.7 The sensitivity of aortic smooth muscle, to nitric oxide was unchanged with increasing age in C57BL/6 mice

Ageing and the presence of PVAT did not elicit any changes in relaxation in phenylephrine-constricted aortic rings upon exposure to 10 μM sodium nitroprusside, an endothelium-independent vasodilator (P = NS all group comparisons, n = 5-8 mice per group Figure 3.7).

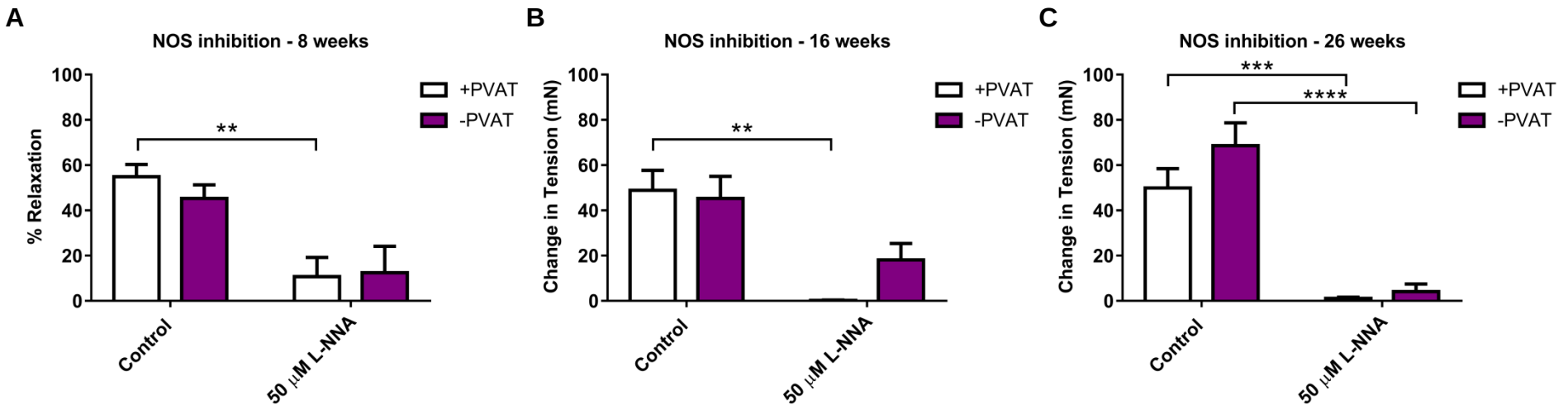

Figure 3.6 Nitric oxide mediates the vasodilatory response to acetylcholine in the aorta of C57BL/6 mice

*NOS inhibition, with 50 μM L-NNA, reduced the vasodilatory responses of phenylephrine-contracted aortic rings to acetylcholine (10 μM) at the A) 8-week, B) 16-week and C) 26-week time-points. Data are expressed as mean ± S.E.M., n = 5-8 mice per group, ** P < 0.01, *** P < 0.001, **** P < 0.0001, two-way ANOVA with Bonferroni's post hoc test.*

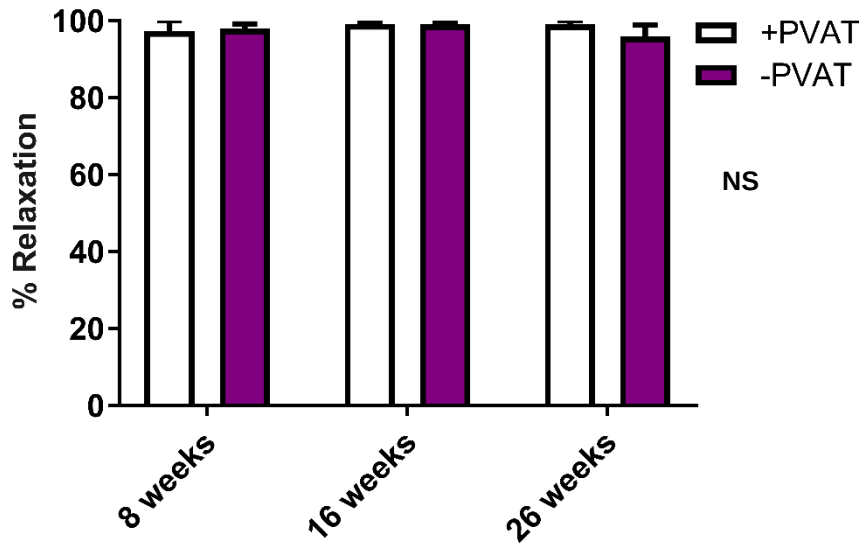

Figure 3.7 Increasing age and the presence of PVAT has no effect on endothelial-independent relaxation *Endothelium-independent relaxation of phenylephrine-constricted aortic rings to 10 μM sodium nitroprusside was unaltered by the presence of PVAT or increasing age in C57BL/6 mice. Data are presented as mean ± S.E.M, n = 5-8 mice per group, two-way ANOVA with post hoc Bonferroni's multiple comparisons tests.*

3.4.8 The weight of PVAT encasing the aorta of C57BL/6 mice increases with ageing in C57BL/6 mice in conjunction with white adipocyte hypertrophy

The effect of ageing on PVAT composition was assessed in the C57BL/6 mice in each group. The weight of PVAT surrounding the aortic arch and thoracic aortae was similar in the 8 and 16-week ND-fed mice (P = NS, n = 4 mice per group, Figure 3.8A). However, an increase in the weight of aortic PVAT was observed in the oldest mice fed a ND for 26 weeks post weaning (8-weeks ND versus 26-weeks ND: P =0.02; 16-weeks ND versus 26-weeks ND: P = 0.04; n = 4-6 mice per group, Figure 3.8A).

Aortic PVAT is a heterogeneous mixture of cell-types, the most predominant of which are brown adipocytes. However, a small population of white adipocytes is present within the aortic PVAT. The composition of aortic PVAT was altered with increasing age and changes to the white adipocyte population within the PVAT were observed. The proportion of aortic PVAT occupied by white adipocytes did not differ significantly between the different age groups (P = NS = 3-4 mice per group, Figure 3.8B and D). Nevertheless, the mean white adipocyte size within the aortic PVAT was significantly increased in the 26-week group (post weaning) compared to the 8-week ND-fed mice (8-weeks ND versus 26-weeks ND P < 0.05; n = 3-4 mice per group, Figure 3.8C and D).

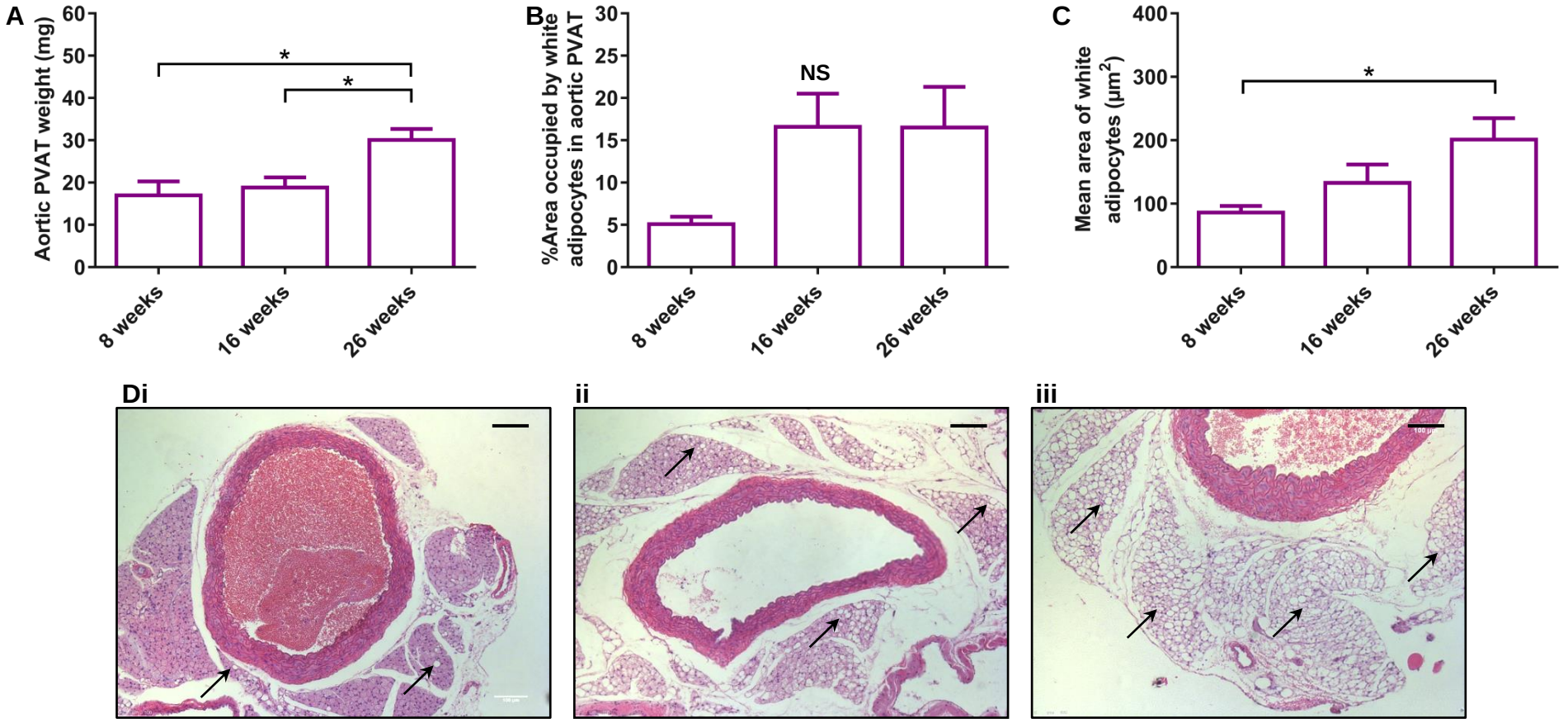

Figure 3.8 The weight of PVAT encasing the aorta increases with ageing in C57BL/6 mice and this corresponds to white adipocyte hypertrophy

*A) PVAT surrounding the aortic arch and thoracic aorta was carefully removed and weighed. A greater amount of PVAT surrounded the aortae of 26-week ND-fed mice compared to the 8 and 16-week ND groups. B) The percentage area of PVAT occupied by white adipocytes did not significantly increase between the different time-points. C) The mean size of aortic white adipocytes was significantly increased in the 26-week ND-fed group compared to the 8-week ND-fed mice. D) Thoracic aortae with intact PVAT from i) 8-week, ii) 16-week and iii) 26-week ND-fed C57BL/6 mice were stained with haematoxylin and eosin to assess PVAT composition and white adipocyte area. Representative images obtained at 10X magnification. Scale bars represent 100 μm with examples of white adipocytes highlighted by arrows. ND = normal diet. PVAT = perivascular adipose tissue. Data are expressed as mean ± S.E.M., * $P < 0.05$, n = 3-6 mice per group, one-way ANOVA with Tukey post hoc multiple comparisons test.*

3.4.9 Superoxide production within aortic PVAT is significantly greater in ageing C57BL/6 mice

Dihydroethidium fluorescent staining (DHE^+) within aortic PVAT was used as an indicator of the presence of superoxide. In the presence of the superoxide anion, DHE is oxidised to 2-hydroxyethidium and emits red fluorescence. DHE^+ nuclei were detected in the aortic PVAT of all age groups but not in the negative DMSO control (Figure 3.9Ai-iv). The amount of DHE^+ staining was significantly elevated between the 16 and-26-week ND-fed groups ($P < 0.05$, n =3 and 4 mice, Figure 3.9B). However, no other differences in DHE^+ staining were observed between the groups (P = NS, n = 3-4 mice, respectively, Figure 3.9B).

Increased superoxide within the aortic PVAT of 26-week ND-fed C57BL/6 mice was associated morphologically with white adipocyte hypertrophy and functionally, the exertion of a pro-contractile effect on aortic rings.

3.4.10 The infiltration of Mac-3^+ macrophages within the aortic PVAT is not altered with ageing

Immunostaining for Mac-3^+ cells was used to detect the number of macrophages infiltrating the aortic PVAT in each group (Figure 3.10Aiii-v). Macrophage infiltration occurred in the PVAT of each experimental group although no statistical differences were found with ageing (8-weeks ND versus 16-weeks ND: $P > 0.99$; 16-weeks ND versus 26-weeks ND: $P = 0.23$; 8-weeks ND versus 26-weeks ND $P = 0.49$; n = 3 mice per group, Figure 3.10B).

Taken together, these data suggest that the increased ROS production within the aortic PVAT was not due to an increase in Mac-3^+ cell infiltration.

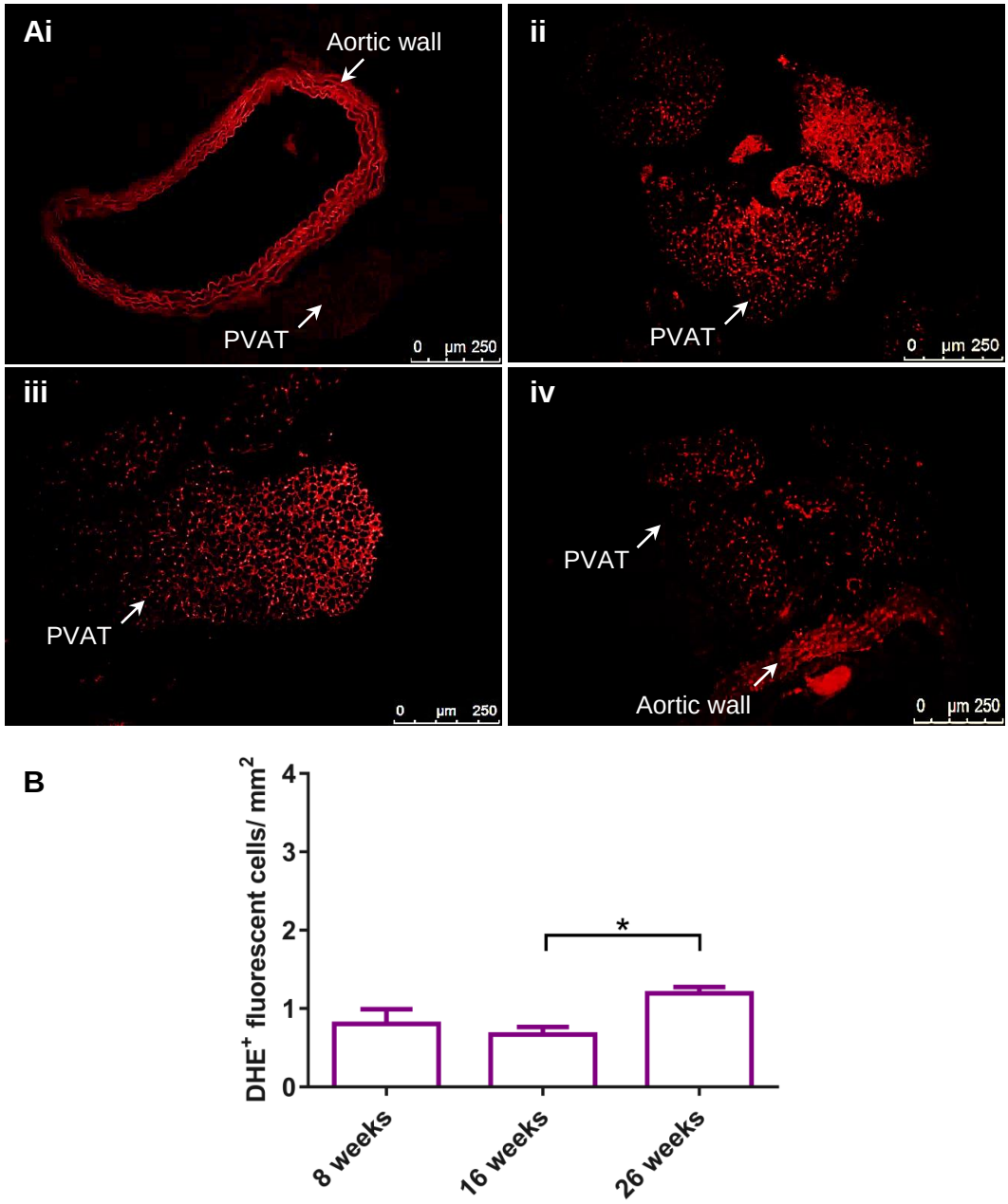

Figure 3.9 The number of dihydroethidium$^+$ cells is increased in the aortic PVAT of ageing C57BL/6 mice

*Sections of PVAT and thoracic aortae were stained with dihydroethidium (DHE) to detect the presence of superoxide Punctate red fluorescence indicates DHE$^+$ cell nuclei and the presence of superoxide. Ai) Autofluorescence was evaluated using a DMSO negative control, elastin fibres within the medial layer of the thoracic aortae emitted fluorescence although PVAT did not exhibit autofluorescence. DHE$^+$ nuclei were observed in all groups with the exception of the negative control: ii) 8-week, ii), 16-week and iv) 26-week ND-fed mice. Representative images obtained at 10 X magnification. Scale bars represent 250 µm. B) DHE$^+$ nuclei were detected within the PVAT of all examined samples. However, higher levels of ROS were found in the PVAT of 26-week time-point mice. Red fluorescent nuclei were counted within 5 fields of view per section per animal. Data are expressed as mean ± S.E.M., DHE = dihydroethidium, ND = normal diet, PVAT = perivascular adipose tissue, DHE$^+$ nuclei presented as cells/mm^2 of PVAT, * $P < 0.05$, n = 3-4 mice per group, one-way ANOVA with Tukey post hoc multiple comparisons test.*

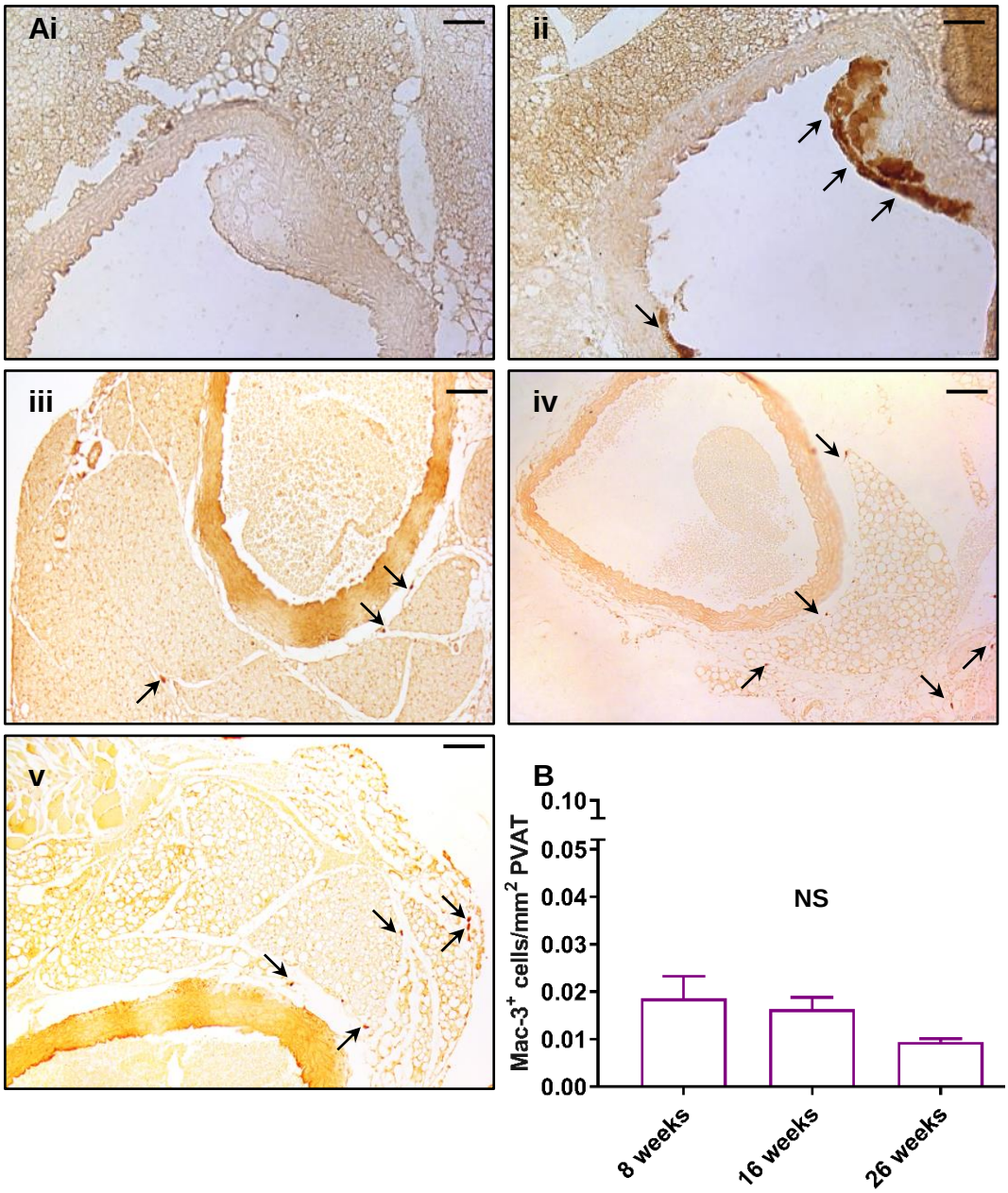

Figure 3.10 Macrophage infiltration occurs within the aortic PVAT of each age-group of C57BL/6 mice

Immunohistochemistry was performed using a marker for macrophages (Mac-3) A) Sections of thoracic aortae with intact PVAT. Tissue from atherosclerotic ApoE$^{-/-}$ mice were used for controls i) IgG negative control, no brown staining within atherosclerotic plaque and ii) Mac-3^{+} positive control, intense brown stain localised within the atherosclerotic plaque indicated by arrows. Aortic sections from C57BL/6 mice fed a ND for iii) 8, iv) 16 and v) 26-weeks. Representative images obtained at 10X magnification. Scale bars represent 100 µm and examples of Mac-3^{+} staining are highlighted by arrows. B) Mac-3^{+} cells were detected within the PVAT of all examined samples. No differences in macrophage infiltration were found between any of the groups. Total PVAT area was measured and all macrophages within the PVAT were counted. ND = normal diet, PVAT = perivascular adipose tissue Data are expressed as Mac-3^{+} cells/mm^{2} PVAT, mean ± S.E.M., n = 3 mice per group, one-way ANOVA with Tukey post hoc multiple comparisons test.

3.4.11 The adipokine profile of C57BL/6 mice is altered with ageing

The adipokine profile of aortic PVAT from 26-week ND-fed C57BL/6 mice was altered in comparison to the 8-week group (Figure 3.11). Of the 38 adipokines tested in the assay, 10 were detected. Lipocalin-2, fibroblast growth factor acidic (FGF acidic), Dipeptidyl Peptidase IV (DPPIV), C-reactive protein (CRP) were found to be more prevalent in the aortic PVAT secretome of ageing 26-week time-point mice (Figure 3.11). Whilst the measured levels of resistin, receptor for advanced glycation end-products (RAGE), Pentraxin-2, insulin-like growth factor binding protein-6 (IGFBP-6), fetuin A and adiponectin were decreased (Figure 3.11).

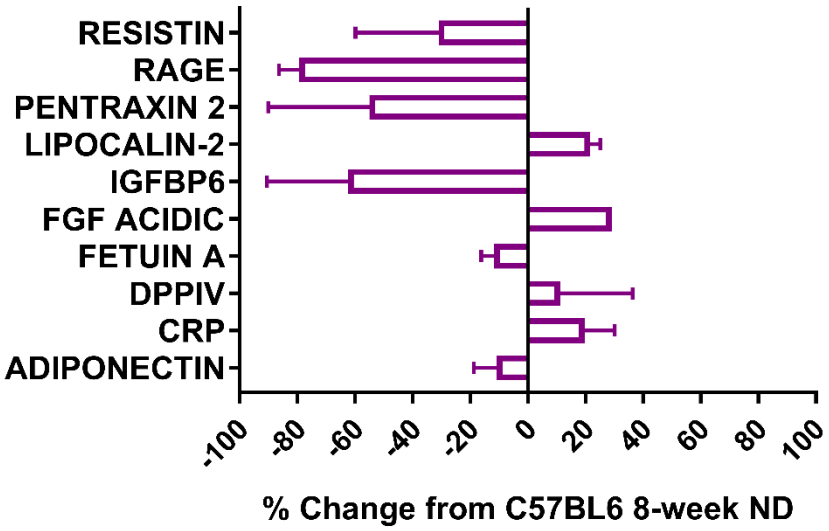

Figure 3.11 The adipokine secretome of 26-week normal diet-fed mice C57BL/6 mice is altered in comparison to the 8-week group.

Aortic PVAT was collected along the aortae from the arch to thoracic aortae at the diaphragm from 3 x 8-week ND and 3 x 26-week ND-fed mice, and stimulated with phenylephrine (3 x 10^{-5} mol/L) in PSS at 37 °C for 45 minutes. The secretomes of age-matched groups were pooled prior to analysis. Experiments were performed in duplicate. Data is expressed as percentage change from 8-week ND-fed mice. ND = normal diet, PVAT = perivascular adipose tissue.

3.5 Discussion

Ageing is an unavoidable cardiovascular risk factor which leads to progressive structural and functional changes in the cardiovascular system (Lakatta 2002). The study of vascular ageing in rodent models has produced results suggesting that certain age-associated phenotypes can be ameliorated (Pacher et al. 2004; Pearson et al. 2008; Sindler et al. 2009; Sindler et al. 2011; Wang et al. 2011; Rammos et al. 2014). Nevertheless, vascular ageing is a complicated process and in humans, additional confounding risk factors and the development of CVD, such as atherosclerosis, make elucidating the direct effects of ageing on the vasculature a difficult undertaking. The C57BL/6 mouse is therefore an intriguing model of healthy vascular ageing because although C57BL/6 have been identified as genetically susceptible to atherosclerosis, the formation of lesions only become apparent following feeding of a high fat high cholesterol diet. Therefore, the effects of vascular ageing to pre-middle age in C57BL/6 mice allows for isolated

age-related changed to be identified without the effects of dyslipidaemia or the development of atherosclerosis (Paigen et al. 1990; Whitman 2004).

The present study aimed to characterise normal vascular ageing, to pre-middle age, in C57BL/6 mice; specifically, the effect of increasing age on endothelial function and the morphology and anti-contractile properties of aortic PVAT was investigated.

The principal findings of this chapter were:

- Endothelial function was maintained in C57BL/6 mice aged to pre-middle age, whilst the anti-contractile effects of aortic PVAT were attenuated in the 26-week ND-fed C57BL/6 mice.
- NOS inhibition revealed that nitric oxide NO mediated the anti-contractile effect of PVAT in the 8 and 16-week ND-fed groups however, NOS inhibition had no effect in the 26-week ND group, which may be indicative of a decrease in PVAT-derived NO.
- The morphology of aortic PVAT was altered with increasing age; an increase in the weight of PVAT surrounding the aortae in combination with white adipocyte hypertrophy, increased superoxide production and an altered adipokine profile may have contributed to the loss of the anti-contractile effect of PVAT in the 26-week ND cohort.

3.5.1 Selection of the age-range and use of C57BL/6 mice in this study

Mouse models are useful for the study of ageing and provide invaluable information relating to the genetics of ageing as a result of their reduced lifespan and high similarities between the genomes of mice and humans, with mice sharing approximately 99% of their genes with humans (Boguski ; Yuan et al. 2011). The genetic manipulation of mice allows for the impact of certain genes on longevity and age-associated diseases to be studied with relative ease (Paigen 1995; Peters et al. 2007; Yuan et al. 2011).

The median lifespan of a male C57BL/6 mouse is approximately 30 months (Yuan et al. 2011) equating to a geriatric human of approximately 80 years of age (Flurkey et al. 2007). Whilst some cardiac changes have been recorded in C57BL/6 mice, the most prevalent cause or contributors to death in ageing C57BL/6 mice are hematopoietic neoplasms and lymphoma. Furthermore, it has been demonstrated that between the ages of 12 and 18-months of age, C57BL/6 mice are likely to develop tumours and other age-related pathologies (Frith et al. 1983; Blackwell et al. 1995; Lipman et al. 1998; Treuting et al. 2008; Sundberg et al. 2011; Brayton et al. 2012). These data demonstrate that in the ages chosen for this study, the C57BL/6 mice should have been healthy and not display overt signs of disease.

The vast proportion of ageing studies conducted in C57BL/6 mice utilise ‘young mice’ of 2-4 months of age and ‘old’ mice exceeding 12 months of age. However, mice between the ages of 3-6 months should be considered mature adults because by this period of time they are sexually mature, are past the developmental stage but are not yet subject to cellular senescence (Flurkey et al. 2007). Age-associated pathologies have been documented in C57BL/6 mice by 12 months of age; these include key hallmarks of vascular ageing such as remodelling of the vascular wall, hypertension, arterial stiffness, up-regulation of the renin-angiotensin system and endothelial

dysfunction (Moon et al. 2001; Stampfli et al. 2010; Song et al. 2012; Georgeon-Chartier et al. 2013; Rammos et al. 2014). In addition, signs of non-vascular ageing such as a decline in spatial learning and memory and decreased motor function have been observed as early as 8 months of age in the C57BL/6 strain (Holguin et al. 1985; Bach et al. 1999; Gasparrini et al. 2009; Steegenga et al. 2012; Shoji et al. 2016). Therefore, post weaning, C57BL/6 mice were fed a ND for 8, 16 or 26-weeks, in order to reflect normal vascular ageing, ensuring that the mice were healthy and did not display overt physiological decline or tumour development (Flurkey et al. 2007).

Furthermore, the oldest group of mice used in this study was of interest because they equate to 'pre-middle age' in humans which is when therapeutic intervention to prevent the progression of CVD could potentially be most effective (Pletcher et al. 2010; Pletcher et al. 2016).

3.5.2 Characterisation of normal ageing, to pre-middle age, in C57BL/6 mice

In this study, the ageing C57BL/6 mice did not display any changes to their lipidemic or glycaemic serum profiles. This is in agreement with previous studies which demonstrate that measurements of total cholesterol, HDL, triglycerides and glucose, remain unchanged in old (18-months old and above) C57BL/6 mice suggesting that when fed a normal rodent diet, C57BL/6 mice do not develop lipid or glycaemic disorders linked to vascular disease (Leiter et al. 1988; Hemmeryckx et al. 2010; Stampfli et al. 2010; Nunes-Souza et al. 2016). Furthermore, in line with these findings, atherosclerotic lesions were not found within the aortae of C57BL/6 mice after 26 weeks on a ND post weaning (Whitman 2004; Stampfli et al. 2010; Rammos et al. 2014).

Although the mice at each of the time-points selected for this study were considered to be fully mature adults, an age-associated increase in body weight was observed. This was attributed to normal growth of the animals and linked to an increase in abdominal fat deposition, evidenced by the increase in size of epididymal fat pads, these findings were similar to other ageing studies in C57BL/6 mice (Gros et al. 2002; Hemmeryckx et al. 2010; Bailey-Downs et al. 2013). Moreover, post 6-months of age, a plateau in body weight of ND-fed mice is generally observed with ageing, indicating that ND-fed C57BL/6 mice do not become overtly obese (Rammos et al. 2014; Nunes-Souza et al. 2016). Further evidence of the healthy state of C57BL/6 mice up to pre-middle age is indicated by the lack of changes to heart weight and the heart weight: body weight ratio, demonstrating that the C57BL/6 did not develop cardiac hypertrophy. Additionally, no alterations in liver or spleen weights were observed which suggests that neither non-alcoholic fatty liver disease or increased inflammation were present in the mice during this time-frame. Conversely, studies of mice between 12 months of age and beyond demonstrate an increase in organ weights, including the heart, liver and spleen, with ageing in both male and female C57BL/6 mice (Rowlatt et al. 1976; Lessard-Beaudoin et al. 2015).

3.5.3 Contractile responses to elevated external potassium are unaffected by PVAT or increasing age

A high concentration potassium solution (KPSS) elicits contraction through the depolarisation of VSM and activation of Ca^{2+} influx via L-type Ca^{2+} channels (Van Hove et al. 2009). Consistent with studies of aortic rings from healthy and obese mice and small arteries of humans, the presence of PVAT did not alter the contraction evoked by stimulation with KPSS (Greenstein et al. 2009; Ketonen et al. 2010; Xu et al. 2012; Meyer et al. 2013). In addition, ageing to pre-middle

age in ND-fed C57BL/6 mice did not induce any alterations in depolarisation responses. However, studies conducted in very old rodents have demonstrated a decline in reactivity to KPSS and whilst the definitive cause for an attenuated response is unclear it is likely because of a reduction in functional SM due to changes to the contractile apparatus (Giordano et al. 2002; Blough et al. 2007; Wheeler et al. 2015). These mechanical findings are congruent with previous observations of increased vascular stiffening with ageing in humans. The contractile responses of the C57BL/6 mice to KPSS in this study indicate that after 26-weeks on a ND, age-associated SM pathologies have not yet occurred.

3.5.3 Endothelial function is maintained in ageing C57BL/6 mice

In accordance with other studies, the relaxation responses of phenylephrine pre-constricted aortic rings from C57BL/6 mice were similar in PVAT-intact or PVAT-denuded conditions (Ketonen et al. 2010). Conversely, although not examined in this study, PVAT has been shown to enhance vasodilation in high potassium pre-constricted aortic rings upon exposure to acetylcholine. Taken together these data suggest that the relaxing capacity of PVAT is modulated by the mechanism of pre-contraction; in these examples α1-adrenorecptor activation or L-type Ca^{2+} channel-mediated, respectively, underlying the complex nature of PVAT (Van Hove et al. 2009; Ketonen et al. 2010).

A hallmark of vascular ageing is the onset of endothelial dysfunction, characterised by an attenuated vasodilatory response to acetylcholine and a decrease in NO bioavailability (Cannon 1998; Donato et al. 2009; Versari et al. 2009; Stampfli et al. 2010). Endothelial dysfunction in a risk factor for CVD and is associated with numerous pathologies including atherosclerosis (Flammer et al. 2010; Seals et al. 2011). NO bioavailability is crucial for the maintenance of a healthy endothelium; the importance of NO in the aorta was demonstrated in this study when the contribution of NO to acetylcholine-induced vasodilation was assessed. Inhibition of NOS with L-NNA dramatically reduced relaxation responses to acetylcholine providing strong evidence that the predominant mechanism of endothelium-dependent dilation in the aorta of the C57BL/6 mouse is mediated via NO. These findings are supported by other studies reporting a high basal production of NO within the aortae and large arteries (Martin et al. 1986; Crauwels et al. 2000).

Endothelial dysfunction did not occur as an effect of ageing in this study, which suggests that the integrity and health of the endothelium is preserved up-to pre-middle age, 26-weeks ND, in C57BL/6 mice. These findings are in contrast with other ageing studies of both large and small arteries which document a decline in endothelial function, as early as the fourth decade in humans and in old rodents, in the absence of clinical CVD and major risk factors for CVD (Celermajer et al. 1994; Taddei et al. 1995; Gerhard et al. 1996; Lyons et al. 1997; Blackwell et al. 2004; Stampfli et al. 2010; Seals et al. 2011). However, these studies involved much older subjects and if the time-points used in this study were advanced it is presumed that endothelial function would diminish with increasing age.

3.5.4 Aortic PVAT attenuates vasoconstriction in young adult C57BL/6 mice but ageing eradicates the PVAT anti-contractile capacity

It is now widely acknowledged that PVAT plays an essential role in modulating vascular tone and homeostasis and its role in the pathogenesis of disease should be considered as significant as

that of the contribution of the endothelium, VSM and adventitia. Nevertheless, little attention has previously been focused on the impact of ageing on the function of PVAT in C57BL/6 mice (Szasz 2012).

In health, PVAT attenuates vasoconstriction via the release of PVAT-derived relaxant factors, (Lohn et al. 2002; Gao et al. 2005; Gao et al. 2007b; Szasz and Webb 2012), but the anti-contractile capacity of PVAT is diminished or completely abolished in diet-induced weight gain (Greenstein et al. 2009; Ketonen et al. 2010; Meyer et al. 2013; Zaborska et al. 2016) and hypertension (Lu et al. 2011a; Galvez-Prieto et al. 2012).

This study demonstrated that aortic PVAT reduced constriction to phenylephrine in aortic rings from 8-week and 16-week ND-fed C57BL/6 mice. However, PVAT was dysfunctional after 26-weeks on the ND, in pre-middle aged mice. The contractions of PVAT denuded aortic rings were unaltered with ageing. However, PVAT-intact aortic rings exhibited significantly increased contractility by the 26-week time-point. Conflicting evidence surrounds the effect of ageing on agonist-induced vascular contractions in very old rodents, ranging from 12-24 months of age. Vasoconstrictions in response to noradrenaline and phenylephrine were found to be unchanged with ageing in rat skeletal muscle resistance arterioles and mouse mesenteric arteries, respectively (Gros et al. 2002; Muller-Delp et al. 2002) . However, ageing to 24-months old resulted in a decrease in contraction in response to endothelin-1 in the coronary arterioles of rats and rings of carotid artery from C57BL/6 mice (Shipley et al. 2005; Meyer et al. 2014) . These findings demonstrate that the effects of ageing on vasoconstriction responses is dependent on the agonist and vascular bed. With regard to this study, these data suggest that the SM and endothelium of the C57BL/6 mouse is healthy at the 26-week time-point, due to the maintained endothelial function and the absence of atherosclerotic lesions, and that PVAT dysfunction precedes endothelial dysfunction, which has not previously been demonstrated in the C57BL/6 mouse. In agreement with this is the finding that maternal obesity in rats predisposes their offspring to PVAT dysfunction prior to the development of endothelial dysfunction or hypertension (Zaborska et al. 2016).

3.5.5 Nitric oxide contributes to the net anti-contractile effect of PVAT in young mice; however, PVAT dysfunction in pre-middle aged mice is associated with a decrease in PVAT-derived nitric oxide

A role for NO contributing to the anti-contractile effect of PVAT has previously been reported (Gil-Ortega et al. 2010; Galvez-Prieto et al. 2012; Victorio et al. 2016; Zaborska et al. 2016). This study provides clear evidence that PVAT-derived NO mediates the anti-contractile effect of PVAT in 8 and 16-week time-point mice, as the PVAT effect was abrogated in the presence of a NOS inhibitor, L-NNA. These data are consistent with reports that NOS inhibition diminished the anti-contractile effect of PVAT in human subcutaneous arteries, mouse aortae and mesenteric arteries (Greenstein et al. 2009; Lynch et al. 2013; Victorio et al. 2016). Nevertheless, NOS inhibition had no effect on aortic rings, either PVAT-intact or PVAT-denuded, from the 26-week time-point mice. These data strongly indicate an age-associated decline of PVAT-derived NO bioavailability, which has been reported in rat mesentery, and may contribute to the pathogenesis of CVD (Melrose et al. 2015).

L-NNA was chosen as the NOS inhibitor for the NO inhibition experiments because it is a competitive inhibitor for the three distinct isoforms of the enzyme, neuronal, endothelial and inducible. However, it may exhibit off-target effects (Moore et al. 1990; Rees et al. 1990; Furfine et al. 1993; Furfine et al. 1994). Whilst the specific NOS isoform responsible for the anti-contractile effect of PVAT was not investigated in this study, recent studies have demonstrated that PVAT from the thoracic aorta of mice and rats express eNOS and produce NO (Araujo et al. 2015; Xia et al. 2016). Nevertheless, thoracic PVAT is mostly comprised of brown adipocytes and iNOS has been shown to be expressed in this tissue, thus a potential contribution of NO from this isoform cannot be discounted (Nisoli et al. 1997; Giordano et al. 2002).

The sensitivity of the VSM to NO was assessed by exposure of phenylephrine pre-constricted aortic rings, in the presence or absence of PVAT to sodium nitroprusside, an endothelium-independent vasodilator. Mechanistically, sodium nitroprusside directly targets vascular SM by stimulation of sGC and induction of hyperpolarisation (Gerhard et al. 1996; Bonaventura et al. 2008). Ageing did not result in altered relaxation to sodium nitroprusside in aortic rings with or without PVAT therefore, sensitivity to NO was unaltered in the C57BL/6 mice. Additionally, pre-constricted NOS-inhibited aortic rings were still able to relax fully to baseline (data not shown). These data are in line with evidence from ageing studies conducted on healthy adult humans and aortic rings of C57BL/6 mice which reported that VSM sensitivity to NO is unimpaired by ageing and further consolidates the idea that reduced endothelial-derived NO bioavailability with ageing contributes to vascular pathologies (Taddei et al. 1995; Gerhard et al. 1996; DeSouza et al. 2000; Ketonen et al. 2010; Seals et al. 2011; Bailey-Downs et al. 2013).

3.5.6 White adipocyte hypertrophy, increased ROS production and an altered adipokine profile may promote age-related PVAT dysfunction

3.5.6.1 The amount of PVAT encasing the aortae of C57BL/6 mice increases with ageing and is associated with white adipocyte hypertrophy

The composition of aortic PVAT was assessed to determine if any age-related morphological changes occurred in conjunction with the observed PVAT dysfunction at the 26-week time-point. Although PVAT has a net beneficial anti-contractile effect, an overabundance has been associated with a decline in PVAT function in ageing and obese mice and increased incidence of CVD in humans (Ketonen et al. 2010; Britton et al. 2012; Szasz 2012). Furthermore, in mice with excess PVAT, a wide range of pathologies are observed including diabetes, hypertension or hypotension depending on the amount of PVAT, altered vasoconstriction and lipodystrophy (Brown et al. 2014). In this study, a significant increase in the weight of PVAT surrounding the thoracic aortae was observed with ageing after 26 weeks on a ND post weaning. This was associated with an increase in the proportion of white adipocytes within the aortic PVAT, although this was non-significant, and significant increase in white adipocyte hypertrophy. Similar age-related morphological changes have been reported in 7 and 24 month old mice, with an increase in the abundance of white adipocytes observed within the aortic PVAT of old mice (Bailey-Downs et al. 2013). It is probable that the increase in white adipocyte size was associated with PVAT dysfunction in the 26-week group.

Expansion of white adipocytes occurs in health and in response to over-nutrition (Rutkowski et al. 2015). However, there are limits to healthy adipocyte hypertrophy and upon reaching a certain size, greater than 100 µm, the cells reach diffusional limits of oxygen which can lead to hypoxia, necrosis and subsequent apoptosis resulting in a highly inflammatory environment (Hosogai et al. 2007; Lee et al. 2014; Rutkowski et al. 2015). Of note, out of the three time-points only the 8-week time-point group exhibited a mean white adipocyte size less than 100 µm (8-weeks: 86.33 ± 10.10 μm^2) whereas the 16 and 26-week time-points exceeded this size (16-weeks: 133.00 ± 28.90 μm^2; 26 weeks: 201.10 ± 33.90 μm^2). This could suggest that by the 16-week time-point the PVAT is in the early stages of dysfunction and that morphological changes occur within the PVAT prior to functional alterations, explaining why the PVAT still exerted an anti-contractile effect at this time-point. In agreement with these findings, adipocyte hypertrophy within PVAT has been observed in the small arteries of obese humans and rodents with diet-induced weight gain and it has been proposed that these adipocytes are in a constant state of hypoxia leading to chronic inflammation and upregulation of pro-inflammatory cytokines such as TNFα (Fesus et al. 2007; Trayhurn et al. 2008; Greenstein et al. 2009; Aghamohammadzadeh et al. 2013; Bussey et al. 2016). If normal vascular ageing results in an increased aortic PVAT weight and white adipocyte hypertrophy and thus induces PVAT dysfunction, weight loss and consequent reduction of PVAT mass could potentially be a novel therapeutic target to reverse or prevent the development of CVD within humans.

3.5.6.2 Superoxide production is increased in ageing C57BL/6 mice

Due to the findings of white adipocyte hypertrophy within the thoracic aortic PVAT, superoxide production was assessed within the PVAT. Subsequently, superoxide levels were found to be elevated in the 26-week time-point mice; these results are supported by similar findings in much older mice, that ageing is associated with increased production of superoxide within the wall of the aorta and the thoracic PVAT (Bailey-Downs et al. 2013). The endothelium, adventitia and PVAT are a major source of vascular ROS. Within the vasculature, ROS can have both beneficial and harmful effects. Whilst superoxide-derived from PVAT has been demonstrated to increase vasoconstriction in mouse mesenteric arteries, hydrogen peroxide has been shown to contribute to the net anti-contractile effect of PVAT (Gao 2007; Gao et al. 2007b). Furthermore, PVAT has been discovered to express both ROS and reactive nitrogen species machinery including NADPH oxidase, a key producer of superoxide, and all superoxide dismutase (SOD) isoforms (Szasz and Webb 2012; Szasz et al. 2013).

Mitochondria are the predominant source of intracellular ROS and elevated superoxide production can predispose the development of CVD due to increased oxidative stress, inflammation and cellular senescence which are all biomarkers of vascular ageing (Rizvi 2009; Bailey-Downs et al. 2013; Costa et al. 2016). Thoracic aortic PVAT is mainly comprised of brown adipose tissue which is mitochondria-rich (Kiefer et al.). ROS production is tightly regulated however, mitochondrial dysfunction in response to ageing and diet-induced weight gain can occur (Ballinger et al. 2002; Trifunovic and Larsson 2008; Bournat and Brown 2010; Payne and Chinnery 2015). Morphological changes in the thoracic PVAT, chiefly white adipocyte

hypertrophy, were observed in the 26-week time-point mice which could potentially have triggered dysregulation of mitochondria resulting in increased superoxide production.

A strong link between elevated superoxide levels and PVAT dysfunction has been observed in states of metabolic disturbance in humans and rodents. In humans, a loss of the anti-contractile effect of PVAT was partially attributed to increased ROS and subsequent treatment with superoxide dismutase and catalase rescued the PVAT function (Greenstein et al. 2009). In further support of the detrimental effects of increased ROS are observations from the mesenteric arteries of the New Zealand obese mouse model which showed that augmented superoxide production was linked to increased NADPH oxidase activity, PVAT hypertrophy, enhanced macrophage infiltration and a loss of the anti-contractile effect of PVAT (Marchesi et al. 2009).

3.5.6.3 The number of Mac-3^{+} cells infiltrating the aortic PVAT is unchanged with ageing

Macrophage infiltration of PVAT has been linked to an attenuation of the anti-contractile effect of PVAT in the small arteries of humans and mice and it has been hypothesised this is due to their abundant secretion of ROS via NADPH oxidase, inducing adipocytokine dysregulation and damage to the endothelium (Greenstein et al. 2009; Rizvi 2009; Ketonen et al. 2010; Withers et al. 2011). PVAT has been demonstrated to secrete a wide variety of factors including adiponectin, leptin and inflammatory cytokines such as IL-6 and TNFα (Szasz and Webb 2012; Szasz et al. 2013). However, it has been proven that the characteristics of PVAT from humans and rodents depends on the location of the vascular bed (Brown et al. 2014). Mesenteric arteries have been shown to comprise mainly of white adipocytes and thus highly prone to inflammation triggered by disease whereas, brown adipose depots such as thoracic PVAT, particularly murine aortic PVAT, has been demonstrated to be resistant to inflammatory insult (Ketonen et al. 2010; Fitzgibbons et al. 2011). In agreement with these findings, this study has demonstrated that macrophage infiltration was not increased with ageing and therefore not directly responsible for the increased generation of superoxide within the PVAT. Also, these observations have been replicated in the PVAT of much older C57BL/6 mice indicating that the elevated levels of ROS within aortic PVAT are not induced by the infiltration of macrophages (Bailey-Downs et al. 2013).

3.5.6.4 The secretion profile of aortic PVAT is altered with ageing in C57BL/6 mice

Finally, the secretion profile of aortic PVAT from 26-week ND-fed mice was demonstrated to be altered in comparison to the youngest, 8-week ND-fed group. Surprisingly, of the 10 detectable adipokines, the relative expression of several well-known ‘bad’ adipokines, that have been associated with increased risk of CVD, were diminished in comparison to younger controls (Mattu and Randeva 2013; Stefan et al. 2013; Nakamura et al. 2014). Resistin, RAGE, Pentraxin-2 (a monocyte/macrophage differentiation marker with high affinity for damaged tissue environment), fetuin A (an inflammatory hepatokine) and IGFBP6 expression were all decreased in comparison to the younger mice, which is in contrast to previous findings (Fenton et al. 2009; Lee et al. 2012; Lu et al. 2012; Du Clos 2013; Stefan and Haring 2013; Fukami et al. 2014). Whilst the reasons behind this decrease are unknown, a potential protective compensatory mechanism could have been induced within the aortic PVAT in response to the morphological changes occurring in the PVAT, i.e. adipocyte hypertrophy. Of note, adiponectin expression, a ‘good’ adipokine with anti-inflammatory and vasodilatory properties, was found to be decreased in the ageing PVAT, in

agreement with other works suggesting that circulating and PVAT-derived adiponectin levels are reduced in states of metabolic disturbance (Fenton et al. 2009; Shibata et al. 2009). This decrease in adiponectin could potentially have further contributed to the loss of the anti-contractile effect of PVAT observed in the 26-week ND-fed group indeed, whilst some work supports this theory, it should be noted that contradictory evidence surround the effect of PVAT from the adiponectin knockout mouse with some research stating the anti-contractile capacity of PVAT is retained and others finding the PVAT effect abolished (Fesus et al. 2007; Lynch et al. 2013). Furthermore, a recent ageing study did not find any alterations in the expression of adiponectin with ageing to 24 months in C57BL/6 mice however, these results could be due to different methods of adipokine analysis (Bailey-Downs et al. 2013).

The adipokine array revealed an increase in the following inflammatory factors: lipocalin-2, FGF acidic, DPPIV and CRP. Lipocalin-2 is highly expressed in murine adipose tissue and has been found to be elevated in diet-induced weight gain and promotes insulin resistance in cultured adipocytes and hepatocytes (Yan et al. 2007). In addition, circulating lipocalin-2 levels have been identified to be positively associated with adiposity in humans (Wang et al. 2007b). The increased expression of CRP and DPPIV in response to disease states has previously been reported. Increased CRP was suggested to promote endothelial dysfunction in rabbits and clinical trial have suggested the possible role of CRP as a pro-atherogenic factor (The Emerging Risk Factors 2010; Chen et al. 2013). DPPIV expression in adipose tissue has been associated with insulin resistance in humans and their presence has been suggested as a marker of increased visceral adipose depots and the metabolic syndrome (Sell et al. 2013; Son et al. 2015). Lastly, FGF-acidic (FGF-1) has been identified to play a key role in adipose tissue remodelling and systemic metabolic homeostasis, and is induced in white adipose tissue in response to a high fat diet in C57BL/6 mice (Jonker et al. 2012).

Taken together, the aforementioned changes to the PVAT secretion profile of ageing C57BL/6 is contradictory. The loss of the anti-contractile effect of PVAT would imply that damaging changes have occurred within the PVAT and as such it was expected that the adipokine profile would show a marked upregulation of pro-inflammatory factors. However, these mixed findings suggest that the PVAT milieu is in constant flux and is subject to both pro and anti-inflammatory actions as such, it is difficult to draw firm conclusions from these data.

3.6. Future experiments to further define the mechanisms underlying age-related PVAT dysfunction

Further investigations could assist with unravelling the complex mechanisms that results in a loss of the beneficial anti-contractile capacity of aortic PVAT with ageing in C57BL/6 mice. Whilst changes to the function of the vascular SM were not observed in the presence of a functional endothelium, it would be interesting to repeat the ageing experiments in endothelium-denuded vessels to ascertain that the healthy endothelium is not somehow masking an underlying smooth muscle dysfunction. Additionally, PVAT transfer experiments could be performed on both ageing and young endothelium-denuded aortic rings to determine if the anti-contractile effect of young PVAT can induce a similar response in older aortic segments and vice versa.

Furthermore, the composition of aortic PVAT was shown to change with ageing and was determined by assessing white adipocyte content. However, ageing could also induce changes to the brown adipocytes and it would be of interest to determine if expression of UCP-1, a marker for brown adipose tissue was altered with ageing to these time-points in C57BL/6 mice and contributed to the loss of the anti-contractile function of PVAT observed in the ageing mice from this study. An age-associated loss of brown adipocytes has previously been demonstrated, (Graja et al. 2015) this loss could potentially contribute to the development of cardiovascular disease.

NOS inhibition experiments indicated that PVAT-derived NO mediated the anti-contractile effect of PVAT in young C57BL/6 mice. This effect was lost in the 26-week ND-fed group and it was proposed that this was due to a decline in the bioavailability of PVAT-derived NO. To test this theory, a nitric oxide assay on PVAT supernatant could be performed at each time-point and total NO assessed (Bryan et al. 2007).

Finally, PVAT dysfunction was observed to occur in the PVAT of pre-middle aged mice in the absence of lipidemic abnormalities, atherosclerosis or endothelial dysfunction. This suggests that PVAT dysfunction occurs as part of the normal ageing process, and may be in part due to an increased PVAT mass and hypertrophy of white adipocytes. Adipose tissue has been shown to have a certain degree of plasticity and it is possible that the increase in white adipocytes within the aortic PVAT, which may have contributed to the loss of function of PVAT, may be reversible. Exercise has been demonstrated to 'brown' white adipocytes and lead to increased eNOS expression and NO production (Sindler et al. 2009; Araujo et al. 2015). Moreover, cold exposure has been shown to re-brown adipocytes although effects on vascular function have not yet been investigated (Sharp et al. 2012; Wu et al. 2012; Park et al. 2014). Conversely, attempts to activate brown adipose tissue pharmacologically, with the sympathomimetic ephedrine, had no effect in humans (Cypess et al. 2012; Kiefer et al.).

3.7 Chapter summary and conclusions

This study has demonstrated that C57BL/6 mice are a valuable tool for the study of vascular ageing in health. During the time-points assessed in this study, C57BL/6 mice were not observed to develop dyslipidaemia, atherosclerosis or endothelial dysfunction. NO contributed to the anti-contractile properties of PVAT in the younger adult mice. Conversely, ageing to approximately 30 weeks (26 weeks ND) was demonstrated to abolish the anti-contractile capacity of aortic PVAT due to a reduction in the bioavailability of PVAT-derived NO and potentially through a series of damaging changes involving: increased PVAT amount, white adipocyte hypertrophy, elevated superoxide production and alterations to the adipokine secretion profile. These data reveal eNOS, and consequently NO bioavailability, as potential therapeutic targets aimed at increasing PVAT-derived NO to restore healthy PVAT function. Moreover, reverting the PVAT to a younger phenotype via browning of the PVAT could also induce beneficial effects.

The principal findings of this chapter were:

- **Endothelial function was maintained in C57BL/6 mice aged to pre-middle age whilst the anti-contractile effects of aortic perivascular adipose tissue (PVAT) were attenuated in the 26-week normal diet (ND) -fed C57BL/6 mice.**

- **NOS inhibition revealed that NO mediated the anti-contractile effect of PVAT in the 8 and 16-week ND-fed groups however, NOS inhibition had no effect in the 26-week ND group, which may be indicative of a decrease in PVAT-derived NO.**
- **The morphology of aortic PVAT was altered with increasing age; an increase in the weight of PVAT surrounding the aortae in combination with white adipocyte hypertrophy, increased superoxide production and an altered adipokine profile may have contributed to the loss of the anti-contractile effect of PVAT in the 26-week ND cohort.**

~ Chapter Four ~

An investigation of perivascular adipose tissue in atherosclerotic ApoE$^{-/-}$ mice

Abstract

Background: The Apolipoprotein E knockout mouse (ApoE$^{-/-}$) is a widely-used model of atherosclerosis and displays characteristics of accelerated ageing. Perivascular adipose tissue (PVAT) surrounds the majority of blood vessels and until recently was not considered important in the pathogenesis of atherosclerosis. PVAT exerts anti-contractile effects that are abolished in disease states. PVAT could potentially modulate the vascular reactivity of aortic ring preparations from ApoE$^{-/-}$ mice and consequently, the development and progression of atherosclerosis, through alterations in PVAT-derived nitric oxide (NO).

Purpose: The following experiments were conducted to determine the influence of PVAT, age, a Western-type and associated progression of atherosclerosis on isolated arterial reactivity on the aortae of ApoE$^{-/-}$ mice. In addition, the morphology of aortic PVAT was assessed to determine the extent (if any) of age or diet-related changes.

Methods: Upon weaning, at approximately 4 weeks of age, male ApoE$^{-/-}$ mice were fed a normal rodent chow (normal diet, ND) or high fat Western-type diet (WD) for a period of 8, 16 or 26-weeks. Vascular reactivity studies were performed on aortic rings with the PVAT remaining intact or PVAT-denuded. The influence of NO on the vasoconstrictor responses of phenylephrine was assessed using the NOS inhibitor L-NNA (50 µM). The morphology of aortic PVAT was assessed via histology and immunohistochemistry.

Results: WD-fed ApoE$^{-/-}$ mice displayed a pro-atherogenic lipoprotein profile and accelerated development of atherosclerosis in comparison to ND-fed mice**.** PVAT was dysfunctional and did not modulate the vascular reactivity of aortic rings in either ND or WD-fed ApoE$^{-/-}$ mice at any of the examined time-points. In addition, endothelial dysfunction was not observed with established atherosclerosis, at the 26-week time-point. NOS inhibition with 50 µM L-NNA did not alter the vascular reactivity of aortic segments at any of the time-points. The amount of PVAT surrounding the aortae of ApoE$^{-/-}$ mouse did not significantly change with ageing or a WD. In addition, the composition of the aortic PVAT, with respect to the proportion and size of white adipocytes, was not significantly altered, nor was there an increase in inflammation with ageing or a WD.

Conclusions: The aortic PVAT of ApoE$^{-/-}$ mice is dysfunctional and does not exert an anti-contractile effect on the aorta. This is possibly due to a combination of reduced PVAT-derived NO within the vasculature and an 'aged' PVAT phenotype

4.1 Introduction

Atherosclerosis is a chronic progressive disease which can remain asymptomatic for decades thus, ageing results in increased incidence and severity of atherosclerotic disease (Toth 2008; Uryga and Bennett 2016). The initial stages of atherogenesis involve the accrual of foam cells along the sub-endothelial layer; this 'fatty streak' has been observed within the aortae of humans in the first decade of life (Strong et al. 1999). By the second and third decades, lesions are manifest within the coronary and cerebral arteries, respectively (Lusis 2000; Singh et al. 2002) .

The ApoE$^{-/-}$ mouse is predisposed to hypercholesterolaemia and spontaneous development of lesions within its vasculature when fed a ND (Plump et al. 1992; Zhang et al. 1992; Jawien et al. 2004). Furthermore, the progression and severity of atherosclerosis can be accelerated by feeding the ApoE$^{-/-}$ mice a high fat WD, as observed in man (Plump et al. 1992).

Relaxation studies performed on the conductance vessels of ApoE$^{-/-}$ mice have demonstrated endothelial dysfunction, which is a predictor of atherosclerosis in humans (Barton et al. 1998; d'Uscio et al. 2001a; Laursen et al. 2001). However, the role of PVAT on vascular reactivity and its potential to modulate both VSM and endothelial cells has not been investigated.

PVAT releases a wide variety of factors which can modulate vascular tone, the inflammatory state of the vessel, VSM characteristics and oxidative stress (Lohn et al. 2002; Gao et al. 2005; Szasz and Webb 2012). Notably in humans, atherosclerotic lesions have been demonstrated to principally occur in epicardial coronary arteries which are surrounded by PVAT (Montani et al. 2004; Sacks et al. 2007; Greif et al. 2009). However, not all arteries encased by PVAT go on to develop atherosclerotic lesions. The role of PVAT and its possible effects on the development of atherosclerosis have only recently begun to be investigated. Studies in humans have reported a strong association between the amount of coronary PVAT and atherosclerotic plaque burden within the artery (Mahabadi et al. 2010; Verhagen and Visseren 2011; Verhagen et al. 2012). Furthermore, PVAT transplant experiments in ApoE$^{-/-}$ mice have reported that transfer of pro-inflammatory adipose to sites of the coronary artery which are not normally predisposed to atherosclerotic lesions caused the development of atheromas and endothelial dysfunction in the recipient mice (Öhman et al. 2011). Atherosclerosis is a highly inflammatory disease and as such, changes to the composition of PVAT, such as increased macrophage infiltration, elevated ROS levels and alterations to the adipocytes which comprise PVAT could potentially contribute to altered vascular reactivity and hence, modulate the progression of atherosclerosis (Ross 1999b).

Nevertheless, little is known regarding the influence of aortic PVAT on the contractility and relaxation responses of isolated aortic preparations from ApoE$^{-/-}$ mice. PVAT could potentially modulate the vascular reactivity of the aortae in ApoE$^{-/-}$ mice via alterations in the release of PVAT-derived factors. A key role NO in mediating the anti-contractile effect of PVAT was observed in C57BL/6 mice in the previous Chapter (3). Furthermore, this study reported that C57BL/6 mice aged to pre-middle age exhibited a loss of the anti-contractile PVAT effect and this potentially was a result of reduced PVAT-derived NO bioavailability. Therefore, alterations within PVAT and in PVAT-derived NO bioavailability in ApoE$^{-/-}$ mice may influence the contractility of the aortae and could potentially modulate atherosclerosis. An increase in aortic contractility through

disturbances in NO signalling and/or release of constricting factors within the PVAT could cause increased blood flow turbulence and therefore, endothelial damage and promote atherosclerosis. Therefore, the role of aortic PVAT and NO in modulating vascular reactivity in both ageing and Western-type diet fed ApoE$^{-/-}$ mice will be evaluated in this study. In addition, the morphology of aortic PVAT will be assessed to determine what, if any, changes occur with accelerated ageing in the ApoE$^{-/-}$ mouse. Insights gained from studies on the aortic PVAT of ApoE$^{-/-}$ mice could, potentially reveal therapeutic targets for the treatment of atherosclerosis.

4.2 Aim and objectives

The aim of this chapter is to determine if PVAT modulates the vascular function of aortic rings from ApoE$^{-/-}$ mice and investigate whether this is modified by ageing, NO bioavailability or a WD and the development of atherosclerosis. The objectives of this chapter are to:

- Phenotype ageing and WD-fed ApoE$^{-/-}$ mice by assessing lipid profiles, body and organ weights and the development of atherosclerotic lesions within the aortae of these mice.
- Determine if endothelial-dependent relaxation is affected by ageing, the presence of PVAT or the development of atherosclerosis in ApoE$^{-/-}$ mice using myography to assess vascular function.
- Establish if the aortic PVAT of ApoE$^{-/-}$ mice exerts an effect on vasoconstrictor responses to cumulative doses of phenylephrine and if pharmacological inhibition of NOS alters this.
- Determine if the structure and morphology of aortic PVAT from ApoE$^{-/-}$ mice is altered by ageing or a WD using histological and immunohistochemical techniques.

4.3 Methods

Male ApoE$^{-/-}$ mice were bred from an in-house colony. At approximately 4 weeks old, the mice were weaned onto either a normal chow diet (ND) or a 21% fat Western-type diet (WD) for 8, 16 or 26 weeks. The lipidemic and glycaemic profiles of ageing ApoE$^{-/-}$ and WD-fed ApoE$^{-/-}$ mice were assessed. Additionally, body and organ weights of ND and WD-fed mice were recorded at sacrifice. En face lesion analysis was performed to determine the extent of atherosclerotic disease progression within the lumen of the aortae in ND and WD-fed mice at each time-point. Relaxation experiments were conducted on aortic rings to determine if PVAT or the pathogenesis of atherosclerosis altered endothelial function. The effect of PVAT on vascular function was assessed using rings of thoracic aortae with the PVAT remaining intact or carefully removed. The influence of NO on the contractile responses of aortic ring preparations was assessed by incubation with a nitric oxide synthase (NOS) inhibitor (L-NNA). The sensitivity of the aortic preparations to exogenous NO was assessed through the application of the endothelium-independent vasodilator, sodium nitroprusside. Aortic PVAT morphology and composition was evaluated using haematoxylin and eosin staining, the superoxide indicator dihydroethidium and a macrophage marker. Detailed methods are provided in Chapter 2.

4.4 Results

4.4.1 Phenotyping normal diet and Western-type diet fed ApoE$^{-/-}$ mice

4.4.1.1 A Western-type diet enhances the pro-atherogenic lipid profile of ApoE$^{-/-}$ mice

Increasing age did not have a significant impact on any of the lipidemic or glycaemic parameters measured in ND-fed ApoE$^{-/-}$ mice (P= NS for all parameters, n = 6 mice per group, Table 4.1). Furthermore, feeding ApoE$^{-/-}$ mice a WD resulted in hypercholesterolaemia in the 16 and 26-week time-points compared to age-matched ND-fed mice (ND versus WD: 8-weeks P = 0.052; 16-weeks P = 0.02; 26-weeks P = 0.03, n = 6 mice per group, Table 4.1). However, there were no observable differences in HDL-cholesterol or triglycerides between age-matched ND and WD-fed mice at any of the experimental times measured (ND versus WD: P = NS each time-points; n = 6 mice per group, Table 4.1). Also, serum glucose levels were unaffected by a WD (ND versus WD: P = NS all time-points; n = 6 mice per group, Table 4.1).

Table 4.1 Lipidemic and glycaemic profiles of normal and Western-type diet-fed ApoE$^{-/-}$ mice

ND	8-weeks	16-weeks	26-weeks	P values for all diet-matched comparisons
Total cholesterol	8.22 ± 0.86	9.77 ± 0.88	10.06 ± 1.16	P = NS
HDL	0.42 ± 0.09	0.49 ± 0.09	0.57 ± 0.11	P = NS
Triglycerides	2.64 ± 0.65	1.71 ± 0.35	1.66 ± 0.30	P = NS
Glucose	15.02 ± 2.84	18.59 ± 0.97	17.55 ± 2.11	P = NS
WD	**8-weeks**	**16-weeks**	**26-weeks**	**P values for all diet-matched comparisons**
Total cholesterol	16.03 ± 1.98	18.42 ± 2.07	18.44 ± 2.66	P = NS
HDL	0.45 ± 0.08	0.58 ± 0.12	0.66 ± 0.12	P = NS
Triglycerides	2.55 ± 0.44	2.32 ± 0.55	2.49 ± 0.49	P = NS
Glucose	19.48 ± 2.42	19.75 ± 0.65	20.66 ± 1.76	P = NS
ND versus WD	**8-weeks**	**16-weeks**	**26-weeks**	
Total cholesterol	NS 0.052	* 0.02	* 0.03	
HDL	NS > 0.999	NS > 0.999	NS > 0.999	
Triglycerides	NS > 0.999	NS > 0.999	NS > 0.999	
Glucose	NS > 0.999	NS > 0.999	NS > 0.999	

Serum obtained at time of sacrifice (mice were weaned at 4 weeks of age then maintained on a normal chow diet (ND) or Western-type diet (WD) for the appropriate length of time. Data are expressed as mean ± S.E.M and measurements are shown in mmol/L. Statistical analysis was carried out by two-way ANOVA, with Bonferroni's post hoc test, n = 6 mice per group.

The lipid and glucose profiles of ND-fed ApoE$^{-/-}$ mice were compared to age and diet-matched C57BL/6 mice (Appendix 2.2). In comparison to the C57BL/6 strain the ApoE$^{-/-}$ mice exhibited hypercholesterolaemia (P < 0.0001; n = 3-6 mice per group) and significantly lower HDL levels (P

< 0.0001; n = 3-6 mice per group). However, serum triglycerides and glucose measurements were similar between the two mouse strains (P = NS; n = 3-6 mice per group).

4.4.1.2 The effect of ageing on the body and organ weights of normal diet-fed ApoE$^{-/-}$ mice

ApoE$^{-/-}$ mice displayed a significant gain in body weight after 16-weeks on the ND, post weaning, compared to the younger 8-week ND-fed mice (8-weeks versus 16-weeks: P = 0.004; n = 26 and 24 mice, respectively, Table 4.2) and this increase was sustained in the 26-week group (8-weeks versus 26-weeks; P = 0.0001; n = 26 and 21 mice, Table 4.2). Also, heart weight was significantly increased between the youngest and oldest groups (8-weeks versus 26-weeks: P = 0.001; n = 26 and 21 mice, Table 4.2). However, no further effects of ageing were observed when heart weight: body weight ratios were compared or in the organ weights of the liver, spleen, and epididymal fat pads and no changes in epididymal adipocyte sizes were observed (P = NS for all parameters and age group comparisons n = 21-26 mice, Table 4.2).

The body and organ weights of ApoE$^{-/-}$ mice were compared to the genetic background, C57BL/6, strain and with the exception of the epididymal fat pads and epididymal adipocyte size no significant difference were observed between the ApoE$^{-/-}$ and C57BL/6 mice (Appendix 2.3). Epididymal fat pad weights and epididymal adipocyte area were significantly decreased in comparison to age-matched 26 week ND-fed C57BL/6 mice and epididymal adipocytes were observed to be significantly enlarged in comparison to ApoE$^{-/-}$ mice after 16 weeks on a ND (P < 0.0001 epididymal fat pad weights: n = 4-6 C57BL/6 mice, n = 20-26 ApoE$^{-/-}$ mice; epididymal adipocyte area: n = 4 mice per group, 100 adipocytes measured per mouse).

4.4.1.3 The effect of A Western-type diet on the body and organ weights of ApoE$^{-/-}$ mice

The impact of a WD on the body and organ weights of ApoE$^{-/-}$ mice was assessed by comparing them to age-matched ND-fed mice. Body weights of ApoE$^{-/-}$ mice were not significantly different until the 26-week time-point (ND versus WD: P = 0.008; n = 26 and 24 mice, respectively, Table 4.2). There were no changes in heart, liver or spleen weight between age-matched mice (Table 4.2) although, a significant decrease in the HW:BW ratio was observed in WD mice after 26-weeks (ND versus WD: P = 0.0004; n = 26 and 24 mice, respectively, Table 4.2). Epididymal fat pads were considerably larger in the 16 and 26 week WD-fed mice in comparison to their age-matched counterparts (ND versus WD: 16-weeks P < 0.0001; 26-weeks P < 0.0001, n = 20-24 mice per group, Table 4.2) and this was related to epididymal adipocyte hypertrophy (ND versus WD: 16-weeks P = 0.04; 26-weeks P = 0.02, n = 20-24 mice per group, Table 4.2).

A WD exacerbated hypercholesterolaemia in ApoE$^{-/-}$ mice. However, extended feeding did not further augment the serum lipid or glycaemic profiles. Although ApoE$^{-/-}$ mice were resistant to diet-induced weight gain, up until the final 26-week time-point, abdominal fat deposition was enhanced in the WD-fed mice at each time-point, and this was associated with adipocyte hyperplasia and not hypertrophy.

Table 4.2 Body and organ weights and epididymal adipocyte size of ApoE$^{-/-}$ mice on a normal or Western-type diet

ND	8-weeks (A)	16-weeks (B)	26-weeks (C)	P values for all diet-matched comparisons
Body weight (g)	28.55 ± 0.45	31.93 ± 0.47	32.88 ± 0.40	A vs B ** 0.004, A vs C *** 0.0001
Heart weight (mg)	153.5 ± 4.55	173.3 ± 5.37	185.0 ± 6.86	A vs C ** 0.001
Heart weight: body weight (mg/g)	5.42 ± 0.11	5.47 ± 0.12	5.61 ± 0.17	
Liver (g)	1.81 ± 0.05	1.95 ± 0.05	2.16 ± 0.13	
Spleen (mg)	106.9 ± 5.53	117.2 ± 8.46	113.7 ± 7.50	
Epididymal fat pad weight (g)	0.29 ± 0.01	0.33 ± 0.02	0.37 ± 0.02	
Epididymal adipocyte area (x10^3 µm^2)	1.42 ± 0.19	1.53 ± 0.31	2.42 ± 0.22	
WD	**8-weeks (D)**	**16 weeks (E)**	**26-weeks (F)**	**P values for all diet-matched comparisons**
Body weight (g)	27.61 ± 0.46	32.93 ± 0.82	36.47 ± 1.26	D vs E **** P <0.0001, D vs F **** P < 0.0001, E vs F ** 0.007
Heart weight (mg)	144.9 ± 4.35	159.0 ± 4.32	164.7 ± 6.55	
Heart weight: body weight (mg/g)	5.11 ± 0.14	4.96 ± 0.15	4.61 ± 0.24	
Liver (g)	1.80 ± 0.05	2.04 ± 0.08	2.37 ± 0.17	D vs F *** 0.0002
Spleen (mg)	116.7 ± 7.01	121.9 ± 7.44	125.5 ± 9.50	
Epididymal fat pad weight (g)	0.51 ± 0.04	0.86 ± 0.09	1.26 ± 0.14	D vs E ** 0.002, D vs F *** 0.0001, E vs F *** 0.0006
Epididymal adipocyte area (x10^3 µm^2)	2.86 ± 0.56	3.2 ± 0.62	4.31 ± 0.51	

ND versus WD	8-weeks	16-weeks	26-weeks
Body weight	NS > 0.999	NS > 0.999	** 0.008
Heart weight	NS > 0.999	NS 0.83	NS 0.18
Heart weight: body weight	NS > 0.999	NS 0.29	*** 0.0004
Liver	NS > 0.999	NS > 0.999	NS > 0.999
Spleen	NS > 0.999	NS > 0.999	NS > 0.999
Epididymal fat pad weight	NS 0.20	**** P < 0.0001	**** P < 0.0001
Epididymal adipocyte area	NS 0.09	* 0.04	* 0.02

ND = normal chow diet, WD = Western-type diet. Data are expressed as mean ± S.E.M.E.M and weights are shown in milligrams or grams. Heart weight: body weight ratio in milligrams/grams and epididymal adipocyte area x10^3 µm^2*. Two-way ANOVA with Bonferroni's post-hoc tests was performed: body and organ weights n = 20-26 mice per group; adipocyte area n = 4 mice per group, 100 adipocytes per mouse.*

4.4.2 A Western-type diet accelerates atherosclerotic lesion formation and plaque burden within the aortae of ApoE$^{-/-}$ mice

Atherosclerotic lesions were present within the aortae of both ND and WD-fed ApoE$^{-/-}$ mice at each time-point investigated (Figure 4.1A). At the initial 8-week time-point, lesions had begun to form in the aortic arch of the WD ApoE$^{-/-}$ mice and to a much lesser extent in the age-matched ND-fed groups (Figure 4.1Ai and ii). After 16 weeks, lesions were visibly more extensive in the aortae of both WD and ND-fed ApoE$^{-/-}$ mice. Lesions were predominantly localised to the aortic arch in ND-fed mice; in contrast to this, in the WD-fed mice, atheromatous lesions had begun to spread along the thoracic aortae and positive lipid staining was observed in the lumen of the intercostal vessels (Figure 4.1Aiii and iv). A dramatic increase in lesion area was observed after extended WD-feeding, 26 weeks, compared to age-matched ND mice (Figure 4.1Av and vi). Large three-dimensional atheromatous plaques, which were concentrated in the aortic arch, were observed along with clusters of lesions which descended along the thoracic aortae (Figure 4.1Avi).

Atherosclerotic burden did not significantly alter with ageing in ND-fed mice (P = NS all time-point comparisons, n = 6-7 mice per group, Figure 4.1B) whereas a large increase in lesions was observed between each experimental time-point in WD-fed mice (8-weeks versus 16-weeks: P = 0.006; 16-weeks versus 26-weeks; P < 0.0001; 8-weeks versus 26-weeks P < 0.0001; n = 6-7 mice per group, Figure 4.1B).

Atherosclerotic plaque burden was more severe in the WD-fed mice, in comparison to ND age-matched ApoE$^{-/-}$ mice, at both the 16 and 26-week time-points (ND versus WD: 16 weeks P = 0.003; 26 weeks P < 0.0001; n = 6-7 mice per group, Figure 4.1B) although no differences were observed between the initial 8-week time-point groups (ND versus WD: P > 0.99; n = 6 and 7 mice, respectively, Figure 4.1B).

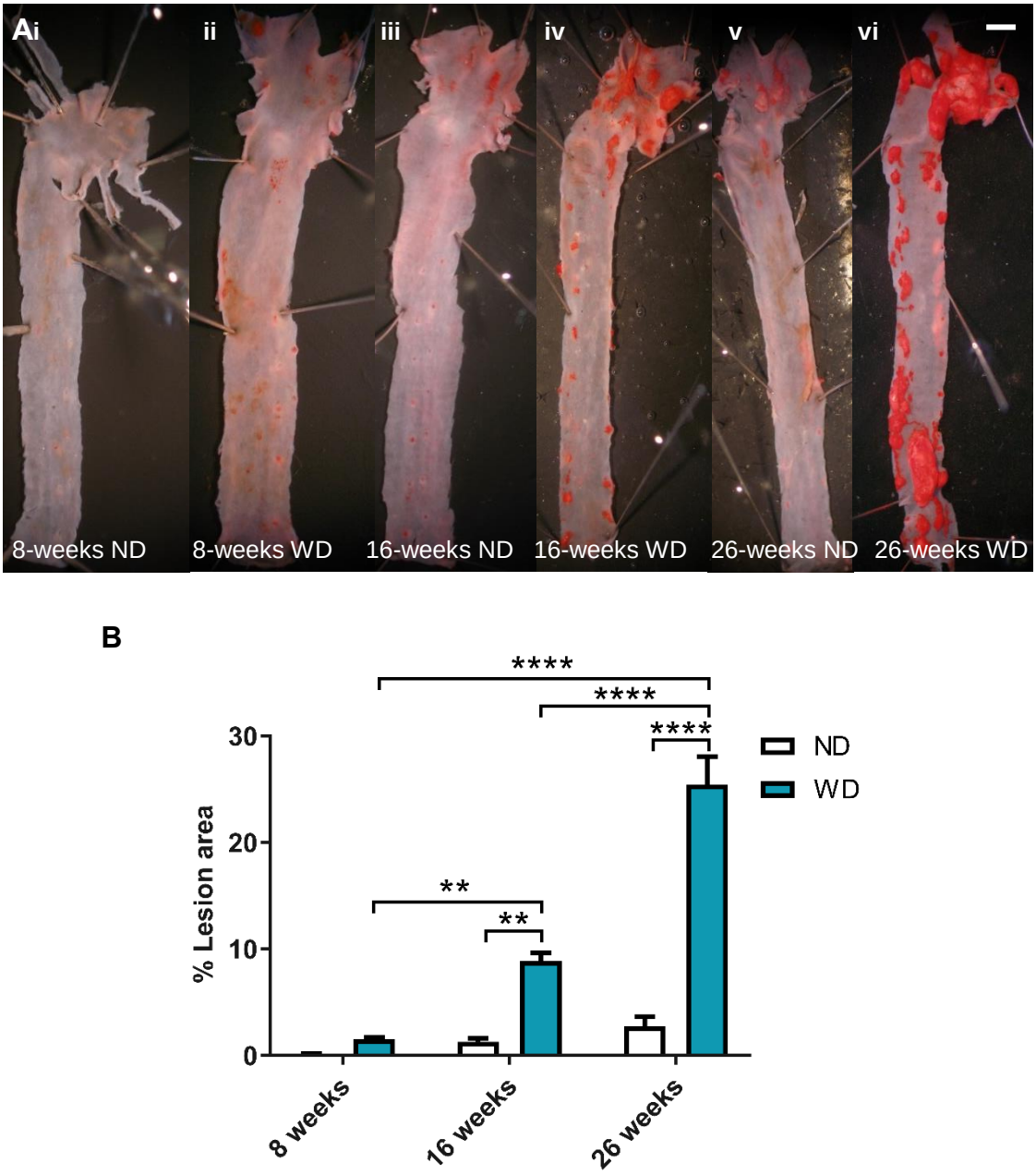

Figure 4.1 En face aortic preparations stained with Oil Red O demonstrating accelerated progression of atherosclerosis in Western-type diet-fed ApoE$^{-/-}$ mice.

*A) Oil Red O was used in order to visualise lipid-laden deposits along the luminal surface of the aortae of ApoE$^{-/-}$ mice after a period of 8-weeks on a ND, i) or WD, ii) 16-weeks on a ND, iii) or WD, iv) or 26 weeks on a ND, v) or WD, vi). Red-stained lesions were traced and total lesion area was expressed as a percentage of the total intimal surface. B) A WD accelerated atherosclerotic disease progression in the aorta of ApoE$^{-/-}$ mice in comparison to ND controls at the 16 and 26-week time-points. Representative images, scale bar, top right hand corner = 1 mm, ND = normal diet, WD = Western-type diet, n=6-7 ApoE$^{-/-}$ mice per group. ** P < 0.01, *** P < 0.001, **** P < 0.0001, Two-way ANOVA with post hoc Bonferroni's post hoc tests.*

4.4.3 Vascular reactivity studies assessing the effect of aortic PVAT on vascular responses

4.4.3.1 The contractions of aortic rings to KPSS are unaffected by the presence of PVAT, ageing or a Western-type diet

The presence of PVAT did not alter the contractile response, evoked by stimulation with 100 mM KPSS, in any of the experimental and a WD did not have a significant effect on aortic ring contraction (P = NS, n = 6-8 mice per group, Figure 4.2).

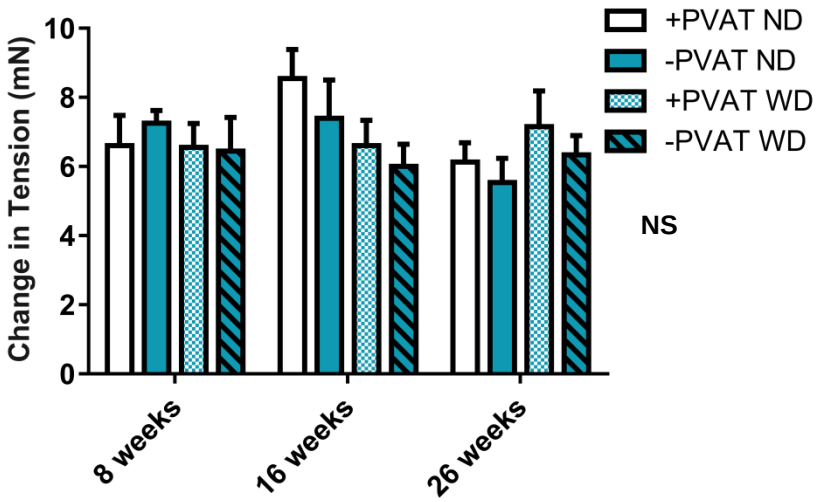

Figure 4.2 Contractile responses to 100 mM KPSS were similar in PVAT-denuded and PVAT-intact aortic rings in each experimental group

*ND = normal diet, WD = Western-type diet Data are presented as mean ± S.E.M, n = 6-8 mice per group***.** *Two-way ANOVA with Bonferroni's post hoc test.*

Furthermore, the responses of ND-fed ApoE$^{-/-}$ mice to KPSS were similar to the contractions observed in ND-fed C57BL/6 mice (P = NS, n = 5-8 mice per group, Appendix 2.4Ai and ii p 221).

4.4.3.2 A decline in endothelium-dependent relaxation is not observed within the aortae of Western-type diet-fed ApoE$^{-/-}$ mice

The presence of PVAT on aortic rings did not have a significant effect on relaxation to 10 µM acetylcholine P = NS; n = 6-8 mice per group, Figure 4.3). In addition, relaxation responses did not decline significantly in either the ND or WD-fed mice despite the fact that atherosclerotic lipid lesions were visible in the aortae of these mice (P = NS; n = 6-8 mice per group, Figure 4.3 and 4.1) Moreover, the relaxation responses of aortic rings from ND and WD-fed mice, in the presence or absence of PVAT, were similar at each time-points (P = NS; n = 6-8 mice per group, Figure 4.3).

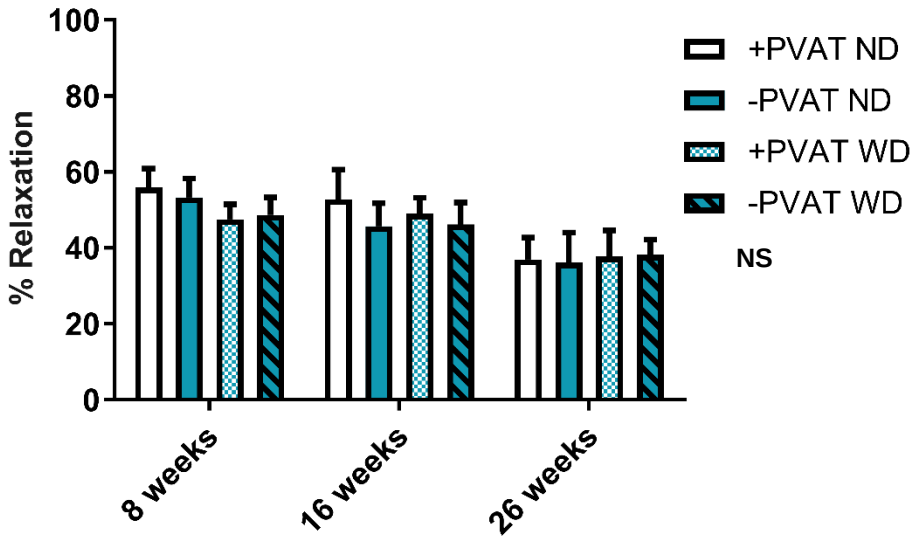

Figure 4.3 Endothelium dependent relaxation does not significantly decline in ApoE$^{-/-}$ mice after prolonged feeding of a Western-type diet.

Phenylephrine pre-constricted aortic rings from ND and WD 26-week time-point ApoE$^{-/-}$ mice did not relax significantly differently from the younger 8 and 16-week groups in response to 10 µM acetylcholine. ND = normal diet, WD = Western-type diet. Data are presented as mean ± S.E.M, n = 6-8 mice per group, with Two-way ANOVA with post hoc Bonferroni's multiple comparison tests.

In addition, endothelial dysfunction was not observed when the relaxation responses of ND-fed ApoE$^{-/-}$ mice were compared to the C57BL/6 strain in the presence or absence of PVAT (P = NS; n = 5-8 mice per group, Appendix 2.4Bi and ii p 221).

4.4.3.3 The aortic PVAT of ApoE$^{-/-}$ mice is dysfunctional and does not exert an anti-contractile effect in normal or Western-type diet fed mice

The PVAT of ApoE$^{-/-}$ mice did not exert an effect on aortic rings in response to cumulative doses of phenylephrine in 8-week ND mice (+PVAT versus -PVAT: P = NS for each group, n = 6-8 mice per condition, Figure 4.4A-C). Similarly, a WD had no impact on the contractility of aortic rings in the presence or absence of PVAT at any of the time-points (+PVAT versus -PVAT: P = NS, n= 6-8 mice per group, Figure 4.4A-C).

4.4.3.4 A Western-type diet does not alter the contractions of aortic rings from ApoE$^{-/-}$ mice, in the presence or absence of PVAT in comparison to normal diet-fed mice

Furthermore, a WD did not alter the contractility of aortic rings, in the presence or absence of PVAT, compared to age and strain-matched ND ApoE$^{-/-}$ mice (ND versus WD: P = NS, Figure 4.4A-C).

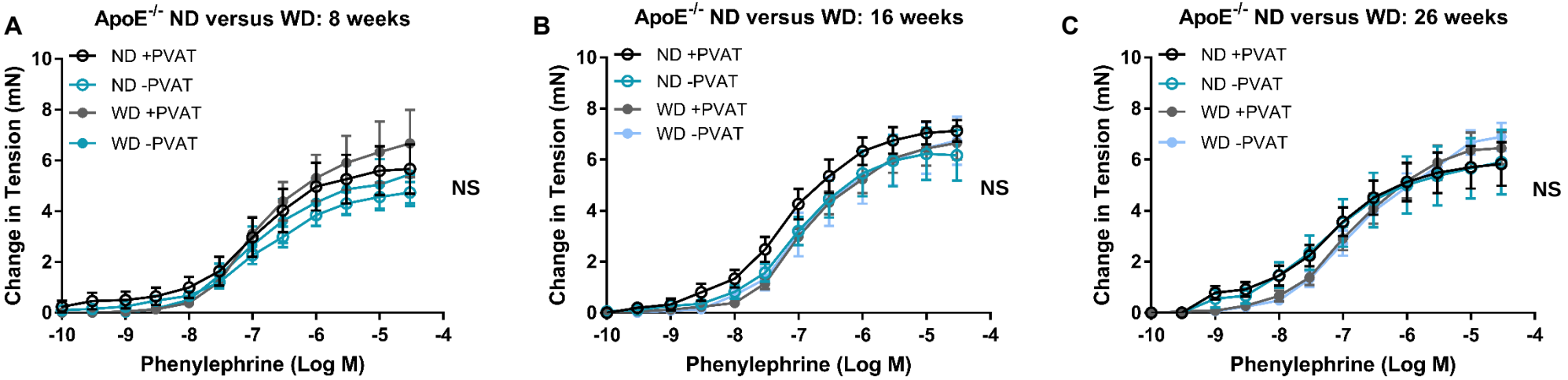

Figure 4.4 The PVAT of ApoE$^{-/-}$ mice is dysfunctional and does not exert an anti-contractile effect in normal or Western-type diet-fed mice

Aortic rings were exposed to cumulative doses of phenylephrine (1 x 10^{-10} - 3 x 10^{-5} mol/L) in the presence or absence of PVAT. Aortic PVAT did not modulate the vascular reactivity of aortic rings in ApoE$^{-/-}$ mice when fed either a ND or WD. Furthermore, the contractions of aortic rings, in the presence or absence of PVAT, from WD-fed ApoE$^{-/-}$ mice were similar to those observed in the age-matched ND mice A) 8 weeks, B) 16 weeks, C) 26 weeks on a ND or WD post weaning. ND = normal diet, PVAT = perivascular adipose tissue, WD = Western-type diet. Dose response data are expressed as mean ± S.E.M., n = 6-8 mice per group, two-way ANOVA with Bonferroni's post hoc tests.

4.4.3.5 Ageing does not alter the contractions of aortic rings from normal or Western-type diet fed ApoE$^{-/-}$ mice in the presence or absence of PVAT

The effect of ageing in ApoE$^{-/-}$ mice was assessed and no significant differences in contraction were observed with increasing age in aortic rings in the absence or presence of PVAT in ND-fed mice (P= NS each age comparison n= 6-8 mice per group, Figure 4.5Ai and ii). Furthermore, ageing and a WD had no significant effect on the contractions of aortic rings with or without PVAT (P = NS; n = 6-8 mice per group, Figure 4.5Bi and ii).

4.4.3.6 The aortic PVAT of normal diet-fed ApoE$^{-/-}$ mice is dysfunctional in comparison to C57BL/6 mice

The contraction of aortic rings from ND-fed ApoE$^{-/-}$ mice, to cumulative doses of phenylephrine, were compared to age and diet-matched C57BL/6 mice (Appendix 2.5). In the absence of PVAT, contractions to phenylephrine were similar in C57BL/6 and ApoE$^{-/-}$ mice at each time-point (ApoE$^{-/-}$ versus C57BL/6: 8-weeks -PVAT P NS for each age group comparison = 6-8 mice per group, Appendix 2.5A-C).

In contrast, the contractions of PVAT-intact aortic rings from ApoE$^{-/-}$ mice were significantly enhanced in both the 8 and 16-week ND-fed groups when compared to age and diet-matched C57BL/6 mice (C57BL/6 versus ApoE$^{-/-}$: 8 weeks: $P < 0.001$; 16 weeks: $P < 0.001$, n = 6-8 mice per group, Appendix 2.5A and B). However, in the 26-week ND-fed group, due to the increase in contractility observed in the PVAT-intact aortic rings of C57BL/6 mice, no differences were observed compared to ApoE contractile responses (P = NS, n = 6-8 mice, Appendix 2.5C).

Thus, PVAT is dysfunctional and does not exert an anti-contractile effect in ApoE$^{-/-}$ mice, prior to or in the presence of overt atherosclerosis, and this is unaffected by ageing. In addition, a WD and the development of extensive atherosclerotic disease does not potentiate the observed PVAT dysfunction.

4.4.3.7 NOS-inhibition does not alter vascular reactivity in ApoE$^{-/-}$ mice

Incubation with the NOS inhibitor, L-NNA (50 μM), did not have a significant effect on the vascular responses of aortic rings, either in the presence or absence of PVAT, in ND-fed mice at any of the examined time-points (P = NS, n = 6-9 mice per group, Figure 4.6Ai-iii). Moreover, these findings were replicated in WD-fed ApoE$^{-/-}$ mice and no effect of NOS-inhibition was observed (P = NS, n = 6-9 mice per group, Figure 4.6Bi-iii).

The lack of a response to NOS inhibition in ApoE$^{-/-}$ mice could potentially suggest reduced NO bioavailability or a decrease in eNOS synthesis/activity within the aorta.

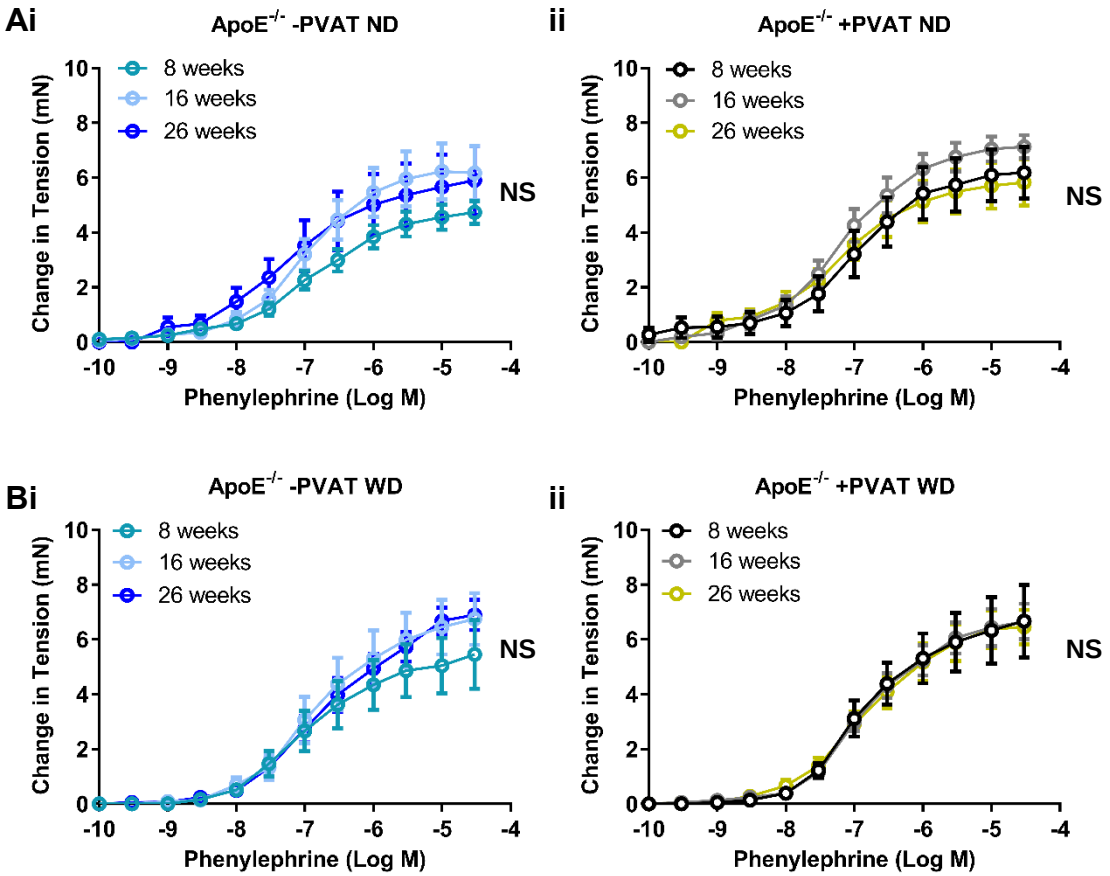

Figure 4.5 Ageing does not alter the contractions of aortic rings from normal or Western-type diet fed ApoE$^{-/-}$ mice in the presence or absence of PVAT

Ai) The contractions of PVAT-denuded and Aii) PVAT-intact aortic rings from ND-fed ApoE$^{-/-}$ mice were unaffected by increasing age, Bi) A WD did not alter the contractility of aortic rings from ApoE$^{-/-}$ mice in the absence of PVAT or in Bii) PVAT-intact conditions, after 8, 16 or 26-weeks on a WD. ND = normal diet, PVAT = perivascular adipose tissue, WD = Western-type diet. Dose response data are expressed as mean ± S.E.M., n = 6-8 mice per group, two-way ANOVA with Bonferroni's post hoc tests.

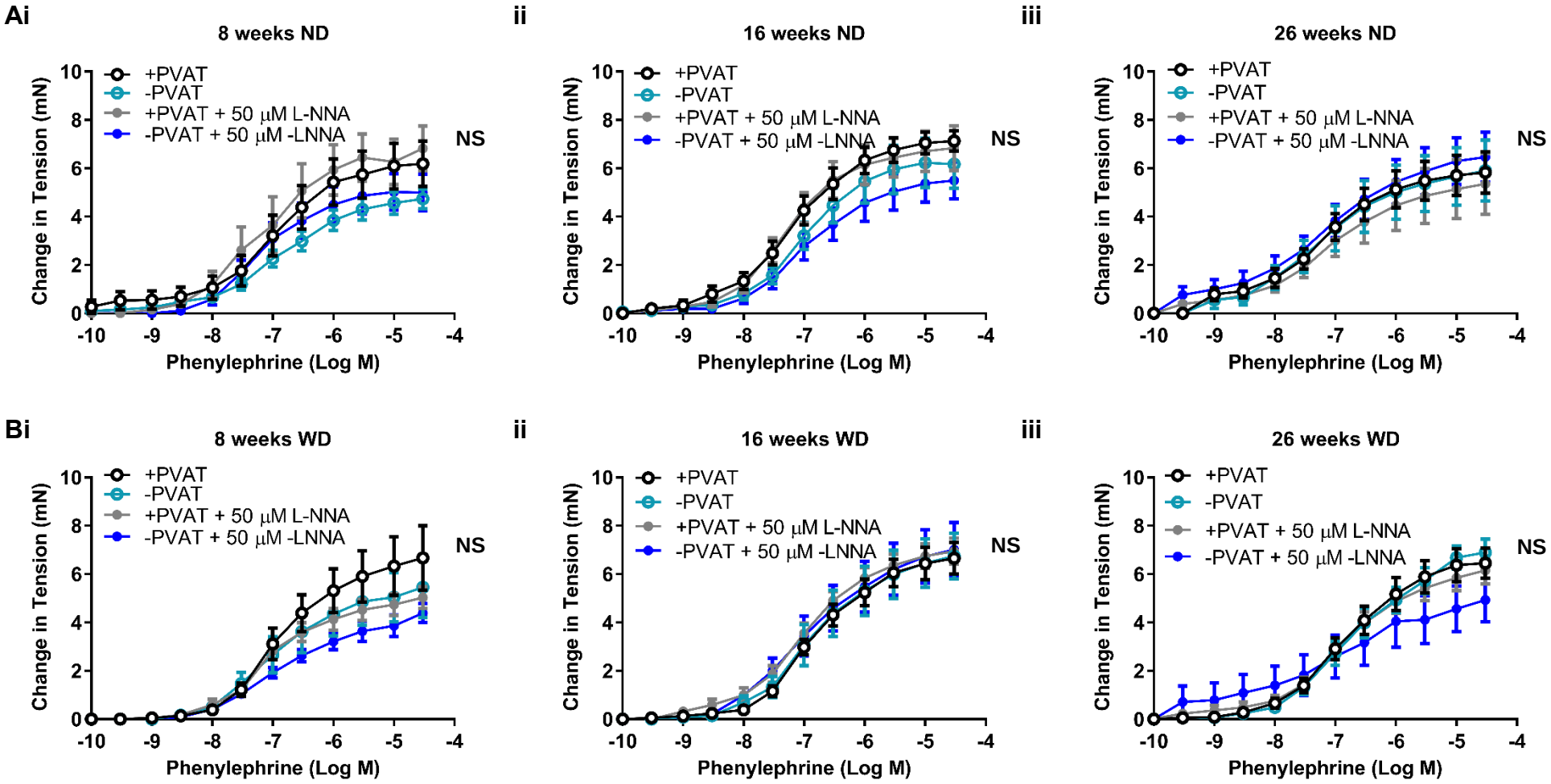

Figure 4.6 Nitric oxide synthase inhibition does not significantly alter aortic contraction in normal diet or Western-type diet-fed ApoE$^{-/-}$ mice

NOS inhibition with 50 μM L-NNA did not significantly alter aortic ring contractions to phenylephrine in A) ApoE$^{-/-}$ mice fed a ND for i) 8, i) 16 or iii) 26 weeks. Additionally, NOS inhibition had no effect on B) ApoE$^{-/-}$ mice fed a WD for i) 8, i) 16 or iii) 26-week time-points. ND = normal diet, NOS = nitric oxide synthase, WD = Western-type diet. Dose response data are expressed as mean ± S.E.M., n = 6-9 mice per group, two-way ANOVA with Bonferroni's post hoc tests.

4.4.3.8 Aortic rings from ApoE$^{-/-}$ mice do not exhibit reduced sensitivity to exogenous nitric oxide

The sensitivity of aortic rings to NO was unaffected by PVAT, increasing age and the development of atherosclerosis in both ND and WD-fed ApoE$^{-/-}$ mice; aortic rings relaxed to baseline when exposed to sodium nitroprusside (10 µM) (P = NS, n = 6-9 mice per group, Figure 4.7). These findings were similar to those observed in C57BL/6 mice (Appendix 2.4Ci and ii).

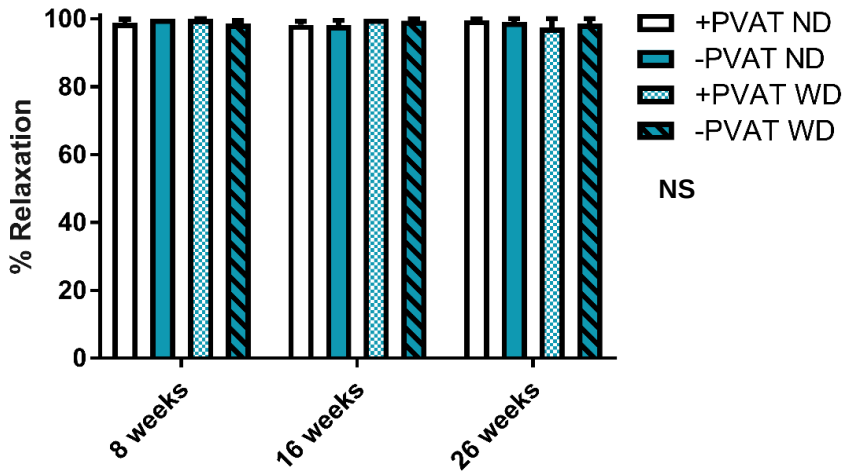

Figure 4.7 The sensitivity of aortic rings to exogenous nitric oxide is unaffected by PVAT, ageing or a Western-type diet in ApoE$^{-/-}$ mice *Endothelium-independent relaxation of phenylephrine-constricted aortic rings to 10 µM sodium nitroprusside, was unaltered by the presence of PVAT, increasing age or a WD. ND = normal diet, NO = nitric oxide, PVAT = perivascular adipose tissue, WD = Western-type diet. Data are presented as mean ± S.E.M, n = 6-9 mice per group, two-way ANOVA with post hoc Bonferroni's multiple comparisons test.*

4.4.4 Ageing and a Western-type diet do not alter the weight of PVAT surrounding the aortic arch and thoracic aortae in ApoE$^{-/-}$ mice

Increasing age had no effect on the measured weight of PVAT surrounding the aortic arch and thoracic aortae (P = NS; n = 3-8 mice per group, Figure 4.8). Additionally, a WD did not alter the weight of PVAT that encased the aortae of ApoE$^{-/-}$ mice at any of the experimental time-points in comparison to ND-fed ApoE$^{-/-}$ mice (ND versus WD: P = NS; n = 3-8 mice each, Figure 4.8).

The weight of PVAT surrounding the aortae of ND-fed ApoE$^{-/-}$ mice was compared to age and diet-matched C57BL/6 mice (Appendix 2.8A). In comparison to 26-week ND-fed ApoE$^{-/-}$ mice, the amount of PVAT encasing the aorta was significantly greater in the C57BL/6 strain (ApoE$^{-/-}$ versus C57BL/6: P = 0.002, n = 3 and 6 mice, respectively, Appendix 2.8A).

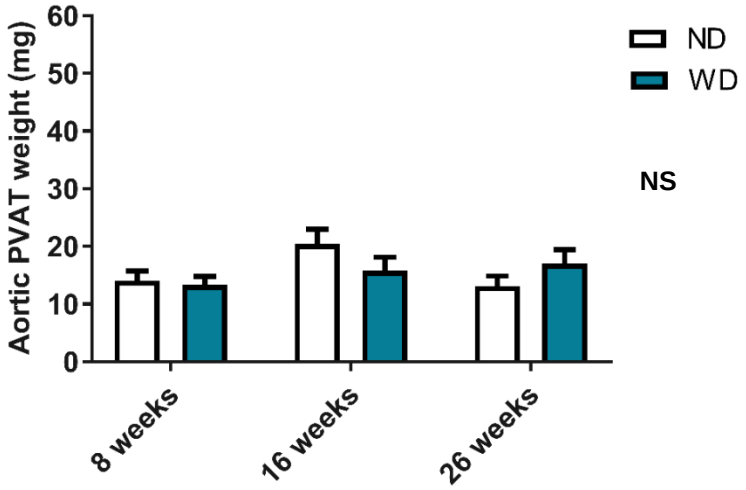

Figure 4.8 The weight of PVAT encasing the aortae of ApoE$^{-/-}$ mice is unaffected by ageing or a Western-type diet

There were no differences in PVAT weight between any of the experimental groups regardless of increasing age or extended periods on a WD. ND = normal diet, PVAT = perivascular adipose tissue, WD = Western-type diet. Data are presented as mean ± S.E.M, n = 3-8 mice per group, two-way ANOVA with post hoc Bonferroni's multiple comparisons test.

4.4.5 The white adipocyte population within the aortic PVAT is unaffected by ageing or a Western-type diet in ApoE$^{-/-}$ mice

The effects of ageing and a WD on ApoE$^{-/-}$ aortic PVAT composition was visualised using haematoxylin and eosin staining (Figure 4.9Ai-vi)

The composition of the aortic PVAT was assessed by calculating the total area occupied by white adipocytes, as a proportion of total PVAT area, and measuring the area of these individual white adipocytes. Ageing in ApoE$^{-/-}$ mice did not have a significant impact on the proportion of white adipocytes within the aortic PVAT (P = NS; n = 3-4 mice per group, Figure 4.9B). Furthermore, a WD did not influence the percentage area occupied by white adipocytes within the aortic PVAT (ND versus WD: P = NS; n = 3-4 mice per group, Figure 4.9B).

The size of white adipocytes within the aortic PVAT was measured. Whilst ageing on a ND had little effect on mean white adipocyte size within the aortic PVAT (P = NS; n = 3-4 mice per group; Figure 4.9C) an increase was observed in WD-fed mice at the 8 and 16-week time-points however, this was not found to be significant with post hoc testing (ND versus WD: 8-weeks: P = 0.06; 16-weeks P = 0.08; 26-weeks P > 0.99; n = 3-4 mice per group, Figure 4.9C).

The aortic PVAT composition data from ND-fed ApoE$^{-/-}$ mice was compared to age and strain matched C57BL/6 mice (Appendix 2.8B and C). Whilst not statistically significant, the percentage area occupied by white adipocytes in 8-week ND-fed ApoE$^{-/-}$ mice was larger than that of the C57BL/6 group and the white adipocyte area was greater. Nevertheless, after 16 weeks on a ND the percentage area of aortic PVAT occupied by white adipocytes was increased in the C57BL/6 mice and more in line with the ApoE$^{-/-}$ measurements. In summary, the aortic PVAT of ApoE$^{-/-}$ mice was resistant to age-induced changes and the effects of a WD.

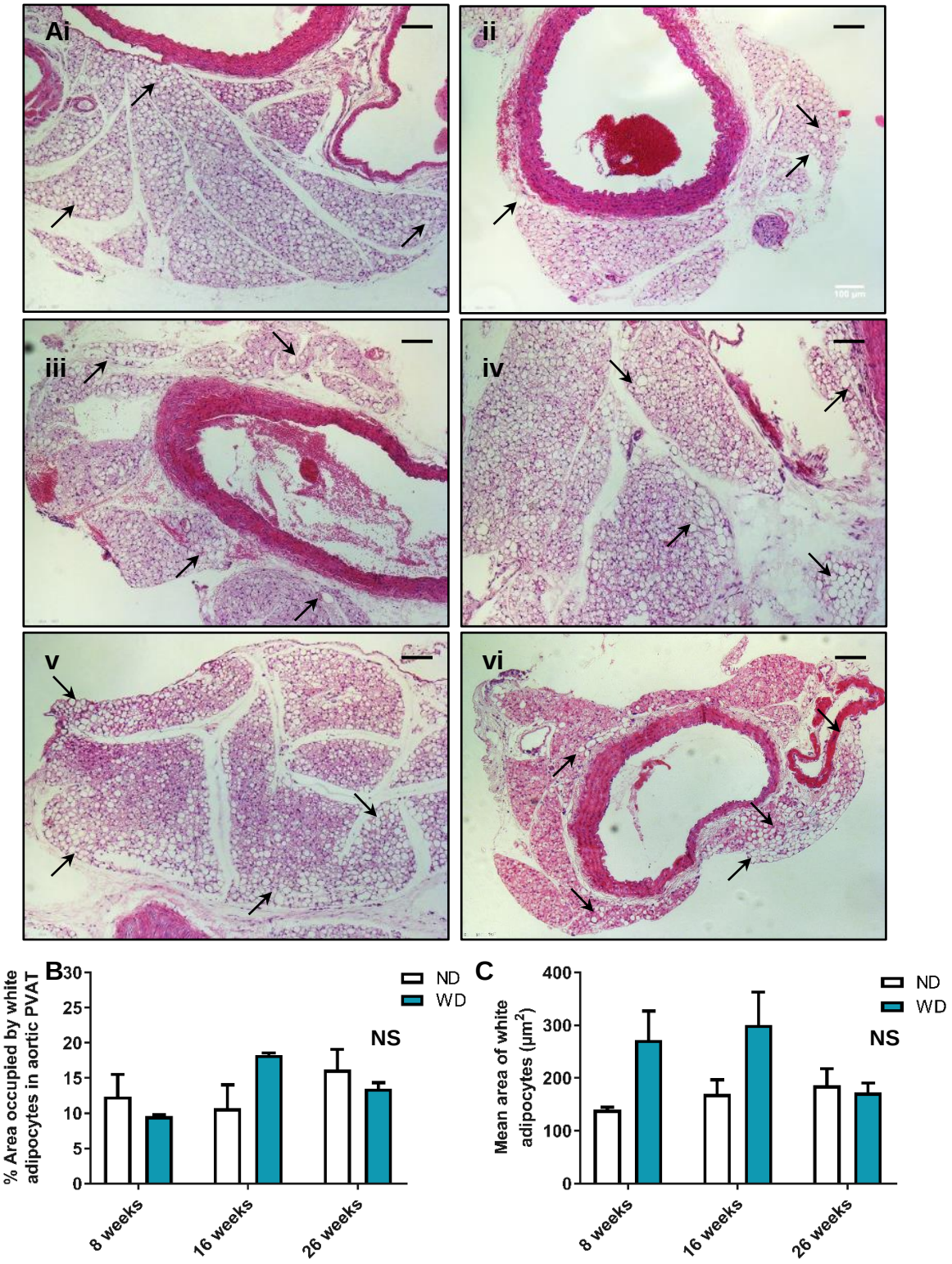

Figure 4.9 The white adipocyte population within the aortic PVAT of ApoE$^{-/-}$ mice is unaffected by ageing or a Western-type diet

A) Haematoxylin and eosin stained thoracic aortae, with PVAT, from 8-week, i) ND, ii) WD, 16-week iii) ND, iv) WD and 26-week v) ND and vi) WD-fed ApoE$^{-/-}$ mice, examples of white adipocytes are highlighted by arrows. B) The percentage area of aortic PVAT occupied by white adipocytes did not significantly increase with ageing or a WD. C) White adipocyte size was unaltered by ageing but a WD resulted in an increased white adipocyte area, but this was not found significant with post hoc tests. Representative images obtained at 10X magnification. Scale bars represent 100 µm. ND = normal diet WD = Western-type diet. Data are expressed as mean ± S.E.M., n = 3-4 mice per group, two-way ANOVA with Bonferroni's post hoc multiple comparisons test.

4.4.6 Superoxide production within the aortic PVAT of ApoE$^{-/-}$ mice is unchanged with ageing or a Western-type diet

The effect of increasing age and a WD on the generation of superoxide within the aortic PVAT of ApoE$^{-/-}$ mice was evaluated using dihydroethidium (DHE) staining. Superoxide was detected in the aortic PVAT of each experimental group (Figure 4.10Ai-vi) although none was detected in the negative DMSO control (Figure 4.10B). The quantity of DHE^{+} nuclei within the PVAT of ND-fed mice was not significantly altered with ageing (P = NS, n = 3-4 mice per group, Figure 4.10C).

In addition, the effect of a WD on superoxide production in aortic PVAT was assessed and no significant differences were found between any of the age-matched groups (ND versus WDP = NS; n = 3-4 mice per group, Figure 4.10C).

The presence of superoxide within the aortic PVAT of ND-fed ApoE$^{-/-}$ mice was compared to the genetic background C57BL/6 strain (Appendix 2.8D). Superoxide was substantially increased in ApoE$^{-/-}$ mice in comparison to the C57BL/6 strain in both the 8 and 16 week ND-fed groups (ApoE$^{-/-}$ versus C57BL/6: 8 weeks: P = 0.002; 16 weeks: P = 0.0007, n = 3 mice per group Appendix 2.8D). However, this effect was lost in the 26-week ND-fed groups and no differences in superoxide levels were observed (P = NS, n = 4 mice per group, Appendix 2.8D).

Superoxide production was elevated in aortic PVAT of ApoE$^{-/-}$ compared to C57BL/6. Additionally, the presence of extensive atherosclerotic lesions within the lumen of the aorta (Figure4.1A) did not influence the amount of superoxide in the surrounding PVAT.

4.4.7 The infiltration of Mac-3^{+} cells within the aortic PVAT of ApoE$^{-/-}$ mice is unchanged with ageing or a Western-type diet

Macrophage infiltration within the aortic PVAT of ageing ApoE$^{-/-}$ mice was assessed using Mac-3 immunostaining (Figure 4.11Bi-vi). Mac-3^{+} cells were observed in the PVAT of each mouse aorta examined.

Ageing did not alter the number of infiltrating Mac-3^{+} cells within the aortic PVAT of ND-fed ApoE$^{-/-}$ mice (P = NS each comparison; n = 3-4 mice per group, Figure 4.12C)

Additionally, a WD was not associated with a change in the number of infiltrated Mac-3^{+} cells within the aortic PVAT of the ApoE$^{-/-}$ mice in comparison to age-matched ND-fed mice (ND versus WD: P = NS; n = 3-4 mice per group, Figure 4.12C).

Furthermore, there were no differences in the numbers of Mac-3^{+} infiltrating cells within the aortic PVAT of ND-fed ApoE$^{-/-}$ and C57BL/6 mice, even though atherosclerotic disease was present within the aortae of ApoE$^{-/-}$ mice (ApoE$^{-/-}$ versus C57BL/6: P = NS, n = 3 mice per group, Appendix 2.8E).

These findings demonstrate that the number of infiltrating Mac-3^{+} cells within the aortic PVAT of ApoE$^{-/-}$ mice is unchanged with ageing or a WD, irrespective of atherosclerotic disease progression within the aortae of ApoE$^{-/-}$ mice.

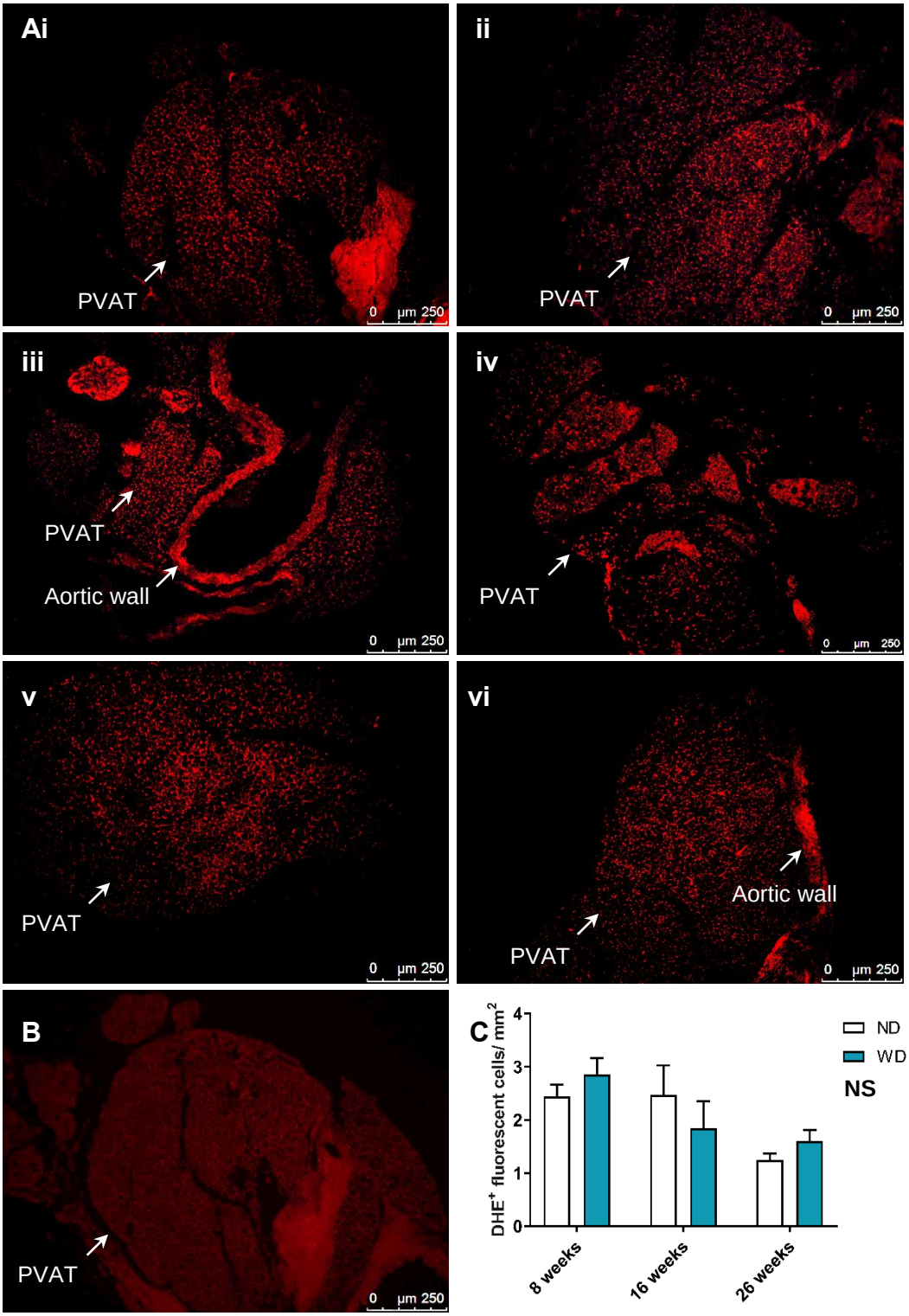

Figure 4.10 ROS production is not significantly altered with ageing or a Western-type diet in the aortic PVAT of ApoE$^{-/-}$ mice

Sections of thoracic aortae with PVAT were stained with DHE to detect the presence of ROS, indicated by punctate fluorescence. A) DHE^{+} nuclei were observed in each group i) 8-week ND, ii) WD, iii) 16-week ND, iv) WD and 26-week v) ND and vi) WD but none was found in the B) DMSO-incubated PVAT control. C) The amount of ROS detected in the 26-week WD group was not significantly lower than the 8-week diet-matched mice. Representative images obtained at 10 X magnification. Scale bars represent 250 µm. ROS was quantified in 5 fields of view per section per animal. DHE = dihydroethidium, ND = normal diet, PVAT = perivascular adipose tissue, WD = Western-type diet. Data are expressed as mean ± S.E.M., DHE^{+} staining presented as cells/mm^2 of PVAT, n = 3-4 mice per group, two-way ANOVA with Bonferroni's post hoc multiple comparisons test.

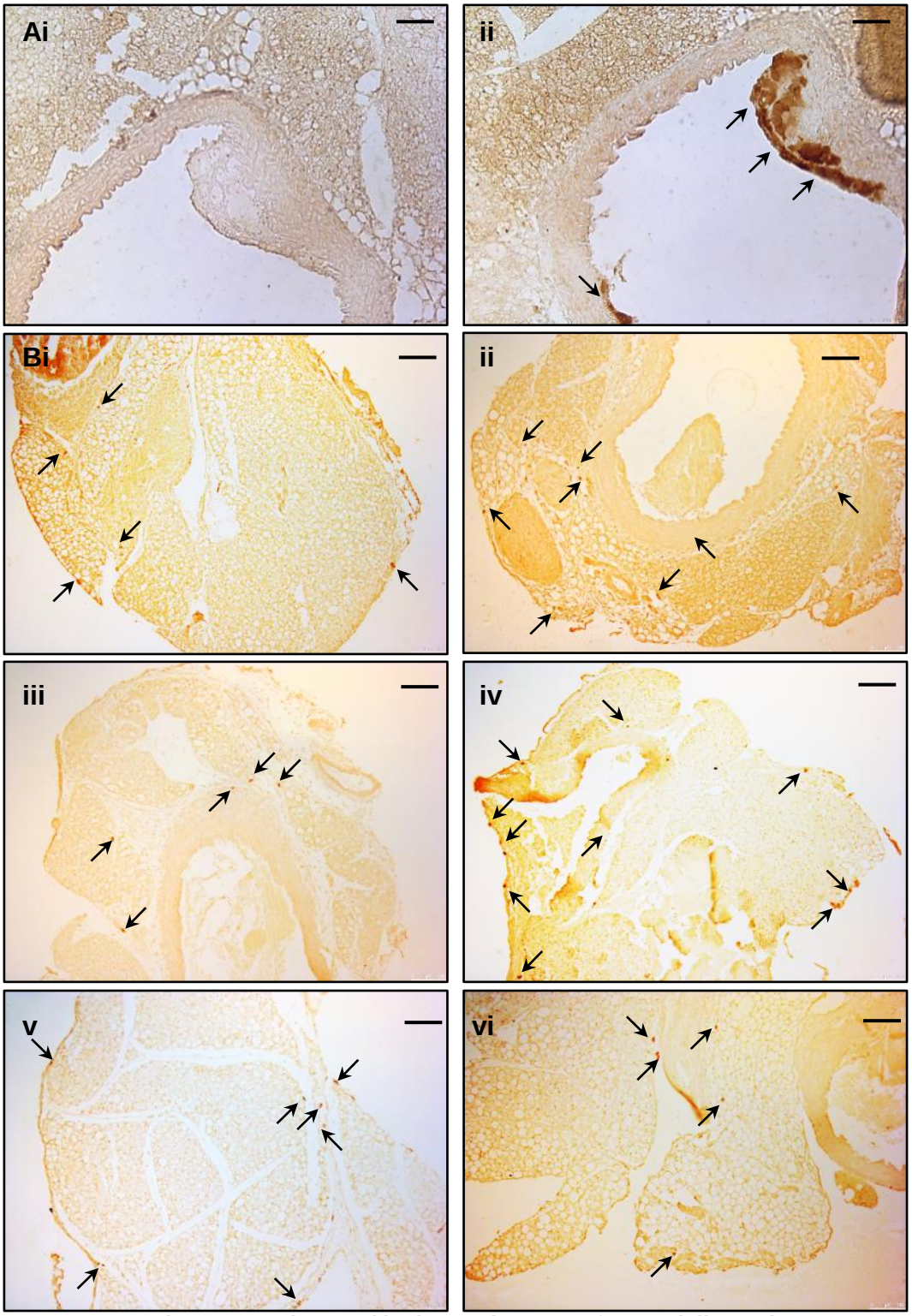

Figure 4.4 Macrophages are observed in the aortic PVAT of normal diet and Western-type diet-fed ApoE$^{-/-}$ mice

Immunostaining for macrophages with Mac-3 was performed on sections of thoracic aortae with PVAT. A) The aortic arch of an atherosclerotic ApoE$^{-/-}$ mouse was used as a control i) IgG and ii) positive control, Mac-3^{+} brown staining was observed within the atherosclerotic plaque. B) Representative images of ApoE$^{-/-}$ mice after: i) 8-weeks ND and ii) WD, iii) 16-weeks ND and iv) WD and 26-weeks v) ND and vi) WD post weaning. Photomicrographs obtained at 10X magnification. Scale bars represent 100 µm and examples of Mac-3^{+} staining are highlighted by arrows.

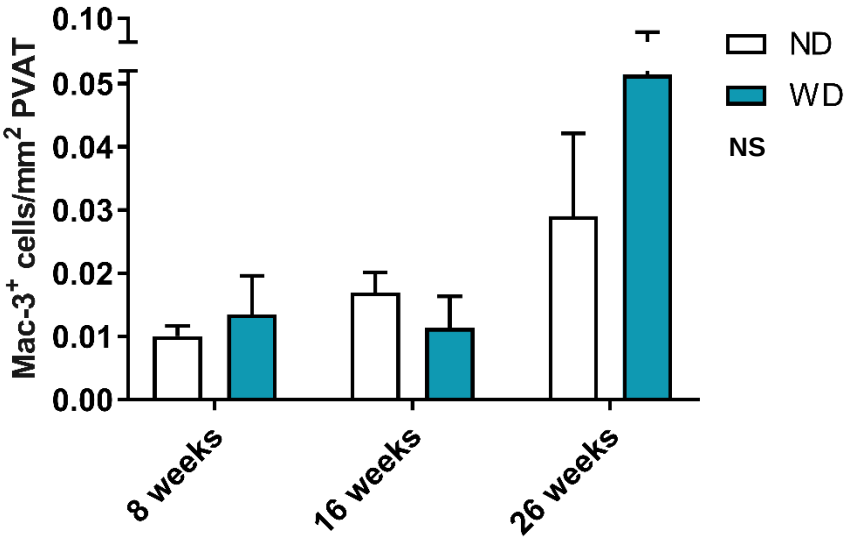

Figure 4.5 Macrophage infiltration of the aortic PVAT of ApoE$^{-/-}$ mice is similar in all experimental groups regardless of age or diet

Total PVAT area was measured and total number of Mac-3^{+} cells within the PVAT quantified. Whilst an increase in Mac-3^{+} cells was observed in the PVAT of the 26-week ND and WD-fed ApoE$^{-/-}$ mice, compared to the younger groups, no significant differences were found. Additionally, a WD did not increase macrophage numbers within the aortic PVAT at any of the time-points in comparison to age-matched ND-fed ApoE$^{-/-}$ mice. ND = normal diet, PVAT – perivascular adipose tissue, WD = Western-type diet. Data are expressed as Mac-3^{+} cells/mm^{2} PVAT, mean ± S.E.M., n = 3-4 mice per group, two-way ANOVA with Bonferroni's post hoc multiple comparisons test.

4.5 Discussion

The present study investigated the impact of ageing and a high fat Western diet on the function and morphology of aortic PVAT in the ApoE$^{-/-}$ mouse.

Key findings:

- Endothelial dysfunction was not observed in the aortae of ND or WD -fed ApoE$^{-/-}$ mice despite the presence of atherosclerotic lesions along the luminal surface of the aortae.
- The aortic PVAT of ApoE$^{-/-}$ mice was dysfunctional and did not exert an anti-contractile effect on aortic rings; this was potentially due to decreased basal eNOS activity resulting in an attenuation of PVAT-derived NO.
- Feeding the ApoE$^{-/-}$ mice a WD did not alter the vascular reactivity of aortic PVAT.
- The aortic PVAT of ApoE$^{-/-}$ mice exhibited an aged phenotype when assessed morphologically.

4.5.1 Hypercholesterolaemia is augmented in Western-type diet ApoE$^{-/-}$ mice

Hypercholesterolaemia and spontaneous lesion development within the vasculature are key features of the ApoE$^{-/-}$ mouse therefore, these aspects along with a number of factors linked with

atherosclerosis and cardiovascular risk factors were investigated to confirm the manifestation of dyslipidaemia and atherosclerotic disease within the ApoE$^{-/-}$ colony housed at The University of Manchester (Zhang et al. 1992).

Three distinct time-points were selected, from the comprehensive observations recorded in other studies, in order to demonstrate the progression of atherosclerosis: 8-weeks (post weaning) when fatty streak formation is first apparent in ApoE$^{-/-}$ mice; 16-weeks (post weaning) when intermediate lesions are present, and finally 26-weeks (post weaning) when extensive atheromas have formed (Zhang et al. 1992; Reddick et al. 1994; Farrell 2008).

For the purposes of this study, cholesterol, HDL-cholesterol, triglycerides and glucose levels were determined to assess how the progression of atherosclerosis and a WD was related to the serum profile of the ApoE$^{-/-}$ mice. In accordance with previous research, WD-fed ApoE$^{-/-}$ mice exhibited severely enhanced hypercholesterolaemia compared to ND age-matched ApoE$^{-/-}$ mice. Hyperlipidaemia is a fundamental prerequisite for the development of atherosclerotic lesions thus, augmented lipid levels accelerate the progression and severity of atherosclerotic disease in humans and ApoE$^{-/-}$ mice (Zhang et al. 1992; Moghadasian et al. 2001). Also of note, ND-fed ApoE$^{-/-}$ mice exhibited elevated cholesterol levels when compared to the background C57BL/6J strain (Plump et al. 1992; Hofmann et al. 2008).

In further agreement with previous works, which demonstrated that ApoE$^{-/-}$ mice develop hyperlipidaemia typified by augmented levels of VLDL and diminished HDL, HDL cholesterol levels were significantly lower in ApoE$^{-/-}$ mice when compared to C57BL/6J (Plump et al. 1992; Zhang et al. 1992). However, no significant differences in HDL levels were observed between ND or WD-fed ApoE$^{-/-}$ mice. This finding is also supported by previous work which found no differences between ND or WD-fed ApoE-deficient mice after two and a half weeks on the respective diets (Plump et al. 1992). This could suggest that lipid metabolism in the ApoE$^{-/-}$ mouse adapts swiftly to diet modification and from that point onwards remains largely unchanged as time progresses. In wild-type mice the greater part of cholesterol is in the form of HDL whilst in ApoE$^{-/-}$ mice ApoB-containing lipoproteins supply the bulk of plasma cholesterol. This shift in lipidemic profile results in a dramatic reduction (approximately 90%) in HDL: total cholesterol or HDL:LDL levels (Moghadasian et al. 2001).

This study did not observe any differences between triglyceride levels in ND or WD-fed ApoE$^{-/-}$ mice nor were there any differences between age and diet-matched C57BL/6J mice. These results were surprising because it has been established in the ApoE-deficient mouse model, regardless of diet, that fasting plasma triglyceride levels are distinctly higher than in wild-type mice counterparts, and this is comparable to what is observed in humans who lack ApoE (Moghadasian et al. 2001; Gao et al. 2007a). This observed discrepancy is likely to be due to the use of non-fasted samples in this study. In humans, the serum lipid profile is routinely assessed after 12-14 hours of fasting. One of the main reasons for this is because postprandial triglycerides remain raised for several hours peaking at approximately 4-5 hours after consumption of food (Campos et al. 2005; Nordestgaard et al. 2007). However, overnight fasting of laboratory rodents has been proven to induce metabolic and cardiovascular stress including: lower heart rates and blood pressure as a result of the animal entering a state of torpor, a drop in body temperature and

reduced oxygen consumption (Swoap 2001; Williams et al. 2002; Tanner et al. 2010). The extent to which fasting challenges the animal may also be affected by the species genotype, gender or the diet the animal had been maintained on prior to fasting (Tanner et al. 2010). Therefore, it was decided that mice would not be fasted before experimentation due to the possible effects that withholding of food could have on vascular reactivity.

There were no observable differences in glucose levels in serum obtained from ApoE$^{-/-}$ mice maintained on either ND or WD over the duration of the experiments. Furthermore, glucose levels were similar to those recorded in age and diet-matched C57BL/6 mice. These data are supported by earlier work in this model that has demonstrated that adult ApoE$^{-/-}$ mice are more glucose tolerant and sensitive to insulin in comparison to wild-type controls (Gao et al. 2007a).

Previous studies in ND-fed ApoE$^{-/-}$ mice have demonstrated a shift in lipoproteins from HDL to VLDL and chylomicron remnants resulting in a pro-atherogenic lipid profile. The elevated cholesterol levels reflect a similar state to the human atherosclerotic condition. The lipid profiles of ApoE$^{-/-}$ mice have previously been shown to not alter with ageing, which is in agreement with the findings of this study (Plump et al. 1992; Zhang et al. 1992; Zhang et al. 1994; Meyrelles et al. 2011).

4.5.2 Phenotyping normal and Western-type diet-fed ApoE$^{-/-}$ mice

Diet-induced weight gain is a risk factor for the development of cardiovascular disease (Lavie et al. 2009). In this study ApoE$^{-/-}$ mice were fed a high fat WD (consisting of 21.4% crude fat and 0.2% cholesterol) to mimic the high-fat/high-sugar food increasingly available to humans, and the primary contributor to diet-induced weight gain (Cordain et al. 2005).

This study reported that the body weight of ApoE$^{-/-}$ mice was unaltered by a WD, in comparison to age-matched ND controls, until the final 26-week time-point post weaning; this suggests that ApoE$^{-/-}$ mice are to some extent resistant to diet-induced weight gain. Similar findings have been reported after 9 weeks of high fat feeding and for longer durations of feeding for up to 24 weeks (Karagiannides et al. 2008; Houtkooper et al. 2011; Pereira et al. 2012). Previous studies also demonstrated that deletion of the ApoE gene in mice genetically predisposed to diet-induced weight gain resulted in an inhibition of adiposity (Crauwels et al. 2000). The body weight of the ND-fed ApoE$^{-/-}$ mice increased over the 8- 26-week time-points post weaning; this observation can most likely be attributed to the normal growth of the animals.

It has previously been demonstrated that plasma cholesterol levels are inversely correlated with an increase in bodyweight and fat accumulation within the ApoE$^{-/-}$ mouse (Karagiannides et al. 2008). Previous studies have demonstrated that the genetic deletion of ApoE$^{-/-}$ impairs the removal of triglycerides and that this confers protection against diet-induced weight gain in the ApoE$^{-/-}$ mouse (Köhn et al. 2012). Also, it has been established that ApoE$^{-/-}$ mice are leaner than wild-type mice and more resistant to high fat diet related increases of adiposity compared to C57BL/6 mice in spite of the fact that the ApoE knockout model is more prone to oxidative stress and inflammation within the adipose tissue (Gao et al. 2007a; Pereira et al. 2012). Whilst no differences in body weight were observed between age and diet-matched ND-fed ApoE$^{-/-}$ mice in comparison to the C57BL/6 strain, C57BL/6J mice were not fed a WD in this study and so

therefore the difference in adiposity of high fat fed ApoE$^{-/-}$ and C57BL/6J mice could not be compared.

The mechanism behind why the deletion of the ApoE$^{-/-}$ gene confers protection against diet-induced weight gain in mice remains unclear. However, it has been postulated that ApoE may regulate triglyceride storage in adipocytes (Yue et al. 2004; Huang et al. 2006). An additional explanation for the observed resistance to diet-induced weight gain in ApoE$^{-/-}$ mice could be due to a reduction in food intake and increased energy expenditure observed in ApoE$^{-/-}$ mice crossed with a genetically obese mouse strain (KKAy), suggesting that ApoE plays a role in energy metabolism (Gao et al. 2007a).

When the heart weight and heart weight to body weight ratio data were assessed in the ApoE$^{-/-}$ mice, similar patterns were observed in both data sets. The obtained measurements from ND-fed ApoE$^{-/-}$ mice tended to be higher than in the WD-fed counterparts, this was significant at the 26-week time-points for both heart weight and heart weight to body weight ratio. This finding could suggest that cardiac hypertrophy, which has previously been reported in WD-fed mice of this strain, did not take place (Qin et al. 2010). This finding is further supported by no differences in heart weight observed between ND-fed ApoE$^{-/-}$ and C57BL/6 mice at any of the time-points.

Deletion of the ApoE$^{-/-}$ gene appeared to confer a protective effect against diet-induced non-alcoholic fatty liver disease (NAFLD) and this is supported by previous works demonstrating that WD-fed C57BL/6 mice were more sensitive to diet-induced NAFLD than ApoE$^{-/-}$ mice (Karavia et al. 2011). Livers from both ND and WD-fed ApoE$^{-/-}$ mice did not exhibit hepatomegaly, this finding is also supported by previous research (Karavia et al. 2011). Additionally, no differences in liver weight were observed between age and diet-matched ND-fed C57BL/6 mice. However, the appearance of livers from WD-fed mice was altered and they appeared significantly paler than the livers of their ND age-matched counterparts. This could indicate that the livers were beginning to undergo steatosis (the infiltration of liver cells with fat) however, this was not examined.

The gross weight of the spleen was used as an indirect marker of inflammation in the ApoE$^{-/-}$ mice. No differences were observed between the ND or WD groups at any of the experimental time-points. These findings conflict with other research which demonstrated a high fat diet induced splenomegaly in ApoE$^{-/-}$ mice. It is possible these differences are due to variations in the composition of the diet used (Marungruang et al. 2016). However, splenomegaly was observed in the ApoE$^{-/-}$ mice after 16 and 26 weeks on a ND in comparison to C57BL/6 mice which may indicate that the inflammatory profile of the ApoE$^{-/-}$ mice is raised.

The epididymal fat pads of the ApoE$^{-/-}$ mice were used as an indicator of diet-induced weight gain because increased abdominal adiposity in humans is associated with increased cardiovascular risk (Després 2012). Whilst the epididymal fat pads of ND-fed ApoE$^{-/-}$ mice did not significantly increase in weight with ageing, a dramatic increase was recorded in WD-fed mice after 16 and 26-weeks of high fat feeding. This finding was also reflected in the observation that the epididymal adipocytes of WD-fed ApoE$^{-/-}$ mice displayed signs of hypertrophy, although no significant differences were observed. Furthermore, when age-matched ND-fed C57BL/6 epididymal fat pads were compared to ND-fed ApoE$^{-/-}$ mice, a dramatic increase in fat pad size was observed in

the C57BL/6 group after 26 weeks on the ND. This was reflected in the adipocyte sizes observed within the fat pads. This data is supported by similar findings which demonstrated that ApoE$^{-/-}$ mice have less body fat and smaller adipocytes compared with wild-type controls (Huang et al. 2006).

Taken together, these data demonstrate that when fed a ND, ageing of ApoE$^{-/-}$ mice up to 26 weeks post weaning does not significantly alter their lipid and glycaemic profiles or organ weights. However, other studies have shown age associated and age-dependent morphological and biochemical changes in 20-week old ApoE$^{-/-}$ mice including fibrosis, elevated pro-inflammatory cytokines and a decrease in anti-oxidant enzymes within the kidney, liver and heart. The absence of these alterations in age-matched controls suggests that physiological ageing is accelerated in the ApoE$^{-/-}$ mouse (Bonomini et al. 2010).

4.5.3 A Western-type diet accelerates the progression and increases the severity of atherosclerotic disease within the aortae of ApoE$^{-/-}$ mice

En face analysis of aortae from ApoE$^{-/-}$ mice demonstrated that a WD accelerated the development and progression of atheromatous lesions on the luminal surface of the aortae in comparison to age-matched ND-fed mice. These results are consistent with previous reports (Zhang et al. 1992). However, no significant increases in lesion burden were observed in ND-fed mice over this time-course. It has been documented that atherosclerotic lesions first begin to develop within the aortic root followed by the aortic arch and eventually descend along the thoracic aorta, a similar lesion distribution was observed within the aortic arch and thoracic aorta in this study (Nakashima et al. 1994).

Oil Red O was used to visualise lipid-laden deposits along the aorta. This stain does not alter or damage plaque composition. This method of lesion analysis is however only a two-dimensional approach and does not take into account the complex three-dimensional plaques that are observed in ApoE$^{-/-}$ mice fed a high fat diet for a long duration (Joshi et al. 2009). It should be acknowledged that Oil Red O staining is not the only approach for the quantification of atherosclerotic lesion burden and other techniques, such as staining sections of the aortic root with Miller's Elastin Van Gieson or the use of Sudan stains for en face analysis, could have been utilised (Venegas-Pino et al. 2013; Agarwal et al. 2014; Lin et al. 2015).

4.5.4 Vascular reactivity studies to assess the influence of aortic PVAT from ApoE$^{-/-}$ mice on contractile and relaxation responses

In the majority of studies conducted on the thoracic aortae of ApoE$^{-/-}$ mice, the adventitia and surrounding PVAT were removed. Subsequently, information detailing the effect of PVAT on vascular function in the ApoE$^{-/-}$ mouse is limited. PVAT has previously been demonstrated to lose its beneficial anti-contractile effects in states of metabolic disturbance and in, in some studies, exert a pro-contractile effect on isolated arteries (Szasz et al. 2013). Increased contraction within the aortae of ApoE$^{-/-}$ mice, mediated by PVAT, could potentially promote the development of atherosclerosis due to increased turbulence of blood flow and consequently, damage the endothelium. Furthermore, the presence of PVAT has, in some studies, been reported to induce endothelial dysfunction (Ketonen et al. 2010; Payne et al. 2010; Xia et al. 2016). Therefore, the

following experiments were conducted on PVAT-intact or denuded aortic rings to determine the influence of PVAT on contraction and relaxation responses in ApoE$^{-/-}$ mice.

The contractile responses of ApoE$^{-/-}$ mice to a depolarising stimulus were unaffected by PVAT, increasing age or a Western-type diet. These findings are similar those observed in this study in the C57BL/6 strain and no differences were observed between the aortic rings, in the presence or absence of PVAT, in comparison to the age-matched ND-fed ApoE$^{-/-}$ mice. These findings are in accordance with previous studies from this lab and others which have demonstrated that the contractions of PVAT-denuded aortic rings from C57BL/6 and ApoE$^{-/-}$ mice were similar in ND and WD-fed conditions (Van Assche et al. 2007; Cobb 2013). Therefore, these data suggest that the L-type calcium channels of ApoE$^{-/-}$ mice are not dysfunctional and that hypercholesterolaemia does not disrupt their function.

4.5.4.1 Endothelial dysfunction is not observed in the aorta of normal or Western-type diet-fed ApoE$^{-/-}$ mice despite the presence of atherosclerotic lesions

In vitro studies on the aortae of ApoE$^{-/-}$ mice have determined that endothelium-dependent relaxation, in response to acetylcholine, is predominantly due to NO (Bonthu et al. 1997). In addition, endothelial dysfunction, a hallmark of atherosclerotic disease in humans, has been reported in ApoE$^{-/-}$ mice (Yang et al. 1999; d'Uscio et al. 2001a). PVAT has been demonstrated to influence relaxation responses of the endothelium both in health and disease (Gao et al. 2007b; Lee et al. 2009; Ketonen et al. 2010; Xia et al. 2016). Therefore, the vasodilatory responses of aortic rings to acetylcholine, an endothelium-dependent vasodilator, were assessed to determine if the presence of PVAT modulated relaxation of isolated aortic rings and to determine if the endothelium remained functional.

The presence of PVAT on aortic ring preparations did not influence vasodilation in any of the ApoE$^{-/-}$ experimental groups. This finding was replicated in the C57BL/6 studies from this investigation (Chapter 3). However, a previous study has reported that abdominal aortic PVAT promotes endothelial dysfunction in diet-induced obese C57BL/6 mice through mechanisms associated with increased NADPH oxidase-derived oxidative stress and elevated pro-inflammatory cytokine production (Ketonen et al. 2010). The discrepancies between the studies could be attributed to the use of different mouse strains, inbred as opposed to knockout, and the use of different sections of the aortae. This present study used aortic rings from the thoracic area, which displays brown adipose tissue (BAT) -like characteristics whereas the previous study used abdominal aortic PVAT which is more white adipose tissue (WAT) -like and more susceptible to inflammation (Fitzgibbons et al. 2011). These data may suggest that the aortic PVAT of ApoE$^{-/-}$ mice does not alter endothelial responses to acetylcholine and, potentially, does not promote endothelial dysfunction within the aortae of ApoE$^{-/-}$ mice.

Endothelial dysfunction has been well characterised in the arteries of ApoE$^{-/-}$ mice and has been attributed to the development of hypercholesterolaemia and the formation of lesions within the aorta (Bonthu et al. 1997; Deckert et al. 1999; Yue et al. 2004; Johansson et al. 2005; Huang et al. 2006; Vasquez et al. 2012). However, no significant impairment of endothelial function was observed at the 26-week time-point in either ND or WD-fed ApoE$^{-/-}$ mice. This finding is supported by previous studies which demonstrated that endothelial dysfunction is not observed until after

more extensive periods of high fat feeding, of up to 29 weeks in ApoE$^{-/-}$ mice (d'Uscio et al. 2001a). Moreover, under ND conditions, the endothelium of ApoE$^{-/-}$ mice has been shown to remain functional up to the age of 6-months (Yaghoubi et al. 2000).

4.5.4.2 The aortic PVAT of ApoE$^{-/-}$ mice is dysfunctional and does not exert an anti-contractile effect in normal diet or Western-type diet-fed mice

The capacity of aortic PVAT from ApoE$^{-/-}$ mice to modulate vascular tone has not previously been investigated. This study demonstrated that the aortic PVAT of ApoE$^{-/-}$ mice did not alter contractions to cumulative doses of phenylephrine in ageing ND or WD-fed mice.

The effect of increasing age was assessed in PVAT-denuded and PVAT-intact aortic preparations of ND-fed ApoE$^{-/-}$ mice. In the absence of PVAT, contractions to cumulative doses of phenylephrine were similar between each time-point. A similar effect was observed in the PVAT-intact aortic rings and no changes in contractility were observed with increasing age. Furthermore, the contractions of WD-fed mice were analogous to the ND-fed mice and severe hypercholesterolaemia did not influence the contractility of aortic rings with or without PVAT. The observation that in the presence of PVAT the aortic rings of WD-fed ApoE$^{-/-}$ mice did not exhibit altered contractions to ND-fed mice was surprising. Previous studies have shown that a high fat diet increased the contraction of arteries, in the presence of PVAT, in rodents due to a variety of mechanisms including decreased PVAT-derived NO bioavailability, increased oxidative stress in the PVAT and the release of PVAT-derived constricting factors (Ketonen et al. 2010; Ma et al. 2010; Meyer et al. 2013; Zaborska et al. 2016). However, these studies were performed in inbred rodent strains that had not been genetically altered therefore they are not directly comparable to the current study. A potential explanation for the lack of an effect of a WD on aortic contractions from ApoE$^{-/-}$ mice could be that the aortic rings were maximally contracted and therefore no further effect of a WD could be observed.

ApoE$^{-/-}$ mice are hypercholesterolaemic and this condition is augmented in mice fed a high fat diet which was demonstrated in this present study (Plump et al. 1992). There are conflicting reports surrounding the effects of hypercholesterolaemia on contractile responses of murine aortic rings to phenylephrine, with studies demonstrating increased, decreased or, similar to this study, no change in contractile response (Fransen et al. 2008; Kurtel et al. 2013; Brinkmann et al. 2014). However, these differences could potentially be due to the use of different mouse strains and experimental conditions. For example, the reported increased contractile response in hypercholesteraemic ApoE$^{-/-}$ mice, in comparison to C57BL/6, was observed in the presence of indomethacin, a cyclooxygenase inhibitor, therefore direct comparisons cannot be made with this study (Fransen et al. 2008). In support of the findings of this study, hypercholesterolaemia has not been found to have an effect on the contractions of arteries from humans (Goode et al. 1995; Cooper et al. 1998). However, these studies were conducted on small arteries and used different agonists to induce contraction.

4.5.4.3 Contractions of PVAT-intact aortic rings from 8 and 16-week normal diet-fed ApoE$^{-/-}$ mice, is significantly enhanced compared to age and diet-matched C57BL/6 responses

The contractile responses of ND-fed ApoE$^{-/-}$ mice were compared to the age and diet-matched C57BL/6 strain in an attempt to elucidate any underlying differences in the responses of PVAT-

intact or PVAT-denuded aortic rings. The contractions of PVAT-denuded aortic preparations were similar, which could suggest that deletion of the ApoE gene does not significantly alter VSM responses to phenylephrine. However, the role of the endothelium in modulating aortic contractility was not assessed and further investigation using endothelium-denuded aortic rings to confirm aortic VSM was unchanged are required.

Conversely, the responses of PVAT-intact aortic rings were significantly increased in ApoE$^{-/-}$ mice fed a ND for 8 or 16 weeks in comparison to age-matched C57BL/6 mice. Previously in the study of the C57BL/6 strain, NO was found to mediate the anti-contractile effect of PVAT in these two groups, but this effect was lost in the oldest mice and was potentially the result of decreased PVAT-derived NO bioavailability. This data potentially suggested that the aortic PVAT of ApoE$^{-/-}$ mice does not exert an anti-contractile effect due to a lack of PVAT-derived NO and subsequently led to the investigation of NO, and its contribution to vascular reactivity, via pharmacological inhibition of NOS in the aortae of ApoE$^{-/-}$ mice.

4.5.4.4 The aortic PVAT of ApoE$^{-/-}$ mice does not exert an anti-contractile effect, which is potentially due to reduced basal activity of endothelial nitric oxide synthase

It has recently been proven that rodent aortic PVAT expresses eNOS (Araujo et al. 2015; Xia et al. 2016). The NOS inhibitor L-NNA was used to dissociate NO-mediated relaxation of the aortic rings from phenylephrine-induced contractions in ApoE$^{-/-}$ mice in this study. NOS inhibition with L-NNA did not result in any significant changes to aortic ring contraction in the presence or absence of PVAT. These data may suggest that eNOS synthesis/activity is decreased in the aortae of the ApoE$^{-/-}$ mouse resulting in a reduction in NO production. However, this requires further investigation as endothelial dysfunction was not observed in WD or ND-fed mice. Previous studies have demonstrated that NOS inhibition in the aortic rings of ApoE$^{-/-}$ mice results in an increase in contraction (Kauser et al. 2000; Fransen et al. 2008). The discrepancy between this study and others could be due to the use of a higher concentration of inhibitor, up to 300 µM in the other studies, or their use of indomethacin to block the production of vasoactive prostanoids (Kauser et al. 2000; Fransen et al. 2008). The concentration of NOS inhibitor used in this study, 50 µM, was chosen in an attempt to limit any possible off-target effects and because of its proven inhibition of NOS, described in the previous Chapter in the C57BL/6 strain.

Taken together, the phenylephrine dose response data may indicate a diminished basal (non-stimulated) NO bioavailability whilst normal agonist-stimulated NO release was retained. Therefore, the lack of an anti-contractile effect of PVAT, in comparison to C57BL/6 mice, may be due to an attenuation of PVAT-derived NO as a result of a reduced basal activity of eNOS.

In agreement with previous studies, the sensitivity of aortic smooth muscle to exogenous NO was unaffected by deletion of ApoE (Deckert et al. 1999; Kauser et al. 2000) . Furthermore, increasing age, the presence of PVAT and a WD had no effect on the ability of aortic preparations to relax when exposed to sodium nitroprusside (a potent NO donor). Contradictory to these findings, another study reported a diminished endothelium-independent relaxation response in the aortae of WD-fed ApoE$^{-/-}$ mice when lesions were present but no change in non-atherosclerotic carotid arteries (d'Uscio et al. 2001a; d'Uscio et al. 2001b). These data would suggest that VSM have reduced sensitivity to NO in the presence of atherosclerotic lesions.

4.5.5 The composition of aortic PVAT from ApoE$^{-/-}$ mice is not significantly altered by increasing age or a Western-type diet

The composition of aortic PVAT from ApoE$^{-/-}$ mice was assessed to determine if any morphological differences were present which could have contributed to the absence of an anti-contractile effect observed in these mice.

4.5.5.1 The weight of PVAT surrounding the aortae and its white adipocyte population is unchanged with increasing age or a Western-type diet in ApoE$^{-/-}$ mice

In this study, ApoE$^{-/-}$ mice were demonstrated to be resistant to diet-induced weight gain up until 26 weeks of high fat feeding. Also, previous studies have observed that ApoE$^{-/-}$ mice exhibit reduced fat deposition and smaller adipocytes than wild-type controls (Huang et al. 2006). This investigation found that the weight of PVAT encompassing the aortic arch and thoracic aorta of ApoE$^{-/-}$ mice is unchanged with increasing age or a WD. Furthermore, whilst no differences were observed after 8 or 16 weeks on a ND, the weight of PVAT surrounding the aortae of C57BL/6 mice was significantly heavier in comparison to age and diet-matched ApoE$^{-/-}$ mice.

The composition of aortic PVAT from ApoE$^{-/-}$ mice was assessed to determine if ageing or a WD induced any changes to the white adipocyte population. However, no statistically significant differences were observed between the groups when the percentage area occupied by white adipocytes were compared or when white adipocyte size was measured. These data were striking due to observations that in C57BL/6 mice fed a high fat diet for 20 weeks, with similar fat content to the one used in this study, the aortic PVAT architecture was distorted and enlarged white lipid droplets were observed (Fitzgibbons et al. 2011). Interestingly, the interscapular brown adipose tissue exhibited enlarged white adipocytes much earlier than the aortic PVAT after only 13 weeks on the high fat diet (Fitzgibbons et al. 2011). This clearly demonstrates that aortic PVAT of C57BL/6 mice is, to a certain extent, resistant to diet-induced weight gain and could imply that the aortic PVAT of ApoE$^{-/-}$ mice is protected even more extensively than C57BL/6 mice from the effects of a high fat diet.

The white adipocytes within the aortae of ApoE$^{-/-}$ mice could be considered to be under chronic hypoxic conditions because the average cell size exceeded 100 µm which is deemed to be the diffusional limit of oxygen (Hosogai et al. 2007). Hypoxia has been demonstrated to exert opposing effects on vascular reactivity and PVAT depending on the species and vascular bed. Mesenteric arteries from rats were exposed to hypoxic conditions for 2 and a half hours which resulted in the loss of the anti-contractile effect of PVAT whereas, when aortic rings from mice were subjected to hypoxic conditions for 30 minutes, the anti-contractile effect of PVAT was potentiated (Greenstein et al. 2009; Maenhaut et al. 2010). However, the aforementioned experiments were examples of acute hypoxia and may not accurately reflect what happens to the influence of PVAT on vascular reactivity when subjected to chronic hypoxia.

The aortic PVAT composition data from ND-fed ApoE$^{-/-}$ mice was compared to age and strain matched C57BL/6 mice. Whilst not statistically significant, the percentage area occupied by white adipocytes and the size of the adipocytes in 8-week ND-fed ApoE$^{-/-}$ mice was larger than that of the C57BL/6 group. These structural differences in the PVAT architecture of ApoE$^{-/-}$ mice could potentially have contributed to the PVAT dysfunction observed in the ApoE$^{-/-}$ mice. However, as

no significant changes occurred with increasing age or a WD this could explain why the contractions of aortic rings in the presence of PVAT were unchanged after extensive high fat feeding or in the oldest, 26-week diet-fed groups. Nevertheless, after 16 weeks on a ND the percentage area of aortic PVAT occupied by white adipocytes was increased in the C57BL/6 group and more in line with the ApoE$^{-/-}$ results. Additionally, the mean aortic white adipocyte areas were similar and as suggested previously, the changes observed in the C57BL/6 strain could potentially have contributed to the eventual loss of the anti-contractile effect of PVAT.

Overall, the PVAT composition data from the ApoE$^{-/-}$ and C57BL/6 mice could point towards the white adipocyte population within the aortic PVAT being an indicator of PVAT 'health'. The aortic PVAT of ApoE$^{-/-}$ mice appeared to have a greater percentage area occupied by white adipocytes and the white adipocytes themselves were larger from the outset in comparison to the C57BL/6 strain after 8 weeks on a ND. This could potentially have contributed to the absence of an anti-contractile effect of PVAT, as a result of hypoxic conditions, leading to lower basal activity of eNOS within the PVAT.

4.5.5.2 Superoxide production in the aortic PVAT of ApoE$^{-/-}$ mice is not significantly altered by increasing age or a Western-type diet

Oxidative stress is a natural physiological process. However, an imbalance of pro and anti-oxidant enzymes can result in the generation of excess ROS, such as superoxide, which can cause damage to the vasculature (Stapleton et al. 2010). The primary producers of ROS within the vasculature are macrophages and mitochondria (Harrison 1997). Hypercholesterolaemia and atherosclerosis have been linked to excess mitochondrial generation of ROS (Elahi et al. 2009). Furthermore, hypercholesterolaemia could potentially trigger upregulation of ROS-producing enzymes.

ApoE has antioxidant and anti-inflammatory properties thus, ApoE$^{-/-}$ mice exhibit a high basal oxidative stress status compared to C57BL/6 mice (Mayr et al. 2005; Tarnus et al. 2009; Pereira et al. 2012). Furthermore, a high fat diet has been demonstrated to induce chronic oxidative stress due to adipocyte hypertrophy which subsequently leads to an inflammatory profile due to the secretion of various cytokines (Eriksson 2007; Park et al. 2007; Vincent et al. 2007; Tarnus et al. 2009; Pereira et al. 2012).

Superoxide production was assessed in the aortic PVAT of ApoE$^{-/-}$ mice because there is a strong association between raised levels of superoxide and PVAT dysfunction which could be due to the depletion of NO by its spontaneous reaction with superoxide anion, resulting in the generation of peroxynitrite, a powerful oxidant. (Greenstein et al. 2009; Marchesi et al. 2009; Victorio et al. 2016). Furthermore, elevated superoxide levels, in conjunction with an attenuation of the anti-contractile effect of PVAT, were observed in the previous C57BL/6 study (described in Chapter 3) in the oldest group of mice. Also, increased superoxide production has been observed in the endothelium and VSM in the aortae of ApoE$^{-/-}$ mice in comparison to C57BL/6 and transgenic ApoE$^{-/-}$ mice with increased endothelial BH_4, a cofactor of NOS (d'Uscio et al. 2001a; Alp et al. 2004). However, until now superoxide production in the aortic PVAT of ApoE$^{-/-}$ mice has largely been ignored.

Although a decrease in superoxide production within the aortic PVAT was observed in both the ND and WD-fed ApoE$^{-/-}$ mice, after 26 weeks feeding, this was not a significant change and may have been a result of an underpowered experiment with 3-4 mice used per group. Therefore, it is difficult to draw firm conclusions from these data. Nevertheless, superoxide production was significantly elevated in both the 8 and 16-week ND-fed groups in comparison to C57BL/6 mice. These data could indicate that the white adipocytes in the aortic PVAT were chronically hypoxic resulting in increased oxidative stress. There were no differences between C57BL/6 and ApoE$^{-/-}$ mice fed a ND for 26 weeks and this may be due to the observed hypertrophy of the white adipocytes within the aortic PVAT of C57BL/6 mice.

Hypoxic conditions in endothelial cells promotes mitochondrial ROS formation (Ishida et al. 2002). Therefore, due to the abundance of mitochondria in aortic PVAT, it is probable that the presumed hypoxic state of the aortic white adipocytes induced the generation of mitochondrial superoxide. Taken together with the aortic PVAT composition data the superoxide findings suggest that the PVAT of ApoE$^{-/-}$ mice displays an accelerated aged phenotype with increased superoxide and enlarged adipocytes both of which were also observed in the PVAT of older C57BL/6 mice (presented in Chapter 3).

4.5.5.3 The number of Mac-3^{+} cells in the aortic PVAT of ApoE$^{-/-}$ mice does not change with increasing age or a Western-type diet

Previous studies have demonstrated that aortic PVAT is highly resistant to inflammation (Ketonen et al. 2010; Fitzgibbons et al. 2011). However, it has been observed that the visceral white adipose depots of ApoE$^{-/-}$ mice exhibit enhanced macrophage infiltration, increased macrophages forming crown-like structures and elevated expression of IL-6 and TNFα compared to C57BL/6 mice, irrespective of diet type (Pereira et al. 2012).

Macrophages were detected in the aortic PVAT of ApoE$^{-/-}$ mice using an antibody of the Mac-3 antigen; Mac-3 expression is increased during macrophage differentiation. Nevertheless, Mac-3 does not detect monocytes or lymphocytes (Ralph et al. 1983). An increase in the number of Mac3^{+} cells was observed in both ND and WD-fed 26-week groups in the PVAT of ApoE$^{-/-}$ mice, but this increase was not statistically significant. Moreover, in comparison to age and diet-matched C57BL/6 mice, no significant differences in infiltrating Mac-3^{+} cells were observed within the PVAT. Although no changes in Mac3^{+} cells were observed in the ApoE$^{-/-}$ mice with ageing or a WD, other inflammatory cells, such as neutrophils, eosinophils, monocytes and lymphocytes may have been present therefore firm conclusions regarding the inflammatory state of the PVAT in these ApoE$^{-/-}$ mice cannot be made.

4.6 Study limitations and future work

Although the experiments in this chapter have provided novel insight into the influence of aortic PVAT from ApoE$^{-/-}$ mice on vascular reactivity and characterised the composition of PVAT with ageing and a WD, several unanswered questions remain. The present study suggests that basal (non-stimulated) eNOS activity within the aortic PVAT and therefore PVAT-derived NO bioavailability is reduced in ApoE$^{-/-}$ mice resulting in an absence of an anti-contractile effect of PVAT whereas, normal agonist-stimulated NO release is maintained (evidenced by retained

endothelial function). However, this hypothesis was not investigated further. A method such as confocal microscopy could be employed to determine basal NO bioavailability within the PVAT and in PVAT-denuded aortic segments. Aortic segments with or without PVAT could be stimulated with phenylephrine or phenylephrine and acetylcholine to mimic the in vitro myography experiments and subsequently incubated with the fluorescent NO indicator 4,5-daminofluorescein diacetate (DAF-2DA), mounted on a confocal microscope and NO production visualised using confocal imaging techniques (Gil-Ortega et al. 2010). Furthermore, this technique could be utilised to determine if 50 µM L-NNA resulted in complete NOS inhibition within the vasculature.

In addition to the above experiments, eNOS expression could be assessed in aortic PVAT and VSM by Western blot. Analogous to the previous experiment, aortic tissue, with or without PVAT, could be incubated in PSS alone, stimulated with phenylephrine or challenged with phenylephrine followed by acetylcholine and then processed for Western blot. The presence and activation of eNOS or any other NOS isoforms could then be analysed.

Superoxide production within the aortic PVAT of ApoE$^{-/-}$ mice did not appear to be the result of increased macrophage infiltration. However, more inflammatory markers could be assessed in the PVAT using immunohistochemical staining markers such as CD68 and F4/80 to further evaluate macrophage infiltration in the PVAT whilst monocytes, and neutrophils could be identified with CD11b and Ly6G (monocytes are negative for Ly6G) (Murray et al. 2011).

It would be interesting to repeat the vascular reactivity studies in endothelium-denuded aortic rings in order to remove the influence of the endothelium and determine if the aortic PVAT still did not exert any effect on VSM contractions. Furthermore, PVAT transfer experiments using young C57BL/6 and ApoE$^{-/-}$ mice where aortic rings, endothelium-intact and endothelium-denuded, were incubated with PVAT from the opposing strain could provide useful information about the nature of the PVAT from both strains. For example, the PVAT of ApoE$^{-/-}$ mice may release a constricting factor which did not have an effect on the host but could increase the contraction of the recipient C57BL/6 aortic rings. Unfortunately, due to limited numbers of ApoE$^{-/-}$ mice, the above experiments could not be performed during the time-frame of this study.

Finally, the histology and immunostaining experiments were potentially under-powered with a 3-4 mice being used per group. Unfortunately, due to the small size of the mouse aorta and the nature of PVAT, many tissue sections were lost during histological and immunohistochemical staining. Numerous attempts were made to prevent the tissue from lifting off the slides, such as using poly-L-lysine coated glass slides, different methods of antigen retrieval, changing the tissue section thickness and gentler washing techniques however, no significant improvements to tissue adhesion were identified

4.7 Chapter summary and conclusions

This study has demonstrated that the aortic PVAT of ApoE$^{-/-}$ mice, in contrast to C57BL/6 mice, does not exert an anti-contractile effect. This is possibly due to a lack of PVAT-derived NO within the vasculature and an ‘aged’ PVAT phenotype in comparison to C57BL/6 mice. These data reiterate the importance of eNOS and NO in promoting the anti-contractile effect of PVAT.

However, further investigation into NO bioavailability within the aortic PVAT of ApoE$^{-/-}$ mice is required.

Key findings:

- **Endothelial dysfunction was not observed in the aortae of ND or WD -fed ApoE$^{-/-}$ mice despite the presence of atherosclerotic lesions along the luminal surface of the aortae.**
- **The aortic PVAT of ApoE$^{-/-}$ mice was dysfunctional and did not exert an anti-contractile effect on aortic rings; this was potentially due to decreased basal eNOS activity resulting in an attenuation of PVAT-derived NO.**
- **Feeding the ApoE$^{-/-}$ mice a WD did not alter the vascular reactivity of aortic PVAT.**
- **The aortic PVAT of ApoE$^{-/-}$ mice exhibited an aged phenotype when assessed morphologically.**

~ Chapter Five ~

An evaluation of perivascular adipose tissue in athero-resistant Cav-1$^{-/-}$ mice

Abstract

Background: The caveolin-1 knockout mouse (Cav-1$^{-/-}$) exhibits enhanced nitric oxide (NO) production within its vasculature due to loss of the tonic inhibitory interaction between Cav-1 and endothelial nitric oxide synthase (eNOS). NO bioavailability is essential in large arteries and confers cardioprotective benefits; a strong association exists between decreased NO production and increased incidence of cardiovascular disease (CVD). Furthermore, NO has been identified as a mediator of the anti-contractile of perivascular adipose tissue (PVAT). High basal NO production within arteries, specifically within PVAT, may prevent the onset of CVD therefore, the influence of PVAT on vascular reactivity was assessed in ageing and Western-type diet-fed Cav-1$^{-/-}$ mice. In addition, Cav-1$^{-/-}$ mice have been reported to exhibit abnormal adipocyte morphology in various fat depots with ageing on a high fat diet

Purpose: The following studies were conducted in order to characterise PVAT composition and the influence of aortic PVAT on vascular function in Cav-1$^{-/-}$ mice of advancing age and in high fat Western-type diet fed Cav-1$^{-/-}$ mice.

Methods: Upon weaning, male Cav-1$^{-/-}$ mice were fed a normal diet (ND) or Western-type diet (WD) for 8, 16 or 26-weeks. Vascular reactivity studies were performed on aortic rings with the PVAT left intact or removed. eNOS was inhibited with 50µM L-NNA to elucidate the contribution of NO -mediated relaxation to the vasoconstrictor response of aortic rings to phenylephrine. Aortic PVAT composition was assessed using a combination of histology and immunostaining.

Results: Cav-1$^{-/-}$ mice were resistant to the development of atherosclerosis after extensive feeding of a WD. In addition, aortic endothelial function was maintained in ageing and in WD-fed mice. PVAT did not modulate vasoconstrictor responses to phenylephrine in ND-fed Cav-1$^{-/-}$ mice. However, after 26-weeks on a WD PVAT exerted a pro-contractile effect on aortic rings ($P = 0.0001$). Additionally, with the exception of the 8-week WD-fed mice, NOS inhibition revealed a pro-contractile effect of PVAT in aortic rings from Cav-1 mice. Morphologically, hypertrophy of the aortic PVAT white adipocyte population was observed after 26 weeks on a WD ($P = 0.02$). However, no other significant changes were observed in regard to superoxide production or macrophage infiltration within aortic PVAT with ageing or a WD.

Conclusions: The aortic PVAT of ND-fed Cav-1 mice is unable to modulate vascular contractions to phenylephrine. However, after 26-weeks on a WD, the contractility of aortic rings in the presence of PVAT was augmented. This may have been the result of PVAT releasing a vaso-constricting factor which counteracted the vaso-relaxant effects of NO as a result of white adipocyte hypertrophy. The contribution of NO-mediated relaxation to the attenuated vasoconstrictor responses of VSM to phenylephrine requires further investigation.

5.1 Introduction

Caveolin-1 (Cav-1) is the main structural component of caveolae which are 'cave-shaped' plasmalemmal invaginations in terminally differentiated cells and are highly expressed throughout all aspects of the vasculature including the endothelium, VSM and adipocytes (Rahman and Sward 2009). Caveolae and Cav-1 are responsible for the tonic inhibition of eNOS the principal generator of NO within the vasculature. eNOS, despite its name, is not solely expressed within endothelial cells and has been detected in VSM and, more recently, perivascular adipose tissue (PVAT) (Buchwalow et al. 2002; Randriamboavonjy and Fleming 2005; Dudzinski and Michel 2007; Xia et al. 2016).

The generation of Cav-1$^{-/-}$ knockout mice, lacking identifiable caveolae structures within the vasculature, allowed the loss of Cav-1 and therefore its inhibitory action on eNOS to be investigated in vitro using isolated aortic preparations (Razani et al. 2001). Aortic rings obtained from Cav-1$^{-/-}$ mice exhibit an impaired vasoconstrictor response to phenylephrine and this has been attributed to increased eNOS activity and high basal production of NO. This attenuated constrictor response was lost upon incubation with 100 µM L-NAME (a NOS inhibitor) and proper contractile responses were restored (Razani et al. 2001). Furthermore, endothelium-dependent relaxations of aortic rings from Cav-1$^{-/-}$ mice were reported to be enhanced in comparison to C57BL/6 mice, the genetic background strain (Razani et al. 2001). Studies of Cav-1$^{-/-}$ mice have demonstrated that loss of Cav-1$^{-/-}$ results in numerous abnormalities including dyslipidaemia, reduced lifespan, premature neuronal ageing, and a prematurely aged phenotype in resistance arteries (Razani et al. 2001; Razani et al. 2002a; Cohen et al. 2003b; Park et al. 2003; Hausman et al. 2012). However, Cav-1$^{-/-}$ mice are resistant to the development of atherosclerosis despite exhibiting hypercholesterolaemia, a prerequisite for the development of atherosclerotic lesions and this may be a result of increased NO bioavailability or disturbed cholesterol handling (Razani et al. 2002a).

Diminished NO within the arteries is associated with ageing and results in increased cardiovascular risk. This is most significant in large arteries, where NO-mediates the majority of endothelium-dependent relaxations. PVAT has repeatedly been demonstrated to be a vital component of the vasculature, providing more than structural support and is able to modulate vascular tone through the release of PVAT-derived factors and subsequent interaction of these factors with the VSM and endothelium (Lohn et al. 2002; Greenstein et al. 2009; Ketonen et al. 2010). A crucial role for NO in contributing to the anti-contractile effect of PVAT has been realised. Decreases in PVAT-derived NO bioavailability have been associated with a loss of the anti-contractile capacity of PVAT in disease states (Marchesi et al. 2009; Gil-Ortega et al. 2010; Aghamohammadzadeh et al. 2013; Victorio et al. 2016; Zaborska et al. 2016). Furthermore, in this present study, NO was observed to play a significant role in aortic PVAT exerting an anti-contractile effect in the aortae of C57BL/6 mice (Chapter 3). Taken together, these findings suggest that increased NO production within the different components of the arteries, in particular PVAT, could confer protection against the development of CVD. Cav-1$^{-/-}$ mice have been reported to exhibit an abundance of NO within the vasculature. However, these studies were conducted in

the absence of PVAT thus, the influence of aortic PVAT on the contractility and relaxation responses of isolated aortic preparations from Cav-1$^{-/-}$ mice was assessed.

High fat feeding of Cav-1$^{-/-}$ mice has been reported to induce hypercholesterolaemia, a risk factor for the development of CVD in humans (Vogel 1997). Furthermore, hypercholesterolaemia has been reported to deplete NO bioavailability through a mechanism involving an increase in the abundance of caveolae and subsequent increase in Cav-1-eNOS interactions (Feron et al. 1999; Grayson et al. 2013). Caveolae and Cav-1 are not detectable within the vasculature of Cav-1$^{-/-}$ mice therefore, Cav-1$^{-/-}$ mice may be protected against the effects of hypercholesterolaemia-induced NO depletion. Cav-1$^{-/-}$ mice have been reported to display altered cholesterol handling and abnormal adipocyte morphology within fat depots when fed a WD diet and subsequently aged (Razani et al. 2002a). Therefore, the effects of increasing age and a WD on aortic PVAT composition and morphology were assessed.

5.2 Aim and objectives

The chapter aims to elucidate the effect of PVAT and the contribution of NO to PVAT function in aortic preparations from Cav-1$^{-/-}$ mice and establish whether this is influenced by ageing or a Western-type diet. This will be achieved by:

- Phenotyping ageing and WD-fed Cav-1$^{-/-}$ mice by assessing lipid and glucose parameters, measuring body and organ weights and assessing en face aortic preparations for the development of atherosclerosis.
- Assessing the effect of Cav-1 deletion on aortic vasoconstrictor and vasodilatory responses, in the presence or absence of PVAT, in ageing and WD-fed Cav-1$^{-/-}$ mice and determining the contribution of NO to these responses using myography techniques.
- Characterising the aortic PVAT of these mice, using histology and immunohistochemistry to determine if ageing or high fat feeding affect its morphology or structure.

5.3 Methods

Male Cav-1$^{-/-}$ mice were obtained from an in-house colony. Mice were weaned at around 4 weeks of age. Upon weaning, the mice were fed either a ND or a high fat (21%) WD for 8, 16 or 26 weeks. The effects of ageing and a WD on blood serum lipid and glucose levels were evaluated. In addition, the body and organ weights of mice from each diet and experimental time-point were recorded. En face Oil Red O staining was performed on aortic preparations to determine whether lipid lesions developed within the aortae of Cav-1$^{-/-}$ mice. Relaxation studies were conducted to determine if loss of Cav-1 resulted in altered vasorelaxation responses to acetylcholine in the aortae of Cav-1$^{-/-}$ mice. Vascular contractility, in the presence or absence of PVAT, was assessed using rings of thoracic aortae. The contribution of NO to vascular reactivity was assessed by incubation with L-NNA (50 µM), a NOS inhibitor. The sensitivity of isolated aortic ring preparations was evaluated using the potent NO donor, sodium nitroprusside. The composition of aortic PVAT was assessed using haematoxylin and eosin staining and the superoxide indicator dihydroethidium (DHE). Immunostaining was performed on PVAT from the thoracic aorta to evaluate macrophage infiltration. Detailed methods are supplied in Chapter 2.

5.4 Results

5.4.1 Characteristics of ageing in normal and Western-type diet-fed Cav-1$^{-/-}$ mice

5.4.1.1 Western-type diet-fed Cav-1$^{-/-}$ mice develop hypercholesterolaemia

The lipid and glucose profiles of ND-fed Cav-1$^{-/-}$ mice did not alter with increasing age (P = NS for all parameters and time-point comparisons; n = 5-6 mice per group, Table 5.1).

In comparison to ND-fed age-matched controls, total serum cholesterol was significantly elevated in WD-fed mice at the 8 and 26-week time-points (ND versus WD: 8-weeks P = 0.03; 16-weeks P = 0.09; 26-weeks P < 0.0001; n = 5-6 mice per group, Table 5.1). Serum HDL was also raised in the 8-week WD-fed group compared to ND mice (P = 0.001, n= 5-6 mice, Table 5.1). Triglyceride and glucose levels of WD-fed mice remained unchanged from age-matched ND mice even after an extensive duration of high fat feeding (ND versus WD: P = NS for triglycerides and glucose at each time-point; n = 5-6 mice per group Table 5.1).

Furthermore, no differences were observed between the serum lipid or glucose profiles of age and diet-matched C57BL/6 mice (Cav-1$^{-/-}$ versus C57BL/6: P = NS for each parameter, n = 4-6 mice per group, Appendix 2.2).

Table 5.1 Lipid and glucose measurements for normal and Western-type diet-fed Cav-1$^{-/-}$ mice

ND	8-weeks	16-weeks	26-weeks	P values for all diet-matched comparisons
Total cholesterol	2.57 ± 0.36	2.75 ± 0.28	3.22 ± 0.25	P = NS
HDL	1.16 ± 0.10	1.51 ± 0.13	1.77 ± 0.14	P = NS
Triglycerides	1.61 ± 0.20	1.74 ± 0.18	2.03 ± 0.22	P = NS
Glucose	17.42 ± 2.42	21.16 ± 2.23	26.03 ± 4.57	P = NS
WD	**8-weeks**	**16-weeks**	**26-weeks**	**P values for all diet-matched comparisons**
Total cholesterol	6.41 ± 1.17	6.08 ± 1.29	9.39 ± 0.72	P = NS
HDL	2.14 ± 0.20	2.03 ± 0.18	2.34 ± 0.14	P = NS
Triglycerides	2.07 ± 0.26	1.27 ± 0.12	1.45 ± 0.14	P = NS
Glucose	24.50 ± 4.89	19.52 ± 1.99	19.00 ± 4.04	P = NS
ND versus WD	**3 months**	**5 months**	**7 ½ months**	
Total cholesterol	* 0.03	NS 0.09	**** P<0.0001	
HDL	** 0.001	NS 0.34	NS 0.18	
Triglycerides	NS > 0.999	NS > 0.999	NS 0.58	
Glucose	NS > 0.999	NS > 0.999	NS > 0.999	

Serum derived from blood obtained at sacrifice. Mice were weaned at 4 weeks of age and maintained on a normal diet (ND) or Western-type diet (WD) for 8, 16 or 26 weeks. Data are expressed as mean ± S.E.M and measurements are shown in mmol/L. Statistical analysis was carried out by two-way ANOVA, with Bonferroni's post hoc tests, n = 5-6 mice per group.

5.4.1.2 The effect of ageing on the body and organ weights of normal diet-fed Cav-1$^{-/-}$ mice

Cav-1$^{-/-}$ mice maintained on a ND displayed a significant gain in weight after 16-weeks compared to the 8-week time-point group (8-weeks versus 26-weeks: $P < 0.0001$, n = 18 and 14 mice, respectively, Table 5.2), this gain was sustained in the 26-week time-point (8-weeks versus 26-weeks: $P < 0.0001$; n = 18 and 15 mice, Table 5.2) but no differences were observed between the 16 and 26-week groups (P = NS, n = 14 and 15 mice, Table 5.2). Heart weights, heart weight: body weight ratio, liver and spleen weights were unaffected by increasing age (P = NS all groups; n = 14-18 mice, Table 5.2). A significant increase in epididymal fat pad weight was observed between the youngest and oldest Cav-1$^{-/-}$ mice (8-weeks versus 26-weeks: $P < 0.0001$; n = 18 and 14 mice, Table 5.2). However, no corresponding increases in epididymal adipocyte area were observed (P = NS; n = 4 mice, 100 adipocytes per mouse, Table 5.2).

The body and organ characteristics of Cav-1$^{-/-}$ mice were compared to the genetic background strain, C57BL/6 (Appendix 2.3). In this present study, no differences were observed between the body weights of C57BL/6 and Cav-1$^{-/-}$ mice (Cav-1$^{-/-}$ versus C57BL/6 mice: P = NS; Cav-1$^{-/-}$ n = 14-18 mice per group; C57BL/6 n = 5-6 mice per group, Appendix 2.3 A). There were no significant differences in the weight of hearts obtained from Cav-1$^{-/-}$ and C57BL/6 mice after 8 weeks on a ND although, cardiac hypertrophy was observed after 16 weeks on a ND, evidenced by a significantly increased heart weight and heart weight: body weight ratio (HW:BW) compared to C57BL/6 mice (Cav-1$^{-/-}$ versus C57BL/6 mice: heart weight: P = 0.008; HW:BW: P = 0.002; Cav-1$^{-/-}$ n = 14-18 mice per group; C57BL/6 n = 5-6 mice per group Appendix 2.3B and C). In addition, whilst the liver weights of Cav-1$^{-/-}$ and C57BL/6 mice were similar in all ND-fed groups (Cav-1$^{-/-}$ versus C57BL/6 mice: P = NS; Cav-1$^{-/-}$ n = 14-18 mice per group; C57BL/6 n = 5-6 mice per group, Appendix 2.3D), the Cav-1$^{-/-}$ mice developed splenomegaly after 16 weeks on a ND and this was sustained in the 26-week ND-fed group (Cav-1$^{-/-}$ versus C57BL/6 mice: 16-weeks ND P = 0.04; 26-weeks ND P =< 0.0001; Cav-1$^{-/-}$ n = 14-18 mice per group; C57BL/6 n = 5-6 mice per group, Appendix 2.3E). The epididymal fat pads of the 26 week ND-fed group were significantly smaller than the C57BL/6 mice (Cav-1$^{-/-}$ versus C57BL/6 mice: $P < 0.0001$, Cav-1$^{-/-}$ n = 14-18 mice per group; C57BL/6 n = 5-6 mice per group, Appendix 2.3 F). Also, epididymal adipocytes from Cav-1$^{-/-}$ mice were significantly smaller than age and diet-matched C57BL/6 mice however, no differences in adipocyte size were observed after 26 weeks on a ND (Cav-1$^{-/-}$ versus C57BL/6 mice: 16 weeks: P = 0.004; Cav-1$^{-/-}$ n = 14-18 mice per group; C57BL/6 n = 5-6 mice per group, Appendix 2.3G).

5.4.1.3 The effect of a Western-type diet on the body and organ weights of Cav-1$^{-/-}$ mice

The effect of a WD in comparison to ND mice on body and organ characteristics was evaluated at each time-point. A WD significantly increased the body weight of Cav-1$^{-/-}$ mice at the 8-week time-point (ND versus WD: P = 0.01, n = 18 mice per group, Table 5.2). However, no further differences in body weight were observed even after extended feeding of a WD (ND versus WD: P = NS; n = 15 and 7 mice, respectively, Table 5.2). Heart weight and heart weight: body weight ratio were unaffected by feeding of a WD at each time-point when compared to age-matched ND-fed mice (P = NS both parameters and all age comparisons; n = 7-18 mice per group, Table 5.2). Hepatomegaly was observed at each time-point in WD-fed mice compared to ND Cav-1$^{-/-}$ controls

(ND versus WD: 8-weeks P = 0.009, n = 18 mice per group; 16-weeks P < 0.0001, n = 14 and 17 mice; 26-weeks P < 0.0001, n = 15 and 7 mice, respectively, Table 5.2). Additionally, splenomegaly occurred at the 26-week time-point in the WD-fed group (ND versus WD: 26 weeks P < 0.0001; n = 15 and 7 mice, Table 5.2). The epididymal fat pads of WD mice were significantly enlarged compared to age-matched ND mice at both the 8 and 16week time-points however, no differences were observed between the oldest 26-week groups (ND versus WD: 8 weeks P < 0.0001, n = 18 mice each; 16 weeks P < 0.0001, n = 14 and 17 mice; 26 weeks P = 0.06; n = 15 and 7 mice, Table 5.2). In addition, epididymal adipocytes were larger in WD-fed mice after the 8 and 16-week time-points (ND versus WD: 8 weeks P = 0.02; 16 weeks P = 0.02; n = 4 mice, 100 adipocytes analysed per mouse, Table 5.2) although no differences were observed between ND and WD-fed mice after 26-weeks (P = NS; n = 4 mice, 100 adipocytes measured per mouse, Table 5.2).

Feeding Cav-1$^{-/-}$ mice a WD resulted in augmented cholesterol levels compared to age-matched ND-fed mice. With the exception of the 8-week time-point, Cav-1$^{-/-}$ mice were resistant to diet-induced weight gain when compared to their ND-fed counterparts. However, hepatomegaly and eventually splenomegaly was observed in WD-fed mice suggesting that fat had begun to accumulate within these organs. Epididymal fat pad weight and the adipocytes that constitute them were significantly enlarged in both the 8 and 16-week WD-fed mice. However, this effect was lost in the oldest group which could imply that the epididymal fat pads and adipocytes had expanded to their maximum capacity.

Table 5.2 Body weight, organ weights and epididymal adipocyte size of normal diet and Western-type diet-fed Cav-1$^{-/-}$ mice

ND	8 weeks (A)	16 weeks (B)	26 weeks (C)	P values for all diet-matched comparisons
Body weight (g)	28.28 ± 0.38	32.70 ± 0.67	34.98 ± 0.63	A vs B **** P < 0.0001, A vs C **** P < 0.0001
Heart weight (mg)	180.6 ± 7.38	203.54 ± 8.41	209.94 ± 9.99	
Heart weight: body weight (mg/g)	6.29 ± 0.22	6.22 ± 0.20	6.00 ± 0.24	
Liver (g)	1.82 ± 0.04	2.09 ± 0.08	2.36 ± 0.131	
Spleen (mg)	119.4 ± 5.77	119.0 ± 5.38	140.28 ± 5.99	
Epididymal fat pad weight (g)	0.31 ± 0.01	0.43 ± 0.04	0.63 ± 0.04	A vs C **** P < 0.0001
Epididymal adipocyte area (x10^3 µm^2)	1.92 ± 0.27	1.91 ± 0.19	3.41 ± 0.37	
WD	**8 weeks (D)**	**16 weeks (E)**	**26 weeks (F)**	**P values for all diet-matched comparisons**
Body weight (g)	31.30 ± 0.59	35.10 ± 0.87	35.32 ± 1.21	D vs E *** 0.0009, D vs F * 0.01
Heart weight (mg)	187.2 ± 8.32	194.1 ± 6.16	203.97 ± 9.29	
Heart weight: body weight (mg/g)	6.14 ± 0.25	5.60 ± 0.26	5.86 ± 0.47	
Liver (g)	2.73 ± 0.19	3.83 ± 0.29	5.15 ± 0.51	D vs E ** 0.001, D vs F **** P < 0.0001, E vs F ** 0.003
Spleen (mg)	143.4 ± 14.38	167.5 ± 6.87	269.7 ± 48.82	D vs E **** P < 0.0001, D vs F **** P < 0.0001, E vs F **** P < 0.0001
Epididymal fat pad weight (g)	0.87 ± 0.06	1.00 ± 0.07	0.87 ± 0.08	
Epididymal adipocyte area (x10^3 µm^2)	4.56 ± 0.41	4.47 ± 0.59	4.39 ± 0.55	
ND versus WD	**8 weeks**	**16 weeks**	**26 weeks**	
Body weight (g)	* 0.01	NS 0.20	NS > 0.999	
Heart weight (mg)	NS > 0.999	NS > 0.999	NS > 0.999	
HW: BW (mg/g)	NS > 0.999	NS > 0.999	NS > 0.999	
Liver (g)	** 0.009	**** P < 0.0001	**** P < 0.0001	
Spleen (mg)	NS > 0.999	NS 0.08	**** P < 0.0001	
Epididymal fat pad weight (g)	**** P < 0.0001	**** P < 0.0001	NS 0.06	
Epididymal adipocyte area (x10^3 µm^2)	* 0. 02	* 0.02	NS > 0.999	

ND = normal chow diet, WD = Western-type diet. Data are expressed as mean ± S.E.M and weights are shown in milligrams or grams. Heart weight: body weight ratio in milligrams/grams and epididymal adipocyte area x10^3 µm^2. *Two-way ANOVA with Bonferroni's post-hoc tests was performed. Body and organ weights n = 14-18 mice per group (with exception of 26 week WD, where n = 7); adipocyte area n = 4 mice per group, 100 adipocytes analysed per mouse.*

5.4.2 Cav-1$^{-/-}$ mice are resistant to the development of atherosclerosis

Atherosclerotic lesions did not develop within the aortae of Cav-1$^{-/-}$ mice fed a ND or after extensive feeding of a WD (Figure 5.1).

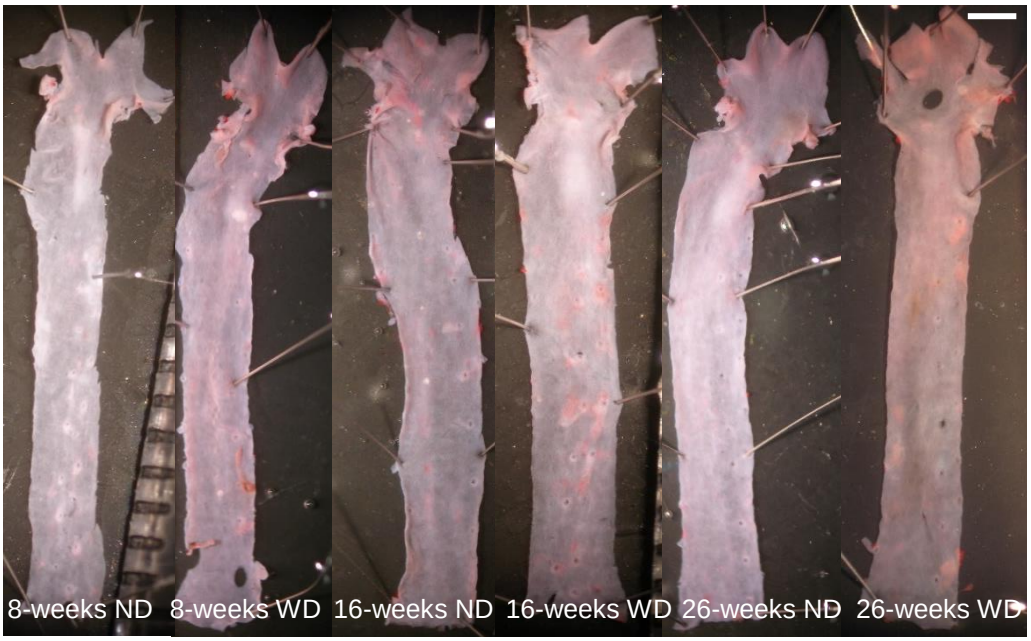

Figure 5.1 En face aortic preparations stained with Oil Red O

Oil Red O was used in order to detect lipid lesions along the surface of the aorta. Lesions did not develop within the aortae of Cav-1 mice$^{-/-}$. Representative images, scale bar, top right-hand corner, = 1 mm, n = 3-6 Cav-1$^{-/-}$ mice per group.

5.4.3 Vascular reactivity studies assessing the effect of aortic PVAT on vascular responses in normal diet and Western-type diet fed Cav-1$^{-/-}$ mice

5.4.3.1 The presence of aortic PVAT does not alter contraction to 100 mM KPSS in Cav-1$^{-/-}$ mice

The contractions of aortic rings to 100 mM KPSS were unaltered by the presence of PVAT in Cav-1$^{-/-}$ mice (+PVAT versus -PVAT: P = NS; n = 4-7 mice per group, Figure 5.2) and a WD did not have a significant effect on aortic ring contraction (ND versus WD: +/-PVAT, P = NS, n = 4-7 mice per group Figure 5.2). Moreover, the contraction stimulated by KPSS was similar between ND-fed Cav-1$^{-/-}$ and C57BL/6 mice (Cav-1$^{-/-}$ versus C57BL/6: +/-PVAT P = NS; n = 4-7 mice per group, Appendix 2.4 Ai and ii).

Nevertheless, considerable variability was observed between the groups and it is therefore difficult to draw firm conclusions regarding the effects of ageing or a WD on the contractile responses of aortic rings in Cav-1$^{-/-}$ mice.

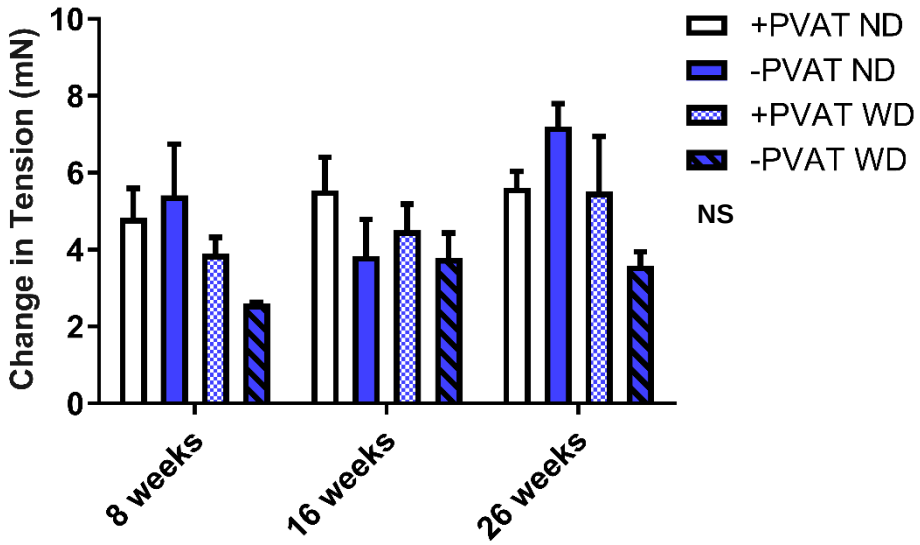

Figure 5.2 Contractions to 100 mM KPSS are similar in aortic rings with or without PVAT

*The contractile responses of PVAT-intact or PVAT-denuded aortic rings were similar. However, significant differences in contractile responses were observed between PVAT-denuded aortic rings in response to increasing age and a WD. ND = normal diet, PVAT = perivascular adipose tissue, WD = Western-type diet. Data are presented as mean ± S.E.M, n = 4-7 mice per group, * P < 0.05, ** P < 0.01, Two-way ANOVA with post hoc Bonferroni's multiple comparisons tests.*

5.4.3.2 Endothelial function, in response to acetylcholine, is maintained with ageing and a Western-type diet in Cav-1$^{-/-}$ mice

The presence of PVAT did not alter the relaxation of phenylephrine-pre-constricted aortic rings to a single dose of acetylcholine, 10 µM, (+PVAT versus -PVAT: P = NS; n = 4-7 mice per group, Figure 5.3). Additionally, endothelial function was unaltered by increasing age in either ND or WD-fed mice (P = NS, n = 4-7 mice per group, Figure 5.3). Moreover, when the responses from ND and WD-fed groups were compared, in PVAT-intact or PVAT denuded aortic rings, no differences in relaxation were observed (ND versus WD: +/-PVAT P = NS; n = 4-7 mice per group, Figure 5.3).

The relaxation responses of ND-fed Cav-1$^{-/-}$ and C57BL/6 mice were compared (Appendix 2.4 Bi and ii). There were no differences in relaxation between PVAT-intact aortic rings from the different of mice (P = NS; n = 4 Cav-1$^{-/-}$ and 8 C57BL/6 mice per group). However, after 26 weeks on a ND the relaxation of Cav-1$^{-/-}$ PVAT-denuded aortic rings was significantly enhanced in comparison to the C57BL/6 strain (Cav-1$^{-/-}$ versus C57BL/: -PVAT P = 0.08, n = 4 Cav-1$^{-/-}$ mice and n = 8 C57BL/6 mice per group, Appendix 2.4Bii).

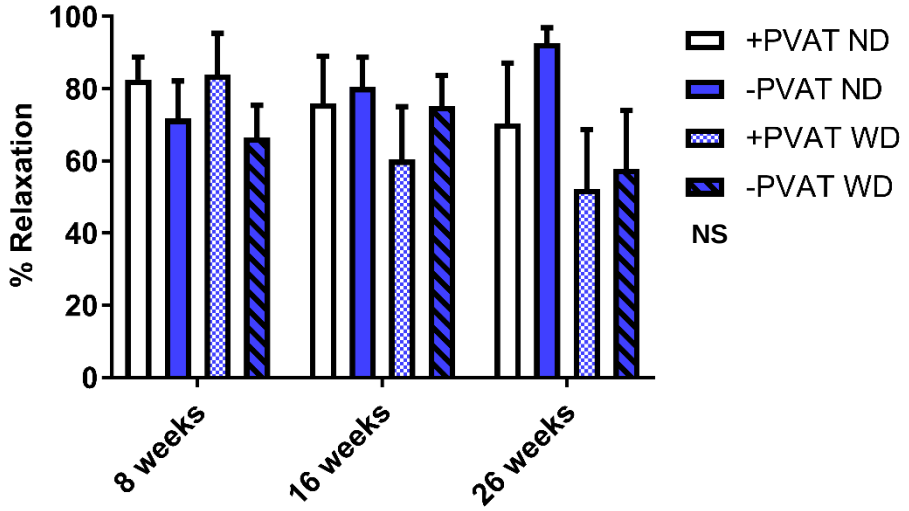

Figure 5.3 Endothelial function is unaffected by PVAT, ageing or a Western-type diet in Cav-1$^{-/-}$ mice

PVAT did not alter relaxations of phenylephrine pre-constricted aortic rings to acetylcholine. ND = normal diet, PVAT = perivascular adipose tissue, WD = Western-type diet. Data are presented as mean ± S.E.M, n = 4-7 mice per group, two-way ANOVA with post hoc Bonferroni's tests.

5.4.3.2 Aortic PVAT from normal diet-fed Cav-1$^{-/-}$ mice does not exert an anti-contractile effect

The PVAT of ND-fed Cav-1/- mice did not modulate the vascular reactivity of aortic rings in response to cumulative doses of phenylephrine at any of the experimental time-points (+PVAT versus -PVAT: P = NS; n = 4-7 mice per group, Figure 5.4A-C).

5.4.3.3 Aortic PVAT from Cav-1$^{-/-}$ mice exerts a pro-contractile effect after extensive high fat feeding

Initially, a WD had no impact on the contraction of aortic rings with or without PVAT. After 8 ad 16 weeks and the vasoconstrictor responses to phenylephrine were similar in the presence or absence of PVAT (+PVAT versus -PVAT: P = NS; n = 5-7 mice per group, Figure 5.4A and B). However, after 26 weeks on a WD the PVAT of Cav-1$^{-/-}$ mice exerted a significant pro-contractile effect on the aortic rings (+PVAT versus -PVAT: P = 0.0001; n = 5 and 4 mice, respectively, Figure 5.4C).

5.4.3.4 PVAT-denuded aortic rings of Cav-1$^{-/-}$ mice exhibit diminished contractions after 26 weeks on a Western-type diet in comparison to normal-diet fed mice

The contractions of aortic rings from WD-fed Cav-1$^{-/-}$ mice were compared to age-matched ND-fed Cav-1$^{-/-}$ mice. Contractions were similar between ND and WD-fed mice up to 16-weeks of high fat feeding (ND versus WD: +/-PVAT P = NS; n = 4-7 mice per group, Figure 5.4A and B). However, contractions of PVAT-denuded aortic rings from mice fed a WD for 26 weeks were significantly reduced when compared to the ND-fed group although this was not replicated in PVAT-intact rings (ND versus WD: 26-weeks -PVAT P < 0.0001; n = 4 mice per group, Figure 5.4C).

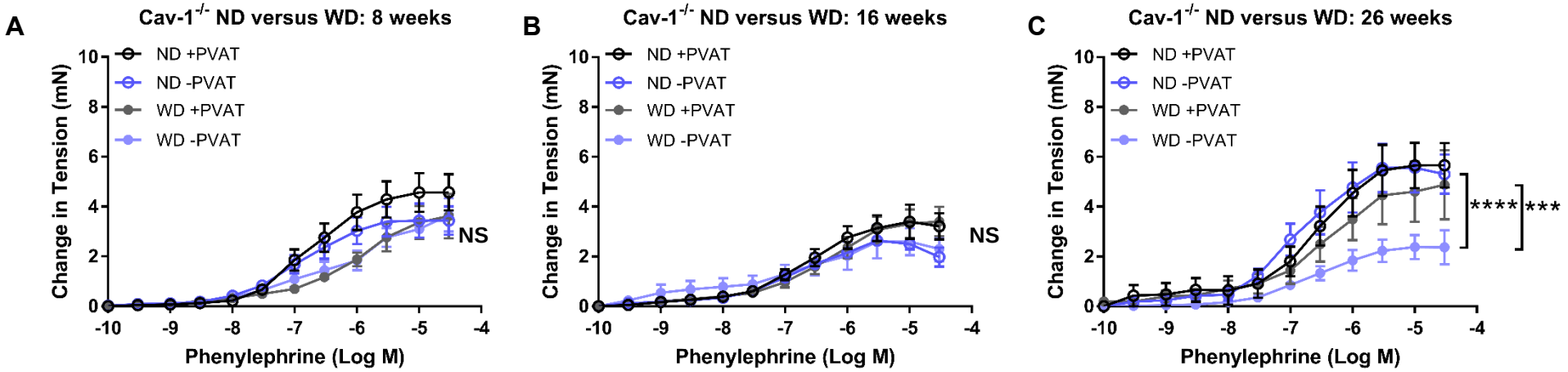

Figure 5.4 The PVAT of Cav-1$^{-/-}$ mice does not modulate vascular contractility on a ND but exerts a pro-contractile effect on aortic rings after 26 weeks on a Western-type diet

*Aortic rings were challenged with cumulative doses of phenylephrine (1 x 10^{-10} - 3 x 10^{-5} mol/L) in the presence or absence of PVAT. A) Aortic PVAT did not modulate vascular reactivity of aortic rings from Cav-1$^{-/-}$ mice when fed either a ND or WD for 8 weeks (post weaning). The contractions of aortic rings, in the presence or absence of PVAT, were similar in WD and ND-fed Cav-1$^{-/-}$ mice. B) A similar pattern was observed in the 16 week ND and WD-fed groups. C) The presence of aortic PVAT did not alter vascular contractions after 26 weeks on a ND (post weaning). However, PVAT exerted a pro-contractile effect after 26 weeks feeding of a WD. No differences were observed between PVAT-intact aortic rings from ND or WD-fed Cav-1$^{-/-}$ mice although, the vasoconstrictor responses of PVAT-denuded aortic rings from ND-fed Cav-1$^{-/-}$ mice were significantly elevated in comparison to aortic preparations from WD-fed mice. ND = normal diet, PVAT = perivascular adipose tissue, WD = Western-type diet. Dose response data are expressed as mean ± S.E.M., n = 4-7 mice per group, two-way ANOVA with Bonferroni's post hoc tests, n = 4-7 mice per group, two-way ANOVA with Bonferroni's post hoc tests. *** P < 0.001, **** P < 0.0001*

5.4.3.5 Ageing alters the contractions of aortic rings from normal diet fed Cav-1$^{-/-}$ mice; however, no effects are observed with ageing on a Western-type diet

The effect of increasing age on the contraction of aortic rings from Cav-1 mice was assessed. Constriction of PVAT-denuded aortic rings from ND-fed mice was similar between the 8 and 16-week groups (P = NS; n = 7 and 4 mice per group, Figure 5.5Ai). Nevertheless, by the 26-week time-point, constriction was significantly increased compared to both the 8 and 16-week time-points (8-weeks versus 26-weeks: -PVAT P < 0.0001; n = 7 and 4 mice, Figure 5.5Ai) (16-weeks versus 26-weeks: -PVAT P < 0.0001; n = 4 mice in each group, Figure 5.5Ai). When PVAT-intact contractions were compared, a significant increase in contractility was observed between the 16 and 26-week time-points but no changes were observed between the other groups (16-weeks versus 26-weeks: +PVAT P < 0.0001; n = 4-7 mice per group, Figure 5.5Aii).

In contrast to the increase in contractility observed with ageing in ND-fed Cav-1$^{-/-}$ mice, ageing had no significant effect on aortic contractions in WD-fed Cav-1$^{-/-}$ mice in either PVAT-denuded or PVAT-intact aortic rings (P = NS for each comparison, n = 4-7 mice per group, Figure 5.5Bi and ii).

5.4.3.6 PVAT-denuded aortic rings exhibit attenuated constriction to phenylephrine in comparison to C57BL/6 mice in the 8 and 16-week normal diet-fed groups

The vasoconstrictor responses of Cav-1$^{-/-}$ mice were compared to age and diet-matched C57BL/6 mice (Appendix 2.6A-C). PVAT denuded aortic rings from ND-fed Cav-1$^{-/-}$ mice exhibited substantially lower contractile responses to phenylephrine, in comparison to C57BL/6 mice, in the 8 and 16 week groups (Cav-1$^{-/-}$ versus C57BL/6: 8-weeks P < 0.0001; 16-weeks P < 0.0001; n = 4-7 mice per group, Appendix 2.6A and B) but no differences were observed after 26 weeks on a ND (Cav-1$^{-/-}$ versus C57BL/6: 26-weeks P = NS; n = 4 and 8 mice, respectively, Appendix 2.6C). In contrast, the responses of PVAT-intact aortic rings were similar between Cav-1$^{-/-}$ and C57BL/6 mice at each time-point (Cav-1$^{-/-}$ versus C57BL/6: P = NS, n = 4-8 mice per group, Appendix 2.6A-C). In summary, the PVAT-denuded aortic rings of Cav-1$^{-/-}$ mice exhibit lower vasoconstrictor responses to phenylephrine, with the exception of 26 week ND-fed mice, when compared to C57BL/6 mice, whilst the contractions of PVAT-intact aortic preparations of Cav-1$^{-/-}$ mice are similar to those of the C57BL/6 strain

5.4.3.7 NOS inhibition in Cav-1$^{-/-}$ mice reveals a pro-contractile effect of PVAT

Inhibition of NOS with L-NNA (50 μM) did not significantly alter the contraction of PVAT-intact or PVAT-denuded aortic rings in ND-fed Cav-1 mice when responses in the presence or absence of L-NNA were compared (control versus L-NNA: P = NS, n = 4-9 mice per group, Figure 5.6Ai-iii). Furthermore, similar responses were produced in the WD-fed mice at each time-point, with the exception of the PVAT-intact 16-week group, where a large increase in contractility was observed in the presence of L-NNA (control versus L-NNA: 16-weeks: +PVAT P < 0.0001; n = 4-7 mice per group, Figure 5.6Bi-iii). However, when contractions of aortic rings in the presence of L-NNA, with or without PVAT were compared, a pro-contractile effect of PVAT was revealed in all the experimental groups, with the exception of the 8 week WD-fed mice (+PVAT + L-NNA versus -PVAT + L-NNA: all time-points, except 8-week WD, P < 0.0001; 8-weeks WD P = 0.08, n = 5-9 mice per group, Figure 5.6).

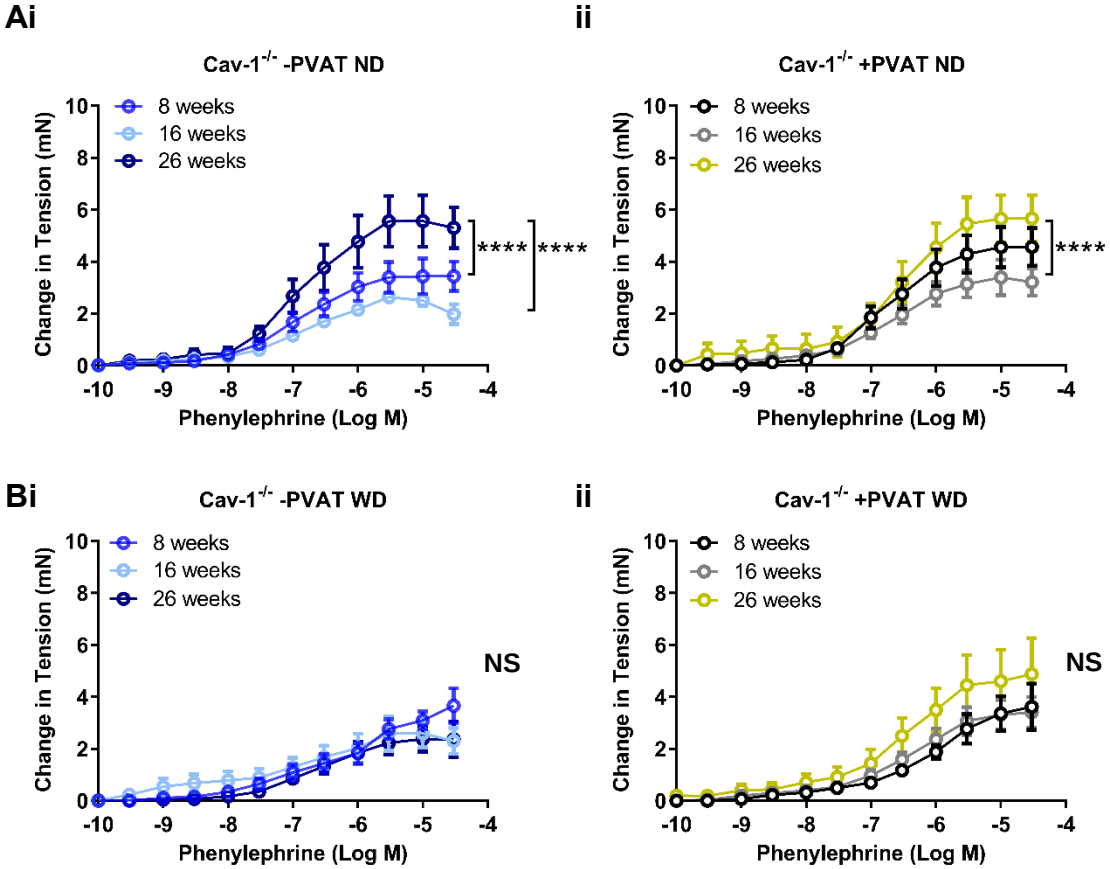

Figure 5.5 Ageing alters the contractions of aortic rings from normal diet fed Cav-1$^{-/-}$ mice; however, no effects are observed with ageing on a Western-type diet

*Ai) Contractile responses of PVAT-denuded aortic rings from ND-fed Cav-1$^{-/-}$ mice exhibited a significant increase in contraction after 26 weeks on a ND (post weaning). Aii) A similar increase in contractility was observed between the 16 and 26-week ND-fed groups in PVAT-intact aortic rings. Bi) A WD did not alter the contractility of aortic rings in the absence of PVAT or in Bii) PVAT-intact conditions, after 8, 16 or 26-weeks on a WD. ND = normal diet, PVAT = perivascular adipose tissue, WD = Western-type diet. Dose response data are expressed as mean ± S.E.M., n = 4-7 mice per group, two-way ANOVA with Bonferroni's post hoc tests. **** P < 0.0001.*

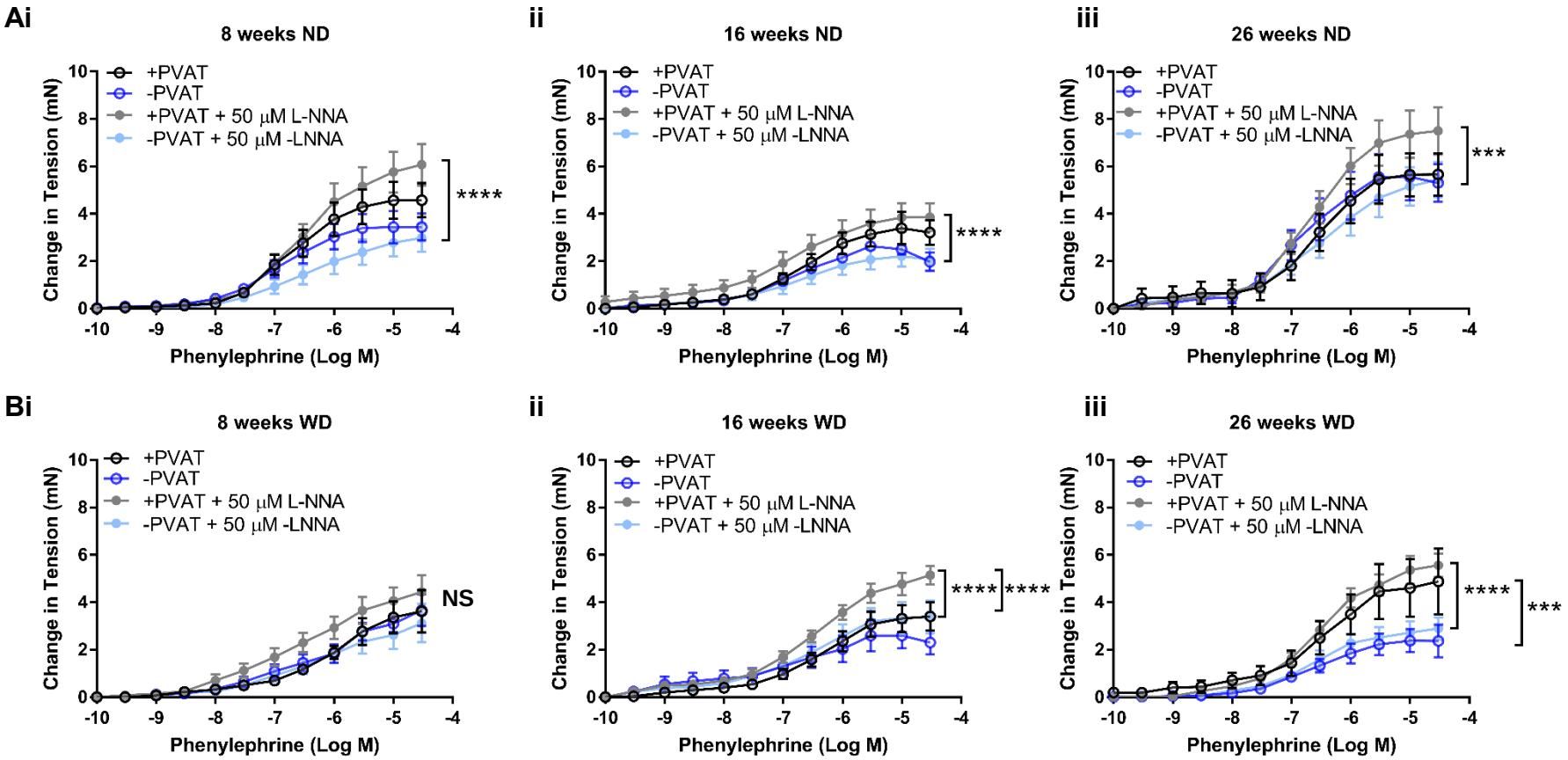

Figure 5.6 Nitric oxide synthase inhibition unmasks a pro-contractile effect of PVAT on aortic rings in Cav-1$^{-/-}$ mice

NOS inhibition with 50 μM L-NNA revealed a significant pro-contractile effect of PVAT in A) ND-fed Cav-1$^{-/-}$ mice at i) 8, i) 16 and the iii) 26-week time-point. NOS inhibition had no effect on B) WD-fed Cav-1$^{-/-}$ mice at the i) 8-week time-point but in the presence of L-NNA, PVAT exerted a pro-contractile effect on aortic rings in the i) 16 and iii) 26-week time-points. ND = normal diet, NOS = nitric oxide synthase, WD = Western-type diet. Dose response data are expressed as mean ± S.E.M., n = 4-9 mice per group, two-way ANOVA with Bonferroni's post hoc tests.

5.4.3.8 The sensitivity of aortic rings to exogenous nitric oxide is unchanged with ageing, the presence of PVAT or a Western-type diet

Pre-constricted aortic rings, in the presence or absence of PVAT, were exposed to the NO donor, sodium nitroprusside (10 µM). Aortic rings relaxed back to baseline in each group of Cav-1$^{-/-}$ mice regardless of the presence of PVAT, the age of the mice or a WD (P = NS each parameter and time-point comparison; n = 4-7 mice per group, Figure 5.7).

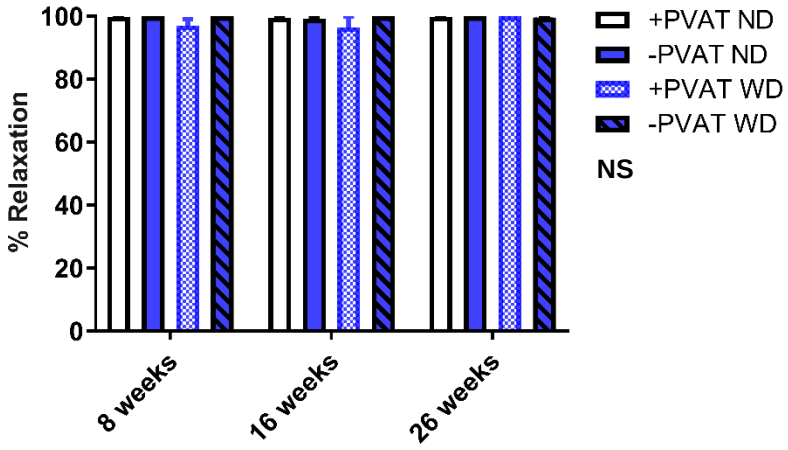

Figure 5.7 Endothelial-independent relaxation is unaffected by PVAT, ageing or a Western-type diet in Cav-1$^{-/-}$ mice

The sensitivity of aortic rings to NO was unaltered by the presence of PVAT, ageing or a WD when exposed to 10 µM sodium nitroprusside, an endothelium-independent vasodilator and potent NO donor. ND = normal diet, NO = nitric oxide, PVAT = perivascular adipose tissue, WD = Western-type diet. Data are presented as mean ± S.E.M, n = 4-7 mice per group, two-way ANOVA with post hoc Bonferroni's multiple comparisons test.

5.4.4 The weight of PVAT surrounding the aortae of Cav-1$^{-/-}$ mice is unaltered by ageing or a Western-type diet

The influence of ageing and a WD on the weight of PVAT encasing the aortae were investigated in Cav-1$^{-/-}$ mice. With increasing age on a ND, the weight of PVAT did not change significantly (P = NS each comparison; n = 3-4 mice per group, Figure 5.8). Additionally, a WD did not appear to increase the weight of PVAT surrounding the aortae in comparison to age and strain-matched ND-fed mice (ND versus WD: P = NS, n= 1-4 mice per group, Figure 5.8). However, firm conclusions cannot be drawn due to a sample size of 1 mouse for the 26-week WD group and 2 mice in the 8-week WD-fed group due to breeding issues with the Cav-1$^{-/-}$ colony.

Also, the weight of PVAT surrounding the aortae of Cav-1$^{-/-}$ mice was compared to the genetic background strain, C57BL/6 mice (Appendix 2.8A). No differences in aortic PVAT weight were observed between the 8-week ND-fed Cav-1$^{-/-}$ and C57BL/6 mice (P > 0.99; n = 3-4 mice per group, Appendix 2.8A). However, the weight of PVAT encasing the aortae of the 16 week ND-fed Cav-1$^{-/-}$ mice was significantly increased compared to the age-matched C57BL/6 group (P = 0.01; n = 3-4 mice per group Appendix 2.8A). After 26 weeks on a ND, the weight of PVAT surrounding

the aortae of C57BL/6 mice was increased and no significant differences were observed between the Cav-1$^{-/-}$ and C57BL/6 mice (P = NS; n = 4-6 mice per group, Appendix 2.8A).

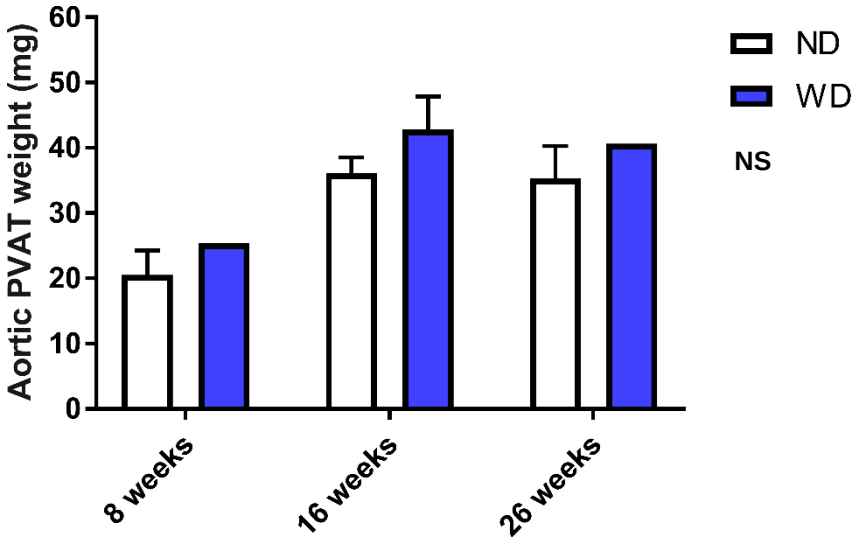

Figure 5.8 Ageing and a Western-type diet do not significantly alter the amount of PVAT surrounding the aortae of Cav-1$^{-/-}$ mice

The PVAT surrounding the aortic arch and thoracic aorta of Cav-1$^{-/-}$ mice was weighed. No significant differences were observed with ageing or a WD at any of the time-points. ND = normal diet, WD = Western-type diet. Data are presented as mean ± S.E.M, n = 1-5 mice per group, two-way ANOVA with post hoc Bonferroni's multiple comparisons test.

5.4.5 White adipocyte hypertrophy is observed in the aortic PVAT of 26-week Western-type diet fed Cav-1$^{-/-}$ mice

The effects of ageing and a WD on the aortic PVAT of Cav-1$^{-/-}$ mice were assessed using haematoxylin and eosin staining (Figure 5.9Ai-vi)

The morphology of the aortic PVAT was evaluated by measuring the total area occupied by white adipocytes, as a percentage of total aortic PVAT area, and subsequently, quantifying the area of each white adipocyte. Increasing age while on a ND did not induce any changes in the proportion of white adipocytes within the aortic PVAT of Cav-1$^{-/-}$ mice (P = NS for each time-point comparison; n = 3-4 mice per group, Figure 5.9B). An increase in the percentage of white adipocytes within the aortic PVAT was observed after 16 weeks (ND versus WD: P = 0.02; n = 4 and 3 mice, respectively, Figure 5.9B) but this was not maintained in the 26-week time-point mice (ND versus WD: P = NS, n = 3 mice per group, Figure 5.9B).

When the white adipocytes within the aortic PVAT were examined, no age-related changes in size were observed in the ND-fed Cav-1$^{-/-}$ mice (P = NS for each time-point comparison; n = 3-4 mice per group, Figure 5.9C). However, upon 26 weeks of high fat feeding, WD-induced white adipocyte hypertrophy was observed within the PVAT of Cav-1$^{-/-}$ mice (ND versus WD: P = 0.02; n = 3 mice per group, Figure 5.9C).

The morphology of aortic PVAT from ND-fed Cav-1$^{-/-}$ mice was compared to age and diet matched C57BL/6 mice (Appendix 2.8B and C). The area occupied by white adipocytes in the aortic PVAT

of ND-fed Cav-1$^{-/-}$ mice was not significantly different to measurements from the C57BL/6 mice (Cav-1$^{-/-}$ versus C57BL/6: 8 weeks: P = NS; n = 3-4 mice per group, Appendix 2.8B). However, after 26 weeks on a ND, the individual white adipocyte area of Cav-1$^{-/-}$ mice was markedly smaller than the adipocyte area observed in the aortic PVAT from C57BL/6 mice of the same age (P = 0.002, n = 3 mice per group, Appendix 2.8C).

Whilst the composition of aortic PVAT of Cav-1$^{-/-}$ mice was unaltered by ageing, it was not protected from the effects of a WD. An increase in the proportion of PVAT occupied by white adipocytes, which was the result of white adipocyte hypertrophy and not hyperplasia, was detected. The morphological changes discovered within the aortic PVAT, after extensive high fat feeding, could have contributed to the observed modulation of vascular reactivity and exertion of a pro-contractile effect on aortic rings (Figure 5.4Biii).

5.4.6 The aortic PVAT of Cav-1$^{-/-}$ mice does not display any age or diet-related changes in superoxide

Superoxide production, within the aortic PVAT of Cav-1$^{-/-}$ mice, was assessed by dihydroethidium (DHE) staining. Superoxide was detected in all experimental groups (Figure 5.10Ai-vi). However, increasing age on a ND did not impact the amount of superoxide detected in the aortic PVAT (P = NS; n = 3 mice per group, Figure 5.10C). Correspondingly, a WD did not augment the production of superoxide within the aortic PVAT of Cav-1$^{-/-}$ mice (ND versus WD: P = NS each comparison; n = 3 mice in each group, Figure 5.10C).

Superoxide production within the aortic PVAT of ND-fed Cav-1$^{-/-}$ mice was compared to the age and diet-matched C57BL/6 strain (Appendix 2.8D). Superoxide was transiently increased in comparison to C57BL/6 mice after 8-weeks on a ND (post weaning) (P = 0.007; n = 3 mice per group, Appendix 2.8D). However, this finding was not maintained in the subsequent groups (P = NS, n = 3-4 mice per group, Appendix 2.8D).

Neither increasing age or a WD had an impact on the presence of superoxide within the aortic PVAT of Cav-1$^{-/-}$ mice. These data suggest that superoxide production within the aortic PVAT of Cav-1$^{-/-}$ mice was not elevated after extensive high fat feeding thus, it is unlikely that superoxide production contributed to the observed exertion of a pro-contractile effect by aortic PVAT after 26 weeks on a WD (Figure 5.4C).

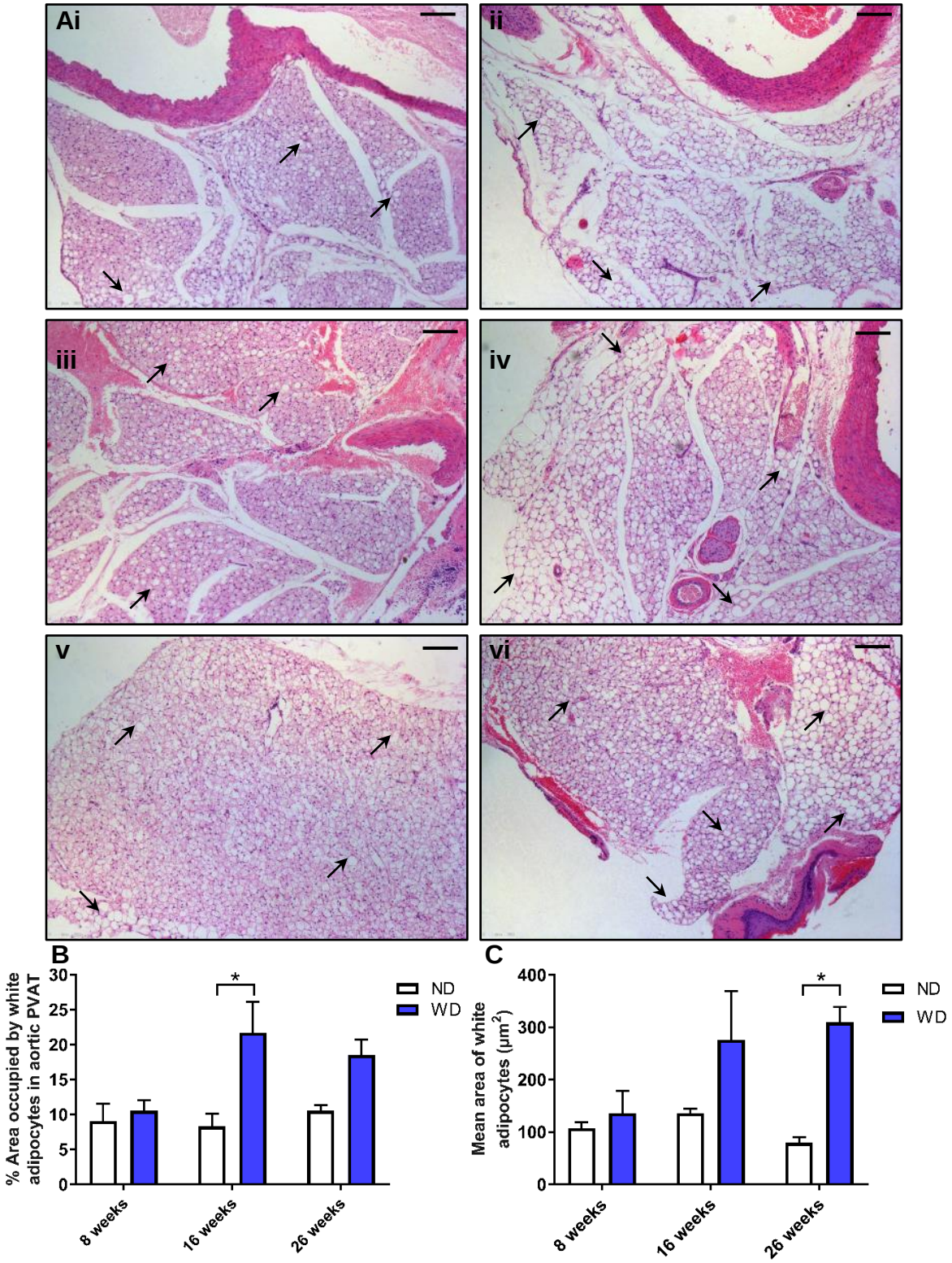

Figure 5.9 White adipocyte hypertrophy is observed in the aortic PVAT of Western-type diet fed Cav-1$^{-/-}$ mice after 26 weeks of feeding

A) Haematoxylin and eosin-stained aortae with PVAT from Cav-1$^{-/-}$ mice after 8-weeks, i) ND, ii) WD, 16-weeks iii) ND, iv) WD and 26-weeks v) ND and vi) WD. Examples of white adipocytes are highlighted by arrows. B) The percentage area of aortic PVAT occupied by white adipocytes was significantly increased in 16-week WD-fed mice. C) White adipocyte hypertrophy was observed after 26 weeks on a WD. Representative images obtained at 10X magnification. Scale bars represent 100 µm. ND = normal diet, WD = Western-type diet. Data are expressed as mean ± S.E.M, n = 3-4 mice per group, two-way ANOVA with Bonferroni's post hoc tests, P < 0.05.*

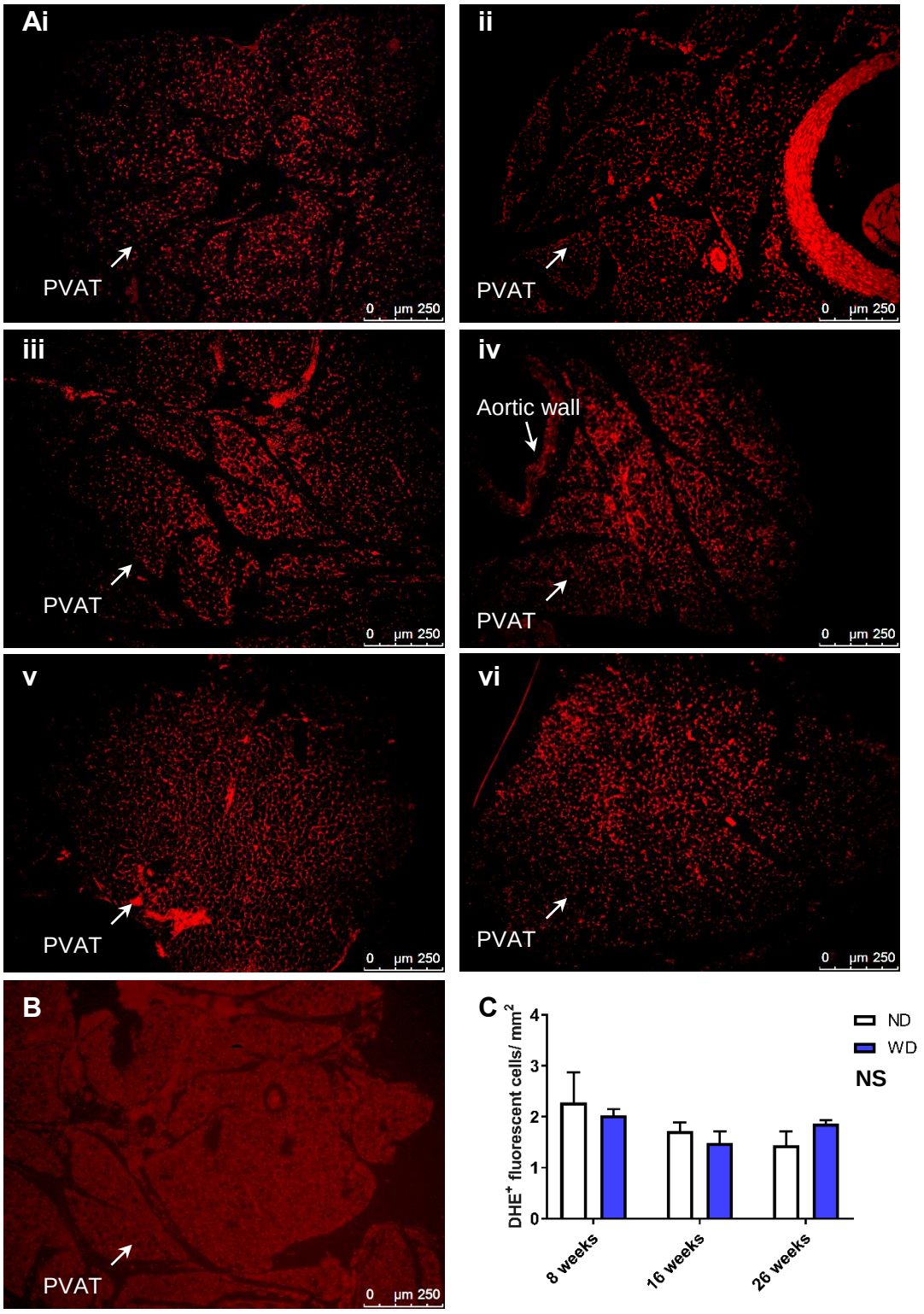

Figure 5.6 Ageing and a Western-type diet do not alter superoxide production within the aortic PVAT of Cav-1$^{-/-}$ mice

Sections of aortic PVAT were stained with DHE a superoxide indicator, and visualised by red punctate fluorescence. A) DHE^{+} nuclei were observed in all sections i) 8-week ND, ii) WD, iii) 16-week ND, iv) WD and 26-week v) ND and vi) WD. B) DHE^{+} staining was not observed in the DHE-omitted control. C) Superoxide production was unaffected by ageing or a WD. Representative images at 10 X magnification. Scale bars represent 250 µm. DHE^{+} nuclei were quantified in 5 fields of view per tissue section. DHE = dihydroethidium, ND = normal diet, PVAT = perivascular adipose tissue, WD = Western-type diet. Data are expressed as mean ± S.E.M., Data presented as cells/mm^2 of PVAT, n = 3-4 mice per group, two-way ANOVA with Bonferroni's post hoc tests.

5.4.7 Macrophage infiltration, within the aortic PVAT of Cav-1 mice is unaffected by ageing or a Western-type diet

The aortic PVAT of Cav-1$^{-/-}$ mice underwent immunostaining for Mac-3 to determine if ageing altered inflammation within the PVAT (Figure 5.11Bi-viii). Ageing did not alter the number of Mac-3^{+} cells infiltrating the aortic PVAT and no changes in Mac-3^{+} cells were observed between the different groups PVAT (8-weeks versus 16-weeks: $P > 0.99$; 16-weeks versus 26-weeks: $P > 0.99$; 8-weeks versus 26-weeks; $P = 0.68$; n = 3 mice per group, Figure 5.12).

Furthermore, a WD did not induce more Mac-3^{+} cells in infiltrate the aortic PVAT of Cav-1$^{-/-}$ mice, even after extensive feeding of a WD (ND versus WD: 8-weeks $P > 0.99$; 16-weeks $P = 0.87$; 26 weeks: $P > 0.99$; n = 3-4 mice per group, Figure 5.12).

Moreover, when Mac-3+ staining of ND-fed Cav-1$^{-/-}$ mice was compared to C57BL/6s, no significant differences were observed between the groups ($P > 0.99$ each diet time-point; n = 3-4 mice per group, Appendix 2.8 E).

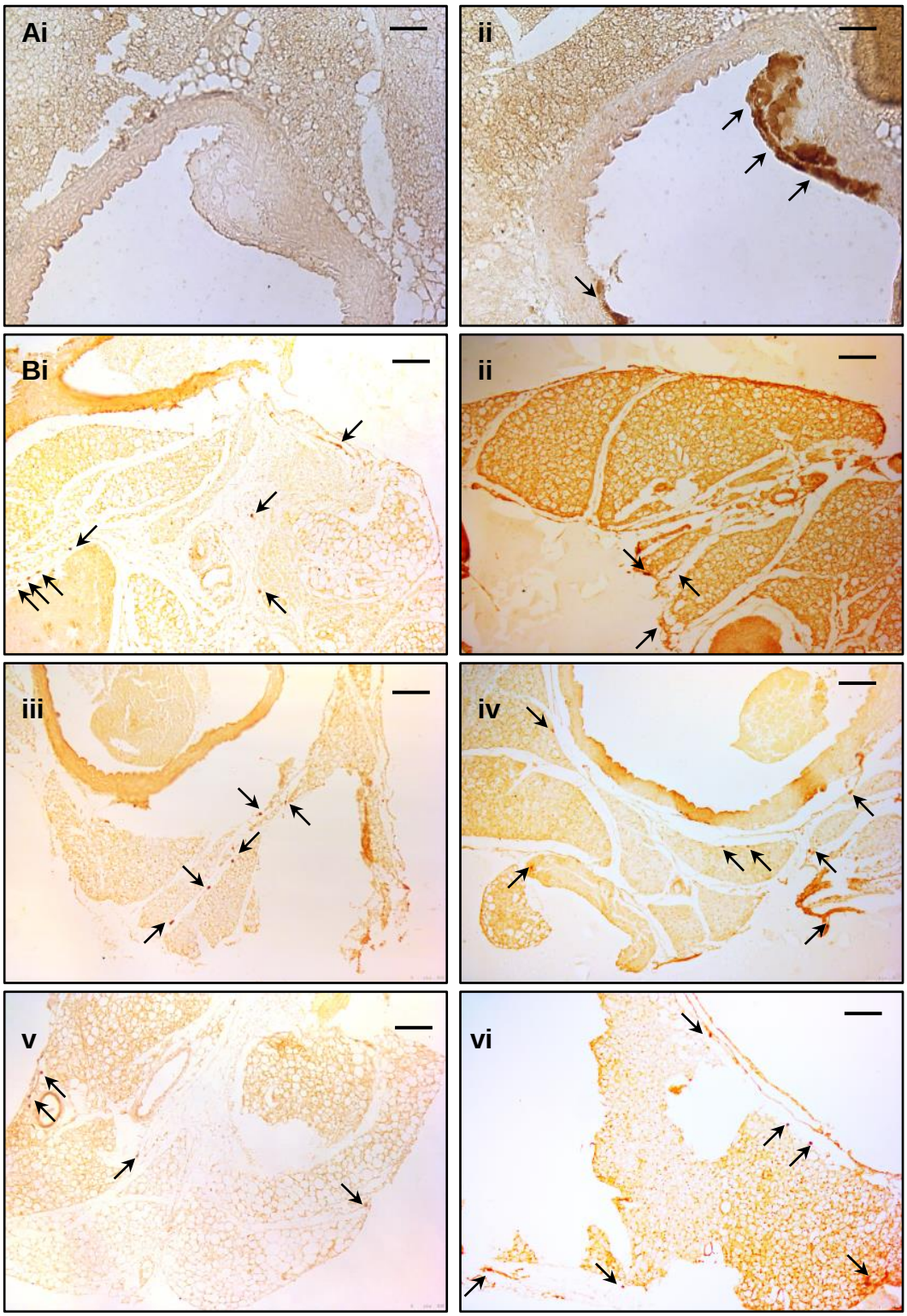

Figure 5.7 Macrophages are present in the aortic PVAT of normal diet and Western-type diet fed Cav-1$^{-/-}$ mice at each time-point

Macrophages were stained with a Mac-3 antibody A) The aortic arch of an atherosclerotic ApoE$^{-/-}$ mouse was used as the control i) IgG and ii) positive control, with specific brown staining within the atherosclerotic plaque. B) Representative images of Cav-1$^{-/-}$ mice at: i) 8-week ND and ii) WD, iii) 16-week ND and iv) WD and 26-week v) ND and vi) WD. Images were obtained at 10X magnification. Scale bars represent 100 µm and examples of Mac-3^{+} staining are highlighted by arrows. ND = normal diet, WD = Western-type diet.

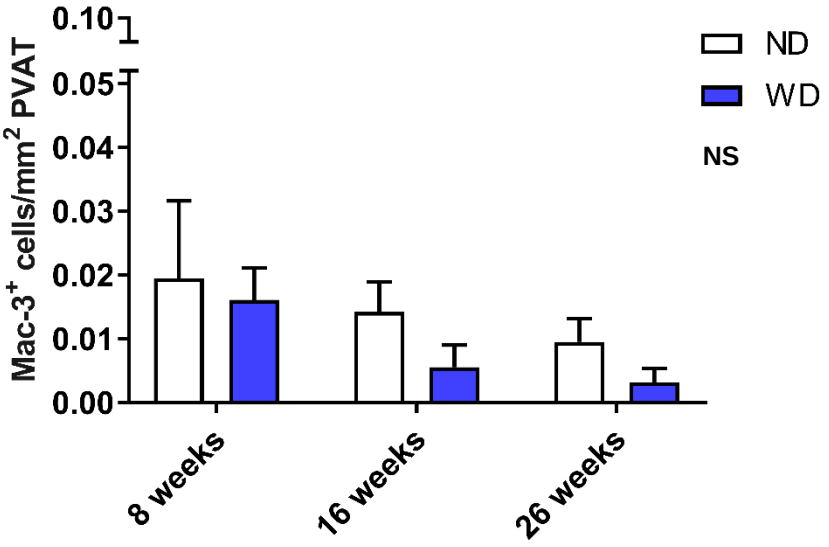

Figure 5.8 The number of Mac-3^{+} cells present within the aortic PVAT of Cav-1$^{-/-}$ mice is unchanged with ageing or a Western-type diet

Macrophage numbers within the aortic PVAT of Cav-1$^{-/-}$ mice were not significantly affected by ageing. Additionally, no differences were observed between ND or WD-fed mice at any of the time-points. ND = normal diet, WD = Western-type diet. Data are expressed as Mac3^{+} cells/mm^{2} PVAT, mean ± S.E.M., n = 3-4 mice per group, two-way ANOVA with Bonferroni's post hoc multiple comparisons test.

5.5 Discussion

This present study aimed to characterise the morphology and influence of aortic PVAT on vascular function in Cav-1$^{-/-}$ mice. In the present study, Cav-1$^{-/-}$ mice were demonstrated to be athero-resistant even though WD-fed mice displayed hypercholesterolaemia. Therefore, Cav-1$^{-/-}$ mice offer an intriguing insight into the effect of Cav-1 deletion on vascular ageing without the added complication of atherogenesis.

The key findings of this chapter were:

- The aortic PVAT of Cav-1$^{-/-}$ mice did not exert an anti-contractile effect on isolated aortic rings.
- The aortic PVAT of Cav-1$^{-/-}$ mice fed a WD for 26 weeks exerted a pro-contractile effect on aortae and this was associated white adipocyte hypertrophy within the aortic PVAT.
- In the presence of the NOS inhibitor, L-NNA, the aortic PVAT of Cav-1$^{-/-}$ mice exerted a pro-contractile effect on aortic ring preparations.
- Extensive feeding of a WD induced white adipocyte hypertrophy within the aortic PVAT of Cav-1$^{-/-}$ mice.

5.5.1 Phenotyping of normal and Western-type diet-fed Cav-1$^{-/-}$ mice

5.5.1.1 The lipidaemic and glycaemic profiles of normal diet-fed Cav-1$^{-/-}$ mice are unchanged with increasing age

The lipid and glucose profiles of ageing Cav-1$^{-/-}$ mice were assessed because Cav-1 has been demonstrated to play a role in cholesterol metabolism and insulin signalling (Nystrom et al. 1999; Fielding and Fielding 2000). There were no overt differences between the non-fasted lipid or glucose levels of ageing Cav-1$^{-/-}$ mice. Furthermore, no differences were observed between the Cav-1$^{-/-}$ serum lipid or glucose profiles of age and diet-matched C57BL/6 mice. These findings are in contrast with published work which observed that Cav-1$^{-/-}$ mice display hypertriglyceridaemia in comparison to C57BL/6 controls and this state is exaggerated in samples obtained postprandially (Razani et al. 2002a; Cohen et al. 2003b). These differences could have occurred due to the use of different assays to measure the triglyceride content or, more likely, due to the use of different rodent chow diets. In the present study, a normal chow diet with 7.52% fat was used whereas; in the previous study mice were maintained on a 10% fat diet (Razani et al. 2002a). Furthermore, a different study observed no differences in the triglyceride levels of Cav-1$^{-/-}$ and C57BL/6 mice at 12 weeks of age (Cohen et al. 2005). The data from this study suggest that Cav-1$^{-/-}$ mice maintained on a ND do not develop dyslipidaemia, a condition which is strongly linked to atherosclerosis and increased cardiovascular risk (Catapano et al. 2011). In line with this finding, atherosclerotic lesions were not observed within the aortae of Cav-1$^{-/-}$ mice, demonstrating that this strain does not spontaneously develop atherosclerosis after 26 weeks of feeding a WD (post weaning).

5.5.1.2 Western-type diet-fed Cav-1$^{-/-}$ mice develop hypercholesterolaemia but are resistant to the development of aortic atherosclerotic lesions

Cav-1$^{-/-}$ mice fed a WD exhibited elevated cholesterol levels and transiently increased HDL after 8 weeks of high fat feeding in comparison to age-matched ND-fed Cav-1$^{-/-}$ mice. However, triglyceride and glucose levels remained similar between ND and WD-fed groups. Moreover, previous studies in Cav-1$^{-/-}$ mice fed a high fat diet, containing 34.9% fat, demonstrated increased HDL-cholesterol esters, free cholesterol, pre-β-HDL, and triglycerides further demonstrating a role of Cav-1 in cholesterol metabolism (Heimerl et al. 2008). These data suggest that Cav-1$^{-/-}$ mice are not resistant to diet-induced hypercholesterolaemia. In humans hypercholesterolaemia is a well-known risk factor for atherosclerosis (Singh et al. 2002). En face lesion analysis demonstrated that atherosclerotic lesions were not present along the luminal surface of the aortae of Cav-1$^{-/-}$ mice after extended high fat feeding (26 weeks WD). Therefore, the athero-resistant phenotype of Cav-1$^{-/-}$ mice is likely to be the result of a lack of uptake and transcytosis of LDL (native or oxidised) into the sub-endothelial space of the vascular wall, which is an important factor in the pathogenesis of atherosclerosis (Cohen et al. 2004a; Fernandez-Hernando et al. 2009; Frank 2010).

5.5.1.3 Normal diet-fed Cav-1$^{-/-}$ mice develop cardiac hypertrophy with ageing

An age-associated increase in body weight was observed in the Cav-1$^{-/-}$ mice and epididymal fat pad weight, but not adipocyte area, was increased after 26 weeks on a ND, in comparison to the

8-week group. However, no other effects of ageing were observed when heart weights, heart weight: body weight ratio, liver and spleen weights were compared.

Although the body weights of Cav-1$^{-/-}$ and C57BL/6 mice were reported to be indistinguishable in the first few months of life, the Cav-1$^{-/-}$ strain has, in previous studies been demonstrated to be leaner than C57BL/6 mice by 12 months of age (Razani et al. 2002a; Cohen et al. 2005). This leaner phenotype of Cav-1$^{-/-}$ mice has been attributed to a reduced cross sectional diameter of adipocytes due to the proposed role of Cav-1 in modulating the structure and biogenesis of lipid droplets and the storage/transport of fatty acids (Razani et al. 2002a; Cohen et al. 2004b). In this present study, no differences were observed between the body weights of C57BL/6 and Cav-1$^{-/-}$ mice after 26 weeks on a ND (post weaning). However, the epididymal fat pads in the 26 week ND group were significantly smaller than the age-matched C57BL/6 group whereas, no differences in epididymal adipocyte size were observed between these groups. Previous studies have demonstrated that the epididymal fat pads of Cav-1$^{-/-}$ mice at approximately 12 weeks old do not display a reduced adipocyte size or aberrations in lipid droplet size (Razani et al. 2002a; Cohen et al. 2004b). These data could suggest that after 26 weeks on a ND the fat depots of Cav-1$^{-/-}$ mice retain characteristics similar to the C57BL/6 mice and age-associated alterations to the adipocytes within the fat pads had not yet occurred.

Whilst no significant differences in the weight of hearts obtained from Cav-1$^{-/-}$ and C57BL/6 mice after 8 weeks on a ND, cardiac hypertrophy was observed after 16 weeks on a ND, evidenced by a significantly increased heart weight and heart weight: body weight ratio compared to C57BL/6 mice. Similar findings have been reported in several different studies of Cav-1$^{-/-}$ mice (Cohen et al. 2003a; Park et al. 2003). It has been suggested that the reported reduction of lifespan of Cav-1$^{-/-}$ mice is potentially due to the development of cardiac hypertrophy with ageing in these mice (Le Lay and Kurzchalia 2005).

Cav-1 is not highly expressed in the liver parenchyma therefore it was not surprising that the liver weights of Cav-1$^{-/-}$ and C57BL/6 mice were similar in all ND-fed groups (Razani et al. 2002a). Nevertheless, splenomegaly was observed after 16 weeks on a ND and this was sustained in the 26-week ND group and this is in line with previous findings and may be indicative of systemic inflammation in Cav-1$^{-/-}$ mice (Percy et al. 2008; Bai et al. 2014).

5.5.1.4 Western-type diet-fed Cav-1$^{-/-}$ mice are resistant to diet-induced weight gain but develop hepatomegaly and splenomegaly

In this present study, Cav-1$^{-/-}$ mice were fed a WD and, except for the 8-week group, were resistant to diet-induced weight gain, an observation which has previously been demonstrated (Razani et al. 2002a). Interestingly, the epididymal fat pads of Cav-1$^{-/-}$ mice were significantly heavier and the epididymal adipocytes enlarged compared to ND-fed mice after 8 and 16 weeks on the WD. However, this effect was lost after 26 weeks on the WD. Previous studies have demonstrated that Cav-1/- mice exhibit only a small gain in fat mass when fed a high fat diet and this is drastically reduced compared to C57BL/6, which suggests that the Cav-1$^{-/-}$ mice are incapable of significant gains in fat mass and display significant adipocyte abnormalities (Razani et al. 2002a). Moreover, in Cav-1$^{-/-}$ mice at 9 months of age the white adipose fat depots were composed of predominantly small adipocytes and were hyper-cellular in comparison to C57BL/6

mice, which could indicate that the adipocytes of Cav-1$^{-/-}$ mice, in response to a high fat diet, are unable to undergo lipogenesis (Razani et al. 2002a). Hepatomegaly was observed in WD-fed Cav-1$^{-/-}$ mice after 8 weeks of feeding and splenomegaly was observed after 26 weeks of feeding (post weaning). This could suggest that a compensatory mechanism occurred in response to the hypercholesterolaemia and explain, in part, why the Cav-1$^{-/-}$ mice did not exhibit diet-induced weight gain, because of an increased uptake of lipids within the liver and spleen and potentially other organ systems.

5.5.2 Vascular reactivity studies assessing the effect of aortic PVAT on vascular responses

Previous experiments on isolated aortic tissue segments from Cav-1$^{-/-}$ mice have been performed in PVAT-denuded conditions. Consequently, the influence of PVAT on vascular reactivity in the Cav-1$^{-/-}$ mouse has not previously been investigated. Therefore, the influence of PVAT, age and a WD on the vascular reactivity of aortic rings from Cav-1$^{-/-}$ mice was investigated.

A high potassium solution, 100 mM KPSS (as used by other studies of large artery preparations), was used to produce membrane depolarisation and stimulate Ca^{2+} entry via voltage-gated channels independently of agonist-induced receptor stimulation (Murphy et al. 2000; Russell et al. 2000; Pojoga et al. 2014; Wheeler et al. 2015). In this study, the presence of PVAT did not significantly alter contractions to KPSS. Furthermore, no significant differences in contractions were observed with increasing age or a WD in PVAT-intact or PVAT-denuded aortic rings. However, there was a substantial amount of variability between the groups and therefore firm conclusions should not be drawn from this data.

A previous study using this specific strain of Cav-1$^{-/-}$ mice demonstrated a reduced constriction of isolated aortic rings to KPSS in comparison to age-matched C57BL/6 mice (Pojoga et al. 2014). This was not observed in the present study and may be due to differences in experimental technique such as the use of different experimental conditions, method of stretching and altered resting tension. In the context of this study, the data suggests that in Cav-1$^{-/-}$ mice the responses of aortic preparations to depolarisation are unaffected by ageing or a WD and contractions are similar to the C57BL/6 strain.

5.5.2.1 Endothelial function is retained in the aorta of normal or Western-type diet-fed Cav-1$^{-/-}$ mice

Cav-1$^{-/-}$ mice have been proposed as a model of premature vascular ageing and one of the main characteristics of vascular ageing is endothelial dysfunction (Taddei et al. 2001; Cho and Park 2005; Ungvari et al. 2010). In this study, neither ageing nor the presence of PVAT altered relaxation responses in ND-fed Cav-1$^{-/-}$ mice which suggests that endothelial function is retained in the Cav-1$^{-/-}$ mice during the studied time-frame and therefore premature vascular ageing is not yet apparent. Furthermore, endothelium-dependent relaxation responses were not significantly altered with increasing age in Cav-1$^{-/-}$ mice fed a WD. Hypercholesterolaemia is strongly associated with dysfunction of endothelial nitric oxide-dependent vasodilation (Bonthu et al. 1997; Kurtel et al. 2013; Brinkmann et al. 2014). Previous studies have demonstrated that this could, at least in part, be due to a mechanism involving an increase in the expression of Cav-1 and caveolae stimulated by increased uptake of cholesterol by endothelial cells and therefore, increased inhibitory Cav-1-eNOS interactions resulting in impaired NO production (Feron et al.

1999; Grayson et al. 2013). However, Cav-1 is not expressed within the vasculature of Cav-1$^{-/-}$ mice and the data from the present study suggest that the bioavailability of NO was unaffected by the development of hypercholesterolaemia and therefore, the aortae of WD-fed Cav-1$^{-/-}$ mice did not display signs of premature vascular ageing after 26 weeks of high fat feeding.

Studies in Cav-1$^{-/-}$ mice have reported an enhanced vaso-relaxation response to acetylcholine in comparison to C57BL/6 mice (Razani et al. 2001; Pojoga et al. 2014). In agreement, this study found that whilst no significant differences in relaxation were observed after 8 or 16 weeks on a ND, relaxation of PVAT-denuded aortic rings was significantly greater after 26 weeks on a ND in comparison to the C57BL/6 strain. Therefore, these data suggest that a healthy endothelium is maintained in ND Cav-1$^{-/-}$ mice for a longer period than in C57BL/6 mice (during the time-frame of this study) due to enhanced eNOS activity and increased basal NO production, an observation previously reported in Cav-1$^{-/-}$ mice (Razani et al. 2001).

Interestingly, the presence of PVAT was not found to significantly alter the vaso-relaxation responses of aortic rings from Cav-1$^{-/-}$ mice in either ND or WD-fed conditions. These data could suggest that either the aortic PVAT of Cav-1$^{-/-}$ mice does not modulate acetylcholine-induced relaxation or, that the aortic rings of Cav-1$^{-/-}$ mice reached their maximal endothelium-dependent relaxation response and this could not be further modulated by PVAT.

5.5.2.2 The aortic PVAT of normal diet-fed Cav-1$^{-/-}$ mice does not exert an anti-contractile effect

PVAT has been proven to modulate vascular reactivity in a range of species, and in various vascular beds, by the release of PVAT-derived vasoactive factors (Brown et al. 2014). However, the influence of PVAT on the vascular reactivity of Cav-1$^{-/-}$ mice has not previously been investigated.

The first study to characterise Cav-1$^{-/-}$ mice demonstrated a diminished vasoconstrictor response, in PVAT-denuded aortic rings, to phenylephrine and this finding has been supported by subsequent works (Razani et al. 2001; Hausman et al. 2012; Pojoga et al. 2014). This observed attenuated vasoconstriction has been attributed to the loss of the Cav-1-eNOS inhibitory interaction resulting in an increase in NO bioavailability (Rahman and Sward 2009; Rath et al. 2009). Previously, (Chapter 3) NO was observed to mediate the anti-contractile effect of PVAT in C57BL/6 mice, and this finding is supported by other works which demonstrate a loss of the anti-contractile effect of PVAT with NOS inhibition (Gao et al. 2007b; Victorio et al. 2016). The recent detection of eNOS within rodent PVAT further supports the theory that NO contributes to the anti-contractile capacity of PVAT (Araujo et al. 2015; Xia et al. 2016). Consequently, the influence of aortic PVAT of Cav-1$^{-/-}$ mice on aortic contractions was assessed. Surprisingly, the aortic PVAT of Cav-1$^{-/-}$ mice did not exert an anti-contractile effect in response to cumulative doses of phenylephrine or a single 10 µm dose of serotonin (data not shown).

5.5.2.3 The aortic PVAT of Cav-1$^{-/-}$ mice fed a WD for 26 weeks exerts a pro-contractile effect on aortae

The effect of a WD on the contractions of arteries from Cav-1$^{-/-}$ mice has not been well-characterised. In this study, the aortic PVAT of WD-fed Cav-1$^{-/-}$ mice did not modulate vascular

contractions, up to 26 weeks of age. However, after 26 weeks on a WD, PVAT-intact aortic rings began to exert a pro-contractile effect on the aortic rings of Cav-1$^{-/-}$ mice, which may suggest that PVAT released a vaso-constricting factor. Similar observations of aortic PVAT exerting a pro-contractile effect on the vasculature have been reported in murine diet-induced weight gain studies. In those studies, the loss of the anti-contractile effect of PVAT was associated with alterations to the brown adipocyte progenitor cell population, increased oxidative stress with the PVAT and the release of pro-inflammatory cytokines (Ketonen et al. 2010; Xu et al. 2012).

5.5.2.4 The contractions of PVAT-denuded aortic rings from Cav-1$^{-/-}$ mice were initially attenuated in comparison to age and diet matched C57BL/6 mice

The contractions of ND-fed Cav-1$^{-/-}$ mice were compared to age and diet-matched C57BL/6 mice to determine if the observed responses were similar to those reported in other studies and if there were differences in the responses of PVAT-intact aortic preparations. In agreement with previous studies, the contraction of the 8 and 16-week ND fed mice were significantly attenuated in comparison to age and diet-matched C57BL/6 mice which suggests enhanced NO bioavailability within the aortae of Cav-1$^{-/-}$ mice in these experimental groups (Razani et al. 2001; Hausman et al. 2012; Pojoga et al. 2014). However, a significant increase in the contraction of PVAT-denuded aortic rings from Cav-1$^{-/-}$ mice was observed after 26 weeks on a ND, resulting in a similar level of constriction to the PVAT-denuded aortic rings of age-matched C57BL/6 mice. These findings are in contrast with a study on the mesenteric arteries of Cav-1$^{-/-}$ mice which demonstrated no age-associated changes between 3 and 12-month-old Cav-1$^{-/-}$ mice (Hausman et al. 2012). This discrepancy may be due to the use of a different vascular bed, the use of a different agonist (phenylephrine versus noradrenaline) and the significantly different ages of mice at the final time-point, 30 weeks in this study (mice were weaned at 4 weeks of age) versus 52 weeks old. The mechanism behind this increase in contraction of PVAT-denuded aortic rings from the 26-week ND fed mice has not been identified. Endothelium-dependent relaxation responses to acetylcholine were preserved in the Cav-1$^{-/-}$ mice which could potentially suggest that decreased NO production was not a factor in the increased vasoconstrictor responses. However, NO bioavailability was not directly assessed in this study and therefore further investigation is required in order to elucidate the mechanism behind the observed increase in contraction.

Strikingly, the contractile responses of PVAT-intact aortic rings from ND-fed Cav-1$^{-/-}$ mice were similar to the contractions of C57BL/6 mice. In C57BL/6 mice (Chapter 3) aortic PVAT exerted an anti-contractile effect on aortic rings in mice fed a ND for 8 and 16 weeks, post weaning. The similar responses of the aortic PVAT from Cav-1$^{-/-}$ and C57BL/6 mice could potentially point to the aortic PVAT of Cav1$^{-/-}$ mice being functional and may indicate that the PVAT was unable to exert an anti-contractile effect due to the dampened vasoconstrictor responses of the PVAT-denuded aortic rings. In addition, the PVAT-intact aortic rings of the 26-week ND-fed Cav-1$^{-/-}$ mice displayed similar contractility to the age-matched C57BL/6 group. After 26 weeks on a ND (post weaning) the aortic PVAT of C57BL/6 mice no longer exerted an anti-contractile effect on aortic preparations and was dysfunctional. This may suggest that the aortic PVAT of Cav-1$^{-/-}$ mice was beginning to display dysfunctional characteristics.

In summary, isolated PVAT-intact aortic rings from ND-fed Cav-1$^{-/-}$ mice did not exert any anti-contractile effects in response to cumulative doses of phenylephrine. However, after extensive feeding of a WD (26 weeks) the aortic PVAT of Cav-1$^{-/-}$ mice was found to exert a pro-contractile effect on aortic preparations. This may indicate that the aortic PVAT of Cav-1$^{-/-}$ mice releases an unidentified PVAT-derived constricting factor which was potentially the cause of the increased contractions observed in the 26-week WD-fed Cav-1$^{-/-}$ mice. These findings led to an investigation of the effects of NOS inhibition on the aortic responses of Cav-1$^{-/-}$ mice.

5.5.2.5 The aortic PVAT of Cav-1$^{-/-}$ mice exerts a pro-contractile effect on aortic ring preparations in the presence of the NOS inhibitor, LNNA

There is evidence that rodent aortic PVAT expresses eNOS and therefore produces NO (Araujo et al. 2015; Xia et al. 2016). Furthermore, previous studies performed in Cav-1$^{-/-}$ mice have demonstrated a key role for eNOS activity and subsequent excess NO contributing to the diminished vasoconstrictor effect observed in the arteries of Cav-1$^{-/-}$ mice (Rath et al. 2009; Raman et al. 2011). Therefore, the NOS inhibitor L-NNA was used to discern the contribution of NO-mediated relaxation from the phenylephrine-induced constriction of aortic rings in the Cav-1$^{-/-}$ mice.

In the presence of L-NNA, PVAT-intact aortic rings exerted a substantial pro-contractile effect in comparison to PVAT-denuded aortic rings, with the exception of the 8-week WD-fed group. These results potentially indicate that, in Cav-1$^{-/-}$ mice, a PVAT-derived constricting factor is released but its effect is counteracted by the antagonistic action of NO. This is in agreement with emerging evidence that PVAT has the capacity to significantly constrict VSM through the release of PVAT-derived constricting factors (Villacorta et al. 2015). PVAT from the thoracic aortae, carotid and mesenteric arteries of C57BL/6 mice has been reported to release epinephrine and prostaglandin which contribute to vascular contraction and these effects were subsequently blocked through incubation of PVAT with a COX inhibitor or α-adrenergic receptor antagonist (Chang et al. 2012b). Furthermore, studies of obese mice have demonstrated that aortic PVAT potentiates aortic contraction as a result of the release of PVAT-derived COX products (Meyer et al. 2013).

Endothelial function was not found to decline significantly in Cav-1$^{-/-}$ mice even after extensive feeding. However, a trend of reduced relaxation was observed in PVAT-intact aortic rings from 26 week WD-fed mice. This reduction in relaxation was associated with PVAT exerting a pro-contractile effect on aortic rings in the absence of L-NNA. Taken together, this could suggest that a small decrease in NO bioavailability disrupts the balance between NO and the PVAT-derived constricting factor thus causing the constricting agent to become predominant.

Successful inhibition of eNOS was achieved in the aortic preparations of C57BL/6 and ApoE$^{-/-}$ mice using 50 µM L-NNA (Chapters 3 and 4 respectively). However, in contrast to previous works, eNOS inhibition in this present study did not result in a substantial increase in contraction of PVAT-intact or PVAT-denuded aortic rings from Cav-1$^{-/-}$ mice (Razani et al. 2001; Hausman et al. 2012; Pojoga et al. 2014). This discrepancy may be due to the use of a lower concentration of NOS inhibitor in this present study (50 µM). In previous studies of isolated aortic and mesenteric preparations from Cav-1$^{-/-}$ mice, higher concentrations of NOS inhibitor (ranging from 100-300 µM) were utilised and this elicited a significant increase in vasoconstriction (Razani et al. 2001;

Hausman et al. 2012; Pojoga et al. 2014). Taken together, these data may suggest that NOS inhibition with 50 μM L-NNA, whilst effective in C57BL/6 and ApoE$^{-/-}$ mice, is insufficient for inhibiting a substantial amount of constitutively active eNOS within the aortae of Cav-1$^{-/-}$ mice. If eNOS inhibition had only partially occurred, some NO may have remained present within the aortae and therefore a true picture of the influence of NO on the contractile responses of Cav-1$^{-/-}$ mice may not have been observed.

Responses to the exogenous NO donor, sodium nitroprusside, were similar in ageing ND and WD-fed Cav-1$^{-/-}$ mice and were relaxation responses were unaffected by the presence of PVAT. Furthermore, no overt differences were observed between age and diet-matched C57BL/6 mice. These findings are in line with other observations of the aortic responses of Cav-1$^{-/-}$ and C57BL/6 mice (Pojoga et al. 2014). These data suggest that the differing contractile responses of PVAT-denuded aortic rings from Cav-1$^{-/-}$ and C57BL/6 mice is not the result of differences in NO sensitivity.

5.5.3 Prolonged feeding of a Western-type diet induces white adipocyte hypertrophy in the aortic PVAT of Cav-1$^{-/-}$ mice but no associated changes in superoxide or Mac3+ cells are observed

The composition of aortic PVAT from Cav-1$^{-/-}$ mice was assessed to determine if ageing or a WD induced any morphological changes. Moreover, Cav-1$^{-/-}$ aortic PVAT composition was compared to that of C57BL/6 mice to ascertain if the lack of an anti-contractile effect of PVAT in Cav-1$^{-/-}$ mice was in-part due to altered aortic PVAT composition.

5.5.3.1 A Western-type diet does not alter the weight of PVAT encompassing the aorta

The PVAT surrounding the aortic arch and thoracic aortae of mice is comprised of predominantly brown adipocytes with a small population of white adipocytes dispersed throughout the tissue. Previous studies have reported that the brown fat depot of high fat fed Cav-1$^{-/-}$ mice (from the sub/intrascapular region) was significantly enlarged (~3- to 4-fold larger) in comparison to diet-matched C57BL/6 mice, after approximately 34 weeks of high fat feeding. However, the composition of lipid droplets and cellular morphology within the fat depot was unaltered; suggesting that the increase in brown adipocyte mass was due to hyper-proliferation resulting from a compensatory response to hypertriglyceridemia (Razani et al. 2002a). Nevertheless, the ND-fed Cav-1$^{-/-}$ mice in this study did not display hypertriglyceridemia whereas, hypercholesterolaemia was induced in WD-fed mice. Subsequently, no significant changes in aortic PVAT weight were observed with increasing age or a WD in the Cav-1$^{-/-}$ mice. This may have been due to low experimental numbers in certain experimental groups because of a lack of available Cav-1$^{-/-}$ mice as a result of a decline in the breeding rates of the Cav-1$^{-/-}$ colony.

Interestingly, whilst no differences in aortic PVAT weight were observed between the 8-week ND Cav-1$^{-/-}$ and C57BL/6 mice, the PVAT encasing the aortae of the 16 week ND-fed Cav-1$^{-/-}$ mice was significantly heavier than the PVAT collected from the age-matched C57BL/6 strain. This effect was transient and no significant differences were observed between the 26-week groups. This may indicate that the total amount of PVAT encasing the aortae of Cav-1$^{-/-}$ mice was not a contributing factor towards the absence of an anti-contractile effect of aortic PVAT in Cav-1$^{-/-}$ mice. This contrasts with observations from studies of human and rodents, which demonstrated

that an increase in PVAT mass was associated with increased risk of CVD and resulted in the loss of an anti-contractile effect of PVAT in studies of isolated arteries (Ketonen et al. 2010; Britton et al. 2012; Szasz 2012). Of note, the area occupied by white adipocytes within the aortic PVAT of ND-fed Cav-1$^{-/-}$ mice was not significantly different to observations from the C57BL/6 mice. In addition, after 26 weeks on a ND, the white adipocytes of the Cav-1$^{-/-}$ mice were substantially smaller than the adipocytes of the C57BL/6 mice at the same age. These data could suggest that the lack of an anti-contractile effect in ND-fed Cav-1$^{-/-}$ mice was not due to changes in the area occupied by white adipocytes or altered white adipocyte size within the aortic PVAT.

5.5.3.2 White adipocyte hypertrophy is observed after 26 weeks feeding of a Western-type diet

The area occupied by white adipocytes within the aortic PVAT of Cav-1$^{-/-}$ mice was altered by feeding the mice a Western-type diet. After 16 weeks of high fat feeding, a significant increase in the amount of PVAT inhabited by white adipocytes was observed; this increase was sustained in the 26-week WD-fed mice although this was not statistically significant. Furthermore, white adipocyte hypertrophy accompanied the increase in area populated by white adipocytes, indicating that the white adipocytes of the aortic PVAT were not hyper-cellular but underwent expansion in response to the WD. The observed white adipocyte hypertrophy is like previous reports from a study of C57BL/6 mice. The study reported that when C57BL/6 mice were fed a high fat for 20 weeks, aortic PVAT morphology was significantly altered and large white lipid droplets were apparent within the PVAT (Fitzgibbons et al. 2011). Also, a similar high fat feeing study reported that altered PVAT composition in high fat fed C57BL/6 mice was associated with a decrease in the anti-contractile capacity of PVAT as a result of decreased NOS activity and a subsequent decrease in NO bioavailability (Xia et al. 2016).

In this present study, the white adipocyte population within the aortic PVAT of 16 and 26-week WD-fed Cav-1$^{-/-}$ mice could be considered hypoxic, as the mean white cell size was greater than 100 µm, the diffusional limit of oxygen (Hosogai et al. 2007). There are conflicting reports surrounding the effects of hypoxia and PVAT on vascular reactivity, with studies demonstrating an attenuation or potentiation of the anti-contractile effect of PVAT (Greenstein et al. 2009; Maenhaut et al. 2010).

The findings of this Cav-1$^{-/-}$ study could indicate a link between the observed increase in aortic white adipocyte size (and potential hypoxic conditions) after 26 weeks on a WD, and the aortic PVAT exerting a pro-contractile effect on the aortae of Cav-1$^{-/-}$ mice. Taken together, these findings indicate that the aortic PVAT of Cav-1$^{-/-}$ mice is not protected from the effects of diet-induced weight gain. Furthermore, in WD-fed mice, a significant increase in aortic white adipocyte size may have been associated with PVAT-intact aortic rings exhibiting increased vasoconstriction to phenylephrine.

5.5.3.3 Neither ageing nor a Western-type diet results in changes to the production of superoxide within the aortic PVAT of Cav-1$^{-/-}$ mice

Enhanced levels of oxidative stress have been linked to increased cellular ageing and play a role in the development of CVD (Elahi et al. 2009). In health, eNOS activation produces NO, a vaso-protective molecule (Dudzinski and Michel 2007). However, a role for eNOS uncoupling and

subsequent production of superoxide within the vasculature has been demonstrated (Guzik et al. 2002; Stapleton et al. 2010). Furthermore, studies of Cav-1$^{-/-}$ mice have reported enhanced oxidative stress and increased superoxide production within the vasculature, which suggests that augmented activity of eNOS may cause some degree of damage to the blood vessels (Wunderlich et al. 2008a; Wunderlich et al. 2008b). Within the vasculature, the major contributors to the generation of ROS are mitochondria and macrophages (Harrison 1997). Aortic PVAT is comprised predominantly of brown adipocytes which are packed with mitochondria therefore, it was of interest to assess superoxide production within the aortic PVAT of Cav-1$^{-/-}$ mice. Furthermore, previous studies of high fat fed C57BL/6 mice have reported increased oxidative stress within PVAT due to adipocyte hypertrophy and the release of pro-inflammatory cytokines (Eriksson 2007; Park et al. 2007; Vincent et al. 2007; Pereira et al. 2012). This Cav-1$^{-/-}$ study observed white adipocyte hypertrophy of aortic adipocytes after 26 weeks on a WD. Consequently, PVAT-derived ROS generation was assessed in WD-fed Cav-1$^{-/-}$ mice to determine if a high fat diet resulted in augmented superoxide production as a result of adipocyte expansion.

The generation of superoxide within the aortic PVAT of Cav-1$^{-/-}$ mice was unaffected by increasing age or a WD. These findings are not in line with previous research, which clearly demonstrated a link between diet-induced weight gain, elevated ROS production and an attenuation of the anti-contractile effect of PVAT in isolated small and large arterial preparations from obese humans and mouse models of diet-induced weight gain (Greenstein et al. 2009; Marchesi et al. 2009). This may suggest that the oxidative state of PVAT from Cav-1$^{-/-}$ mice is elevated but does not undergo anymore oxidative stress in response to ageing or a WD.

Nevertheless, superoxide production in the aortic PVAT of 8-week ND-fed Cav-1$^{-/-}$ mice was significantly elevated in comparison to age-matched C57BL/6 mice and this trend was continued after 16 weeks on the ND however, this was not statistically significant. There were no apparent differences between the amount of superoxide in Cav-1$^{-/-}$ or C57BL/6 mice after 26 weeks on a ND. In conjunction with this, the PVAT of C57BL/6 mice was no longer observed to exert an anti-contractile effect. These data potentially indicate that baseline superoxide production is elevated in Cav-1$^{-/-}$ mice and may have contributed to the lack of an anti-contractile effect of PVAT.

5.5.3.4 The number of Mac-3^{+} cells within the aortic PVAT were unchanged with ageing or a Western-type diet

Murine thoracic PVAT has been reported to exhibit a less inflammatory profile than other fat depots due to its brown adipose tissue characteristics (Ketonen et al. 2010; Fitzgibbons et al. 2011). In addition, Cav-1 has been reported to promote monocyte to macrophage differentiation (Fu et al. 2012). Macrophage infiltration within the aortic PVAT of Cav-1$^{-/-}$ mice was investigated to determine if loss of Cav-1 altered the inflammatory profile of aortic PVAT and to determine if a WD. influenced this

A Mac-3 marker was used to detect infiltrating macrophages within the aortic PVAT of the Cav-1$^{-/-}$ mice. No significant changes in infiltrating Mac-3^{+} cells were observed with increasing age or a WD in the aortic PVAT of Cav-1$^{-/-}$ mice, which is in line with previous reports indicating that the aortic PVAT of high fat-fed C57BL/6 mice was resistant to inflammation (Ketonen et al. 2010;

Fitzgibbons et al. 2011). Mac-3 expression is associated with macrophage differentiation therefore it was expected that loss of Cav-1$^{-/-}$ would result in a decrease in Mac-3^{+} cells within the aortic PVAT in comparison to C57BL/6 mice because of the role Cav-1 plays in promoting this process. Nonetheless, no differences in Mac-3^{+} cells were observed between the aortic PVAT of Cav-1$^{-/-}$ and C57BL/6 mice. These data suggest that the process of monocyte to macrophage differentiation is preserved in the Cav-1$^{-/-}$ mouse, which is similar to other published reports (Fu et al. 2012). This study cannot definitively state that the inflammatory profile of Cav-1$^{-/-}$ mice is unaffected by ageing or a WD as the presence of other inflammatory cells, such as lymphocytes, neutrophils and eosinophils within the aortic PVAT was not confirmed.

5.6 Limitations and future work

Although it is widely acknowledged that Cav-1$^{-/-}$ mice lack identifiable caveolae structures and do not express Cav-1$^{-/-}$ within the different component vasculature, including aortic SM and adipocytes, this was not confirmed in the present study (Razani et al. 2001; Adebiyi et al. 2007; Peterson et al. 2009). Therefore, in future studies of Cav-1$^{-/-}$ mice, the lack of Cav-1$^{-/-}$ expression in VSM and aortic PVAT should be ideally confirmed by Western blot.

Furthermore, the concentration of NOS inhibitor used in this study appeared to be insufficient for the enhanced amount of active eNOS present in the Cav-1$^{-/-}$ mice. Previous vascular reactivity studies involving Cav-1$^{-/-}$ mice used significantly higher concentrations of NOS inhibitors (100 µM and upwards) and consequently, reported an increase in aortic contractions (Razani et al. 2001; Martin et al. 2012; Pojoga et al. 2014). If this study were to be repeated, a higher concentration of inhibitor, of at least 100 µM, should be utilised to appropriately determine the contribution of NO-induced vaso-relaxation to the observed dampened vasoconstrictor responses of phenylephrine in Cav-1$^{-/-}$ mice, and to assess if NO modulates the vascular reactivity of PVAT-intact aortic rings. In addition, eNOS expression could be assessed within the aortic PVAT and VSM by Western blot to elucidate if eNOS activation or expression is enhanced in the aortae of Cav-1$^{-/-}$ mice in comparison to C57BL/6 mice.

Previous studies in Cav-1$^{-/-}$ mice have demonstrated a role of endothelium-derived vasodilators in contributing to the dampened vasoconstrictor responses in Cav-1$^{-/-}$ mice (Pojoga et al. 2014). This finding could be investigated, in the presence or absence of PVAT, by mechanical removal of the endothelium. These experiments would give an insight into the ability of PVAT to modulate the vascular reactivity of smooth muscle without the added complication of endothelium-derived vasoactive factors.

In this study, after 26 weeks on a WD, the PVAT of Cav-1$^{-/-}$ mice was indicated to release an unknown PVAT-derived constricting factor. It would be of considerable interest to identity this factor using pharmacological tools in myography experiments.

5.7 Summary and conclusions

This present study demonstrated that the aortic PVAT of Cav-1$^{-/-}$ mice does not exhibit an anti-contractile capacity. However, the aortic PVAT itself may have been functional but unable to modulate vascular reactivity due to the observed dampened vasoconstrictor responses of PVAT-

denuded aortic rings. After extensive feeding of a WD, the aortic PVAT of Cav-1$^{-/-}$ mice exerted a significant pro-contractile effect on aortic rings and this was associated with white adipocyte hypertrophy. Furthermore, NOS inhibition revealed a pro-contractile effect of aortic PVAT from Cav-1$^{-/-}$ mice which may have been due to the release of a PVAT-derived vaso-constricting factor. The bioavailability of NO within the aortae of Cav-1$^{-/-}$ mice requires further investigation.

The principal findings of this chapter were:

- **The aortic PVAT of Cav-1$^{-/-}$ mice did not exert an anti-contractile effect on isolated aortic rings.**
- **The aortic PVAT of Cav-1$^{-/-}$ mice fed a WD for 26 weeks exerted a pro-contractile effect on aortae and this was associated white adipocyte hypertrophy within the aortic PVAT.**
- **In the presence of the NOS inhibitor, L-NNA, the aortic PVAT of Cav-1$^{-/-}$ mice exerted a pro-contractile effect on aortic ring preparations.**
- **Extensive feeding of a WD induced white adipocyte hypertrophy within the aortic PVAT of Cav-1$^{-/-}$ mice.**

~ Chapter Six ~

A study of aortic perivascular adipose tissue in ApoE$^{-/-}$Cav-1$^{-/-}$ double knockout mice

Abstract

Background: Apolipoprotein E-Caveolin-1 double knockout mice (ApoE$^{-/-}$Cav-1$^{-/-}$) have previously revealed a key involvement of Cav-1 in the pathogenesis of atherosclerosis. ApoE$^{-/-}$ Cav-1$^{-/-}$ mice display a severely pro-atherogenic lipid profile yet Cav-1 ablation confers significant protection against the development of atherosclerosis within the aortae of these mice. The vascular reactivity of ApoE$^{-/-}$Cav-1$^{-/-}$ mice and the potential influence of aortic PVAT has not previously been investigated. The atheroprotected phenotype of ApoE$^{-/-}$Cav-1$^{-/-}$ mice may be in part due to enhanced nitric oxide (NO) production within the components of the aortae due to the loss of the Cav-1-eNOS inhibitory complex.

Purpose: The following experiments were conducted to characterise the morphology of aortic PVAT from ApoE$^{-/-}$Cav-1$^{-/-}$ mice and to determine the influence of PVAT, age, and Western-type diet (WD) on isolated aortic reactivity.

Methods: Upon weaning, at approximately 4 weeks old, male ApoE$^{-/-}$Cav-1$^{-/-}$ mice were fed a normal diet (ND) or high fat WD for 8, 16 or 26-weeks. Vascular reactivity studies were performed on aortic rings with or without PVAT. The effect of NO on contractile responses to phenylephrine were assessed via nitric oxide synthase (NOS) inhibition. The structure of the aortic PVAT was assessed using histology and immunostaining.

Results: ApoE$^{-/-}$Cav-1$^{-/-}$ mice were successfully generated by interbreeding ApoE$^{-/-}$ and Cav-1$^{-/-}$ mice. However, less than 50% of viable. offspring produced survived to weaning. ApoE$^{-/-}$Cav-1$^{-/-}$ mice exhibited a pro-atherogenic lipid profile which was further exacerbated by feeding of a WD. Nevertheless, atherosclerotic lesion burden within the aortae of WD-fed ApoE$^{-/-}$Cav-1$^{-/-}$ mice was significantly lower than age and diet-matched ApoE$^{-/-}$ mice. ApoE$^{-/-}$Cav-1$^{-/-}$ mice were not resistant to diet induced weight gain after 16 weeks on a WD and this was sustained in the 26-week group (16-weeks: $P = 0.002$; 26-weeks: $P = 0.005$). In addition, splenomegaly was observed at each time-point in the WD-fed mice and hepatomegaly was recorded after 16 weeks on the WD. Although atherosclerosis occurred within the aortae of the ApoE$^{-/-}$Cav-1$^{-/-}$ mice, endothelial function was maintained. PVAT did not modulate vascular reactivity at any of the time-points and a WD had no effect on contractions to phenylephrine. Furthermore, incubation with a NOS inhibitor revealed a pro-contractile effect of PVAT in 8-week ND-fed ApoE$^{-/-}$Cav-1$^{-/-}$ mice however, NOS inhibition had no effect on the other experimental groups. Hypertrophy of the aortic white adipocytes was observed after 26-weeks on a WD although no associated effects on vascular reactivity were observed. ROS production and Mac-3^{+} infiltration of aortic PVAT was unaltered by ageing or a WD in ApoE$^{-/-}$Cav-1$^{-/-}$ mice.

Conclusions: WD-fed ApoE$^{-/-}$Cav-1$^{-/-}$ mice exhibit an athero-protected phenotype. In addition, endothelial function is preserved within the aortae of these mice. Furthermore, PVAT does not

influence the vascular reactivity of aortic rings in ND or WD-fed conditions. However, NOS inhibition revealed a pro-contractile effect of aortic PVAT in the 8-week ND mice which may have been due to the release of a pro-contractile factor. These data demonstrate the importance of Cav-1 in the development of atherosclerosis.

6.1 Introduction

Deletion of Caveolin-1 was discovered to confer significant protection against the development of atherosclerotic disease within ApoE$^{-/-}$ mice (Frank et al. 2004a). A key role of Cav-1 in the pathogenesis of atherosclerosis was highlighted by the athero-protective phenotype displayed by ApoE$^{-/-}$Cav-1$^{-/-}$ double knockout mice despite an atherogenic lipoprotein profile characterised by elevated serum cholesterol and triglycerides in comparison to ApoE$^{-/-}$ mice (Frank et al. 2004a). These findings indicate that caveolae and Cav-1 are crucial mediators of cholesterol homeostasis and transcytosis of lipoproteins into the sub-endothelial space, a vital initiating step in the development of atherosclerosis within the arteries (Vasile et al. 1983; Ghitescu et al. 1986; Kim et al. 1994; Schubert et al. 2001). Moreover, additional mechanisms for how genetic lack of Cav-1$^{-/-}$ confers an atheroprotected phenotype have been proposed. These include a role of elevated NO bioavailability exerting cardio-protective effects within the endothelial cells of ApoE$^{-/-}$Cav-1$^{-/-}$ mice, due to loss of tonic inhibition of eNOS by Cav-1, resulting in enhanced eNOS activity and thus increased NO production (Garcia-Cardena et al. 1996; Fernandez-Hernando et al. 2009). Furthermore, follow-up studies of ApoE$^{-/-}$Cav-1$^{-/-}$ double knockout mice have highlighted that Cav-1 exerts significant pro-or anti-atherogenic effects depending on specific cell type. Expression of Cav-1 in endothelial cells has been reported to promote and even accelerate atherosclerosis whilst lack of Cav-1 in macrophages promotes apoptosis and increases inflammation (Fernandez-Hernando et al. 2009), (Pavlides et al. 2014).

The vascular reactivity of ApoE$^{-/-}$Cav-1$^{-/-}$ mice and the potential influence of PVAT on vascular contractility has not previously been explored. Lack of Cav-1 within the aortic PVAT of ApoE$^{-/-}$ Cav-1$^{-/-}$ mice may promote an atheroprotected phenotype due to enhanced PVAT-derived NO production. Augmented NO bioavailability could potentially contribute to an attenuation of vasoconstrictor responses, prevention of turbulent blood flow and thus protect against the development of atherosclerotic lesions within the aortae of ApoE$^{-/-}$Cav-1$^{-/-}$ mice. Therefore, the aim of this study was to characterise the effects of ageing on vascular reactivity of the aortae of ApoE$^{-/-}$Cav-1$^{-/-}$ mice in the presence or absence of PVAT. The effect of feeding ApoE$^{-/-}$Cav-1$^{-/-}$ mice a Western-type diet and its potential influence on vascular reactivity was investigated. In addition, the morphological characteristics of aortic PVAT were assessed.

6.2 Aim and objectives

The chapter aims to investigate the influence of PVAT on the vascular function of aortic rings from ApoE$^{-/-}$Cav-1$^{-/-}$ mice, the role of NO, and establish if PVAT function is altered by ageing or a Western-type diet and atherosclerosis. This will be achieved by:

- Characterising the effect of ageing and a WD on ApoE$^{-/-}$Cav-1$^{-/-}$ mice by evaluating lipid and glucose parameters, measuring body and organ weights, and assessing the development of atherosclerosis using en face aortic preparations.
- Establishing if the presence of aortic PVAT modulates vascular responses to vasoconstrictor or vasodilator agents, and if ageing or high fat feeding alter this.
- Determining the extent to which NO affects vascular responses by pharmacological inhibition of NOS.
- Assessing if the aortic PVAT of the ApoE$^{-/-}$Cav-1$^{-/-}$ mice is altered by ageing or a WD, using histology and immunohistochemistry.

6.3 Methods

Male ApoE$^{-/-}$Cav-1$^{-/-}$ double knockout mice were bred in-house by crossing ApoE$^{-/-}$ and Cav-1$^{-/-}$ mice and the subsequent mating of specific offspring. Genotyping of ear snips was performed to determine the specific genotype of the offspring. At approximately 4-5 weeks of age, ApoE$^{-/-}$Cav-1$^{-/-}$ mice were weaned and maintained on either a standard rodent chow diet (normal diet ND) or a high fat (21%) WD for 8, 16 or 26 weeks. The effects of ageing and a WD were characterised in ApoE$^{-/-}$Cav-1$^{-/-}$ mice by analysis of serum lipid and glucose levels and recording of body and organ weights. Atherosclerotic disease progression was assessed via en face lipid lesion analysis of aortic preparations. Endothelial relaxation, in response to acetylcholine, was measured to determine whether the development of atherosclerosis impeded endothelial function. Contractility studies were performed in PVAT-intact or PVAT-denuded thoracic aortic rings to determine if PVAT influenced vascular reactivity to phenylephrine. The involvement of NO in vascular responses in aortic rings with or without PVAT was evaluated by incubation with 50 µM L-NNA, a NOS inhibitor. Sensitivity of aortic rings to exogenous NO was determined through the use of sodium nitroprusside, a potent NO donor. The aortic PVAT environment was assessed via a combination of histology, the use of a superoxide indicator and immunostaining to determine if macrophages were present. Full methods are available in Chapter 2.

6.4 Results

6.4.1 Genetic screening of ApoE and Cav-1 deletions

The ApoE$^{-/-}$Cav-1$^{-/-}$ colony was generated by an initial cross between ApoE$^{-/-}$ and Cav-1$^{-/-}$ mice and selection of the desired offspring for subsequent breeding (refer to breeding strategy in Chapter 2, Figure 2.1). Genotypes were confirmed by performing PCR amplification on DNA extracted from ear snips using two different PCR reactions for Cav-1 and ApoE alleles.

The knockout alleles for Cav-1 and ApoE were amplified to 410 bp and 245 bp, respectively whilst wild type alleles were amplified to 690 bp for Cav-1 and 155 bp for ApoE (Figure 6.1A and B). No bands were observed in the negative water control.

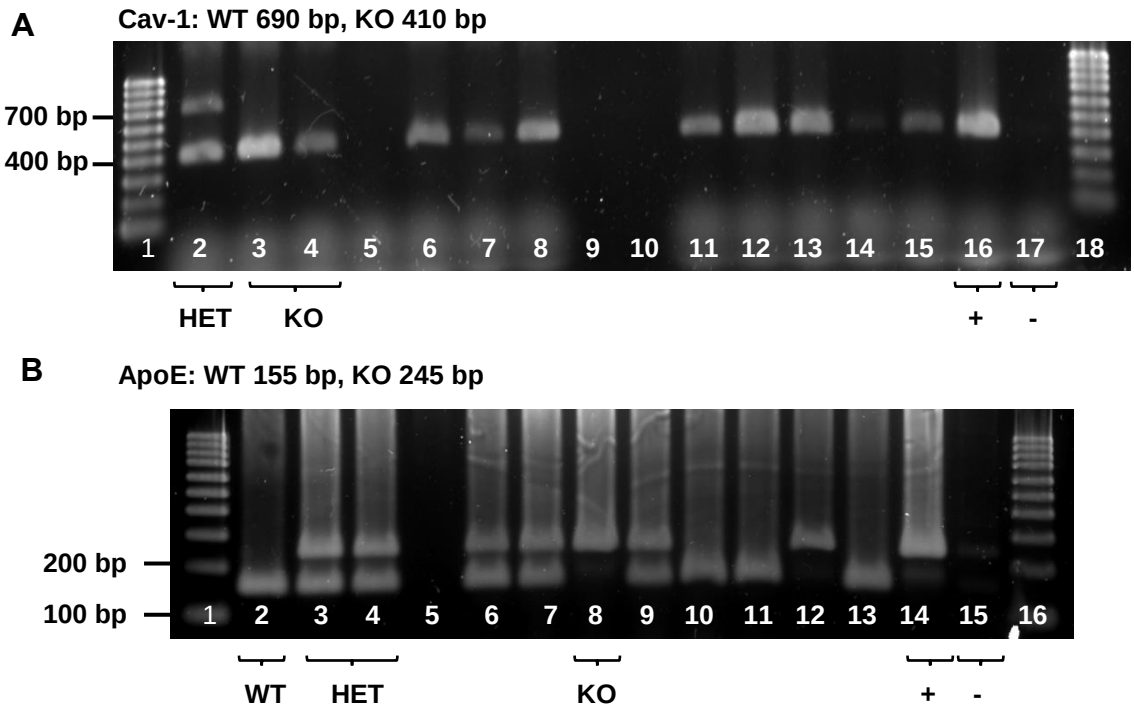

Figure 6.9 Genotyping of the Apoe$^{-/-}$Cav-1$^{-/-}$ double knockout mouse

Lanes show the DNA extracted from the interbreeding of ApoE$^{-/-}$ and Cav-1$^{-/-}$ mice at the second and third stages of the ApoE$^{-/-}$Cav-1$^{-/-}$ breeding strategy. A) Cav-1 PCR, DNA was amplified using primers oIMR1972, oIMR1973 and oIMR1974. Observed bands were 690 base pairs (bp) and 410 bp for WT and KO DNA respectively. Lanes 1 and 18 depict a 100 bp ladder whilst lane 2 depicts HET bands, and lanes 3,4, 6-8 and 11-15 depict KO bands. A positive control (+) band is in lane 16 whilst a negative water control (-) is in lane 17 with no observable bands. Lanes 9 and 10 were empty due to a broken gel comb whilst lane 5 is a failed PCR. B) ApoE PCR, DNA was amplified with primers oIMR0180, oIMR0181 and oIMR0182. The targeted KO allele was amplified to 245 bp whilst the WT produced a band at 155 bp. Lanes 1 and 16 depict a 100 bp ladder whilst lane 2 depicts a WT band, lanes 3,4,6,7 and 9 depict HET bands whilst lanes 8 and 12 demonstrate KO bands. A positive control (+) band is in lane 14 whilst a negative water control (-) is in lane 15. Lane 5 is an unsuccessful PCR. Lane 8 in both gels demonstrates the successful generation of the ApoE$^{-/-}$Cav-1$^{-/-}$ mouse. HET (heterozygous) KO (knockout) WT (wild-type).

6.4.2 Colony maintenance

The ApoE$^{-/-}$Cav-1$^{-/-}$ colony was difficult to maintain and the output of experimental mice was low due to the relatively poor survival rates of the offspring. The table below (Table 6.1) is representative of the general breeding patterns observed, with greater than 50% of litters lost to cannibalism or found dead soon after birth. Numerous methods to improve breeding outcomes were implemented including: placing breeding cages in a quieter room on an opposite light/dark cycle, separating sires from dams prior to litters being born, fostering pups with FVB mice and using full Cav-1 knockout ApoE heterozygotes for breeding. however, none of these approaches resulted in an improvement.

Table 6.1 Representative breeding outcomes from the ApoE$^{-/-}$Cav-1$^{-/-}$ double knockout colony

Breeders	Sire	Dam	Set-up	Litter ID	DOB	Born	Weaned	Males	Females
Trio 18	**#83**	**#129**	**23/07/14**	**18:1**	**27/8/14**	**5**	**0**	**---**	**---**
	DOB 15/03/14	**DOB 21/05/14**		**18:2**	**29/8/14**	**5**	**0**	**---**	**---**
	batch 9:3	**batch 10:3**		**18:3**	**30/9/14**	**7**	**2**	**1**	**1**
		#133		**18:4**	**20/10/14**	**†**	**---**	**---**	**---**
		DOB 23/05/14							
		batch 9:6							
Trio 19	**#126**	**#107**	**19/08/14**	**19:1**	**10/09/14**	**6**	**4**	**2**	**2**
	DOB 23/05/14	**DOB 07/05/14**		**19:2**	**24/09/14**	**7**	**0**	**---**	**---**
	batch 9:6	**batch 6:3**		**19:3**	**26/11/14**	**8**	**7**	**---**	**---**
		#108		**19:4**	**30/12/14**	**†**	**---**	**---**	**---**
		DOB 07/05/14							
		batch 6:3							
Trio 21	**#147**	**#148**	**19/08/14**	**21:1**	**09/09/14**	**10**	**0**	**---**	**---**
	DOB 13/06/14	**DOB 13/06/14**		**21:2**	**12/10/14**	**10**	**7**	**5**	**2**
	batch 14:1	**batch 14:1**		**21:3**	**15/10/14**	**10**	**9**	**3**	**6**
		#163		**21:4**	**06/12/14**	**7**	**0**	**---**	**---**
		DOB 01/07/14		**21:5**	**10/12/14**	**5**	**0**	**---**	**---**
		batch 10:4		**21:6**	**22/01/15**	**†**	**---**	**---**	**---**
				21:7	**24/01/15**	**†**	**---**	**---**	**---**
Trio 30	**#271**	**#261**	**21/01/15**	**30:1**	**18/02/15**	**4**	**4**	**2**	**2**
	DOB 16/11/14	**DOB 26/10/14**		**30:2**	**17/03/15**	**1**	**---**	**---**	**---**
	batch 22:1	**batch 19:3**		**30:3**	**26/03/15**	**6**	**6**	**3**	**3**
		#273		**30:4**	**06/05/15**	**8**	**7**	**2**	**5**
		DOB 16/11/14		**30:5**	**20/05/15**	**†**	**---**	**---**	**---**
		batch 22:1		**30:6**	**28/06/15**	**3**	**---**	**---**	**---**
				30:7	**05/07/15**	**6**	**2**	**1**	**1**
				30:8	**13/08/15**	**10**	**3**	**2**	**1**
				30:9	**20/11/15**	**†**	**---**	**---**	**---**

† Litter found dead or no pups were found. Litters highlighted in bold survived to weaning

6.4.3 Characteristics of ageing in normal diet-fed ApoE$^{-/-}$Cav-1$^{-/-}$ double knockout mice and the impact of a Western-type diet

6.4.3.1 The lipid profile of normal diet-fed ApoE$^{-/-}$Cav-1$^{-/-}$ mice is markedly more pro-atherogenic than ApoE$^{-/-}$ mice

Increasing age had no effect on the lipid or glycaemic profiles of ND-fed ApoE$^{-/-}$Cav-1$^{-/-}$ mice (P = NS all parameters; n = 5-6 mice per group, Table 6.2).

The lipid profiles of ND-fed ApoE$^{-/-}$Cav-1$^{-/-}$ mice was compared to the profiles of ApoE$^{-/-}$ and Cav-1$^{-/-}$ mice (Appendix 2.2A-D). The lipid profile of ApoE$^{-/-}$Cav-1$^{-/-}$ mice was more pro-atherogenic than age and diet-matched ApoE$^{-/-}$ mice. Total cholesterol and triglycerides were substantially elevated in ND-fed ApoE$^{-/-}$Cav-1$^{-/-}$ mice in comparison to age and diet-matched ApoE$^{-/-}$ mice (P < 0.0001; cholesterol and triglycerides, n = 4-6 mice per group, Appendix 2.2A-B). No significant differences were observed between HDL measurements of ApoE$^{-/-}$ and ApoE$^{-/-}$Cav-1$^{-/-}$ mice at any of the time-points (P = NS for all comparisons; n = 4-6 mice per group Appendix 2.2C) and glucose levels of ApoE$^{-/-}$ and ApoE$^{-/-}$Cav-1$^{-/-}$ mice were similar (P = NS for all comparisons; n = 4-6 mice per group, Appendix 2.2D).

Cholesterol and triglyceride levels were significantly augmented in ND-fed ApoE$^{-/-}$Cav-1$^{-/-}$ mice in comparison to Cav-1$^{-/-}$ mice (P < 0.0001; cholesterol and triglycerides, n = 4-6 mice per group Appendix 2.2A-B). However, in comparison to Cav-1$^{-/-}$ mice, the HDL levels of the ApoE$^{-/-}$Cav-1$^{-/-}$ double knockout were substantially lower at each time-point (P < 0.0001; n = 4-6 mice per group Appendix 2.2C). No significant differences in glucose levels were observed between the ApoE$^{-/-}$ Cav-1$^{-/-}$ double knockout, or Cav-1$^{-/-}$ mice (P = NS for all comparisons; n = 4-6 mice per group, Appendix 2.2D).

6.4.3.2 The lipid profile of Western-type diet fed ApoE$^{-/-}$Cav-1$^{-/-}$ double knockout mice is severely pro-atherogenic

Hypercholesterolemia was more severe in WD-fed ApoE$^{-/-}$Cav-1$^{-/-}$ mice compared to ND strain-matched mice at each time-point (ND versus WD: 8-weeks P = 0.0002; 16-weeks P = 0.0001; 26-weeks P < 0.0001, n = 6 mice per group, Table 6.2). Also, there was a trend of reduced HDL-cholesterol in WD-fed ApoE$^{-/-}$Cav-1$^{-/-}$ mice although this was only significantly depleted after 16 weeks on the WD compared to ND mice (ND versus WD: P = 0.03; n = 6 mice per group, Table 6.2). However, serum triglyceride and glucose levels were not significantly affected by a WD (P = NS for triglyceride and glucose for all time-point comparisons; n = 5-6 mice per group, Table 6.2).

Table 6.2 Lipidemic and glycaemic profiles of ApoE$^{-/-}$Cav-1$^{-/-}$ double knockout mice after 8, 16 or 26 weeks on a normal diet or Western-type diet

ND	8-weeks	16-weeks	26-weeks	P values for all diet-matched comparisons
Total cholesterol	13.50 ± 1.98	15.18 ± 1.68	16.52 ± 1.96	P = NS
HDL	0.48 ± 0.06	0.55 ± 0.08	0.39 ± 0.07	P = NS
Triglycerides	4.24 ± 0.81	4.79 ± 0.37	4.03 ± 0.79	P = NS
Glucose	21.01 ± 2.21	19.78 ± 2.58	14.75 ± 2.75	P = NS
WD	**8-weeks**	**16-weeks**	**26-weeks**	**P values for all diet-matched comparisons**
Total cholesterol	35.65 ± 3.96	38.08 ± 3.92	47.43 ± 3.63	P = NS
HDL	0.36 ± 0.08	0.23 ± 0.06	0.17 ± 0.05	P = NS
Triglycerides	3.76 ± 0.64	4.87 ± 0.78	6.41 ± 0.91	P = NS
Glucose	28.27 ± 1.56	22.21 ± 3.08	18.24 ± 3.45	P = NS
ND versus WD	**8-weeks**	**16-weeks**	**26-weeks**	
Total cholesterol	*** 0.0002	*** 0.0001	**** P < 0.0001	
HDL	NS > 0.999	* 0.03	NS 0.39	
Triglycerides	NS > 0.999	NS > 0.999	NS > 0.999	
Glucose	NS > 0.999	NS > 0.999	NS > 0.999	

Serum derived from blood obtained at time of sacrifice (mice were weaned at 4-5 weeks of age then maintained on a normal chow diet (ND) or Western-type diet (WD) for the appropriate length of time. Data are expressed as mean ± S.E.M and measurements are shown in mmol/L. Statistical analysis was carried out by two-way ANOVA, with Bonferroni's post hoc test, n = 5-6 mice per group.

6.4.3.3 The body and organ weights of normal diet-fed ApoE$^{-/-}$Cav-1$^{-/-}$ double knockout mice are largely unaffected by increasing age; however, the mice develop cardiac hypertrophy

ApoE$^{-/-}$Cav-1$^{-/-}$ mice fed a ND displayed a significant increase in body weight at the 16-week time-point (8-weeks versus 16-weeks: P = 0.03; n = 17 mice each, Table 6.3). However, no further differences were observed between the time-points (P = NS for all comparisons, n = 8-17 mice per group, Table 6.3). Moreover, heart weight, heart weight: body weight ratio, liver, spleen, epididymal fat pad weights and mean epididymal adipocyte sizes were unaffected by increasing age (P = NS for all parameters and time-point comparisons, n = 8-17 mice per group, Table 6.3).

There were no differences in body weight between the ApoE$^{-/-}$Cav-1$^{-/-}$ double knockout mice and the ApoE$^{-/-}$ or Cav-1$^{-/-}$ strains after feeding of a ND (P = NS for all comparisons n = 8-26 mice per group, Appendix 2.3A). However, cardiac hypertrophy was observed in the 16 week ND-fed ApoE$^{-/-}$Cav-1$^{-/-}$ mice in comparison to age-matched ApoE$^{-/-}$ mice when isolated heart weights and heart weight: body weight ratios were compared (ApoE$^{-/-}$Cav-1$^{-/-}$ versus ApoE$^{-/-}$: heart weight: P = 0.007; heart weight: body weight ratio: P = 0.002; n = 15 and 24 mice, respectively, Appendix 2.3B and C). No differences in heart weight or heart weight: body weight ratio, were observed between the

ApoE$^{-/-}$Cav-1$^{-/-}$ and Cav-1$^{-/-}$ mice (P = NS for all time-point comparisons; n = 14-18 mice per group Appendix 2.3B and C).

The liver weights of ApoE$^{-/-}$Cav-1$^{-/-}$ double knockout mice and the ApoE$^{-/-}$ and Cav-1$^{-/-}$ strains were similar (P = NS; all comparisons, n = 8-26 mice per group, Appendix 2.3D). However, splenomegaly was observed in the 16 week ND-fed ApoE$^{-/-}$Cav-1$^{-/-}$ double knockout mice in comparison to the ApoE$^{-/-}$ and Cav-1$^{-/-}$ strains (ApoE$^{-/-}$Cav-1$^{-/-}$ versus ApoE$^{-/-}$: P = 0.007; ApoE$^{-/-}$ Cav-1$^{-/-}$ versus Cav-1$^{-/-}$: P = 0.003; n = 8-26 mice per group, Appendix 2.3E). Epididymal fat pads were assessed and there were no differences in epididymal fat pad weights or adipocyte size between age-matched ApoE and ApoE$^{-/-}$Cav-1$^{-/-}$ mice (P = NS; all comparisons, n = 8-24 mice per group Appendix 2.3F and G). Epididymal fat pads of ApoE$^{-/-}$Cav-1$^{-/-}$ mice were significantly smaller than Cav-1$^{-/-}$ mice (P < 0.0001; all comparisons, n = 8-21 mice per group, Appendix 2.3F) although no significant differences in epididymal adipocyte sizes were observed (P = NS; all comparisons, n = 8-21 mice per group, Appendix 2.3G).

6.4.3.4 A Western-type diet resulted in diet-induced weight gain, hepatomegaly and splenomegaly in the ApoE$^{-/-}$Cav-1$^{-/-}$ double knockout mice

In comparison to ND-fed ApoE$^{-/-}$Cav-1$^{-/-}$ mice, a WD significantly augmented the body weights of the 16 and 26-week time-point groups (ND versus WD: 16-weeks; P = 0.002; 26-weeks P = 0.005, n = 8-17 mice per group, Table 6.3) although heart weights and heart weight: body weight ratio remained unchanged (P = NS for both heart weight and HW:BW and each age comparison; n = 8-17 mice per group, Table 6.3). Hepatomegaly was observed after 16 weeks on a WD (ND versus WD: P = 0.0008; n = 17 and 15 mice, Table 6.3) and persisted at the 26-week time-point (ND versus WD: P = 0.0001; n = 8 and 13 mice, respectively, Table 6.3). Similarly, splenomegaly occurred in all WD groups compared to their age-matched counterparts (ND versus WD: 8-weeks P = 0.02; 16-weeks P = 0.0001; 26-weeks P = 0.0008, n = 8-17 mice per group, Table 6.3). An increase in epididymal fat pad weight was observed in both the 8-week (ND versus WD: P = 0.007; n = 17 and 14 mice, Table 6.2) and 16-week time-points (ND versus WD: P < 0.0001; n = 17 and 15 mice, Table 6.3). Conversely, this increase was not sustained by the 26-week time-point (ND versus WD: P = 0.22; n = 8 and 13 mice, Table 6.3). Epididymal adipocyte hypertrophy was only observed in the 16-week WD group (ND versus WD: 16 weeks; P < 0.002, Table 6.3).

ApoE$^{-/-}$Cav-1$^{-/-}$ mice displayed a markedly more pro-atherogenic cholesterol profile than age and diet-matched ApoE$^{-/-}$ mice. Additionally, ApoE$^{-/-}$Cav-1$^{-/-}$ mice were more susceptible to diet-induced weight gain, which was observed from the 16-week time-point. Furthermore, splenomegaly and hepatomegaly occurred in WD-fed ApoE$^{-/-}$Cav-1$^{-/-}$ mice, which suggests that as in the Cav-1$^{-/-}$ mice, fat had begun to accumulate within these organs. Similarly, to the Cav-1$^{-/-}$ mice, epididymal fat pads were only significantly enlarged compared to age-matched ND-mice at the 8 and 16-week time-points however, epididymal adipocytes were only significantly enlarged at the 16-week time-point

.

Table 6.3 Body weight, organ weights and epididymal adipocyte size of the ApoE$^{-/-}$Cav-1$^{-/-}$ double knockout (ApoE$^{-/-}$Cav-1$^{-/-}$, ApoE$^{-/-}$Cav-1$^{-/-}$) mice

ND	8 weeks (A)	16 weeks (B)	26 weeks (C)	P
Body weight (g)	28.27 ± 0.57	32.27 ± 0.43	31.79 ± 1.22	A vs B * 0.03
Heart weight (mg)	174.0 ± 5.62	200.6 ± 7.53	190.7 ± 10.01	
Heart weight: body weight ratio (mg/g)	6.16 ± 0.16	6.22 ± 0.21	5.99 ± 0.19	
Liver (g)	2.08 ± 0.07	2.16 ± 0.08	2.10 ± 0.14	
Spleen (mg)	118.3 ± 4.63	149.0 ± 7.58	140.9 ± 7.70	
Epididymal fat pad weight (g)	0.26 ± 0.01	0.27 ± 0.02	0.33 ± 0.04	
Epididymal adipocyte area (x10^3 µm^2)	1.79 ± 0.24	2.19 ± 0.13	2.72 ± 0.18	
WD	**8 weeks (D)**	**16 weeks (E)**	**26 weeks (F)**	**P**
Body weight (g)	32.02 ± 0.73	37.52 ± 1.71	37.85 ± 0.75	D vs E ** 0.002, D vs F ** 0.001
Heart weight (mg)	183.2 ± 9.48	214.8 ± 14.17	210.76 ± 8.88	
Heart weight: body weight ratio (mg/g)	5.71 ± 0.33	5.82 ± 0.40	5.58 ± 0.23	
Liver (g)	2.30 ± 0.10	3.93 ± 0.51	5.82 ± 0.55	D vs E ** 0.004, D vs F **** P < 0.001, E vs F *** 0.0008
Spleen (mg)	165.3 ± 5.91	228.5 ± 20.56	219.7 ± 9.15	D vs E *** 0.0008, D vs F ** P < 0.01
Epididymal fat pad weight (g)	0.59 ± 0.07	0.92 ± 0.13	0.62 ± 0.05	D vs E * 0.01
Epididymal adipocyte area (x10^3 µm^2)	3.10 ± 0.76	5.12 ± 0.53	4.65 ± 0.27	
ND versus WD	**8 weeks**	**16 weeks**	**26 weeks**	
Body weight (g)	NS 0.07	** 0.002	** 0.005	
Heart weight (mg)	NS > 0.999	NS > 0.999	NS > 0.999	
HW: BW (mg/g)	NS > 0.999	NS > 0.999	NS > 0.999	
Liver (g)	NS > 0.999	*** P = 0.0008	**** P = 0.0001	
Spleen (mg)	* P < 0.02	**** P = 0.0001	*** P = 0.0008	
Epididymal fat pad weight (g)	** 0.007	**** P < 0.0001	NS 0.22	
Epididymal adipocyte area (x10^3 µm^2)	NS 0.87	** 0.002	NS 0.07	

ND = normal chow diet, WD = Western-type diet. Data are expressed as mean ± S.E.M and weights are shown in milligrams or grams. Heart weight: body weight ratio was presented as milligrams/grams and epididymal adipocyte area x10^3 µm^2*. Two-way ANOVA with Tukey's multiple comparison post-hoc tests, body and organ weights n = 8-17 mice per group, adipocyte area n = 3-4 mice per group, 100 adipocytes measured per mouse.*

6.4.4 Loss of Cav-1 confers protection against the development of atherosclerosis in Western-type diet-fed ApoE$^{-/-}$Cav-1$^{-/-}$ double knockout mice

A WD did not significantly alter the atherosclerotic lesion burden of ApoE$^{-/-}$Cav-1$^{-/-}$ mice, in comparison to ND-fed ApoE$^{-/-}$Cav-1$^{-/-}$ mice, until 26 weeks of high fat feeding (ND versus WD: 0.94 ± 0.40% versus 6.85 ± 0.68% P = 0.02, n = 5-6 mice per group, Figure 6.2A and B).

No differences were apparent between ND-fed ApoE$^{-/-}$Cav-1$^{-/-}$ and age-matched ApoE$^{-/-}$ mice at any of the experimental time-points (P = NS for all comparisons; 26-weeks: n = 5-7 mice per group, Figure 6.2B). However, ApoE$^{-/-}$Cav-1$^{-/-}$ mouse were more resistant to the development of atherosclerotic lesions when fed a WD compared to ApoE$^{-/-}$ mice (Figure 6.2 B).

In the initial stages of atherosclerosis, the 8-week time-point, no significant differences in atherosclerotic burden were observed between ApoE$^{-/-}$Cav-1$^{-/-}$ or ApoE$^{-/-}$ mice fed a WD (P = NS, n = 6 mice per group, Figure 6.2B). Nevertheless, by the 16-week time-point, atherosclerosis was markedly more severe in the aortae of WD-fed ApoE$^{-/-}$ mice compared to age and diet-matched ApoE$^{-/-}$Cav-1$^{-/-}$ mice (P = 0.04, n = 4-6 mice per group, Figure 6.2B). By the final 26-week time-point the extent of atherosclerotic disease within the aortae of WD-fed ApoE$^{-/-}$ mice remained significantly enhanced compared to ApoE$^{-/-}$Cav-1$^{-/-}$ mice (P < 0.0001; n = 6-7 mice per group, Figure 6.2B).

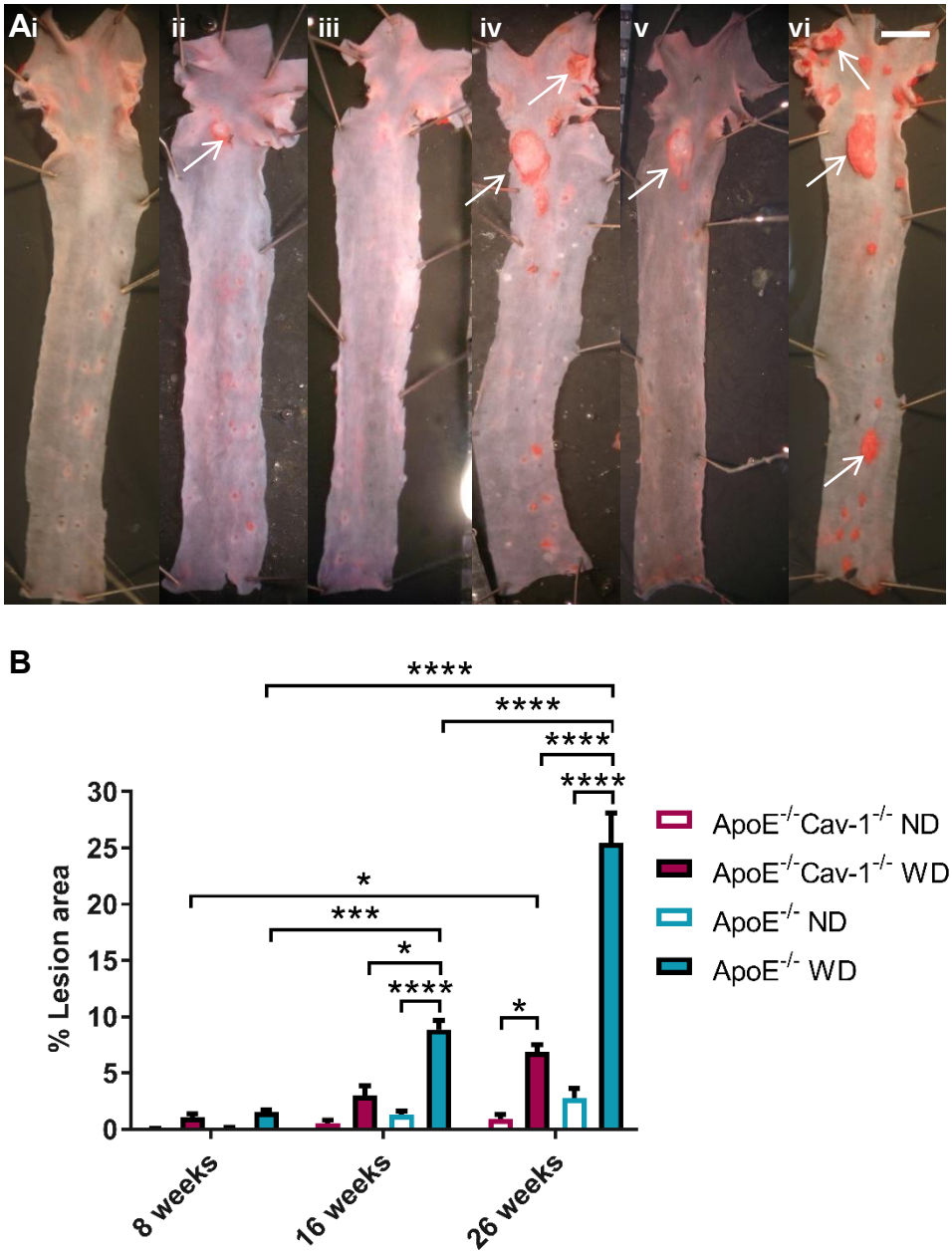

Figure 6.2 Atherosclerotic lesion burden within the aortae of Western-type diet-fed ApoE$^{-/-}$Cav-1$^{-/-}$ double knockout mice is drastically reduced compared to age and diet-matched ApoE$^{-/-}$ mice

*A) En face Oil red O staining of lipid lesions along the luminal surface of the aortae of ApoE$^{-/-}$ Cav-1$^{-/-}$ mice at 8-weeks on a i) ND, or ii) WD, 16-weeks on a iii) ND, or WD iv) WD, and 26-weeks on a v) ND or vi) WD. Atheromatous lesions are stained red and highlighted by arrows. B) Atherosclerotic disease progression was accelerated in WD fed ApoE$^{-/-}$Cav-1$^{-/-}$ and ApoE$^{-/-}$ mice. However, WD-fed ApoE$^{-/-}$Cav-1$^{-/-}$ mice were more resistant to the development of atherosclerosis than age and diet-matched ApoE$^{-/-}$ mice. Representative images. scale bar, top right-hand corner, = 1 mm, ND = normal diet, WD = Western-type diet. Data are presented as mean ± S.E.M, n = 4-7 mice per group, * P <0.05, *** P < 0.001, **** P < 0.0001. Two-way ANOVA with post hoc Bonferroni's test. ApoE$^{-/-}$ data previously shown in Chapter 3, Figure 4.1.*

6.4.5 Vascular reactivity studies assessing the effect of aortic PVAT on vascular responses

6.4.5.1 The contraction of aortic rings to 100 mM KPSS were unaltered by the presence of PVAT in the ApoE$^{-/-}$Cav-1$^{-/-}$ double knockout mice

The contractile responses of PVAT-intact or PVAT-denuded aortic rings were similar in response to 100 mM KPSS (+PVAT versus -PVAT: P = NS; n = 5-8 mice per group, Figure 6.3). In addition, no significant changes in contraction were observed between the aortic rings of ND and WD-fed ApoE$^{-/-}$Cav-1$^{-/-}$ double knockout mice in the presence of PVAT (ND versus WD: P = NS, n = 5-8 mice per group) or in PVAT-denuded preparations (ND versus WD: P = NS).

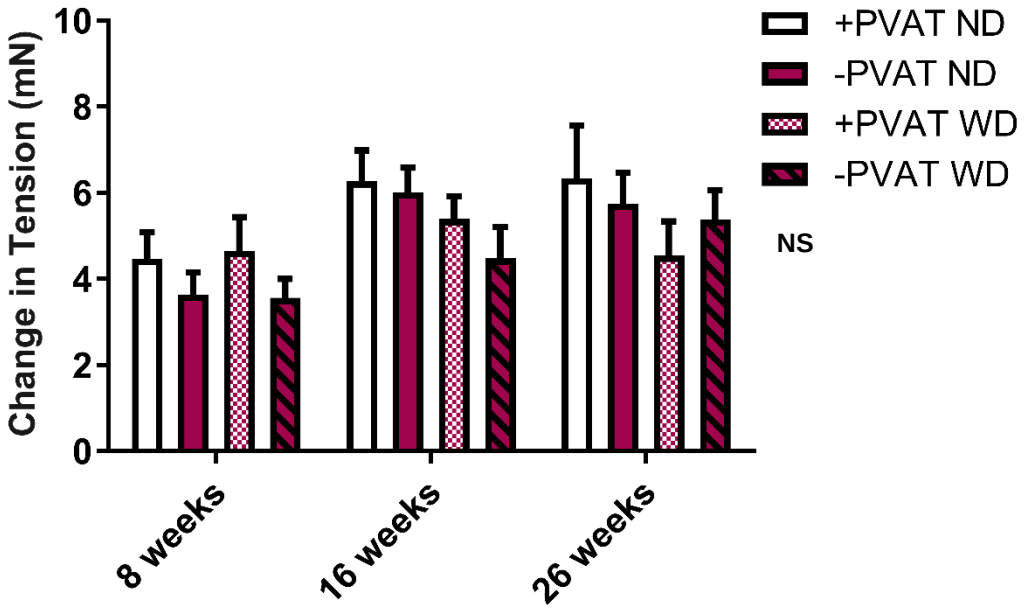

Figure 6.3 The contractility of aortic rings, in response to 100 mM KPSS, were unaltered by the presence of PVAT in the ApoE$^{-/-}$Cav-1$^{-/-}$ double knockout mice.

The contraction of PVAT-intact or PVAT-denuded aortic rings were similar at each time-point. ND = normal diet, PVAT = perivascular adipose tissue WD = Western-type diet. Data are presented as mean ± S.E.M, n = 5-8 mice per group, Two-way ANOVA with post hoc Bonferroni's multiple comparisons test.

Additionally, the responses of aortic rings to KPSS from ND-fed ApoE$^{-/-}$Cav-1$^{-/-}$ double knockout mice were compared to ApoE$^{-/-}$ and Cav-1$^{-/-}$ mice (Appendix 2.4Ai and ii). No significant differences were observed between the ApoE$^{-/-}$Cav-1$^{-/-}$ or Cav-1$^{-/-}$ mice ether in the presence or absence of PVAT (ApoE$^{-/-}$Cav-1$^{-/-}$ versus Cav-1$^{-/-}$: P = NS for all comparisons n = 4-8 mice per group, Appendix 2.4Ai and ii).

The contractions of PVAT-intact aortic rings from ApoE$^{-/-}$Cav-1$^{-/-}$ mice were similar to those observed from the ApoE$^{-/-}$ mice (Appendix 2.4Ai). However, the contraction of PVAT-denuded aortic rings from 8 week ND-fed ApoE$^{-/-}$Cav-1$^{-/-}$ mice was significantly reduced in comparison to aortic rings from age and diet-matched ApoE$^{-/-}$ mice (ApoE$^{-/-}$Cav-1$^{-/-}$ versus ApoE$^{-/-}$: -PVAT: P = 0.004, n = 6-8 mice per group, Appendix 2.4Aii).

6.4.5.2 A functional endothelium is retained during the progression of atherosclerosis in ApoE$^{-/-}$Cav-1$^{-/-}$ double knockout mice

Although atherosclerotic lesions were present along the luminal surface of the aortae of the ApoE$^{-/-}$Cav-1$^{-/-}$ mice endothelial relaxations were not significantly altered in either the ND or WD-groups (P = NS for all comparisons, n = 5-8 mice per group , Figure 6.4). In addition, no differences were found between the relaxations of ND and WD aortic rings in the presence, or absence of PVAT (ND versus WD: P = NS; n = 4-8 mice per group, Figure 6.4).

The presence of PVAT had no effect on the relaxation of aortic rings to 10 µM acetylcholine in ND or WD conditions (+/-PVAT: P = NS for all comparsons; n = 5-8 mice per group, Figure 6.4).

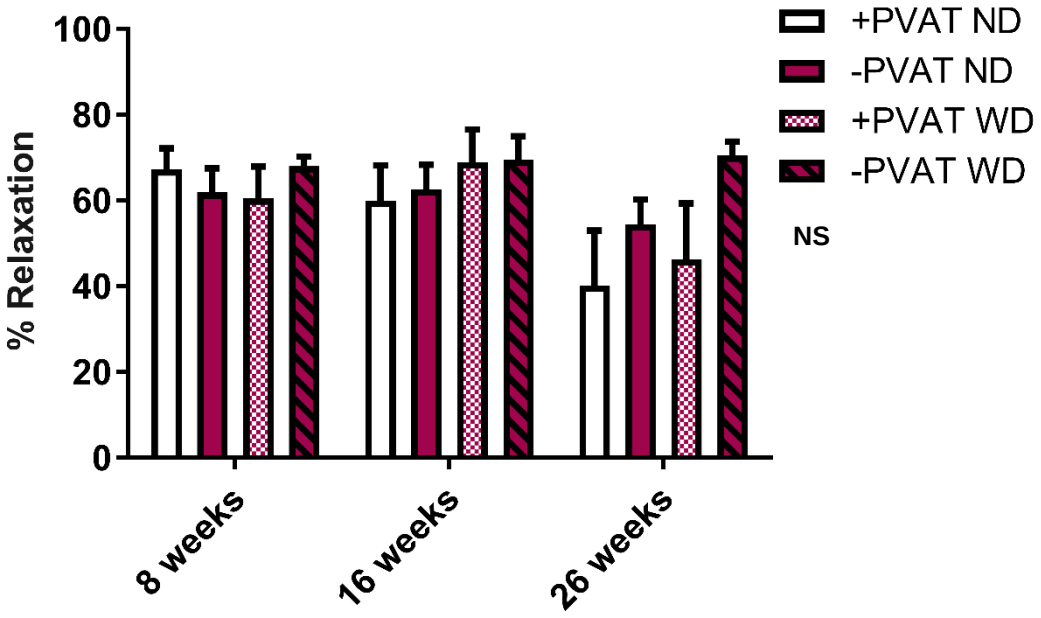

Figure 6.4 Endothelial dysfunction does not occur in the aortae of the ApoE$^{-/-}$Cav-1$^{-/-}$ double knockout mice at any of the examined time-points

Phenylephrine pre-constricted aortic rings from 26-week time-point ND and WD-fed mice did not display significantly altered vasodilatory responses to 10 µM acetylcholine in comparison to the younger diet-matched groups. In addition, the presence of PVAT did not affect the relaxations of aortic rings Data are presented as mean ± S.E.M, n = 5-8 mice per group, with Two-way ANOVA and post hoc Bonferroni's multiple comparison tests.

Endothelium-dependent relaxation responses of ND-fed ApoE$^{-/-}$Cav-1$^{-/-}$ double knockout mice were similar to those observed from the aortic rings of ApoE$^{-/-}$ mice (ApoE$^{-/-}$Cav-1$^{-/-}$ versus ApoE$^{-/-}$ P = NS for each age-matched comparison, n = 5-8 mice per group (Appendix 2.4Bi and ii).

However, in comparison to Cav-1$^{-/-}$ mice, the endothelium-dependent relaxation responses of PVAT-denuded aortic rings from ApoE$^{-/-}$Cav-1$^{-/-}$ mice were significantly reduced after 26 weeks on a ND (post weaning) (ApoE$^{-/-}$Cav-1$^{-/-}$ versus Cav-1$^{-/-}$: -PVAT: P = 0.01; n = 4-5 mice per group, Appendix Bii).

6.4.5.3 The aortic PVAT of ApoE$^{-/-}$Cav-1$^{-/-}$ double knockout mice does not exert an anti-contractile effect in normal diet or Western-type diet-fed mice

PVAT did not modulate contractions to phenylephrine in ND-fed ApoE$^{-/-}$Cav-1$^{-/-}$ mice at any of the examined time-points (+/-PVAT: P = NS, n = 5-8 mice per group, Figure 6.A-C). Moreover, these findings were replicated in age-matched WD-fed ApoE$^{-/-}$Cav-1$^{-/-}$ mice; the contractility of aortic rings were similar in the presence or absence of PVAT at each time-point (+PVAT versus -PVAT: P =NS, n = 5-8 mice per group, Figure 6.5A-C).

6.4.5.4 A Western-type diet does not alter the contractions of aortic rings in the ApoE$^{-/-}$Cav-1$^{-/-}$ double knockout mice in comparison to normal diet-fed mice

High fat feeding ApoE$^{-/-}$Cav-1$^{-/-}$ mice did not have a significant impact on aortic ring contractions. No differences in contractile responses were observed between PVAT-denuded aortic rings of ND and WD-fed ApoE$^{-/-}$Cav-1$^{-/-}$ mice (ND versus WD: P = NS for each comparison; n = 4-8 mice per condition, Figure 6.5A-C). Furthermore, a WD had no impact on the contraction of aortic rings, in the presence of PVAT, in comparison to ND-fed mice at any of the time-points (ND versus WD: P = NS for each comparison n = 5-8 mice per condition, Figure 6.5A-C).

6.4.5.5 Ageing increases the contractility of PVAT-denuded aortic rings from normal and Western-type diet-fed ApoE$^{-/-}$Cav-1$^{-/-}$ double knockout mice

The effect of ageing on vascular reactivity in ND ApoE$^{-/-}$Cav-1$^{-/-}$ mice was evaluated. In the absence of PVAT, the contractility of aortic rings significantly increased after the initial 8-week ND time-point (8-weeks versus 16-weeks: P = 0.04, 8-weeks versus 26-weeks: P = 0.02, n = 5-7 mice per group, Figure 6.6Ai) although no differences in contraction were observed between the 16 and 26-week groups. However, ageing had no effect on the vascular reactivity of PVAT-intact aortic rings from ND-fed ApoE$^{-/-}$Cav-1$^{-/-}$ mice (P = NS for each time-point comparison, n = 5-7 mice per group, Figure 6.6Aii).

Similar findings were observed with ageing on a WD in ApoE$^{-/-}$Cav-1$^{-/-}$ mice. A significant increase in contraction was observed between the 8 and 26 week WD-fed groups when the contractile responses of PVAT-denuded aortic rings were compared (8-weeks versus 26-weeks: P = 0.008, n = 4 and 7 mice, respectively, Figure 6.6Bi) although no differences were observed between the 8 and 16-week WD-fed responses (8-weeks versus 16-weeks: P = NS, n = 4 and 8 mice, respectively, Figure 6.6Bi). No differences in the contractile responses of PVAT-intact aortic rings from ageing WD-fed mice were observed (P = NS; n = 7-10 mice per group, Figure 6.6Bii).

In summary, the aortic PVAT of ApoE$^{-/-}$Cav-1$^{-/-}$ mice did not exert an anti-contractile effect and a WD did not augment the contractions of aortic rings in comparison to age-matched ND-fed ApoE$^{-/-}$Cav-1$^{-/-}$. Furthermore, a significant increase in the contractile responses of PVAT-denuded aortic rings were observed with ageing on a ND and WD although no such age-associated changes were observed in PVAT-intact aortic preparations.

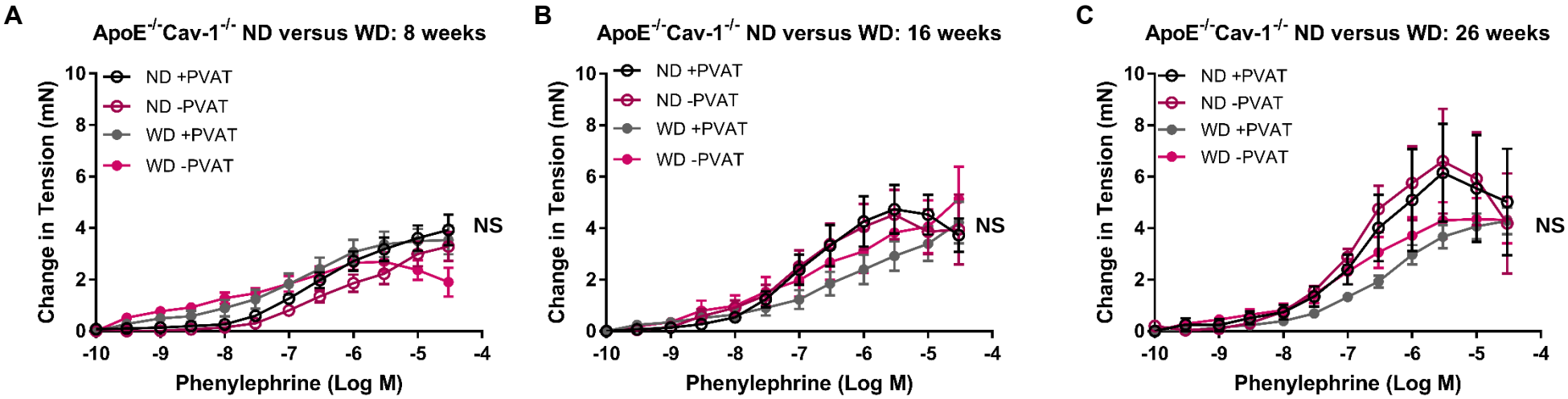

Figure 6.5 Aortic PVAT does not modulate vascular reactivity in normal or Western-type diet-fed ApoE$^{-/-}$Cav-1$^{-/-}$ double knockout mice

Aortic rings were challenged with cumulative doses of phenylephrine (1 x 10^{-10} - 3 x 10^{-5} mol/L) in the presence or absence of PVAT. A) Aortic PVAT did not exert an anti-contractile effect on aortic rings from ApoE$^{-/-}$Cav-1$^{-/-}$ mice when fed either a ND or WD for 8 weeks (post weaning). In addition, the contractions of aortic rings, in the presence or absence of PVAT, were similar when WD and ND-fed responses were directly compared. B) A similar pattern was observed in the 16 week ND and WD-fed groups and PVAT did not modulate aortic contractions. The contractions of aortic rings from ND and WD-fed ApoE$^{-/-}$Cav-1$^{-/-}$ mice were comparable with or without PVAT. C) The presence of aortic PVAT did not alter vascular contractions after 26 weeks on a ND or WD (post weaning) and a WD did not alter the contractions of PVAT-denuded or PVAT-intact aortic rings in comparison to ND responses. ND = normal diet, PVAT = perivascular adipose tissue, WD = Western-type diet. Dose response data are expressed as mean ± S.E.M., n = 4-7 mice per group, two-way ANOVA with Bonferroni's post hoc tests, n = 4-10 mice per group, two-way ANOVA with Bonferroni's post hoc test.

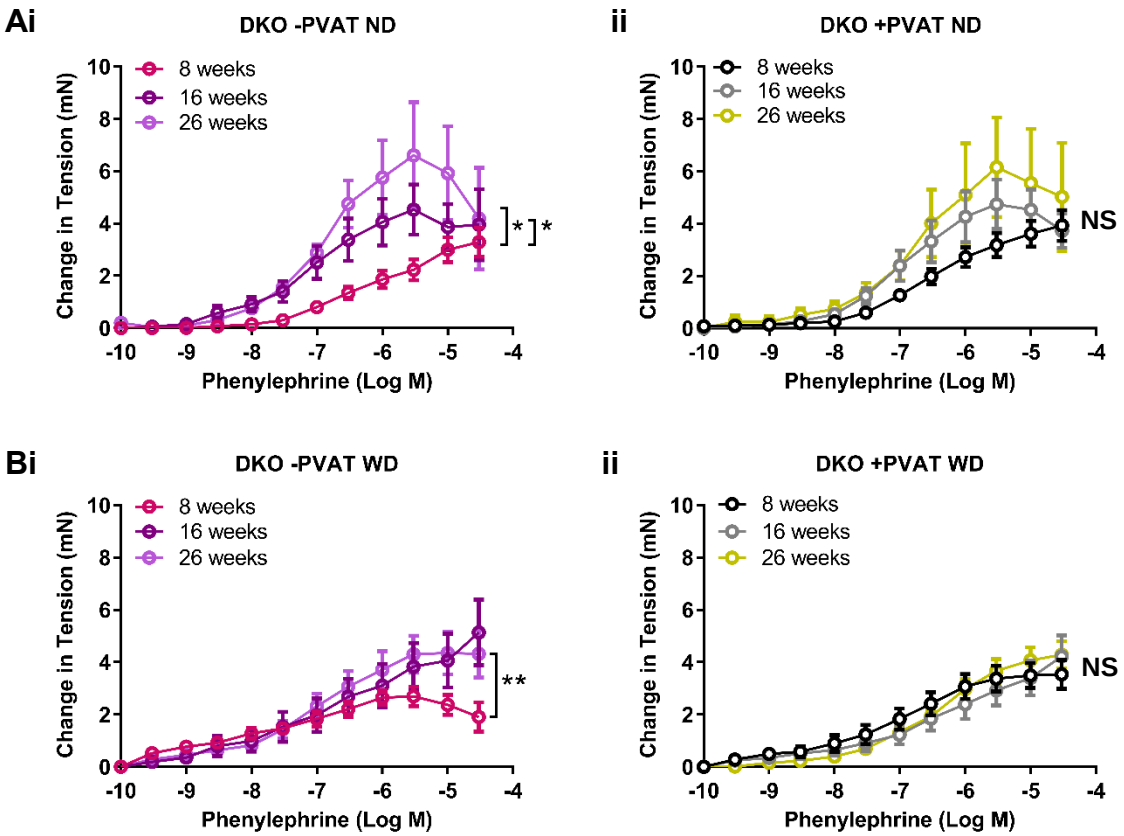

Figure 6.6 Ageing increases the contractility of PVAT-denuded aortic rings from normal diet and Western-type diet fed ApoE$^{-/-}$Cav-1$^{-/-}$ double knockout mice *Ai) The contractions of PVAT-denuded aortic rings from ND-fed ApoE$^{-/-}$Cav-1$^{-/-}$ mice were significantly increased with ageing on a ND. Aii) No age-related changes in contraction were observed in PVAT-intact aortic rings. Bi) A significant increase in contraction of PVAT-denuded aortic rings was observed between the 8 and 26-week WD-fed ApoE$^{-/-}$Cav-1$^{-/-}$ mice. Bii) PVAT-intact aortic rings from WD-fed ApoE$^{-/-}$Cav-1$^{-/-}$ mice were unaffected by increasing age. ND = normal diet, PVAT = perivascular adipose tissue, WD = Western-type diet. Dose response data are expressed as mean ± S.E.M., n = 4-8 mice per group, two-way ANOVA with Bonferroni's post hoc tests. * P < 0.05, ** P < 0.01.*

6.4.5.6 The aortic ring preparations of normal diet-fed ApoE$^{-/-}$Cav-1$^{-/-}$ double knockout mice exhibit characteristics of both ApoE$^{-/-}$ and Cav-1$^{-/-}$ mice

The contractions of PVAT-denuded aortic rings from ND-fed ApoE$^{-/-}$Cav-1$^{-/-}$ mice were compared to age and diet-matched ApoE$^{-/-}$ and Cav-1$^{-/-}$ mice (Appendix 2.7Ai-iii). The constriction of PVAT-denuded aortic rings from 8-week ND-fed ApoE$^{-/-}$Cav-1$^{-/-}$ mice was significantly lower than the ApoE$^{-/-}$ responses (ApoE$^{-/-}$Cav-1$^{-/-}$ versus ApoE$^{-/-}$: 8-weeks P = 0.002, n = 7 and 8, respectively, Appendix 2.7Ai). However, the contractions of ApoE$^{-/-}$Cav-1$^{-/-}$ mice were similar to Cav-1$^{-/-}$ mice at this time-point (P = NS, n = 4-7 mice per group, Appendix 2.7Ai). After 16 weeks on a ND no significant differences were observed between PVAT-denuded aortic rings from ApoE$^{-/-}$ and ApoE$^{-/-}$Cav-1$^{-/-}$ mice (P = NS, n = 5-8 mice per group, Appendix 2.7Aii) although the contractions of aortic rings from the ApoE$^{-/-}$Cav-1$^{-/-}$ mice were significantly increased compared to their Cav-1$^{-/-}$ counterparts (ApoE$^{-/-}$Cav-1$^{-/-}$ versus Cav-1$^{-/-}$: 16-weeks P = 0.002 n = 6 and 4 mice, respectively, Appendix 2.7Aii). After 26 weeks on a ND, the contractile responses of ApoE$^{-/-}$Cav-1$^{-/-}$ mice were similar to those observed in the ApoE$^{-/-}$ and Cav-1$^{-/-}$ mice (P = NS, n = 4-8 mice per group, Appendix 2.7Aiii).

Furthermore, PVAT-intact aortic responses from ND-fed ApoE$^{-/-}$Cav-1$^{-/-}$ mice were compared to age and diet-matched ApoE$^{-/-}$ and Cav-1$^{-/-}$ mice (Appendix 2.7Bi-iii). When the contraction of aortic rings, in the presence of PVAT, were compared to ApoE$^{-/-}$ responses, the contractions of ApoE$^{-/-}$ Cav-1$^{-/-}$ aortic rings were found to be significantly diminished in both the 8 and 16-week groups (ApoE$^{-/-}$Cav-1$^{-/-}$ versus ApoE$^{-/-}$: 8-weeks P < 0.0001; 16-weeks P < 0.0001; n = 8 for all groups, Appendix 2.7Bi and ii). However, by the 26-week time-point no differences in contractions were apparent (P = NS, n = 5 and 6 mice, Appendix 2.7Biii and iii). The responses of PVAT-intact aortic rings from ApoE$^{-/-}$Cav-1$^{-/-}$ mice were similar to those of Cav-1$^{-/-}$ mice at each time-point (P = NS for each group comparison; n = 4-8 mice per group, Appendix 2.7Bi-iii).

In summation, the contractile responses of aortic rings from ND-fed ApoE$^{-/-}$Cav-1$^{-/-}$ mice displayed characteristics of both ApoE$^{-/-}$ and Cav-1$^{-/-}$ mice. Initially, contractions to phenylephrine were dampened in PVAT-denuded aortic rings in a similar fashion to Cav-1. However, this reduced contraction, compared to ApoE$^{-/-}$ mice, was lost after 16-weeks on a ND post weaning. The contractile responses of PVAT-intact aortic rings were again similar to Cav-1$^{-/-}$ mice and displayed significantly reduced contractions compared to ApoE$^{-/-}$ mice at the 8 and 16-week time-points.

6.4.5.7 Nitric oxide synthase inhibition causes a pro-constrictor effect in PVAT from 8-week normal diet-fed ApoE$^{-/-}$Cav-1$^{-/-}$ mice but exerts no effect in the other groups

Incubation with 50 µM L-NNA, a NOS inhibitor revealed a significant pro-constrictor effect of PVAT in the 8-week ND-fed ApoE$^{-/-}$Cav-1$^{-/-}$ mice (+PVAT + L-NNA versus -PVAT + L-NNA: P = 0.02; n= 8 and 7 mice, Figure 6.7Ai). However, this effect did not persist in ageing ND ApoE$^{-/-}$Cav-1$^{-/-}$ mice and contractions were similar in NOS-inhibited PVAT-intact and PVAT-denuded aortic rings (P = NS in the presence of L-NNA for the 16 and 26-week ND-fed groups; n= 5-9 mice per group, Figure 6.7Aii and iii). Additionally, NOS inhibition had no effect on contractile responses of aortic rings, in the presence or absence of PVAT, in the WD-fed groups (P = NS in the presence of L-NNA for each WD-fed time-point n = 7-9 mice per group, Figure 6.7Bi-iii).

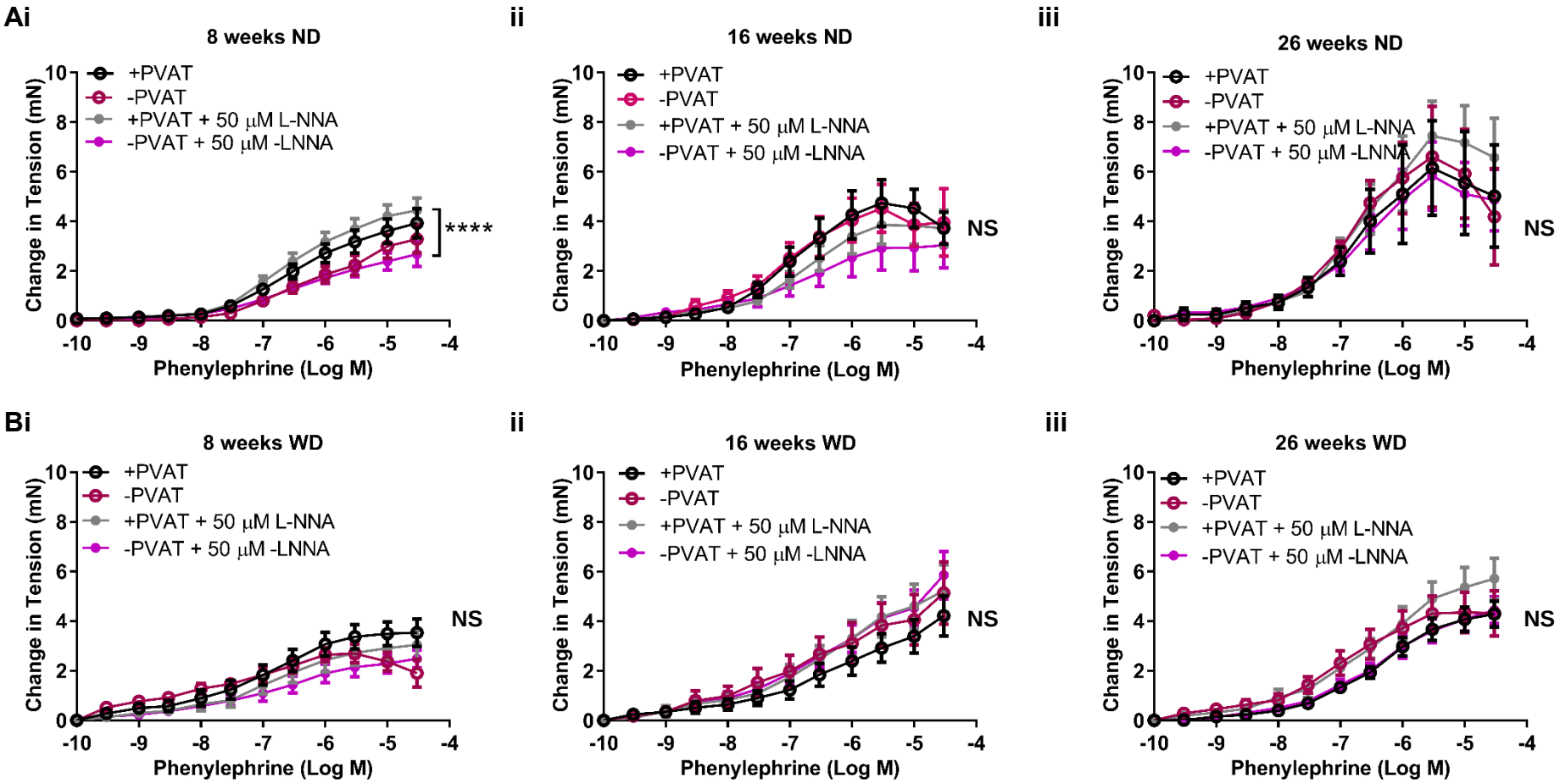

Figure 6.7 Nitric oxide synthase inhibition reveals a pro-constrictor effect in PVAT from 8-week normal diet-fed ApoE$^{-/-}$Cav-1$^{-/-}$ mice but exerts no effect in the other groups

*NOS inhibition with 50 μM L-NNA revealed a pro-contractile effect of PVAT in Ai) 8-week ND-fed ApoE$^{-/-}$Cav-1$^{-/-}$ mice. However, this effect did not persist and no significant differences in contractions were observed in the presence of NOS in Aii) 16 or iii) 26-week ND-fed ApoE$^{-/-}$Cav-1$^{-/-}$ mice. Furthermore, NOS inhibition had no effect on B) WD-fed ApoE$^{-/-}$Cav-1$^{-/-}$ mice at any of the time-points i) 8, i) 16 or iii) 26-weeks on the diet post weaning. ND = normal diet, NOS = nitric oxide synthase, WD = Western-type diet. Dose response data are expressed as mean ± S.E.M., **** P < 0.0001, n = 4-10 mice per group, two-way ANOVA with post hoc tests.*

6.4.5.8 The aortic rings of double knockout mice do not exhibit reduced sensitivity to exogenous nitric oxide

Vaso-relaxation of aortic rings from ApoE$^{-/-}$Cav-1$^{-/-}$ mice to the NO donor sodium nitroprusside, were unchanged with ageing, a WD or the presence of PVAT (P = NS; n = 4-10 mice per group, Figure 6.8).

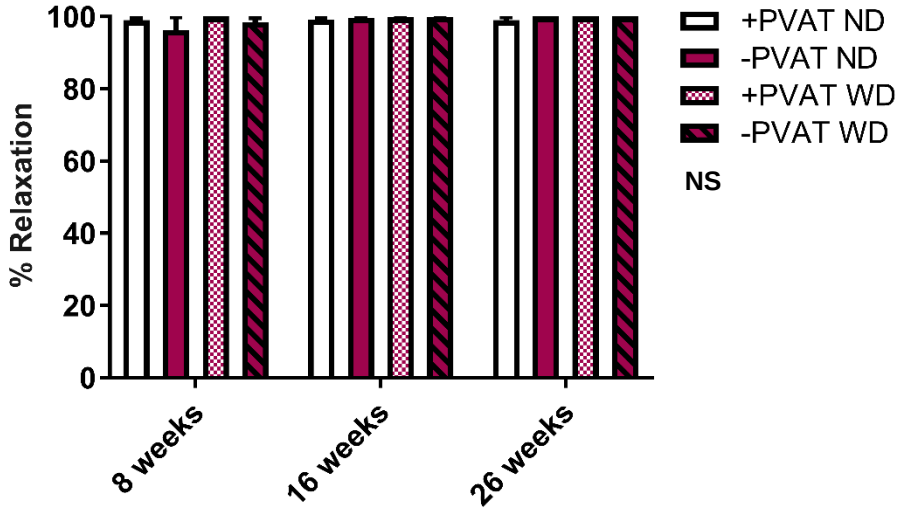

Figure 6.8 Endothelial-independent relaxation is unaffected by PVAT, ageing or the development of atherosclerosis in ApoE$^{-/-}$Cav-1$^{-/-}$ double knockout mice

The sensitivity of phenylephrine-constricted aortic rings to 10 μM sodium nitroprusside, a NO donor, was unaltered by the presence of PVAT, ageing or atherosclerosis in ND or WD-fed ApoE$^{-/-}$Cav-1$^{-/-}$ mice. ND = normal diet, WD = Western-type diet. Data are presented as mean ± S.E.M, n = 4-7 mice per group, two-way ANOVA with post hoc Bonferroni's multiple comparisons test.

These findings reflect the observations of the ApoE$^{-/-}$ and Cav-1$^{-/-}$ mice, that upon exposure to 10 μM sodium nitroprusside the aortic rings relax back to baseline regardless of age, diet or the presence or absence of PVAT (Appendix 2.4Ci and ii).

6.4.6 White adipocyte hypertrophy occurs within the aortic PVAT of ApoE$^{-/-}$Cav-1$^{-/-}$ double knockout mice after extensive duration on a Western-type diet

Aortic PVAT weight could not be assessed in the ApoE$^{-/-}$Cav-1$^{-/-}$ because of incomplete data sets due to breeding issues within the colony.

The impact of ageing and a WD on aortic PVAT morphology was assessed in the ApoE$^{-/-}$Cav-1$^{-/-}$ mouse using haematoxylin and eosin staining (Figure 6.9Ai-vi). Ageing of ApoE$^{-/-}$Cav-1$^{-/-}$ mice on a ND from 8 to 26-weeks did not produce any alterations in the proportion of white adipocytes within the aortic PVAT (P = NS between each time-point; n = 3-4 mice per group, Figure 6.9B). Furthermore, a WD did not elicit any further changes (ND versus WD: P = NS, comparisons between groups; n = 3-4 mice per group, Figure 6.9B).

Additionally, upon examination of individual white adipocyte size, no age-associated changes in size were observed in ND-fed ApoE$^{-/-}$Cav-1$^{-/-}$ mice (P > 0.99 each time-point comparison; n = 3-4 mice per group, Figure 6.9C). Whilst no effects of a WD were observed after 8 or 16 weeks on a WD (ND versus WD: P = NS; n = 3-4 mice per group Figure 6.9C) prolonged high fat feeding induced white adipocyte hypertrophy within the aortic PVAT (ND versus WD: 26-weeks: P = 0.01; n = 4 ND and 3 WD-fed mice, Figure 6.9C).

The aortic PVAT of ApoE$^{-/-}$Cav-1$^{-/-}$ mice displayed hybrid characteristics relating to the ApoE$^{-/-}$ and Cav-1$^{-/-}$ mice. Whilst the proportion of white adipocytes occupying the aortic PVAT remained unaltered by increasing age or a WD, which was an ApoE$^{-/-}$-like phenotype (Appendix 2.8B), after 26 weeks of a WD the adipocytes became hypertrophied, similar to the Cav-1$^{-/-}$ mice (Appendix 2.8C).

In 26-week ND-fed C57BL/6 mice and 26-week WD-fed Cav-1$^{-/-}$ mice, white adipocyte hypertrophy was associated with PVAT causing vasoconstriction of aortic rings and exerting a pro-contractile effect. However, in age-matched WD-fed ApoE$^{-/-}$Cav-1$^{-/-}$ mice PVAT was still unable to modulate vascular reactivity.

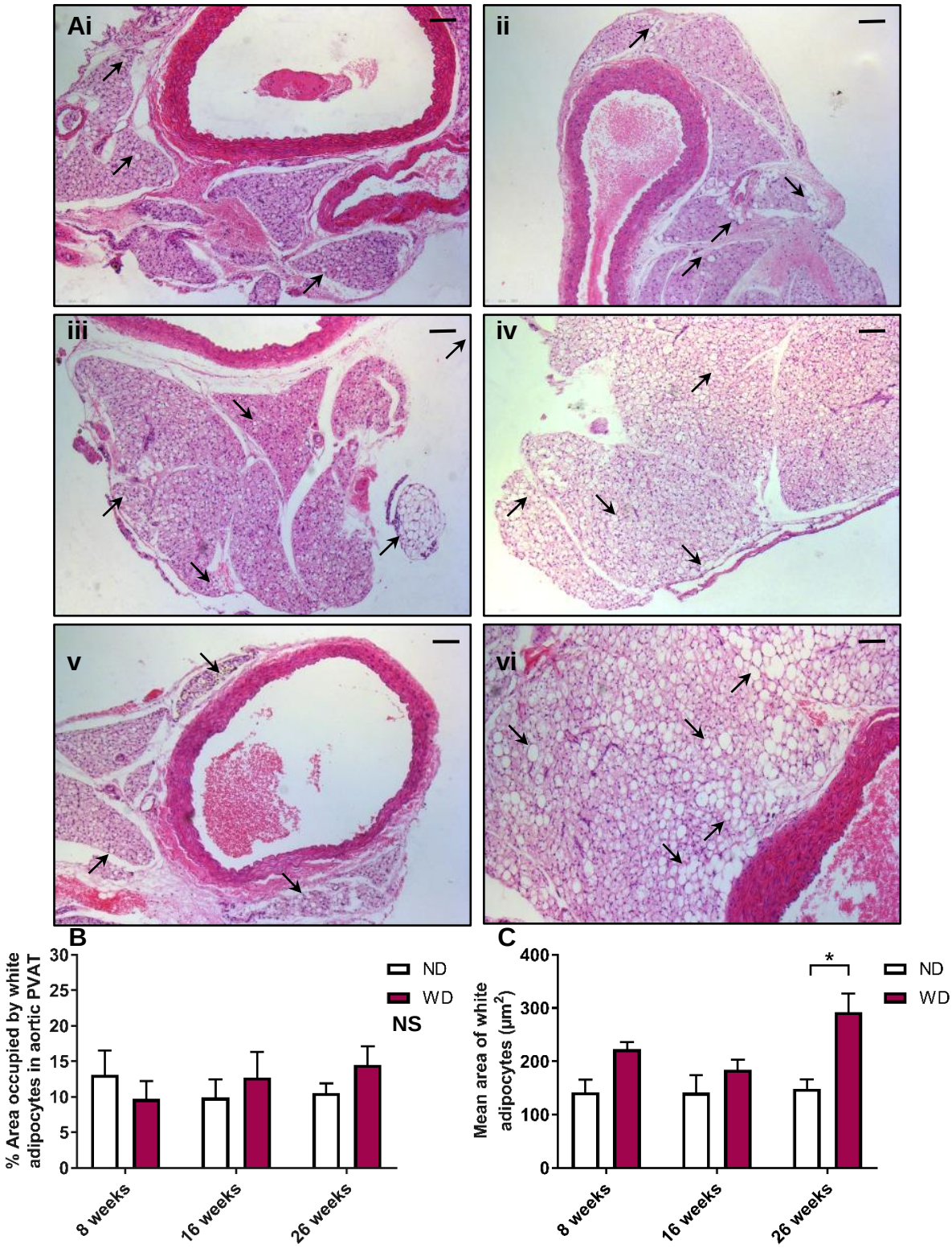

Figure 6.9 The proportion of aortic PVAT occupied by white adipocytes is unaltered by ageing or a Western-type diet; however, white adipocyte hypertrophy is observed after prolonged high fat feeding in the ApoE$^{-/-}$Cav-1$^{-/-}$ double knockout mice

*A) Haematoxylin and eosin-stained thoracic PVAT and aortae sections from ApoE$^{-/-}$Cav-1$^{-/-}$ mice at 8-weeks, i) ND, ii) WD, 16-weeks iii) ND, iv) WD and 26-weeks v) ND and vi) WD. Examples of white adipocytes are highlighted by arrows. B) The percentage area of aortic PVAT occupied by white adipocytes did not change with ageing or a WD. C) White adipocyte hypertrophy was observed after 26 weeks on a WD. Representative images obtained at 10X magnification. Scale bars represent 100 μm. ND = normal diet, WD = Western-type diet. Data are expressed as mean ± S.E.M, * P < 0.05, n = 3-4 mice per group, two-way ANOVA with Bonferroni's post hoc tests.*

6.4.7 The PVAT of ApoE$^{-/-}$Cav-1$^{-/-}$ double knockout mice does not display elevated levels of superoxide with ageing or a Western-type diet

The presence of superoxide within the aortic PVAT of ApoE$^{-/-}$Cav-1$^{-/-}$ mice was visualised via DHE fluorescent staining. Superoxide was detected in each of the experimental groups (Figure 6.10Ai-vi). Ageing had no effect on superoxide levels within the aortic PVAT of ApoE$^{-/-}$Cav-1$^{-/-}$ mice (P = NS for each group comparison; n = 3-5 mice per group, Figure 6.10C). Furthermore, a high fat WD did not promote an increase in superoxide production within the aortic PVAT (ND versus WD: P = NS for each comparison; n = 3-5 mice in each group, Figure 6.10C).

Atherosclerotic lesion burden was markedly less severe in WD-fed ApoE$^{-/-}$Cav-1$^{-/-}$ mice at both the 16 and 26-week time-points in comparison to age and diet-matched ApoE$^{-/-}$ mice. However, superoxide production within the aortic PVAT of ApoE$^{-/-}$Cav-1$^{-/-}$ was similar to the PVAT of ApoE$^{-/-}$ mice (Appendix 2.8D). Also, the amount of ROS within the PVAT of ApoE$^{-/-}$Cav-1$^{-/-}$ mice did not differ when compared to age and diet-matched Cav-1$^{-/-}$ mice. ROS levels were not elevated in either of the 26 week WD-fed Cav-1$^{-/-}$ or ApoE$^{-/-}$Cav-1$^{-/-}$ mice even though adipocyte hypertrophy was observed in the white adipocyte population of the aortic PVAT.

6.4.8 Ageing and a Western-type diet does not affect the number of macrophages infiltrating the aortic PVAT of ApoE$^{-/-}$Cav-1$^{-/-}$ double knockout mice

Inflammation was assessed in the aortic PVAT of ageing and WD-fed ApoE$^{-/-}$Cav-1$^{-/-}$ mice via Mac-3 immunostaining (Figure 6.11Bi-vi).

The number of macrophages infiltrating the PVAT was unchanged by ageing (P = NS for each time-point comparison; n = 3-5 mice per group, Figure 6.12). In addition, a WD did not alter the numbers of infiltrating macrophages observed within the aortic PVAT of ApoE$^{-/-}$Cav-1$^{-/-}$ mice when compared to age-matched ND-fed mice (ND versus WD: P = NS for each comparison; n = 3-5 mice per group, Figure 6.12).

These data could suggest that the development of atherosclerosis within the aortae of the ApoE$^{-/-}$Cav-1$^{-/-}$ mice has no impact on the infiltration of Mac-3^{+} macrophages within the surrounding aortic PVAT.

Additionally, the macrophage infiltration of aortic PVAT from ApoE$^{-/-}$Cav-1$^{-/-}$ mice was compared to ApoE$^{-/-}$ and Cav-1$^{-/-}$ mice and no significant differences in macrophage numbers were observed between the different groups of mice (P = NS for each time-point, n = 3-4 mice per group, Appendix 2.8E).

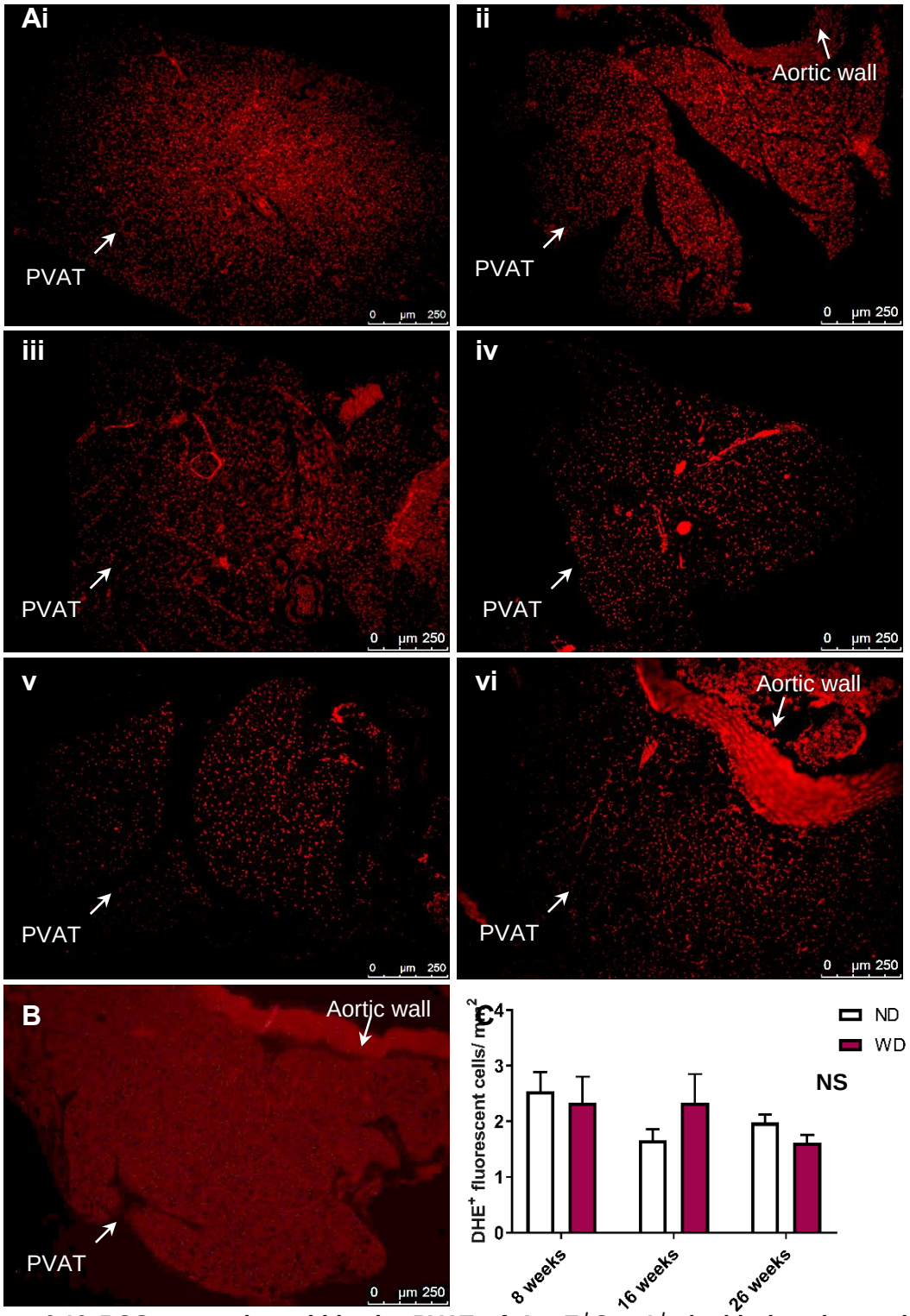

Figure 6.10 ROS generation within the PVAT of ApoE$^{-/-}$Cav-1$^{-/-}$ double knockout mice is unaltered by ageing or a Western-type diet

Thoracic aortae with PVAT were sectioned and incubated with DHE to detect ROS, indicated by red punctate fluorescence. A) DHE^{+} nuclei were observed in all sections i) 8-week ND, ii) WD, iii) 16-week ND, iv) WD and 26-week v) ND and vi) WD. B) No DHE^{+} nuclei were observed in the DMSO control. C) ROS production within the aortic PVAT was unaffected by ageing or a WD. Representative images at 10 X magnification. Scale bars represent 250 µm. DHE^{+} nuclei were quantified in 5 fields of view per section per mouse. DHE =dihydroethidium, ND = normal diet, WD = Western-type diet. Data are expressed as mean ± S.E.M., DHE^{+} nuclei presented as cells/mm^{2} of PVAT, n = 3-5 mice per group, two-way ANOVA with Bonferroni's post hoc test.

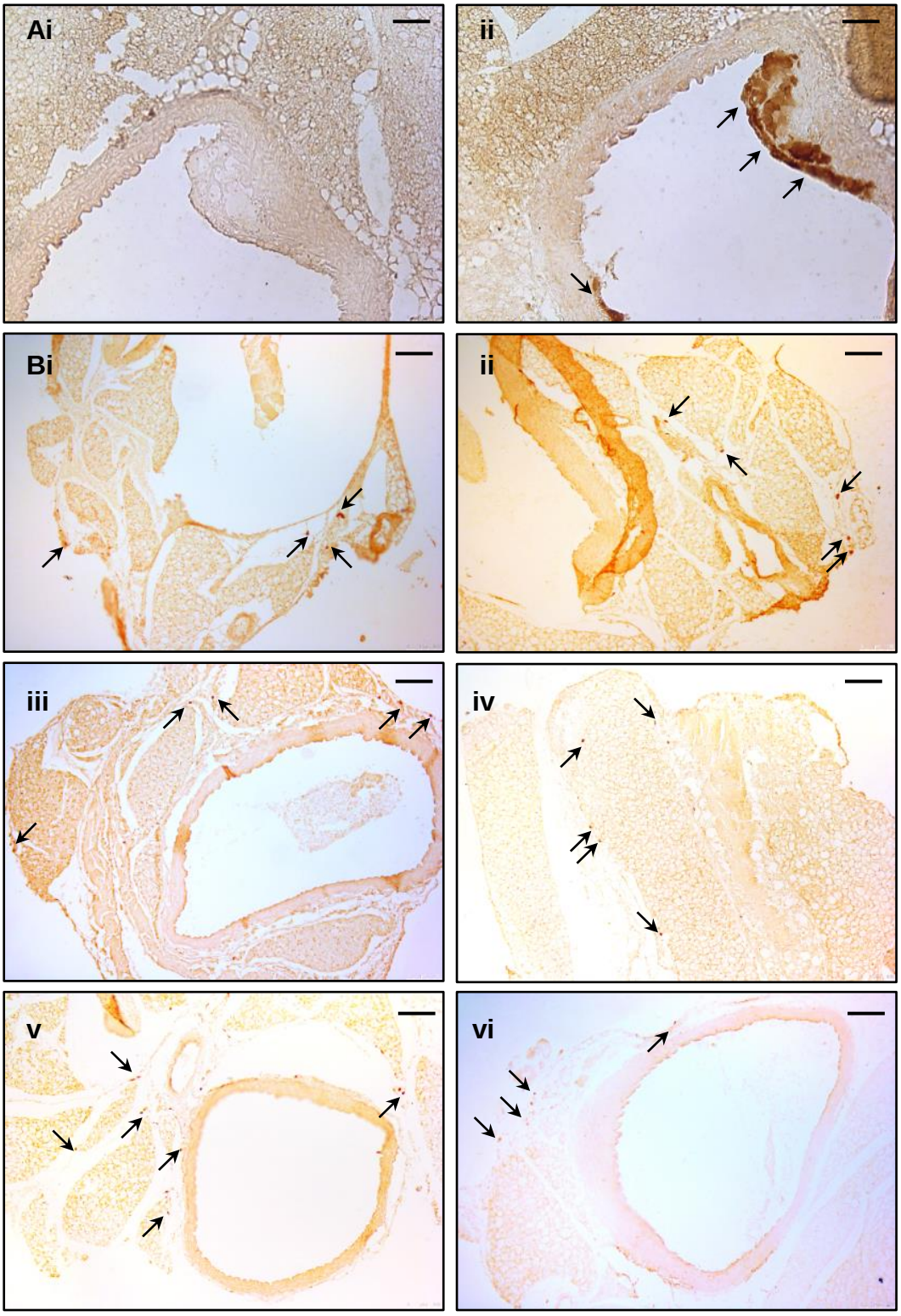

Figure 6.11 Macrophages are present in the aortic PVAT of ApoE$^{-/-}$Cav-1$^{-/-}$ double knockout mice

Inflammation was assessed in the aortic PVAT of ApoE$^{-/-}$Cav-1$^{-/-}$ mice using a Mac-3 macrophage marker. A) The aortic arch of an atherosclerotic ApoE$^{-/-}$ mouse was used as a control i) IgG and ii) positive control, macrophages were stained brown in the atherosclerotic plaque. B) Representative images of ApoE$^{-/-}$Cav-1$^{-/-}$ mice at: i) 8-week ND and ii) WD, iii) 16-week ND and iv) WD and 26-week v) ND and vi) WD. Images were obtained at 10X magnification. Scale bars represent 100 µm and examples of Mac-3^{+} staining are highlighted by arrows. ND = normal diet, WD = Western-type diet.

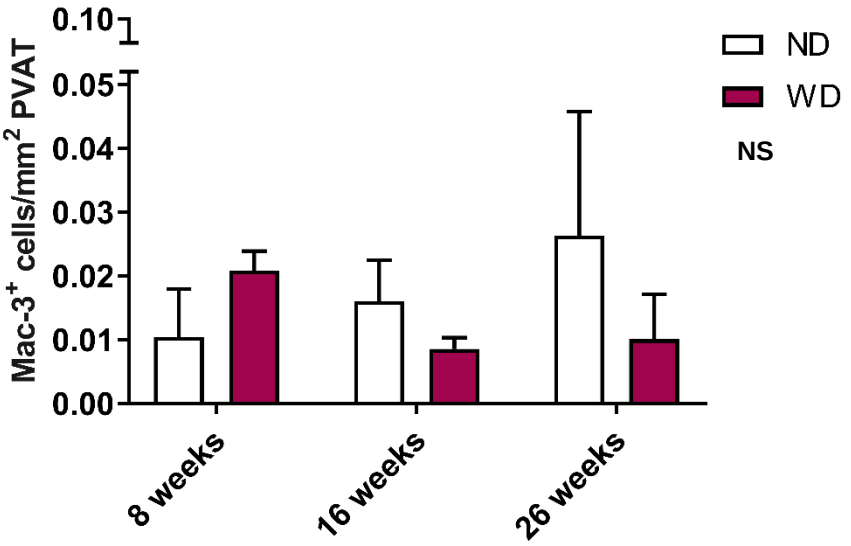

Figure 6.11 Ageing and a Western-type diet do not alter the number of infiltrating macrophages within the aortic PVAT of the ApoE$^{-/-}$Cav-1$^{-/-}$ double knockout mice

The macrophages within the aortic PVAT were quantified. No differences in macrophage number were observed with ageing or in WD-fed ApoE$^{-/-}$Cav-1$^{-/-}$ mice. Images were obtained at 10X magnification. ApoE$^{-/-}$Cav-1$^{-/-}$ (double knockout) ND = normal diet, WD = Western-type diet. Data are expressed as Mac-3^{+} cells/mm^{2} PVAT, mean ± S.E.M., n = 3-5 mice per group, two-way ANOVA with Bonferroni's post hoc multiple comparisons test.

6.5 Discussion

This study was the first to characterise the aortic PVAT composition of the ApoE$^{-/-}$Cav-1$^{-/-}$ double knockout mice and assess the influence of PVAT on isolated aortic reactivity in ageing and WD-fed mice.

The key findings of this chapter were:

- The lipid profile of ApoE$^{-/-}$Cav-1$^{-/-}$ mice was significantly more pro-atherogenic than age and diet-matched ApoE$^{-/-}$ mice. However, atherosclerotic lesion burden was significantly attenuated in WD-fed ApoE$^{-/-}$Cav-1$^{-/-}$ mice in comparison to the ApoE$^{-/-}$ mice.
- Endothelial function was retained in ND and WD-fed ApoE$^{-/-}$Cav-1$^{-/-}$ mice, despite the development of atherosclerotic lesions along the luminal surface of the aortae.
- The aortic PVAT of ApoE$^{-/-}$Cav-1$^{-/-}$ mice did not exert an anti-contractile effect on aortic rings.
- A WD did not alter the influence of aortic PVAT on vascular reactivity in ApoE$^{-/-}$Cav-1$^{-/-}$ mice.
- NOS inhibition revealed a pro-constrictor effect in PVAT from 8-week ND-fed ApoE$^{-/-}$Cav-1$^{-/-}$ mice.
- A WD induced white adipocyte hypertrophy within the aortic PVAT of ApoE$^{-/-}$Cav-1$^{-/-}$ mice.

6.5.1 Generation and maintenance of the ApoE$^{-/-}$Cav-1$^{-/-}$ double knockout colony

The generation of the ApoE$^{-/-}$Cav-1$^{-/-}$ mouse took significantly longer than expected; the length of time between the first ApoE$^{-/-}$ and Cav-1$^{-/-}$ cross and the successful generation of male experimental ApoE$^{-/-}$Cav-1$^{-/-}$ mice was approximately 18 months. Furthermore, once the ApoE$^{-/-}$ Cav-1$^{-/-}$ mouse was established, the breeding and survival rate of litters was poor. This finding is in line with those observed in the Cav-1$^{-/-}$ mice which demonstrated a diminished reproductive performance on the C57BL/6J background (Razani et al. 2001). The low weaning survival rate of male ApoE$^{-/-}$Cav-1$^{-/-}$ mice was reflected in reduced numbers for some of the following experiments. The genotypes of ApoE$^{-/-}$Cav-1$^{-/-}$ mice were verified throughout the study to ensure the veracity of the mouse strain.

6.5.2 Phenotyping of normal and Western-type diet-fed ApoE$^{-/-}$Cav-1$^{-/-}$ double knockout mice

The phenotypic characteristics of the ApoE$^{-/-}$Cav-1$^{-/-}$ mice were assessed to determine whether they displayed similar characteristics as those previously reported in the literature. As such, lipid and glucose profiles, body and organ weights and the development of atherosclerosis within the aortae were determined.

6.5.2.1 The lipid profile of normal diet-fed ApoE$^{-/-}$Cav-1$^{-/-}$ double knockout mice is markedly more pro-atherogenic compared with ApoE$^{-/-}$ mice, although no associated increase in atherosclerotic disease progression is observed

Ageing was not associated with any significant alterations in lipid or glucose measurements in ND-fed ApoE$^{-/-}$Cav-1$^{-/-}$ double knockout mice. ApoE$^{-/-}$Cav-1$^{-/-}$ mice have been observed to display a shift towards a more pro-atherogenic lipid profile than age and diet-matched ApoE$^{-/-}$ mice when fed a ND (Frank et al. 2004a; Engel et al. 2011). In line with these reports, total cholesterol and triglycerides were substantially elevated in ND-fed ApoE$^{-/-}$Cav-1$^{-/-}$ mice in comparison to age and diet-matched ApoE$^{-/-}$ and Cav-1$^{-/-}$ mice. Furthermore, whilst no changes were observed in HDL measurements between ApoE$^{-/-}$ and ApoE$^{-/-}$Cav-1$^{-/-}$ mice, in comparison to Cav-1$^{-/-}$ mice, HDL was significantly lower and these data are similar to previous reports (Engel et al. 2011).

En face lesion analysis with Oil Red O was performed along the aortic arch and thoracic aortae of the ApoE$^{-/-}$Cav-1$^{-/-}$ mice. Atherosclerotic lesions were present in each ND-fed group. However, no statistically significant increases in lesion burden were observed with ageing in these mice. Furthermore, despite the enhanced pro-atherogenic lipid profile of the ApoE$^{-/-}$Cav-1$^{-/-}$ mice, lesion burden appeared to be reduced in comparison to age and diet-matched ApoE$^{-/-}$ mice, although this was not statistically significant. These findings contrast with those observed previously. In the original study of the ApoE$^{-/-}$Cav-1$^{-/-}$ mice, atherosclerotic lesion burden was significantly reduced in comparison to ApoE$^{-/-}$ mice. However, this comparison was performed at 11 months of age and could therefore account for the observed differences (Frank et al. 2004a). An additional study in ND-fed ApoE$^{-/-}$Cav-1$^{-/-}$ and ApoE$^{-/-}$ mice, at similar ages to those used in this study, 17 and 26 weeks old, observed a significant reduction in atherosclerotic lesions in haematoxylin and eosin-stained sections of aortic arch from the ApoE$^{-/-}$Cav-1$^{-/-}$ double knockout mice at both ages (Engel et al. 2011). Moreover, the plaques of ApoE$^{-/-}$Cav-1$^{-/-}$ mice were observed to exhibit lower levels of inflammation, with fewer macrophages, neutrophils and T-cells present. The differences

between those findings and the ones reported in this present study may be a result of the different quantification methods to assess atherosclerotic lesions, with the current study assessing the presence of lesions along the aortic arch and thoracic aortae whilst the previous study focussed on one specific area. Nevertheless, these data could demonstrate that whilst no age-associated changes occur in the lipid or glucose profiles of ApoE$^{-/-}$Cav-1$^{-/-}$ mice, the strain exhibits a pro-atherogenic lipid profile due to the loss of Cav-1 and caveolae structures. Therefore, this loss could potentially limit the transcytosis of LDL into the sub-endothelial space of the vascular wall which is a key initiating step in atherogenesis (Frank et al. 2004a).

6.5.2.2 Western-type diet-fed ApoE$^{-/-}$Cav-1$^{-/-}$ double knockout mice exhibit protection against the development of atherosclerosis despite a proatherogenic lipidaemic serum profile in comparison to ApoE$^{-/-}$ mice

Maintaining the ApoE$^{-/-}$Cav-1$^{-/-}$ mice on a WD was observed to further exacerbate their pro-atherogenic lipid profile resulting in severe hypercholesterolaemia in comparison to ND-fed ApoE$^{-/-}$Cav-1$^{-/-}$ mice. Furthermore, when compared to age-matched WD-fed ApoE$^{-/-}$ mice, the ApoE$^{-/-}$Cav-1$^{-/-}$ strain showed substantially augmented cholesterol and triglyceride levels. Similar observations were recorded in the original study of the ApoE$^{-/-}$Cav-1$^{-/-}$ mice, further validating the findings of the current study (Frank et al. 2004a).

The extent of atherosclerotic disease progression within the aortae of the ApoE$^{-/-}$Cav-1$^{-/-}$ was assessed using the Oil Red O lipid stain. A WD resulted in a significant increase in lesion burden after 26 weeks of feeding in comparison to age-matched ND-fed ApoE$^{-/-}$Cav-1$^{-/-}$ mice. Subsequently, the extent of atherosclerotic disease within the aortae of ApoE$^{-/-}$Cav-1$^{-/-}$ mice was compared to the age and diet- matched ApoE strain. Strikingly, atherosclerotic lesions were substantially more prevalent in the aortae of ApoE$^{-/-}$ mice after 16 and 26-weeks of a WD in comparison to the ApoE$^{-/-}$Cav-1$^{-/-}$ mice. These data reflect the observations of previous studies of the ApoE$^{-/-}$Cav-1$^{-/-}$ mice, which demonstrated that deletion of Cav-1 conferred significant protection against the development of atherosclerosis in WD-fed mice (Frank et al. 2004a; Fernandez-Hernando et al. 2009). Furthermore, a crucial role for endothelial Cav-1 expression in the pathogenesis of atherosclerosis has been identified previously. Cav-1 was observed to promote the development of atherosclerosis when expressed specifically in the endothelium, and over-expression accelerated atherosclerotic disease progression (Fernandez-Hernando et al. 2009; Fernandez-Hernando et al. 2010). Overall, the lipid profile and athero-protected phenotype of ApoE$^{-/-}$Cav-1$^{-/-}$ mice suggests a critical role for Cav-1 in facilitating the infiltration of lipids into the wall of the artery thus, loss of Cav-1 potentially results in an attenuation of LDL transcytosis into the sub-endothelial space therefore reducing the progression and development of atherosclerosis (Fernandez-Hernando et al. 2009).

6.5.2.3 The body and organ weights of normal diet-fed ApoE$^{-/-}$Cav-1$^{-/-}$ double knockout mice are largely unaffected by increasing age; however, the mice develop cardiac hypertrophy

The ApoE$^{-/-}$Cav-1$^{-/-}$ mouse has not been extensively characterised and therefore little is known about the effect of combined ApoE and Cav-1 deletion on the organ weights. Except for an increase in body weight after 16 weeks on a ND, in comparison to the 8-week group, ageing in the ApoE$^{-/-}$Cav-1$^{-/-}$ mice did not result in any major differences between the different experimental

groups when body and organ weights were assessed. This study found that there were no differences in body weight between the ApoE$^{-/-}$Cav-1$^{-/-}$ double knockout mice and the ApoE$^{-/-}$ or Cav-1$^{-/-}$ strains after feeding a ND. In agreement with this, the original ApoE$^{-/-}$Cav-1$^{-/-}$ study observed that there were no significant differences in body weight at 11 months of age in ND-fed ApoE$^{-/-}$Cav-1$^{-/-}$ and ApoE$^{-/-}$ mice (Frank et al. 2004a).

However, when other characteristics were assessed, some differences between the ApoE$^{-/-}$Cav-1$^{-/-}$ double knockout mice and the ApoE$^{-/-}$ and Cav-1$^{-/-}$ strains were recorded. Cardiac hypertrophy was observed after 8 and 16 weeks on the ND but no differences were found after 26 weeks of feeding. These data are not surprising because Cav-1$^{-/-}$ mice have been reported to develop cardiac hypertrophy (and this was observed in Chapter 5) and in line with these findings, no differences in heart weight or heart weight: body weight ratio were observed between the ApoE$^{-/-}$ Cav-1$^{-/-}$ and Cav-1$^{-/-}$ mice (Cohen et al. 2003b; Park et al. 2003). Furthermore, whilst there were no differences in epididymal fat pad weights between age-matched ApoE and ApoE$^{-/-}$Cav-1$^{-/-}$ mice, the fat pads of ApoE$^{-/-}$Cav-1$^{-/-}$ mice were significantly smaller than Cav-1$^{-/-}$ mice after 16 weeks on a ND. However, no significant differences in epididymal adipocyte size were found between the ApoE$^{-/-}$Cav-1$^{-/-}$ and ApoE$^{-/-}$ or Cav-1$^{-/-}$ mice. These data suggest that the increased fat deposition in Cav-1$^{-/-}$ mice is due to hyperplasia, as previously reported, and that this does not occur within the epididymal fat depots of ApoE$^{-/-}$Cav-1$^{-/-}$ mice, suggesting regulation of fat depots and adipocytes is altered in these mice (Razani et al. 2001; Razani et al. 2002a).

6.5.2.4 A Western-type diet causes diet-induced weight gain, hepatomegaly and splenomegaly in the ApoE$^{-/-}$Cav-1$^{-/-}$ double knockout mice

The impact of a WD on the organ weights of ApoE$^{-/-}$Cav-1$^{-/-}$ mice has not previously been assessed. A WD resulted in diet induced weight gain, after 16 weeks of feeding, in comparison to age-matched ApoE$^{-/-}$Cav-1$^{-/-}$ mice. High fat feeding resulted in significant increases in liver and spleen weight but no changes to heart weight or heart weight: body weight ratio. Furthermore, although the epididymal fat pads of the ApoE$^{-/-}$Cav-1$^{-/-}$ mice were initially enlarged, no differences were found between ND or WD-fed ApoE$^{-/-}$Cav-1$^{-/-}$ mice at the 26-week time-point and a significant difference in adipocyte size was only observed after 16 weeks on a WD. Taken together, these data suggest that ApoE$^{-/-}$Cav-1$^{-/-}$ mice are not resistant to diet induced weight gain. However, the combined lack of ApoE$^{-/-}$ and Cav-1$^{-/-}$ appears to result in a compensatory shunting of the excess circulating lipids into other organs such as the liver and spleen. Moreover, in humans a fatty liver can develop in response to increased adiposity (Stapleton et al. 2010).

6.5.3 Vascular reactivity studies assessing the effect of aortic PVAT on vascular responses in normal diet and Western-type diet fed ApoE$^{-/-}$Cav-1$^{-/-}$ double knockout mice

Until now, the vascular reactivity of the ApoE$^{-/-}$Cav-1$^{-/-}$ mouse has not been investigated. Furthermore, the influence of PVAT on vascular responses in this mouse model is unknown thus, experiments were conducted on PVAT-intact or PVAT-denuded aortic rings to determine the effect of PVAT, age and a WD on vascular reactivity in the ApoE$^{-/-}$Cav-1$^{-/-}$ mouse.

The responses of aortic rings to a depolarising solution, KPSS, were not significantly affected by the presence of PVAT, age or a WD. Furthermore, the constrictions of aortic rings from ND-fed ApoE$^{-/-}$Cav-1$^{-/-}$ mice did not differ significantly from the responses of ApoE$^{-/-}$ or Cav-1$^{-/-}$ mice.

6.5.3.1 Endothelial function does not significantly decline in the aortae of normal or Western-type diet-fed ApoE$^{-/-}$Cav-1$^{-/-}$ double knockout mice despite the presence of atherosclerotic lesions

Endothelial dysfunction, characterised by altered NO signalling, is a risk factor for the development of atherosclerosis and is a hallmark of vascular ageing. Furthermore, hypercholesterolaemia has been demonstrated to contribute to endothelial dysfunction and promote the development of atherosclerosis in humans (Feron et al. 1999; Landmesser et al. 2004; Fu et al. 2010). Previous studies have described a decline in aortic endothelial function in ApoE$^{-/-}$ mice which was associated with hypercholesterolaemia and the development of atherosclerotic lesions (Bonthu et al. 1997; Vasquez et al. 2012). However, aortic endothelial function did not decline in ApoE$^{-/-}$ mice in this study (Chapter 4). In addition, endothelial integrity was assessed in Cav-1$^{-/-}$ mice and observed to be retained with ageing in both ND and hypercholesterolaemic WD-fed Cav-1$^{-/-}$ mice. Furthermore, endothelial function was discovered to be enhanced, similarly to previous studies, in comparison to the C57BL/6 group in PVAT-denuded aortic rings from 26 week ND-fed mice (Razani et al. 2001; Pojoga et al. 2008).

ApoE$^{-/-}$Cav-1$^{-/-}$ mice exhibit severe hypercholesterolaemia in ND and WD-fed conditions however, the mice exhibit a certain degree of protection against the development of atherosclerosis. It was therefore of significant interest to determine if the endothelial relaxation responses of ApoE$^{-/-}$Cav-1$^{-/-}$ mice were preserved with advancing age and extreme hypercholesterolaemia. Furthermore, aortic PVAT has previously been reported to promote endothelial dysfunction in atherosclerosis and in states of metabolic disturbance thus, the influence of PVAT on endothelium-independent vaso-relaxation was assessed (Gao et al. 2005; Marchesi et al. 2009; Ketonen et al. 2010; Payne et al. 2010).

Endothelial function was not altered by the presence of PVAT, increasing age or a WD in the aortic rings of ApoE$^{-/-}$Cav-1$^{-/-}$ mice. Moreover, severe hypercholesterolaemia and the presence of atherosclerotic lesions did not lead to a significant decline in relaxation responses to acetylcholine. In addition, the relaxation responses of age and diet-matched ApoE$^{-/-}$ and Cav-1$^{-/-}$ mice were compared and no significant differences were observed between the different mouse genotypes. The preserved endothelial relaxation responses of aortic rings from ND and WD-fed ApoE$^{-/-}$Cav-1$^{-/-}$ mice potentially lends further support to the argument that genetic deletion of Cav-1 confers protection against the development of atherosclerosis as a result of reduced cholesterol transcytosis into the sub-endothelial space (Everson et al. 2001; Frank et al. 2006; Sun et al. 2010).

6.5.3.2 The aortic PVAT of ApoE$^{-/-}$Cav-1$^{-/-}$ double knockout mice does not exert an anti-contractile effect

Vascular reactivity of the aortae from ApoE$^{-/-}$Cav-1$^{-/-}$ mice had not been investigated prior to the commencement of this study. Furthermore, the influence of aortic PVAT on the contractile responses of the ApoE$^{-/-}$Cav-1$^{-/-}$ mice was unknown.

The responses of PVAT-intact and PVAT-denuded aortic rings from ND-fed ApoE$^{-/-}$Cav-1$^{-/-}$ mice exhibited similar constriction in response to cumulative doses of phenylephrine, indicating that PVAT did not exert an anti-contractile effect on the aortic rings of ApoE$^{-/-}$Cav-1$^{-/-}$ double knockout

mice. Furthermore, a WD did not influence the vascular responses of PVAT-intact aortic rings. The lack of an anti-contractile effect in the ApoE$^{-/-}$Cav-1$^{-/-}$ mice is in line with the previous findings of this study, that the aortic PVAT of ND-fed ApoE$^{-/-}$ and Cav-1$^{-/-}$ mice did not exert an anti-contractile effect. Nonetheless, this study concluded that a WD did not modulate the responses of PVAT-intact aortic rings when challenged with cumulative doses of phenylephrine. These data may suggest that there are significant differences in the factors release by the PVAT of Cav-1$^{-/-}$ and ApoE$^{-/-}$Cav-1$^{-/-}$ mice in response to a WD and this requires further investigation.

In addition, when the responses of ND and WD aortic rings were compared no significant differences were observed between the PVAT-intact or PVAT-denuded- aortic rings. This data further demonstrates that a WD did not significantly alter the contractions of aortic rings from the ApoE$^{-/-}$Cav-1$^{-/-}$ mice regardless of the presence of PVAT. Both the ND and WD-fed ApoE$^{-/-}$Cav-1$^{-/-}$ mice exhibited severe hypercholesterolaemia. Previous reports have suggested that hypercholesterolaemia may augment vascular reactivity via a Cav-1 dependent mechanism (Feron et al. 1999; Grayson et al. 2013). It has been reported that in hypercholesterolaemic conditions there is increased uptake of cholesterol by endothelial cells with results in upregulation of Cav-1 expression (Feron et al. 1999). Elevated Cav-1 expression increases the number of Cav-1-eNOS inhibitory interactions and therefore hinders NO signalling within the endothelium, which in turn can result in decreased NO and potentially, an imbalance in the release of pro and anti-contractile factors within the arteries leading to increased contraction (Feron et al. 1999). If this is indeed the case, then the aortae of ApoE$^{-/-}$Cav-1$^{-/-}$ mice should be protected from hypercholesterolaemic-induced endothelial damage due to the absence of Cav-1$^{-/-}$ within the vasculature of the ApoE$^{-/-}$Cav-1$^{-/-}$ mice (Frank et al. 2004a). However, there are conflicting findings surrounding the effect of hypercholesterolaemia on the contractile responses of arteries. Furthermore, this present study demonstrated that in ApoE$^{-/-}$ mice there were no changes in aortic contraction associated with augmented hypercholesterolaemia when fed a WD. Nevertheless, both mouse models are genetically modified and exhibit hypercholesterolaemia in ND-fed conditions thus, the effect of hypercholesterolaemia on aortic contractility should be investigated in a mouse model, such as C57BL/6 mice, that does not display elevated cholesterol levels, under normal chow conditions, and subsequent hypercholesterolaemia can be induced via feeding of a WD.

The PVAT-denuded aortic rings from 8 week ND and WD-fed ApoE$^{-/-}$Cav-1$^{-/-}$ mice exhibited lower contractions than the diet-matched 16 and 26-week groups suggesting that this was an age-associated effect. To tease out the separate effects of ApoE$^{-/-}$ and Cav-1$^{-/-}$ deletion, the contractions of ND-fed ApoE$^{-/-}$Cav-1$^{-/-}$ mice were compared to age and diet matched ApoE$^{-/-}$ or Cav-1$^{-/-}$ mice.

This current study reported similar findings in PVAT-denuded aortic segments from young Cav-1$^{-/-}$ mice (a dampened vasoconstrictor response to phenylephrine) but not ApoE$^{-/-}$ mice. In the ApoE$^{-/-}$ study, it was proposed that aortic PVAT exhibited a reduced basal activity of eNOS whereas, it has been widely reported that eNOS activity and therefore NO production is enhanced in Cav-1$^{-/-}$ mice resulting in a significantly attenuated vasoconstrictor response, in previous studies and in the present investigation (Razani et al. 2001; Hausman et al. 2012; Pojoga et al.

2014). The reasons behind the altered contractility of ApoE$^{-/-}$Cav-1$^{-/-}$ mice with ageing is unclear. However, the increased aortic contractions are unlikely to be attributed to a decrease in NO, as a result of increased presence of atherosclerotic lesions within the aortae, because there were no significant differences in atherosclerotic lesion burden at these time-points and consequently, there were no alterations in endothelium-dependent vaso-relaxations.

6.5.3.3 The presence of a NOS inhibitor, L-NNA, does not augment contractions to phenylephrine in PVAT-intact or PVAT-denuded aortic rings in ApoE$^{-/-}$Cav-1$^{-/-}$ double knockout mice

Recently, evidence has been provided that rodent aortic PVAT expresses NO and is therefore a source of NO (Araujo et al. 2015; Xia et al. 2016). Therefore, the contribution of NO-mediated vaso-relaxation to phenylephrine-induced contraction of the aortic rings of the ApoE$^{-/-}$Cav-1$^{-/-}$ mice was assessed using L-NNA because of the presumed enhanced eNOS activity due to the loss of Cav-1.

In the presence of a NOS inhibitor, the aortic rings of 8-week ND-fed ApoE$^{-/-}$Cav-1$^{-/-}$ mice exhibited Cav-1$^{-/-}$-like responses; the contraction of PVAT-intact+L-NNA aortic rings was significantly enhanced compared to PVAT-denuded+L-NNA responses. This increase in contraction may have resulted from a reduction of NO bioavailability due to the inhibition of eNOS. However, NO bioavailability was not directly assessed therefore firm conclusions cannot be drawn. An increase in contraction in the presence of L-NNA was not observed in any of the other experimental groups, regardless of diet. This data could indicate that the aortic rings of ApoE$^{-/-}$Cav-1$^{-/-}$ mice, preceding the development of overt atherosclerosis (8-week ND-fed mice) have an enhanced eNOS/NO bioavailability than the other groups as part of a compensatory mechanism prior to the onset of atherosclerosis. However, this requires further investigation of NO bioavailability within the aortic PVAT and aortae. Alternatively, the PVAT from the 8-week ND-fed ApoE$^{-/-}$Cav-1$^{-/-}$ mice may have released a vaso-constricting factor although the lack of a similar response, increased vasoconstriction of PVAT in response to NOS inhibition, in the other experimental groups make this seem unlikely.

In the previous Cav-1$^{-/-}$ experiments from this study, it was suspected that the concentration of inhibitor used did not result in complete inhibition of NOS and thus, did not result in a significant increase in contraction of the aortic rings which was observed in other Cav-1$^{-/-}$ studies (Razani et al. 2001; Hausman et al. 2012; Pojoga et al. 2014). Therefore, it is possible that eNOS was not fully inhibited in the aortic rings of the ApoE$^{-/-}$Cav-1$^{-/-}$ mice indicating that some NO may have been present within the vasculature and may have continued to suppress phenylephrine-induced constrictions. Nevertheless, in the ApoE$^{-/-}$ study, NOS inhibition did not result in a significant increase in contraction of PVAT-intact or PVAT-denuded aortic rings and this was proposed to be due to a reduced basal activity of eNOS. Taken together, it is difficult to draw firm conclusions from this data without conducting further experiments to verify NOS inhibition occurred within the aortic rings of the ApoE$^{-/-}$Cav-1$^{-/-}$ mice.

The sensitivity of the aortic rings to sodium nitroprusside, a potent NO donor, was tested. The relaxation responses were similar in the presence or absence of PVAT regardless of age or diet type. Moreover, no differences were observed between age and diet-matched ApoE$^{-/-}$ and Cav-

$1^{-/-}$ mice. These findings suggest that the sensitivity of aortic rings to NO is unaltered in the ApoE$^{-/-}$Cav-1$^{-/-}$ mice and is unaffected by the development of atherosclerosis or hypercholesterolaemia. These findings are in agreement with previous studies demonstrating no change in NO sensitivity with ageing or across the different mouse genotypes used in this study (Deckert et al. 1999; Kauser et al. 2000; Ketonen et al. 2010; Pojoga et al. 2014).

6.5.4 A WD induces white adipocyte hypertrophy within the aortic PVAT of ApoE$^{-/-}$Cav-1$^{-/-}$ double knockout mice after 26 weeks of feeding; however, no associated changes in the generation of superoxide or Mac-3^{+} cells are observed

The composition of aortic PVAT from the ApoE$^{-/-}$Cav-1$^{-/-}$ mice has not previously been morphologically assessed. Therefore, the effect of increasing age and a WD on the structure of aortic PVAT was evaluated to determine if there were any overt differences between the different ApoE$^{-/-}$Cav-1$^{-/-}$ groups. Furthermore, these findings were compared to the ApoE$^{-/-}$ and Cav-1$^{-/-}$ mice to highlight any similarities or differences between the three strains which could explain the altered vascular responses between the groups.

The amount of PVAT encasing the aorta could not be assessed in the ApoE$^{-/-}$Cav-1$^{-/-}$ mice because of breeding issues within the colony and subsequent low numbers of ApoE$^{-/-}$Cav-1$^{-/-}$ mice.

6.5.4.1 A WD induces white adipocyte hypertrophy within the aortic PVAT of ApoE$^{-/-}$Cav-1$^{-/-}$ double knockout mice after 26 weeks of feeding

Alterations to the morphology of PVAT have been associated with changes in function and loss of the anti-contractile effect of PVAT (Greenstein et al. 2009; Fitzgibbons et al. 2011; Bussey et al. 2016). This study found that the amount of total aortic PVAT area occupied by white adipocytes was unchanged by ageing or a WD. A similar observation was made in the ApoE$^{-/-}$ mice whereas, in the Cav-1$^{-/-}$ strain, a WD resulted in an increase in the area occupied by white adipocytes after 16 weeks of high fat feeding.

Upon assessment of white adipocyte size, a WD was observed to induce white adipocyte hypertrophy within the aortic PVAT of the ApoE$^{-/-}$Cav-1$^{-/-}$ mice after 26 weeks on a WD, which was analogous to the observation of the aortic PVAT of Cav-1$^{-/-}$ mice. In contrast, no significant white adipocyte hypertrophy was observed in ApoE$^{-/-}$ mice. Nevertheless, the percentage area occupied by white adipocytes was similar in ND-fed ApoE$^{-/-}$Cav-1$^{-/-}$ mice, Cav-1$^{-/-}$ and the ApoE$^{-/-}$ mice and in addition, there were no significant differences in mean adipocyte area between the different groups of mice under ND conditions.

The average white adipocyte size within the aortic PVAT of the ApoE$^{-/-}$Cav-1$^{-/-}$ mice was greater than 100 µm for each experimental group, which could have resulted in the adipocytes experiencing chronic hypoxic conditions (Hosogai et al. 2007; Lee et al. 2014; Rutkowski et al. 2015).. When a cell exceeds 100 µm in size the ability of oxygen to diffuse across the cell is reduced and hypoxia followed by necrosis and apoptosis may be induced, causing a highly inflammatory environment (Hosogai et al. 2007). As stated previously, the data surrounding hypoxia and its modulation of the anti-contractile effect of PVAT is conflicting (Greenstein et al. 2009; Maenhaut et al. 2010). However, in 26-week ND-fed C57BL/6 mice and 26-week WD-fed

Cav-1$^{-/-}$ mice, white adipocyte hypertrophy and potentially hypoxic conditions was associated with PVAT causing vasoconstriction of aortic rings and exerting a pro-contractile effect. However, in age-matched WD-fed ApoE$^{-/-}$Cav-1$^{-/-}$ mice, PVAT was still unable to modulate vascular reactivity. This data could suggest that lack of ApoE$^{-/-}$ is protective and prevents the release of constricting factors or lessens the damage associated with adipocyte hypertrophy.

6.5.4.2 The aortic PVAT of ApoE$^{-/-}$Cav-1$^{-/-}$ double knockout mice does not undergo any changes in superoxide production with ageing or a Western-type diet

Elevated levels of oxidative stress through enhanced production of free radicals, such a superoxide anion, have been associated with vascular damage, and this is a risk factor for the development of CVD (Elahi et al. 2009). ApoE confers anti-inflammatory and anti-oxidant properties therefore; its loss has been linked with high basal oxidative stress in ApoE$^{-/-}$ mice (Mayr et al. 2005; Tarnus et al. 2009; Pereira et al. 2012). In addition, Cav-1$^{-/-}$ mice exhibit increased oxidative stress and superoxide production within their arteries (Wunderlich et al. 2008a; Wunderlich et al. 2008b). Therefore, superoxide production within the aortic PVAT of ApoE$^{-/-}$Cav-1$^{-/-}$ mice was assessed.

Increasing age of the ND ApoE$^{-/-}$Cav-1$^{-/-}$ mice did not result in a significant alteration of superoxide within the aortic PVAT. Surprisingly, when compared to ND ApoE$^{-/-}$ and Cav-1$^{-/-}$ mice, no significant differences were observed between the different genotypes. This suggests that deletion of ApoE$^{-/-}$ and Cav-1$^{-/-}$ does not augment thoracic PVAT-derived superoxide production. Furthermore, feeding the ApoE$^{-/-}$Cav-1$^{-/-}$ mice a WD did not result in any changes in the generation of superoxide. This is in line with the previous observations of WD-fed ApoE$^{-/-}$ and Cav-1$^{-/-}$ mice in this study. Aortic PVAT is a heterogeneous mix of white and brown adipose tissue (BAT) and whilst white adipocytes are present within thoracic PVAT, the majority of aortic PVAT is composed of BAT. BAT is a thermogenic tissue and is abundantly packed with mitochondria and upon activation, promotes thermogenesis through the dissipation of chemical energy as heat, a process facilitated by mitochondrial uncoupling protein 1 (UCP-1) (Rebiger et al. 2016). UCP-1 has been demonstrated to play a key role in modulating the oxidative status of BAT through mediating the uncoupling of oxidative phosphorylation and thus limits oxidative stress in BAT thus his may explain why superoxide production was unchanged in the aortic PVAT of the ApoE$^{-/-}$Cav-1$^{-/-}$ mice (Oelkrug et al. 2010; Rebiger et al. 2016).

6.5.4.3 The number of infiltrating Mac3^{+} cells within the aortic PVAT of ApoE$^{-/-}$Cav-1$^{-/-}$ double knockout mice is unaffected by increasing age or a WD

Previous studies have demonstrated that thoracic aortic PVAT is resistant to inflammation (Ketonen et al. 2010; Fitzgibbons et al. 2011). The population of infiltrating Mac3^{+} cells was assessed in the aortic PVAT of the ApoE$^{-/-}$Cav-1$^{-/-}$ mice and no significant differences were observed with increasing age in ND-fed ApoE$^{-/-}$Cav-1$^{-/-}$ mice. In addition, a WD and the presence of atherosclerotic lesions within the aortae did not alter the number of Mac3^{+} cells observed infiltrating the aortic PVAT. These findings agree with the observations of WD-fed Cav-1$^{-/-}$ and ApoE$^{-/-}$ mice used in this study and reports from other investigations of murine aortic PVAT (Ketonen et al. 2010; Fitzgibbons et al. 2011). However, the populations of other inflammatory

cells were not assessed and therefore it is not possible to draw firm conclusions regarding the inflammatory profile of the aortic PVAT from the ApoE$^{-/-}$Cav-1$^{-/-}$ mice.

6.6 Limitations and future experiments

A limiting factor of this study was the amount of time taken to generate the ApoE$^{-/-}$Cav-1$^{-/-}$ mouse and the subsequent poor breeding output resulting in the generation of fewer ApoE$^{-/-}$Cav-1$^{-/-}$ mice for use in experiments than required.

Although the genotype of all experimental ApoE$^{-/-}$Cav-1$^{-/-}$ mice was confirmed by PCR, Western blots confirming the absence of ApoE and Cav-1 were not performed. In previous studies, Cav-1$^{-/-}$ mice have been demonstrated to lack caveolae structures and do not express Cav-1$^{-/-}$ within the vasculature, specifically the aortic SM and adipocytes. However, due to low numbers of mice this was not confirmed in the present study thus, in future investigations of the ApoE$^{-/-}$Cav-1$^{-/-}$ mice the absence of Cav-1 and ApoE$^{-/-}$ should be confirmed by performing a Western blot on the PVAT and aortae of the mice.

The Cav-1$^{-/-}$ eNOS inhibition experiments indicated that the concentration of L-NNA, a NOS inhibitor, was too low. This may have resulted in incomplete inhibition of eNOS in the aortic preparations of the ApoE$^{-/-}$Cav-1$^{-/-}$ mice. Therefore, it would be important to determine if NO bioavailability was substantially depleted after NOS inhibition, using 50 µM L-NNA, via confocal microscopy utilising an indicator of NO. Additionally it would be interesting to repeat the myography and proposed confocal experiments using a higher concentration of L-NNA, 100 µM for example, to determine if this resulted in altered aortic contractility or diminished NO bioavailability.

Atherosclerotic lesion burden was assessed via en face lesion analysis using an Oil Red O stain. However, additional histological quantifications of lesions should be performed, for example examination of the aortic root using Elastin Van Gieson's stain, in order to verify the findings of this study, that the ApoE$^{-/-}$Cav-1$^{-/-}$ mice are athero-protected in comparison to ApoE$^{-/-}$ mice.

Although aortic PVAT has been demonstrated to be resistant to inflammation it would be of interest to perform a more detailed characterisation of the inflammatory profile of the aortic PVAT and determine if other inflammatory cells populate the aortic PVAT of the ApoE$^{-/-}$Cav-1$^{-/-}$ mice (Ketonen et al. 2010; Fitzgibbons et al. 2011).

6.7 Summary and conclusions

This present study demonstrated that when fed a WD, ApoE$^{-/-}$Cav-1$^{-/-}$ mice display an athero-protected phenotype despite a severely pro-atherogenic lipid profile. Furthermore, the aortic PVAT of ApoE$^{-/-}$Cav-1$^{-/-}$ double knockout mice did not influence vascular reactivity although the morphology of white adipocytes within the aortic PVAT was altered after extensive high fat feeding. In addition, the PVAT from 8-week ND fed ApoE$^{-/-}$Cav$^{-/-}$ mice exerted a pro-contractile effect in response to NOS inhibition however, the reason for this remains unclear. The athero-protected phenotype of ApoE$^{-/-}$Cav-1$^{-/-}$ mice has previously been proposed to be due to the reduced transcytosis of LDL into the sub-endothelial space of the vascular wall, which may provide a potential therapeutic target for the treatment or prevention of atherosclerosis.

The main findings of this chapter were:

- **The lipid profile of ApoE$^{-/-}$Cav-1$^{-/-}$ mice was significantly more pro-atherogenic than age and diet-matched ApoE$^{-/-}$ mice. However, atherosclerotic lesion burden was significantly attenuated in WD-fed ApoE$^{-/-}$Cav-1$^{-/-}$ mice in comparison to the ApoE$^{-/-}$ mice.**
- **Endothelial function was retained in ND and WD-fed ApoE$^{-/-}$Cav-1$^{-/-}$ mice, despite the development of atherosclerotic lesions along the luminal surface of the aortae.**
- **The aortic PVAT of ApoE$^{-/-}$Cav-1$^{-/-}$ mice did not exert an anti-contractile effect on aortic rings.**
- **A WD did not alter the influence of aortic PVAT on vascular reactivity in ApoE$^{-/-}$Cav-1$^{-/-}$ mice.**
- **NOS inhibition revealed a pro-constrictor effect in PVAT from 8-week ND-fed ApoE$^{-/-}$Cav-1$^{-/-}$ mice.**
- **A WD induced white adipocyte hypertrophy within the aortic PVAT of ApoE$^{-/-}$Cav-1$^{-/-}$ mice.**

~ Chapter Seven ~

General Discussion

7.1 Main findings of this thesis

Refer to Figure 7.1 and 7.2 for a schematic summary of the findings.

The effect of ageing and the role of nitric oxide in PVAT and vascular function in C57BL/6 mice:

- Endothelial function was maintained in C57BL/6 mice aged to pre-middle age whilst the anti-contractile effects of aortic perivascular adipose tissue (PVAT) were attenuated in the 26-week normal diet (ND) -fed C57BL/6 mice.
- Nitric oxide synthase (NOS) inhibition revealed that nitric oxide (NO) mediated the anti-contractile effect of PVAT in the 8 and 16-week ND-fed groups however, NOS inhibition had no effect in the 26-week ND group, which may be indicative of a decrease in PVAT-derived NO.
- The morphology of aortic PVAT was altered with increasing age; an increase in the weight of PVAT surrounding the aortae in combination with white adipocyte hypertrophy and increased superoxide production and an altered adipokine profile may have contributed to the loss of the anti-contractile effect of PVAT in the 26-week ND cohort.

The effect of ageing, a Western-type diet and the contribution of nitric oxide to the function of PVAT in atherosclerotic ApoE$^{-/-}$ mice:

- Endothelial dysfunction was not observed in the aortae of ND or Western-type diet (WD) -fed ApoE$^{-/-}$ mice despite the presence of atherosclerotic lesions along the luminal surface of the aortae.
- The aortic PVAT of ApoE$^{-/-}$ mice was dysfunctional and did not exert an anti-contractile effect on aortic rings; this was potentially due to decreased basal endothelial NOS (eNOS) activity resulting in an attenuation of PVAT-derived NO.
- Feeding the ApoE$^{-/-}$ mice a WD did not alter the vascular reactivity of aortic PVAT.
- The aortic PVAT of ApoE$^{-/-}$ mice exhibited an aged phenotype when assessed morphologically.

The influence of nitric oxide and PVAT on vascular function in ageing and Western-type diet-fed athero-resistant Cav-1$^{-/-}$ mice

- The aortic PVAT of Cav-1$^{-/-}$ mice did not exert an anti-contractile effect on isolated aortic rings.

- The aortic PVAT of Cav-1$^{-/-}$ mice fed a WD for 26 weeks exerted a pro-contractile effect on isolated aortic rings and this was associated with white adipocyte hypertrophy within the aortic PVAT.
- In the presence of the NOS inhibitor, L-NNA, the aortic PVAT of Cav-1$^{-/-}$ mice exerted a pro-contractile effect on aortic ring preparations.
- Extensive feeding of a WD induced white adipocyte hypertrophy within the aortic PVAT of Cav-1$^{-/-}$ mice.

The effect of ageing, a Western-type diet and nitric oxide on PVAT and vascular function in athero-protected ApoE$^{-/-}$Cav-1$^{-/-}$ mice

- The lipid profile of ApoE$^{-/-}$Cav-1$^{-/-}$ mice was significantly more pro-atherogenic than age and diet-matched ApoE$^{-/-}$ mice. However, atherosclerotic lesion burden was significantly attenuated in WD-fed ApoE$^{-/-}$Cav-1$^{-/-}$ mice in comparison to the ApoE$^{-/-}$ mice.
- Endothelial function was retained in ND and WD-fed ApoE$^{-/-}$Cav-1$^{-/-}$ mice, despite the development of atherosclerotic lesions along the luminal surface of the aortae.
- The PVAT of ApoE$^{-/-}$Cav-1$^{-/-}$ mice did not exert an anti-contractile effect on aortic rings.
- A WD did not alter the influence of aortic PVAT on vascular reactivity in ApoE$^{-/-}$Cav-1$^{-/-}$ mice.
- NOS inhibition revealed a pro-contractile effect in PVAT from 8-week ND-fed ApoE$^{-/-}$Cav-1$^{-/-}$ mice.
- A WD induced white adipocyte hypertrophy within the aortic PVAT of ApoE$^{-/-}$Cav-1$^{-/-}$ mice.

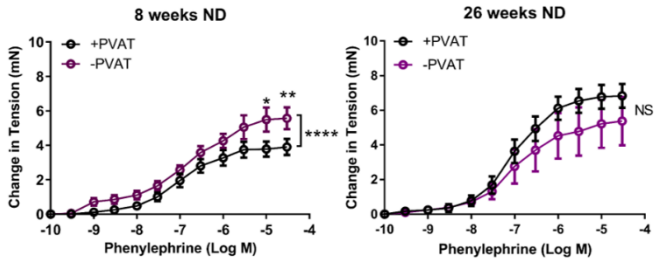

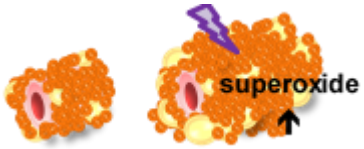

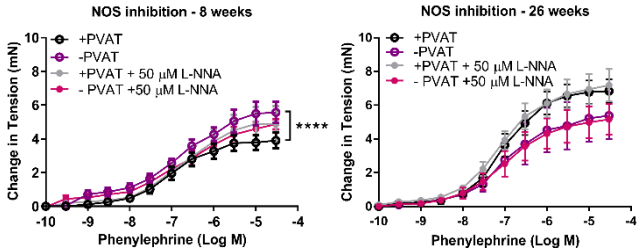

PVAT dysfunction in pre-middle aged mice was associated with increased aortic PVAT weight, white adipocyte hypertrophy, increased superoxide and altered adipokine profile.

Aortic PVAT exerted an anti-contractile effect in young C57BL/6 mice. This effect was lost with ageing.

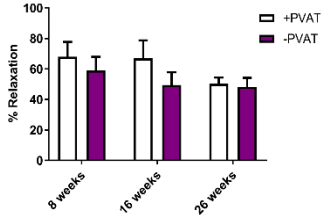

PVAT dysfunction preceded endothelium dysfunction and therefore could be used as an early indicator of cardiovascular disease. PVAT did not modulate endothelium-dependent relaxation.

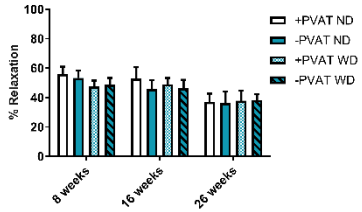

Endothelium-dependent relaxations did not decline with age or a WD. The presence of PVAT did not alter relaxation responses.

PVAT was dysfunctional and had an 'aged' phenotype that was unaffected by diet.

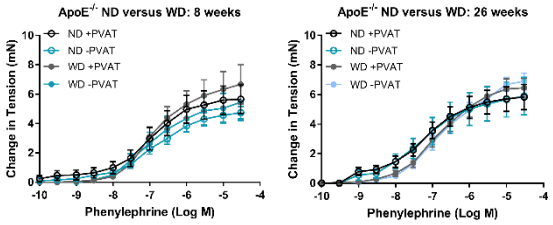

Summary of key findings

NOS inhibition experiments in young C57BL/6 mice abolished the anti-contractile effect of PVAT in young C57BL/6 mice indicating that PVAT-derived NO mediates the anti-contractile effect of aortic PVAT. NOS inhibition had no effect in pre-middle age mice indicating diminished PVAT-derived NO bioavailability

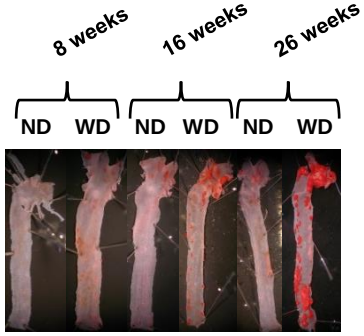

Atherosclerotic lesion development was accelerated within the aortae of WD-fed mice.

NOS inhibition had no effect on aortic ring contractility with or without PVAT and this was attributed to reduced basal eNOS activity.

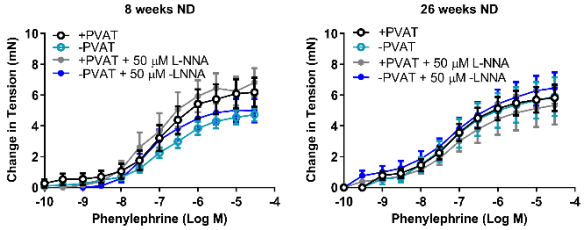

The amount of PVAT surrounding the aortae did not alter with age or a WD nor did the population or mean size of the white adipocytes within the PVAT.

Figure 7.12 Summary of key findings in C57BL/6 and ApoE$^{-/-}$ mice

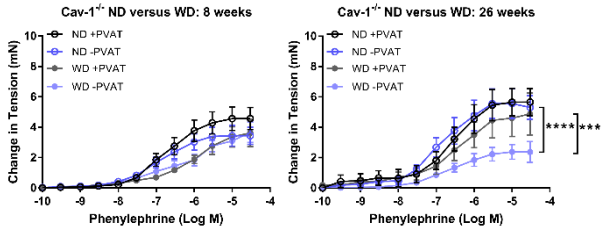

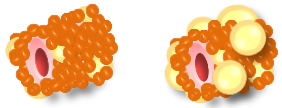

White adipocytes within the PVAT of 26 week WD-fed mice were significantly enlarged compared to ND mice. Also, this was observed in the ApoE$^{-/-}$Cav-1$^{-/-}$ mice

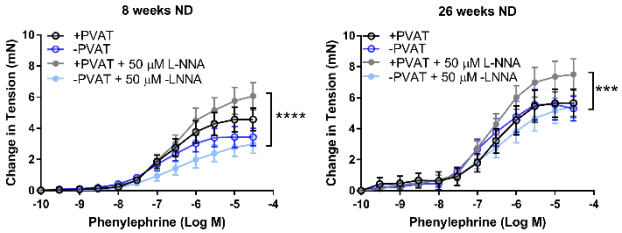

PVAT did not exert an anti-contractile effect this may have been due to dampened vasoconstrictor responses of PVAT-denuded aortic rings preventing further modulation of relaxation or, the release of a contracting factor opposing the effect of excess NO. Aortic PVAT exerted a pro-contractile effect after 26 weeks on a WD and this was associated with white adipocyte hypertrophy

Cav-1$^{-/-}$

NOS inhibition revealed a pro-contractile effect of PVAT which may indicate the release of a PVAT-derived constricting factor.

Atherosclerotic lesions did not form within the aorta.

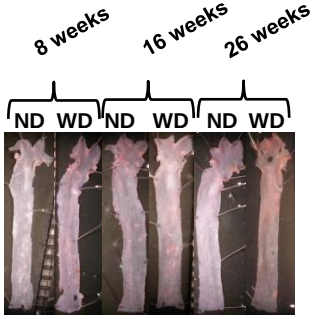

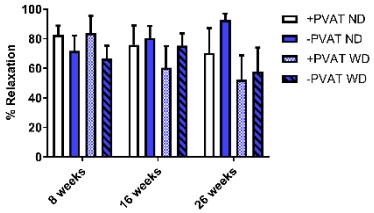

PVAT did not modulate endothelium-dependent relaxations and no significant changes in were observed with ageing or a WD.

Summary of key findings

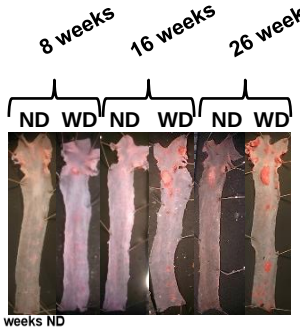

Atherosclerotic lesion burden was reduced in 5 and 7 ½ month old WD-fed mice compared to ApoE$^{-/-}$ mice.

ApoE$^{-/-}$Cav-1$^{-/-}$

PVAT did not modulate vascular reactivity with ageing or a WD.

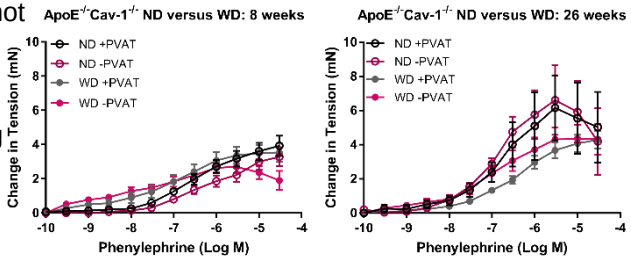

Endothelium-dependent relaxations were unchanged with ageing or a WD and PVAT did not modulate relaxation responses

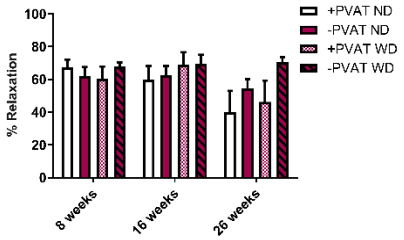

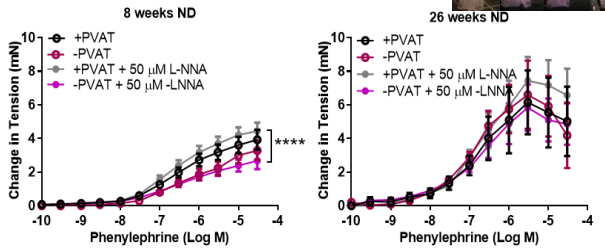

NOS inhibition revealed a Cav-1$^{-/-}$-like response in the 8 week ND-fed group, which may suggest enhanced eNOS activity prior to the onset of overt atherosclerosis. However, no effects of NOS inhibition were observed in the rest of the groups, similar to the ApoE$^{-/-}$ responses.

Figure 7.2 Summary of key findings from Cav-1$^{-/-}$ and ApoE$^{-/-}$Cav-1$^{-/-}$ mice

7.2 Summary of the main findings of this thesis and future directions

7.2.1 Nitric oxide mediates the anti-contractile effect of aortic PVAT in young C57BL/6 mice, but this is attenuated with ageing to pre-middle age and this is potentially due to a decrease in PVAT-derived NO bioavailability and alterations to PVAT composition

The data in this thesis indicate that NO within the thoracic aortic PVAT of C57BL/6 mice is a key mediator of the anti-contractile effect of PVAT, as inhibition of NOS attenuated the anti-contractile influence of PVAT in the 8 and 16-week ND fed mice. However, this anti-contractile effect of aortic PVAT was abolished in ageing C57BL/6 mice and was attributed to a loss of PVAT-derived NO bioavailability, as NOS inhibition no longer influenced aortic preparations from mice of this age group. Similar findings have been observed in the small arteries of humans and rodents, where inhibition of NOS diminished the anti-contractile effect of PVAT although this was absent in states of diet-induced weight gain (Greenstein et al. 2009; Gil-Ortega et al. 2010; Lynch et al. 2013; Bussey et al. 2016; Zaborska et al. 2016). Additionally, eNOS and NO in PVAT have been demonstrated to be substantially downregulated in diet-induced weight gain, with C57BL/6 mice fed a high fat diet for 32 weeks exhibiting undetectable levels in mesenteric PVAT (Fernández-Alfonso et al. 2013). This study did not investigate the mechanism of action of aortic PVAT-derived NO on the aortic SM. Nevertheless, it has been demonstrated previously that NO modulates vasoconstriction of vascular SM predominantly through stimulating sGC to cGMP and activates protein kinase G, which subsequently stimulates the re-uptake of cytosolic Ca^{2+} into the sarcoplasmic reticulum and the opening of Ca^{2+}-activated K^+ channels resulting in relaxation of SM (Furchgott and Vanhoutte 1989; Carvajal et al. 2000; Derbyshire and Marletta 2012; Zhao et al. 2015). Furthermore, a role for the activation of protein kinase G in the anti-contractile effect of murine PVAT has recently elucidated (Withers et al. 2014).

In the present study, the altered influence of aortic PVAT on the vasculature was associated with an increased amount of aortic PVAT, white adipocyte hypertrophy, increased superoxide production and an altered adipokine profile. Furthermore, NOS inhibition experiments indicated that PVAT-derived NO bioavailability may have been diminished in the ageing C57BL/6 mice. Together, these changes may have promoted the observed age-associated aortic PVAT dysfunction. These findings agree with previous studies which clearly demonstrated a link between an overabundance of PVAT with altered vascular reactivity in ageing and obese mice and a greater cardiovascular (CVD) risk in humans (Ketonen et al. 2010; Britton et al. 2012; Szasz 2012). Furthermore, the loss of the anti-contractile effect of PVAT has been linked to decreases in PVAT-derived NO bioavailability in humans and rodent models (Gao et al. 2007b; Greenstein et al. 2009; Zaborska et al. 2016).

This study demonstrated that the ageing C57BL/6 mice exhibited a greater percentage area of PVAT occupied of white adipocytes within the aortic PVAT and these adipocytes were enlarged. Also, similar findings in much older mice have been recorded (Bailey-Downs et al. 2013). Furthermore, the size of the white adipocytes indicated that they could have been under chronic hypoxic conditions due to exceeding the oxygen diffusion limit which can lead to hypoxia, necrosis, and an inflammatory environment (Hosogai et al. 2007; Lee et al. 2014; Rutkowski et al. 2015). Intriguingly, these alterations to the influence and morphology of aortic PVAT occurred

prior to endothelial dysfunction or dyslipidaemia, which has long been used as an indicator of cardiovascular health.

These findings pose two main questions for future research. Firstly, do the findings in ageing C57BL/6 mice translate to those observed in vivo in humans? If normal vascular ageing induces a loss of the net beneficial anti-contractile capacity of PVAT in humans, imaging of sites such as the coronary artery, to assess the amount of PVAT, or as referred to in humans at this site, epicardial adipose tissue (EAT), surrounding the artery could be important for determining if detrimental changes are present within the fat. An increase in the amount of EAT could be used as an early indicator of increase CV risk. Currently, echocardiography, CT and MRI have been used to assess EAT thickness in humans and a link between larger quantities of EAT encasing the coronary arteries has been linked to increased CVD incidence (Britton et al. 2012; Fitzgibbons et al. 2014). Furthermore, diet, exercise and gastric bypass have been demonstrated to decrease visceral and epicardial fat mass and could have potentially improved the function of EAT with regards to vascular reactivity as an added a side-effect (Willens et al. 2007; Iacobellis et al. 2008; Kim et al. 2009; Fitzgibbons and Czech 2014). However, there is conflicting evidence concerning the morphology of the EAT surrounding human coronary arteries, with some studies finding brown adipose tissue characteristics and others a white adipose tissue profile (Chatterjee et al. 2009; Sacks et al. 2009; Miao and Li 2012).

Functional or histological assessment of human arteries to determine if PVAT undergoes similar age-related changes, such as a loss of anti-contractile capacity, adipocyte hypertrophy, increased superoxide production and altered adipokine profile, as observed in the ageing C57BL/6 mice, would be of interest. However, collecting human arteries for PVAT studies is understandably difficult. The internal thoracic artery is one of the most accessible human arteries and is obtained during coronary artery bypass graft operations (Gao et al. 2005; Malinowski et al. 2008). Also, in relation to the findings of this study, it is the most clinically relevant as it has been demonstrated to exert an anti-contractile effect ex vivo in response to various agonists including phenylephrine (Gao et al. 2005). Furthermore, additional studies demonstrated that the PVAT of the internal thoracic artery and not adipose tissue in general, i.e. fat derived from another fat depot, elicited the anti-contractile effect of PVAT through the release of vasoactive factors and adipokines, as pleural fat had no effect on vascular reactivity (Malinowski et al. 2008). However, in contrast to this study, the anti-contractile effect of PVAT from the internal thoracic artery was determined to occur through two discrete mechanisms via an endothelium-dependent pathway involving NO release and subsequent K_{Ca} channel activation but also by a NO-independent pathway involving hydrogen peroxide (H_2O_2) (Gao et al. 2005; Gao et al. 2007b; Malinowski et al. 2008).

If similar alterations occurred in the PVAT of humans, as observed in ageing mice in this study, this raises the second important question, can the age-associated changes in PVAT morphology and vascular reactivity be reversed? As stated previously, diet, exercise and gastric bypass have been proven to decrease visceral and epicardial fat mass (Willens et al. 2007; Iacobellis et al. 2008; Kim et al. 2009; Fitzgibbons and Czech 2014). These findings may translate to other PVAT depots. The current study demonstrated that the aortic PVAT of ageing C57BL/6 mice displayed white adipocyte hypertrophy. However, adipose tissue is known to exhibit plasticity, to a certain

extent, and it is possible that white adipocyte hypertrophy, which may have contributed to the PVAT dysfunction observed, may be reversible. Previous studies in rodents have demonstrated that exercise can lead to the 'browning' of white adipocytes within aortic PVAT and led to increased eNOS expression and NO production (Araujo et al. 2015; DeVallance et al. 2016). However, a period of exercise training over 8 weeks was not sufficient to alter the anti-contractile capacity of PVAT in rat aortic preparations. In addition, PVAT-derived adipokine profiles were unchanged although a reduction in PVAT amount was observed (Araujo et al. 2015). Furthermore, studies on the left circumflex coronary artery in swine demonstrated no effect of exercise on PVAT function (Bunker and Laughlin 2010). Nevertheless, the effect of exercise on the influence of PVAT on vascular function in humans has not yet been assessed and its potential therapeutic effects remain to be seen. Alternative approaches such as cold exposure and pharmacological targeting of brown adipose tissue are currently under investigation. Therapeutic 'browning' of adipose tissue may be a potential method to rescue PVAT function and reverse the effects of white adipocyte hypertrophy observed in PVAT with ageing, diet-induced weight gain and other CVD in humans (Cypess et al. 2012; Kiefer et al. ; Sharp et al. 2012; Wu et al. 2012; Park et al. 2014).

In conjunction with the observed morphological and compositional changes within the aortic PVAT of pre-middle aged C57BL/6 mice, NOS inhibition experiments indicated a reduction in PVAT-derived NO in the ageing C57BL/6 mice and this may have contributed to the loss of the anti-contractile effect of PVAT. This finding may reveal eNOS and NO as a potential therapeutic target for the restoration of the PVAT effect. Specific targeting of the NO pathway in order to maintain or restore PVAT anti-contractile function could potentially reduce CVD incidence, as diminished NO bioavailability is a key factor in the pathogenesis of many CVDs. Current mainstream therapeutic strategies in the treatment of reduced NO bioavailability involve the use of NO donors and agents to increase NO bioactivity in vivo (Lundberg et al. 2015). However, a better understanding of NO signalling may lead to therapies which can enhance eNOS activity in vivo and limit the reaction of NO with ROS in the vasculature and thus maintain PVAT and endothelium function.

7.2.2 The aortic PVAT of ApoE$^{-/-}$ mice does not exert an anti-contractile effect which may be due to reduced basal eNOS activity and an aged PVAT phenotype

In this study the aortic PVAT of ageing ND and WD-fed ApoE$^{-/-}$ mice was assessed for the first time. Aortic PVAT was not shown to alter vascular reactivity and did not exert an anti-contractile effect in the early or later stages of atherosclerosis. However, in comparison to healthy C57BL/6 mice, the contractile responses of PVAT-intact aortic rings in the 8 and 16-week ND ApoE$^{-/-}$ mice was augmented in comparison to the age and diet matched C57BL/6 strain, which indicated a dysfunction of the PVAT. Additionally, a WD did not have an impact on vascular responses. The PVAT dysfunction in the ApoE$^{-/-}$ mice could potentially be attributed to reduced basal eNOS activity in comparison to C57BL/6 mice, as NOS inhibition had no effect on the ApoE$^{-/-}$ aortic preparations. However, this needs to be explored further and eNOS activity and NO bioavailability experiments performed on the aortae and its PVAT in order to verify or refute this assertion.

In addition to vascular reactivity studies, the morphology of aortic PVAT from ApoE$^{-/-}$ mice was assessed and found to be unchanged with ageing or a WD. However, the aortic PVAT of ApoE$^{-/-}$ mice appeared to differ to that of the C57BL/6 strain. Ageing and a WD did not alter the weight of PVAT encasing the aortae of ApoE$^{-/-}$ mice whereas in the C57BL/6 study, PVAT amount increased significantly with age. In addition, studies of C57BL/6 mice have clearly demonstrated high fat feeding results in an increase in PVAT amount and a loss of the anti-contractile capacity (Ketonen et al. 2010). Although not statistically significant, the area occupied by white adipocytes within the aortic PVAT of ApoE$^{-/-}$ mice, and indeed the size of the white adipocytes themselves were initially greater than age-matched C57BL/6 mice. The enlarged white adipocyte size within the aortic PVAT of the ApoE$^{-/-}$ mice may have contributed to a hypoxic environment and therefore contributed to the lack of an anti-contractile effect of the PVAT from ApoE$^{-/-}$ mice. Furthermore, superoxide production was substantially elevated in the younger ApoE$^{-/-}$ mice in comparison to the C57BL/6 strain. Taken together, this data may indicate that the morphology and oxidative status of aortic PVAT from ApoE$^{-/-}$ mice contributes to the observed PVAT dysfunction, as these characteristics, increased white adipocyte size and superoxide, were observed in the ageing C57BL/6 mice when age-associated PVAT dysfunction occurred. Furthermore, previous studies in high fat-fed C57BL/6 mice have demonstrated that changes to PVAT composition, such as increases in white adipocyte number and adipocyte hypertrophy (as observed from the outset in the aortic PVAT of ApoE$^{-/-}$ mice) results in a decrease in PVAT-derived NO bioavailability (Xia et al. 2016).

The ApoE$^{-/-}$ mouse is a model of atherosclerosis and ageing and as such, it would be interesting to assess NO bioavailability and eNOS activity in the PVAT of humans in close proximity to atherosclerotic plaques to determine if the characteristics of PVAT from ApoE$^{-/-}$ mice, e.g. decreased NO, increased white adipocyte hypertrophy and enhanced superoxide production, are observed in humans. In addition, investigations using samples of arteries from humans where atherosclerotic lesions are present, and determining if PVAT could modulate vascular reactivity and exert an anti-contractile effect would be of interest. Furthermore, if NO bioavailability and eNOS activity were found to be reduced in the PVAT surrounding atherosclerotic lesions, current treatments such as statins, and therapies aimed at increasing NO production in vivo could potentially restore PVAT function and prevent further development of atherosclerosis.

However, significant differences between the findings of this study and that of PVAT and atherosclerosis in humans were observed. The aortic PVAT of ApoE$^{-/-}$ mice was observed to be resistant to the effects of diet induced weight gain and no significant increases in Mac-3^{+} macrophage infiltration were observed in the aortic PVAT. This is not representative of the human condition. A recent theory of ‘outside-in’, regarding vascular inflammation suggests that inflammation within PVAT could promote atherosclerosis. This hypothesis suggests that inflammation originates in the adipose tissue surrounding the vasculature and spreads inward towards the artery wall; this was supported by immunostaining of human atherosclerotic aortae demonstrating inflammatory macrophages and T cells at the junction of PVAT and adventitia (Henrichot et al. 2005; Maiellaro et al. 2007; Britton et al. 2011). Previous studies have demonstrated that atherosclerotic plaques develop predominantly within epicardial coronary

arteries that are surrounded by PVAT and this fat depot expands with increasing adiposity (Montani et al. 2004; Sarin et al. 2008; Payne et al. 2012). Furthermore, atherosclerotic burden has been associated with the amount of epicardial PVAT surrounding the artery (Greif et al. 2009; Mahabadi et al. 2010; Wang et al. 2010; Verhagen et al. 2012). However, although several atherosclerotic lesions were present in the aortae of ApoE$^{-/-}$ mice, no significant increases in the amount of PVAT surrounding the aortae were observed, demonstrating that the aortic PVAT of ApoE$^{-/-}$ mice is resistant to diet-induced weight gain a finding that is not observed in humans.

7.2.3 The aortic PVAT of Cav-1$^{-/-}$ mice does not exert an anti-contractile effect

The studies of aortic PVAT in C57BL/6 mice indicated that PVAT-derived NO played an important role in mediating the anti-contractile effect of PVAT. Therefore, the effect of excess NO production in the aortic PVAT of Cav-1$^{-/-}$ mice was assessed and, surprisingly, the aortic PVAT of Cav-1$^{-/-}$ was not observed to exert an anti-contractile effect (Razani et al. 2001). The lack of an anti-contractile effect could potentially be due to the observed dampened contractile responses of PVAT-denuded aortic rings. Potentially, the reduced contraction of the aortae of the Cav-1$^{-/-}$ mice prevented any further modulation by aortic PVAT in these mice thus preventing an anti-contractile effect of PVAT from being revealed. However, loss of Cav-1 within the vasculature of Cav-1$^{-/-}$ mice may have led to compensatory mechanisms and the release of vaso-constricting factors. This theory is supported by the finding that after 26 weeks on a WD, the PVAT of Cav-1$^{-/-}$ mice significantly augmented contractile responses to phenylephrine, suggesting the release of a PVAT-derived constricting factor and this was observed in conjunction with white adipocyte hypertrophy. This finding is in line with other studies of large arteries which have demonstrated that PVAT can exert vaso-constricting factors and these have been identified in states of health and disease (Chang et al. 2012b; Meyer et al. 2013; Villacorta and Chang 2015).

Furthermore, after incubation with the NOS inhibitor, L-NNA, PVAT-intact aortic rings were demonstrated to exert pro-contractile effects on aortic preparations (with the exception of the 8-week WD-fed group) and this reinforces the idea that the aortic PVAT of Cav-1$^{-/-}$ mice releases a vaso-constricting factor but its effect is masked by PVAT-derived NO. Inhibition of eNOS may have resulted in diminished NO bioavailability, and therefore disrupted the balance between PVAT-derived NO and the constricting factor, enabling the vaso-constricting factor to modulate aortic contractions.

Superoxide production was assessed within the aortic PVAT of Cav-1$^{-/-}$ mice and although no changes were observed with ageing or a WD, significant differences in superoxide production were observed in comparison to C57BL/6 mice. Superoxide was elevated in 8-week ND-fed Cav-1$^{-/-}$ mice in comparison to age matched C57BL/6 mice and may indicate some dysfunction of the PVAT of Cav-1$^{-/-}$ mice. This is supported by findings that augmented ROS production within PVAT resulted in a loss of the PVAT anti-contractile effect (Greenstein et al. 2009; Marchesi et al. 2009).

It would be interesting to observe the effects of excess NO production in another mouse model, for example a transgenic mouse globally over-expressing eNOS, or targeted overexpression within aortic PVAT to determine if the aortic PVAT exerts an anti-contractile effect or responds in a similar fashion to the Cav-1$^{-/-}$ mice. Transgenic mice overexpressing eNOS within the vascular wall display attenuated vasoconstrictor responses and are hypotensive which has been attributed

to elevated basal NO within the vasculature (Ohashi et al. 1998). In addition, another line of transgenic mice overexpressing eNOS demonstrated a two-fold increase in eNOS within epididymal adipose tissue and a six-fold increase in the aorta (Sansbury et al. 2012). Moreover, enhanced eNOS overexpression was demonstrated to prevent diet-induced weight gain and hyperinsulinaemia and increased metabolic activity was observed in the adipose tissue (Sansbury et al. 2012). However, enhanced NO production within the aortae of the Cav-1 mice was not directly confirmed therefore additional experiments are required to determine the nature of eNOS activity, NO bioavailability and the contribution of NO to the vascular reactivity of PVAT and the aortae of Cav-1$^{-/-}$ mice.

7.2.4 Western-type diet fed ApoE$^{-/-}$Cav-1$^{-/-}$ double knockout mice exhibit an athero-protected phenotype; however, aortic PVAT from these mice does not modulate vascular reactivity

The aortic PVAT of ApoE$^{-/-}$Cav-1$^{-/-}$ double knockout mice did not modulate vascular reactivity. Furthermore, a WD did not alter the contractile responses of PVAT. However, white adipocyte hypertrophy was observed after 26 weeks of high at feeding and a link between adipocyte hypertrophy and PVAT dysfunction has been extensively reported on. In Cav-1$^{-/-}$ mice, white adipocyte hypertrophy was associated with PVAT exerting a pro-contractile effect although no change in contractility were observed in ApoE$^{-/-}$Cav-1$^{-/-}$ mice. This potentially suggests that there are fundamental differences in the secretion profiles of Cav-1$^{-/-}$ and ApoE$^{-/-}$Cav-1$^{-/-}$ mice in response to a WD and this requires further investigation.

A contributing factor to the absence of an anti-contractile effect in the PVAT of ApoE$^{-/-}$Cav-1$^{-/-}$ mice may have been that it appears to display an aged phenotype from the outset, with enlarged white adipocytes (greater than 100 µm in each group) and elevated superoxide production (Hosogai et al. 2007; Lee et al. 2014; Rutkowski et al. 2015). The aortic PVAT of ApoE$^{-/-}$Cav-1$^{-/-}$ mice may have been exposed to chronic hypoxic conditions due to the enlarge white adipocytes which could have prevented the aortic PVAT from exerting an anti-contractile effect as reported in other studies (Greenstein et al. 2009).

In the presence of the NOS inhibitor L-NNA, the aortic PVAT of 8-week ND-fed ApoE$^{-/-}$Cav-1$^{-/-}$ mice exerted a pro-contractile effect (as observed in the PVAT of NOS-inhibited Cav-1$^{-/-}$ mice) although this effect was not replicated in any of the other experimental groups. The increased contraction may suggest the release of a vaso-constricting factor by the PVAT. On the other hand, it may suggest enhanced eNOS activity at this time-point and may have been a consequence of a compensatory mechanism prior to the development of overt atherosclerosis. Altered vaso-relaxation responses have been reported in ApoE$^{-/-}$ mice prior to the development of atherosclerosis as a result of altered Ca^{2+} handling and the release of COX-2-derived products and these were attributed to a compensatory mechanism to counteract the effects of a dysfunctional endothelium (Cobb C. 2013; Ewart et al. 2014). However, this requires further investigation of eNOS activity/NO bioavailability within the aortic PVAT and aortae.

It has been suggested that excess NO production within the aortae of ApoE$^{-/-}$Cav-1$^{-/-}$ mice, due to the loss of the inhibitory Cav-1-eNOS complex, contributes to its atheroprotected phenotype (Le Lay and Kurzchalia 2005). However, eNOS activity and NO bioavailability were not directly

assessed in this study and therefore further investigation, through Western blot, Griess reagent assay or confocal microscopy, is required in order to fully evaluate eNOS activity, NO bioavailability and the influence of NO on vascular reactivity within the aortae and aortic PVAT of Cav-1$^{-/-}$ mice.

Despite the fact that atherosclerosis is a major factor in the development of coronary artery disease, most treatments are aimed at mechanically opening occluded vessels or bypassing established plaques. Although atherosclerotic lesions have been recorded within the vasculature in the first couple of decades of life, therapies aimed at preventing the initiation and very early development of atherosclerosis are limited (Piepoli et al. 2016). Current statin treatments have been demonstrated to halt or indeed possibly reverse atherosclerosis in the middle-aged and elderly population (Smilde et al. 2001; Nissen et al. 2004; Taylor et al. 2004; Steinberg 2010). However, a genetic predisposition to low LDL cholesterol levels appears to confer greater protection against coronary heart disease (Cohen et al. 2006). These data suggest that over a lifetime, therapeutically lowering LDL may be more effective against the development of CVD then targeting LDL later in life (Lloyd-Jones et al. 2003; Forrester 2010; Steinberg 2010). The Coronary Artery Risk Development in Young Adults study (CARDIA) demonstrated that in young adults, ranging in age from 18 to 30 years of age, even slightly augmented cholesterol levels resulted in damage to the coronary arteries and increased the likelihood of the development of coronary artery calcification and atherosclerosis (Pletcher et al. 2010). Additional research by the Framingham Offspring study suggests that lowering LDL-cholesterol within the young adult population could reduce the incidence of CVD in later life (Pletcher et al. 2016). However, much remains unclear about the long term beneficial effects of prophylactic statin treatment.

Although beyond the remit of this thesis, the athero-protected phenotype of the ApoE$^{-/-}$Cav-1$^{-/-}$ double knockout mice requires further investigation. The prevailing theory of how lack of Cav-1 confers protection in this strain is that a key initiating step in atherosclerosis, the transcytosis of LDL into the sub-endothelial space, is impaired in this mouse (Frank et al. 2004a; Frank et al. 2006; Fernandez-Hernando et al. 2009; Fernandez-Hernando et al. 2010; Engel et al. 2011). Therefore, experiments investigating LDL transcytosis in the ApoE$^{-/-}$Cav-1$^{-/-}$ double knockout mice should be performed as the information obtained from these experiments could provide potential therapeutic targets for the treatment and prevention of atherosclerosis.

Looking forward, the role of endothelial Cav-1 in LDL transcytosis into the sub-endothelial space and endothelial cell activation may provide potential therapeutic targets. Modification of LDL in vivo to prevent its binding with Cav-1 and subsequent transcytosis into the vascular wall could present a way of reducing atherosclerosis in humans. However, this would be a considerable undertaking due to the important role of native LDL in the body and potential side effects. Alternatively, the therapeutic application of a drug-eluting stent to locally inhibit Cav-1 at sites prone to atherosclerosis could offer another potential treatment. Local and targeted inhibition of Cav-1 could have the benefit of increasing eNOS activity and NO bioavailability, which are proven to be decreased in atherosclerosis, and could theoretically limit oxidised LDL transcytosis into the

artery wall thus, protecting against the development or progression of atherosclerosis. However, possible unwanted side-effects may occur as previously stated, cell-specific Cav-1 has been demonstrated to exert both anti or pro-atherogenic effect (Frank et al. 2004a; Frank and Lisanti 2004b; Le Lay and Kurzchalia 2005; Frank et al. 2006; Sedding et al. 2006; Fernandez-Hernando et al. 2009; Fernandez-Hernando et al. 2010; Fu et al. 2010; Pavlides et al. 2014).

7.3 Limitations

7.3.1 The clinical relevance of animal models

Although studies in humans provide invaluable understanding of human physiology and the mechanisms behind the pathogenesis and progression of disease, there are numerous limitations associated with the use of human tissue. The influence of lifestyle, diet, comorbidities and the availability of appropriate tissue samples necessitates the use of animal models. Furthermore, access to human arteries that are undergoing atherogenesis is difficult. The complex nature of atherogenesis has necessitated the use of a range of animal models including transgenic mice, rabbits, pigs and non-human primates.(Getz and Reardon 2012) This is primarily due to the ease with which the confounding effects of diet and environmental factors can be controlled and the shorter life-spans of the animals, allowing evaluation for the duration of the animal's life cycle (Leong et al. 2015). The use of an inbred mouse strain, C57BL/6 mice, and genetically modified ApoE$^{-/-}$, Cav-1$^{-/-}$ and ApoE$^{-/-}$Cav-1$^{-/-}$ mice used in the present study presented significant advantages due to the controlled environment the mice were housed in and a presumed lack of genetic variation within each mouse strain.

As previously described, the study of healthy ageing in humans is often complicated by the presence of CVDs such as atherosclerosis and other comorbidities, which can make extricating the direct effects of ageing on the vasculature challenging. Nevertheless, the use of C57BL/6 mice allowed for the complications often observed in humans to be circumvented. The C57BL/6 strain does not spontaneously develop atherosclerosis, a hallmark of vascular ageing, and in this study displayed no signs of dyslipidaemia (Lakatta 2002; Ungvari et al. 2010). Therefore, this enabled a direct assessment of healthy ageing. Furthermore, the use of the ApoE$^{-/-}$ mouse provided an insight into the effects of hypercholesterolaemia and atherosclerosis, often observed in ageing humans, on the vascular reactivity of the aorta and its surrounding PVAT. The Cav-1$^{-/-}$ mouse did not exhibit premature vascular ageing. Nevertheless, the development of hypercholesterolaemia in WD-fed Cav-1 mice enabled the effects of elevated cholesterol on vascular responses to be assessed without the added complications of atherogenesis. Finally, the use of the athero-protected ApoE$^{-/-}$Cav-1$^{-/-}$ double knockout model clearly highlighted the importance of Cav-1 in the pathogenesis of atherosclerosis, and Cav-1/ LDL transcytosis as a possible therapeutic target in humans. Additionally, this study characterised the vascular reactivity of the ApoE$^{-/-}$Cav-1$^{-/-}$ double knockout mouse for the first time.

Male mice were used in the investigations of this thesis in an effort to eliminate the effects of continuous polyoestrous observed in female rodents (Caligioni 2009). Previous reports have demonstrated gender differences in the generation of NO within the vasculature and adipose as

a result of a stimulatory effect induced by oestrogen on the activity of eNOS (Dominiczak et al. 1997; Forte et al. 1998; Kypreos et al. 2014; Menazza et al. 2016).

Studies of CVD in humans have clearly demonstrated that during their reproductive years, women are less susceptible to the development of CVD and atherosclerosis than men. However, men and post-menopausal women of a similar age display the same risk for CVD thus, women develop CVD an average of 10 years later than men (Perez-Lopez et al. 2010; Meyrelles et al. 2011). In addition, studies of mouse models of atherosclerosis, ApoE$^{-/-}$ or LDLR$^{-/-}$ mice, demonstrated that endogenous/exogenous oestrogen plays an athero-protective role in these mice (Thomas et al. 2007). Nevertheless, conflicting evidence has arisen indicating that the atherosclerotic lesion burden in ApoE$^{-/-}$ mice is greater in females than in males whereas in the ApoE$^{-/-}$Cav-1$^{-/-}$ double knockout mice no differences in lesions were observed (Frank et al. 2004a; Meyrelles et al. 2011). Furthermore, studies of gender differences in male and female ApoE$^{-/-}$ mice demonstrated that during the progression of atherosclerosis, female mice were more vulnerable to endothelial dysfunction (Zhou et al. 2015) Taken together, these data indicate that the use of both male and female mice would have added more confounding factors to the studies. Additionally, the majority of rodent studies on PVAT have solely relied on male animas and therefore it is not known if gender differences in PVAT exist. However, this would be an intriguing future area of research.

Studies of mouse models have contributed significantly to the understanding of the pathogenesis of diseases such as atherosclerosis, and ageing. However, it is important to acknowledge that the physiology of mice differs considerably from that of humans and the observations of this study may not be reflected in humans. In addition, the use of a knockout model and the lack of a specific gene and protein may result in compensatory changes. The development of atherosclerosis within the ApoE$^{-/-}$ mice, while providing invaluable insight into the mechanisms behind the pathogenesis of atherosclerosis, differs from humans in several key ways (Bentzon et al. 2010). The plasma cholesterol of ApoE$^{-/-}$ mice is predominantly carried in lipoprotein remnant particles as opposed to LDL, which is the most common lipid to undergo transcytosis into the sub-endothelial space in humans. Furthermore, it is widely recognised that a low HDL to LDL cholesterol ratio increases the risk of atherosclerosis and CVD in humans (Miller 1982; Getz and Reardon 2012). However, while incredibly rare, humans without ApoE display raised remnant cholesterol in a similar fashion to ApoE$^{-/-}$ mice (Schaefer et al. 1986). In contrast to humans, mice rarely develop atherosclerotic lesions within the coronary arteries but lesions are present in the aortic root. However, the significantly elevated heart rate of mice, resulting in turbulent flow of blood, is thought to be the main reason behind this (Getz and Reardon 2012). Nevertheless, mouse models of atherosclerosis, especially ApoE$^{-/-}$ mice, have revealed crucial information about the development of atherosclerosis, including that hyperlipidaemia is fundamental in the development of atherosclerosis and vital information about the pathogenesis of atherosclerosis has been obtained due to similarities between the lesions of the ApoE$^{-/-}$ mouse and those observed in man (Pendse et al. 2009).

Thus, while no animal model exactly mirrors human conditions, mice offer extremely useful models to study the underlying mechanisms involved in the progression of diseases.

7.3.2 Generation and maintenance of the ApoE$^{-/-}$Cav-1$^{-/-}$ colony

A limiting factor for this study was the considerable length of time, (approximately 18 months) taken to generate the ApoE$^{-/-}$Cav-1$^{-/-}$ mouse. Initially, this was the result of several factors including the smaller litter sizes produced by the ApoE$^{-/-}$ mice and the low output of mice from the Cav-1$^{-/-}$ colony. In the initial stages of this study, the breeding and survival rates of the Cav-1$^{-/-}$ colony were so low that the generation of the ApoE$^{-/-}$Cav-1$^{-/-}$ mouse was hindered by lack of available Cav-1$^{-/-}$ mice. Therefore, the Cav-1$^{-/-}$ mice were backcrossed to the C57BL/6 background strain to rescue the colony. The Cav-1$^{-/-}$/C57BL/6 backcross significantly improved the breeding and survival rates of the colony and enabled the generation of the ApoE$^{-/-}$Cav-1$^{-/-}$ mouse to continue. However, upon successful generation of the ApoE$^{-/-}$Cav-1$^{-/-}$ mice the balance between maintenance of the colony and the production of experimental mice became problematic. The DKO mice were extremely poor breeders and less than half of the offspring survived to weaning age. Despite various attempts to improve the breeding and survival outcomes of the offspring, including: moving the mice to a room where they would be disturbed less, separating sires and dams prior to litters being born, fostering pups with FVB mice and breeding heterozygotes (ApoE$^{+/-}$Cav-1$^{-/-}$) no improvements were made. Consequently, some of the experiments performed, using the ApoE$^{-/-}$Cav-1$^{-/-}$ strain, have lower than optimal numbers of mice.

7.3.3 Myography as an ex vivo technique for the assessment of vascular function

Myography is a useful technique for the study of isolated vessels as it allows mechanisms underlying vasoconstriction and dilation to be studied in a controlled manner, thus circumventing the problems posed by in vivo work, for example the release of endogenous hormonal and sympathetic activity. However, the concentration of substances used in the organ bath may not correspond or be comparable to those observed physiologically. In addition, the conditions that vessels are exposed to, specifically in the 'open-ended' preparation, permit the direct exposure of the luminal surface to substances released by the PVAT, which would not occur in vivo (Malinowski et al. 2008; Gollasch 2012). Nevertheless, the anti-contractile effects of PVAT have been demonstrated, using a murine perfused isolated mesenteric bed, to occur through the release of a PVAT-derived relaxant factor outside from outside the artery (Fesus et al. 2007). Technical issues can arise during the initial dissection and mounting of the aortic ring preparations. If not performed carefully the endothelium and vascular SM can easily become damaged. Over-stretching of the aortic segments during normalisation can also result in an insult to the vascular components. To overcome this, controls were introduced to ascertain the viability of the aortic rings by stimulation with KPSS and ensuring a stable contraction was achieved.

The aorta was chosen to assess vascular function because this is the site of most lesion development within the ApoE$^{-/-}$ and ApoE$^{-/-}$Cav-1$^{-/-}$ mice and one of the purposes of this study was to evaluate the effect of atherosclerotic lesion progression in the ApoE$^{-/-}$ and ApoE$^{-/-}$Cav-1$^{-/-}$ mice (VanderLaan et al. 2004). Furthermore, in health, large arteries, such as the aorta and carotid, display a high basal release of NO. Attenuation of NO bioavailability is an indicator of endothelial dysfunction, which is associated with ageing and atherosclerosis, and was another focus of this study (Martin et al. 1986).

7.4 Concluding remarks

The data presented in this thesis have provided novel insights into the influence of aortic PVAT on vascular reactivity and the morphology of aortic PVAT in normally ageing mice (C57BL/6), atherosclerotic ApoE$^{-/-}$ mice, athero-resistant Cav-1$^{-/-}$ mice and the athero-protected ApoE$^{-/-}$Cav-1$^{-/-}$ double knockout mice.

This study demonstrated that ageing to pre-middle age in C57BL/6 mice resulted in significant changes to the function and morphology of aortic PVAT and a loss of the anti-contractile effect of PVAT, prior to the development of endothelial dysfunction and in the absence of dyslipidaemia. This raises intriguing questions about whether the loss of the beneficial anti-contractile capacity of PVAT with ageing can be restored either through exercise or pharmacological intervention and if similar age-associated changes occur in the PVAT of humans.

The aortic PVAT of ApoE$^{-/-}$ mice did not exert an anti-contractile effect and was dysfunctional from the outset of the experiments; this was attributed to a lack of PVAT-derived NO as a result of low basal eNOS activity furthermore, the PVAT exhibited an aged phenotype and displayed elevated superoxide production in comparison to C57BL/6 mice. However, ageing and a WD did not induce any further changes. This data could implicate low basal NO production within PVAT as a contributory factor to the development of atherosclerosis.

Studies of Cav-1$^{-/-}$ mice demonstrated that the aortic PVAT of ND-fed Cav-1$^{-/-}$ mice did not exert an anti-contractile effect. However, after 26 weeks on a WD a pro-contractile effect of PVAT was observed and this was associated with hypertrophy of the white adipocytes within the aortic PVAT. NOS inhibition also revealed a pro-contractile effect of aortic PVAT which may suggest that the PVAT of Cav-1$^{-/-}$ mice releases a PVAT-derived vaso-constricting factor and its action is antagonised by NO. The aortic PVAT of ApoE$^{-/-}$Cav-1$^{-/-}$ mice does not exert an anti-contractile effect and vascular responses are not modulated by ageing or a WD. However, aortic PVAT composition was altered after extensive high fat feeding. The investigation of the ApoE$^{-/-}$Cav-1$^{-/-}$ double knockout mice verified that lack of Cav-1$^{-/-}$ confers protection against the development of atherosclerosis. Although beyond the remit of this study, the previously proposed mechanism of reduced LDL transcytosis into the sub-endothelial space, provides an exciting potential therapeutic target for the prevention of atherosclerosis.

~Appendix One~

Appendix 1.1 Reagents and consumables

Product	*Code*	*Supplier*
General		
Acetic acid	10171460	Fisher Scientific, Leicestershire, UK
Calcium chloride	10050070	Fisher Scientific, Leicestershire, UK
EDTA	ED	Sigma-Aldrich, Poole, UK
EDTA dipotassium salt	ED2P	Sigma-Aldrich, Poole, UK
Ethanol	12468750	Fisher Scientific, Leicestershire, UK
Glucose	10141520	Fisher Scientific, Leicestershire, UK
Hydrochloric acid	258148	Sigma-Aldrich, Poole, UK
IMS	11482874	Fisher Scientific, Leicestershire, UK
Magnesium sulphate	10224680	Fisher Scientific, Leicestershire, UK
Methanol	10284580	Fisher Scientific, Leicestershire, UK
Paraformaldehyde	441244	Sigma-Aldrich, Poole, UK
PBS Tablets	18912-014	Gibco, Warrington, UK
Potassium chloride	10010310	Fisher Scientific, Leicestershire, UK
Potassium phosphate	P0662	Sigma-Aldrich, Poole, UK
Sodium bicarbonate	71630	Sigma-Aldrich, Poole, UK
Sodium chloride	10735921	Fisher Scientific, Leicestershire, UK
Sodium hydroxide	S5881	Sigma-Aldrich, Poole, UK
Animal husbandry		
Rodent breeder and grower BK001	801960	Special Diets Services, Essex, UK
'Western' high fat diet (21%)	829100	Special Diets Services, Essex, UK
Molecular biology		
0.2 ml PCR tubes	1402-8100	Starlab, Milton Keynes, UK
DNA Loading Buffer Blue (5x)	BIO-37045	Bioline, London, UK
Hyperladder	V 33031	Bioline, London, UK
Nancy-520	01494	Sigma-Aldrich, Poole, UK
Primers		Sigma-Aldrich, Poole, UK
REDExtract-N-Amp Tissue PCR Kit	XNAT	Sigma-Aldrich, Poole, UK
SeaKem LE agarose	50004	Lonza, Castleford, UK
Histology/immunostaining		
Avidin/biotin blocking kit	004303	Invitrogen, Warrington, UK
Bovine serum albumin	A7906	Sigma-Aldrich, Poole, UK
Coverslips No 1.5 22x50mm	MIC3246	Scientific Laboratory supplies, Hessle, UK
DAB substrate kit	SK-4100	Vector Labs, Peterborough, UK
DPX mounting medium	LAMB/DPX	Raymond Lamb, Sussex, UK
Eosin Y	230251	Sigma-Aldrich, Poole, UK
Horse serum	16050-130	Invitrogen, Warrington, UK
Hydrogen peroxide	H1009	Sigma-Aldrich, Poole, UK
ImmEdge Hydrophobic Barrier Pen	H-4001	Vector Labs, Peterborough, UK
Mac-3 (CD107b Clone M3/84) rat anti-mouse monoclonal antibody	550292	BD Biosciences, Oxford, UK
Mayer's haematoxylin	H3136	Sigma-Aldrich, Poole, UK
Methyl green	H-3402	Vector Labs, Peterborough, UK
Oil red O powder	00625	Sigma-Aldrich, Poole, UK

Poly-lysine slides	631-0107	VWR International, UK
Rabbit anti-rat, biotin conjugated secondary	E0468	Dako, Cambridge, UK
Rat IgG	559072	BD Biosciences, Oxford, UK
Triethyl phosphate	538728	Sigma-Aldrich, Poole, UK
Tris base	T1503	Sigma-Aldrich, Poole, UK
Tris hydrochloride	T5941	Sigma-Aldrich, Poole, UK
Tween – 20	P1379	Sigma-Aldrich, Poole, UK
Vectastain elite ABC kit	PK-6100	Vector Labs, Peterborough, UK
Xylene	10784001	Fisher Scientific, Leicestershire, UK
Myography		
Acetylcholine	A6625	Sigma-Aldrich, Poole, UK
L-NNA	N5501	Sigma-Aldrich, Poole, UK
Phenylephrine	P6126	Sigma-Aldrich, Poole, UK
Sodium nitroprusside	13451	Sigma-Aldrich, Poole, UK
PVAT secretome		
Mouse Adipokine Array	ARY013	R&D systems, Minneapolis, USA
Serum analysis		
Cholesterol assay		Randox Laboratories, Crumlin, UK
Glucose assay		Randox Laboratories, Crumlin, UK
HDL assay		Randox Laboratories, Crumlin, UK
Triglyceride assay		Randox Laboratories, Crumlin, UK

Appendix 1.2 Recipes

Molecular biology
TAE buffer, 50X, pH 8.5 (1 litre)
242 g Tris base
57.1 ml acetic acid
100 ml 0.5M EDTA
Make up to volume with distilled water

Histology and Immunohistochemistry
Oil Red O, 0.5% (50ml)
0.25g Oil Red O dissolved in 60% aqueous triethyl phosphate
Filter and use immediately

100 mM Tris-HCl, pH 8.2 (100 ml)

1.21 g Tris-HCl
Make up to volume with distilled water
pH to 8.2 with HCl

1 x TBS (1 litre)
6.06 g Tris-base
8.76 g sodium chloride
800 ml distilled water
Make up to 1 litre with distilled water
pH to 7.5

1 x TBS/T (1 litre)
1 mL of Tween 20 in 1 litre of TBS buffer

Citrate Buffer (1 litre)
2.94 g tri-sodium citrate
0.5 ml Tween
Make up to 1 litre with distilled water,
pH to 6.0

Myography

PSS, pH 7.4, 10 litres

69.544 g NaCl (119 mmol/L)
3.504 g KCl (4.7 mmol/L)
2.884 g $MgSO_4 \cdot 7H_2O$ (1.17 mmol/L)
21.003 g $NaHCO_3$ (25 mmol/L)
1.592 g KH_2PO_4 (1.17 mmol/L)
*0.121 g K_2EDTA (0.03 mmol/L)
9.909 g Glucose (5.5 mmol/L)
*2.352 g $CaCl_2$ (1.6 mmol/L)
Made up to 10 litres with distilled water

100 mM KPSS, pH 7.4, 2 litres

2.770 g NaCl (23.7 mmol/L)
14.912 g KCl (100 mmol/L)
0.577 g $MgSO_4 \cdot 7H_2O$ (1.17 mmol/L)
4.201 g $NaHCO_3$ (25 mmol/L)
0.318 g KH_2PO_4 (1.17 mmol/L)
*0.0241 g K_2EDTA (0.03 mmol/L)
1.982 g Glucose (5.5 mmol/L)
*0.470 g $CaCl_2$ (1.6 mmol/L)
Made up to 2 litres with distilled water

*dissolved in distilled water prior to addition to solution

Appendix 1.3 Tissue processing for Immunohistochemistry

Automatic schedule for the Shandon Citadel 2000 processor:

50% IMS	90 minutes
70% IMS	60 minutes
99% IMS	60 minutes
99% IMS	60 minutes
99% IMS	60 minutes
99% IMS	90 minutes
99% IMS	90 minutes
Xylene	90 minutes
Xylene	90 minutes
Xylene	90 minutes
Molten wax	90 minutes
Molten wax	120 minutes

Appendix 1.4 Haematoxylin and Eosin automatic staining protocol (program 1)

Xylene	5 minutes
Xylene	3 minutes
Xylene	3 minutes
Ethanol	3 minutes
Ethanol	2 minutes
90% IMS	2 minutes
70% IMS	2 minutes
Distilled water	2 minutes
Gill's haematoxylin #2	2 minutes
Distilled water	1 minute
5% acetic acid	10 seconds
Distilled water	1 minute
Blueing agent	30 seconds
Distilled water	2 minutes
70% IMS	1 minute
90% IMS	1 minute
Ethanol	1 minute
Eosin alcoholic	1 ½ minutes
Ethanol	2 minutes
Ethanol	2 minutes
Ethanol	2 minutes
Xylene	2 minutes
Xylene	3 minutes
Xylene	5 minutes

Appendix 1.5 Field of view reproducibility study for the quantitation of superoxide within sections of aortic perivascular adipose tissue

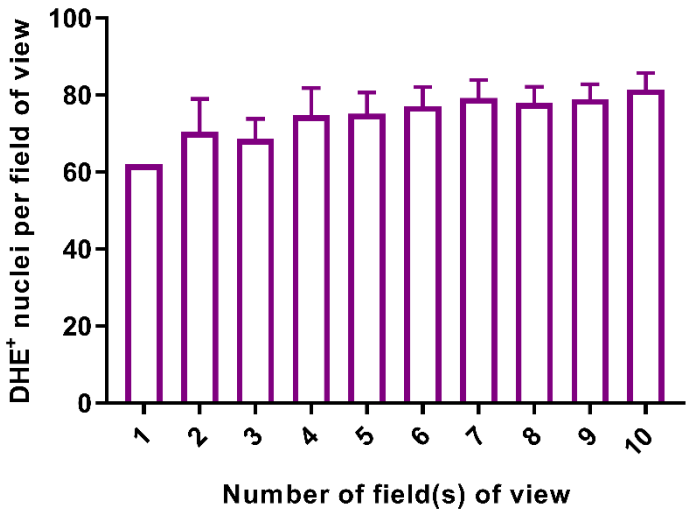

Appendix 1.5 Preliminary study to determine the number of fields of view required for quantitation of superoxide within aortic PVAT using dihydroethidium staining.

An increasing number of fields of view (FOV, 200 x 150 µm) were used to determine when the number of dihydroethidium$^+$ (DHE$^+$) nuclei within the aortic PVAT would become consistent. The number of DHE$^+$ nuclei within each FOV was quantified. Each bar represents the number of FOV measured and the number of DHE$^+$ stained nuclei. It was concluded that the number of DHE$^+$ stained nuclei ceased to increase significantly after 5 FOV. Representative results from a section of aortic PVAT from one mouse.

Appendix 1.6 Mouse adipokine array

A

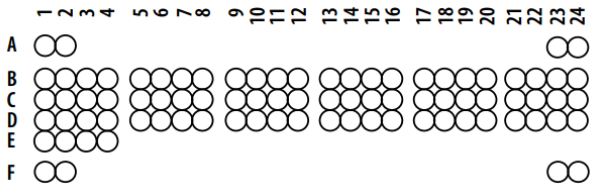

B

Coordinate	Adipokine/control	Alternative nomenclature
A1, A2	Reference spots	------
A23, A24	Reference spots	------
B1, B2	Adiponectin	GBP-28, apM1, AdipoQ, Acrp30
B3, B4	Agouti-related peptide	AgRP, ART
B5, B6	Angiopoietin-like 3	ANGPTL3
B7, B8	C-reactive protein	CRP
B9, B10	Dipeptidylpeptidase IV	DPPIV, CD26,DPP4
B11. B12	Endocan	ESM-1
B13, B14	Fetuin A	AHSG
B15, B16	Fibroblast growth factor acidic	FGF acidic, FGF-1
B17, B18	Fibroblast growth factor-21	FGF-21)
B19, B20	Hepatocyte growth factor	HGF
B21, B22	Intercellular Adhesion Molecule 1	ICAM-1, CD54
B23, B24	Insulin-like growth factor-I	IGF-I, Somatomedin C
C1, C2	Insulin-like growth factor -II	IGF-II, Somatomedin A
C3, C4	Insulin-like growth factor binding protein-1	IGFBP-1
C5, C6	Insulin-like growth factor binding protein-2	IGFBP-2
C7, C8	Insulin-like growth factor binding protein-3	IGFBP-3
C9, C10	Insulin-like growth factor binding protein-5	IGFBP-5
C11, C12	Inulin-like growth factor binding protein-6	IGFBP-6
C13, C14	Interleukin 6	IL-6
C15, C16	Interleukin 10	IL-10
C17, C18	Interleukin 11	IL-11
C19, C20,	Leptin	OB
C21, C22	*Leukaemia inhibitory factor*	LIF
C23, C24	Lipocalin-2	NGAL
D1, D2	Monocyte chemoattractant protein-1	MCP-1, CCL2, JE
D3, D4	Macrophage colony-stimulating factor	M-CSF, CSF-1
D5, D6	Oncostatin M	OSM
D7, D8	Pentraxin 2	PTX2, SAP
D9, D10	Pentraxin 3	PTX3, TSG-14
D11, D12	Preadipocyte factor 1	Pref-1, DLK-1, FA1
D13, D14	RAGE	------
D15, D16	RANTES	CCL5
D17, D18	Retinol binding protein 4	RBP4
D19, D20	Resistin	ADSF/FIZZ3
D21, D22	Serpin E1	PAI-1
D23, D24	Tissue inhibitor of metalloproteinase-1	TIMP-1
E1, E2	*Tumour necrosis factor-α*	TNF-α, TNFSF1A
E3, E4	*Vascular endothelial growth factor*	VEGF, VEGF-1
F1, F2	Reference spots	------
F23, F24	PBS (negative control)	------

Appendix 1.6 Mouse adipokine array layout A, and list of adipokines and their co-ordinates found on the array membrane B.

Adipokines were dotted on the membrane in duplicates**.**

Appendix 1.7 Mouse adipokine array validation

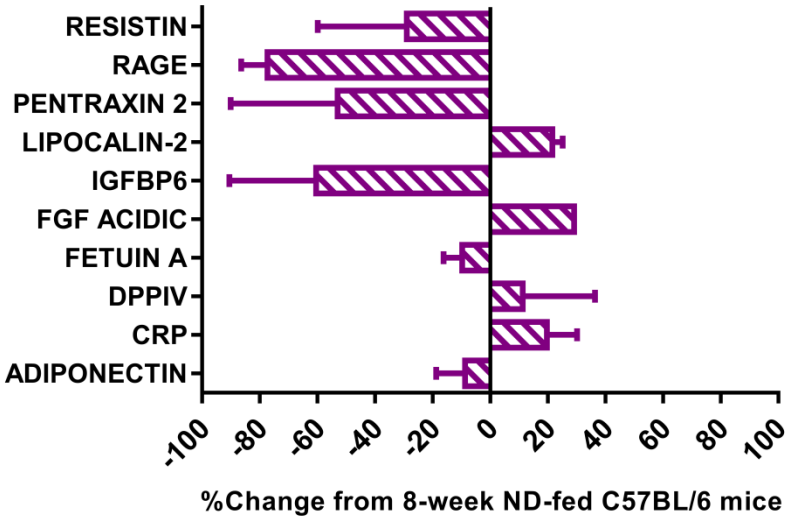

Appendix 1.7 The reliability of the Proteome Profiler Adipokine array

The array was validated by repeating experiments for C57BL/6 26-week ND-fed mice using the same pooled samples.

~Appendix Two - Supplementary Results~

Appendix 2.1 The anti-contractile effect of PVAT is endothelium-independent

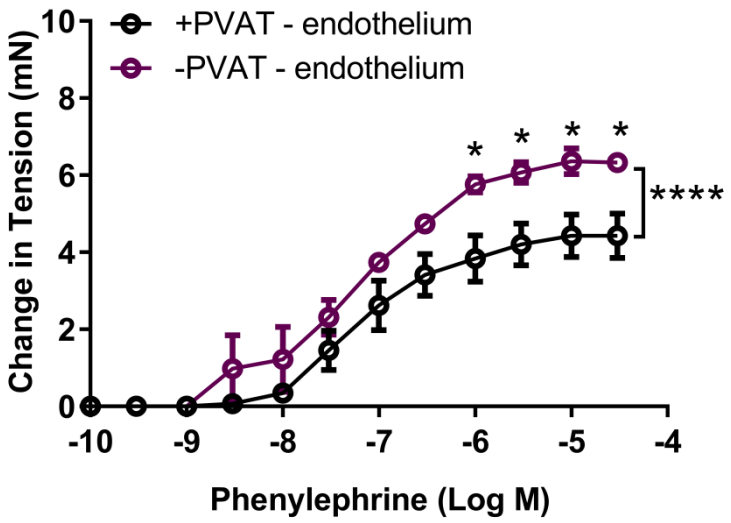

Appendix 2.1 The anti-contractile effect of aortic PVAT is endothelium-independent in 8-week normal diet-fed C57BL/6 mice

The presence of PVAT on aortic rings from young adult C57BL/6 mice reduced vasoconstrictor responses to cumulative doses of phenylephrine (1x10-10 - 3x10-5 mol/L). Endothelium denuded aortic rings exhibited < 30% relaxation to acetylcholine. Dose response data are expressed as mean ± S.E.M., n = 3 mice, * P < 0.05, **** P < 0.0001, two-way ANOVA with Bonferroni post hoc test.

The following supplementary results display comparisons for all mouse strains fed a normal diet (ND). Statistical analyses were performed between mice of the same background strain, i.e.:

- **ApoE$^{-/-}$ mice versus C57BL/6**
- **Cav-1$^{-/-}$ versus C57BL/6**
- **ApoE$^{-/-}$Cav-1$^{-/-}$ versus ApoE$^{-/-}$**
- **ApoE$^{-/-}$Cav-1$^{-/-}$ versus Cav-1$^{-/-}$**

Appendix 2.2 Lipidemic and glycaemic profiles of normal diet-fed C57BL/6, ApoE$^{-/-}$, Cav-1$^{-/-}$ and ApoE$^{-/-}$Cav-1$^{-/-}$ mice

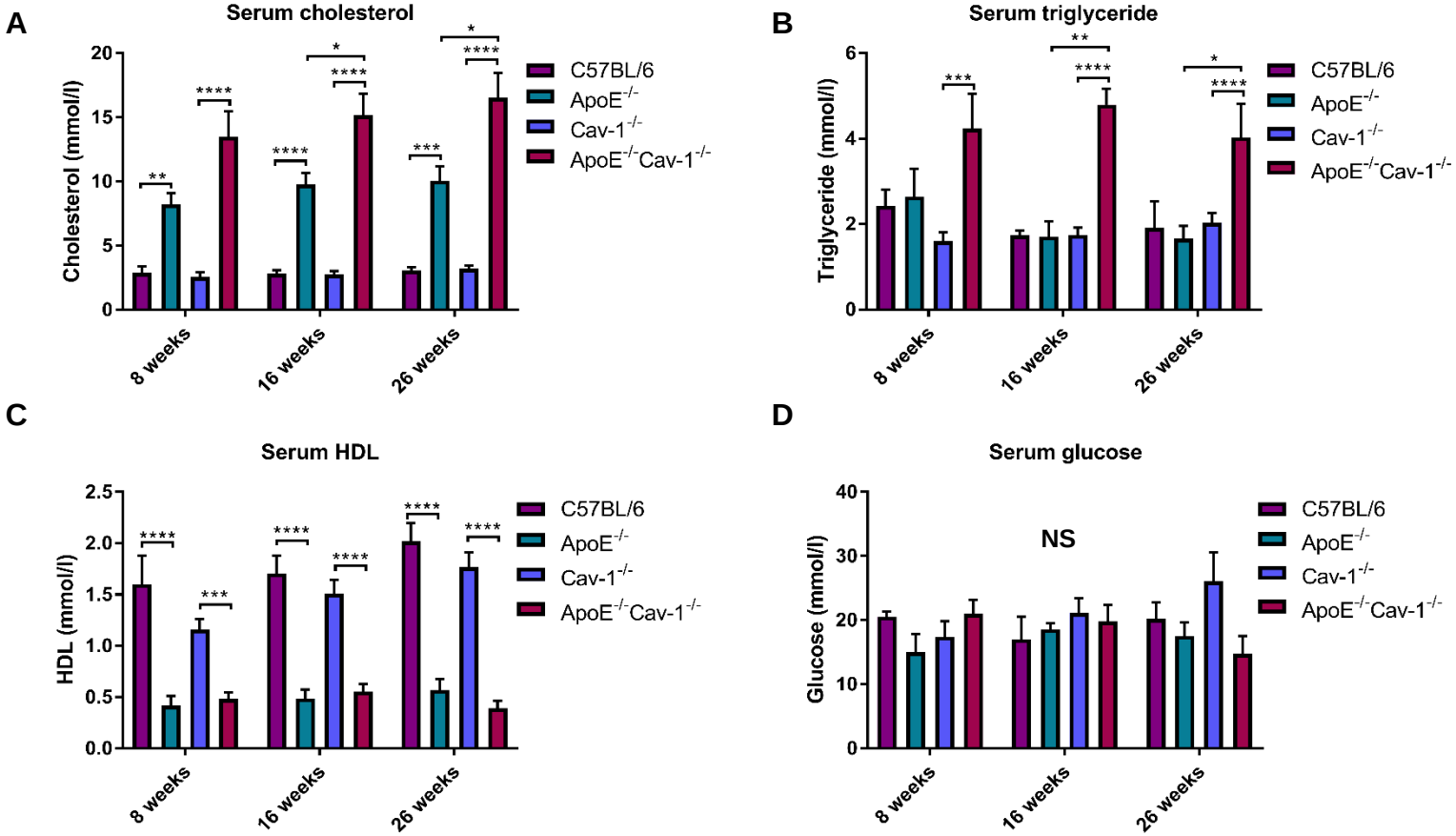

Appendix 2.2 Lipidemic and glycaemic profiles of normal diet-fed C57BL/6, ApoE$^{-/-}$, Cav-1$^{-/-}$ and ApoE$^{-/-}$Cav-1$^{-/-}$ mice

*Serum obtained at time of sacrifice (mice weaned at 4 weeks old then maintained on a normal chow diet (ND) for the appropriate length of time. Serum levels of A) cholesterol, B) triglyceride, C) HDL and D) glucose were assessed in the ageing mice. Data are expressed as mean ± S.E.M, measurements are in mmol/L. Statistical analysis carried out by two-way ANOVA, with Bonferroni's post hoc test, n = 4-6 mice per group, * P < 0.05, ** P < 0.01, *** P < 0.001, **** P < 0.0001*

Appendix 2.3 Body, organ weights and epididymal adipocyte size of normal diet-fed C57BL/6, ApoE$^{-/-}$, Cav-1$^{-/-}$ and ApoE$^{-/-}$Cav-1$^{-/-}$ mice

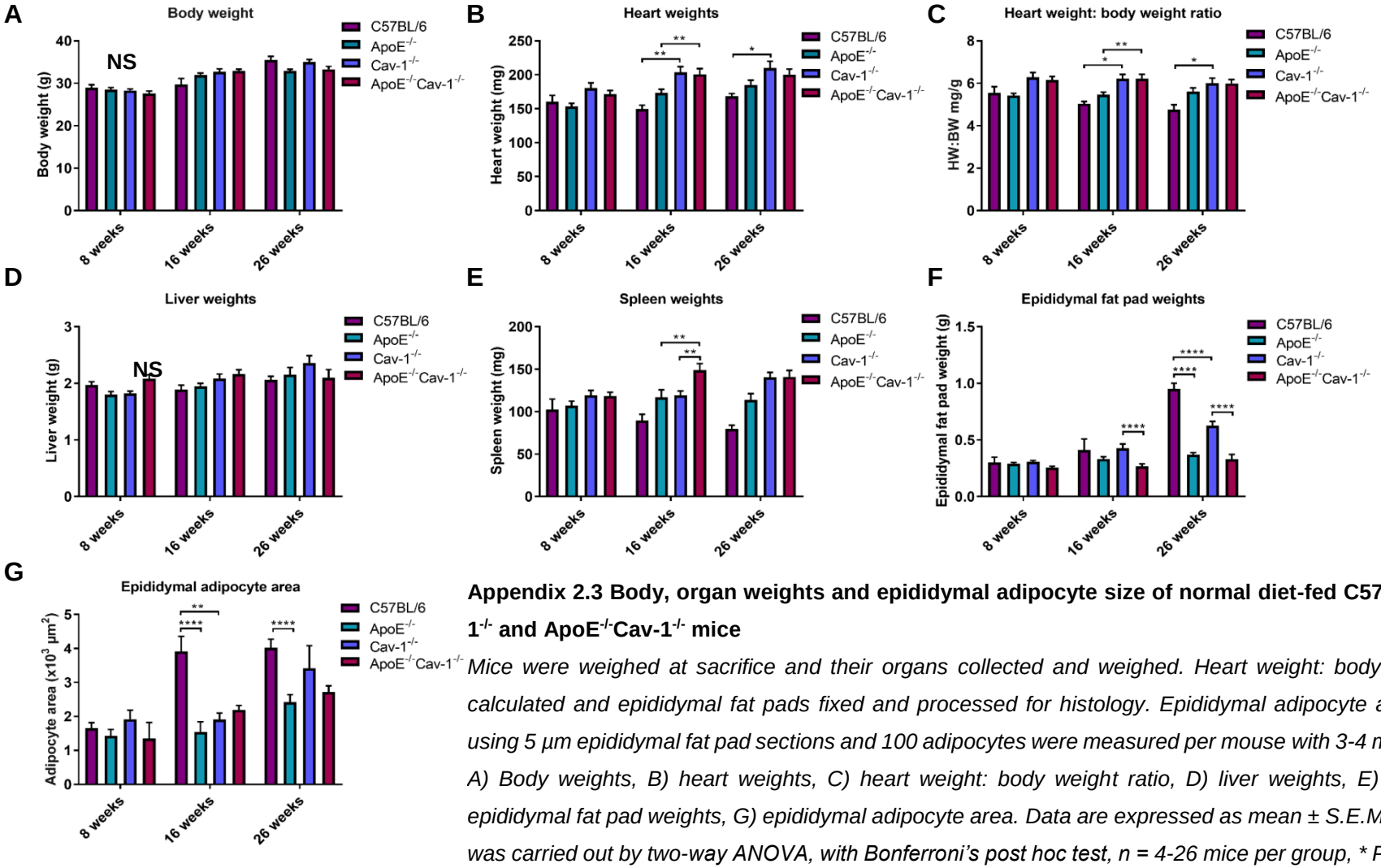

Appendix 2.3 Body, organ weights and epididymal adipocyte size of normal diet-fed C57BL/6, ApoE$^{-/-}$, Cav-1$^{-/-}$ and ApoE$^{-/-}$Cav-1$^{-/-}$ mice

*Mice were weighed at sacrifice and their organs collected and weighed. Heart weight: body weight ratios were calculated and epididymal fat pads fixed and processed for histology. Epididymal adipocyte area was calculated using 5 µm epididymal fat pad sections and 100 adipocytes were measured per mouse with 3-4 mice used per group. A) Body weights, B) heart weights, C) heart weight: body weight ratio, D) liver weights, E) spleen weights, F) epididymal fat pad weights, G) epididymal adipocyte area. Data are expressed as mean ± S.E.M. Statistical analysis was carried out by two-way ANOVA, with Bonferroni's post hoc test, n = 4-26 mice per group, * P < 0.05, ** P < 0.01, **** P < 0.0001*

Appendix 2.4 KPSS contraction responses, endothelial function and endothelium-independent relaxations of PVAT-intact or PVAT-denuded isolated aortic rings from C57BL/6, ApoE$^{-/-}$, Cav-1$^{-/-}$ and ApoE$^{-/-}$Cav-1$^{-/-}$ mice fed a normal diet

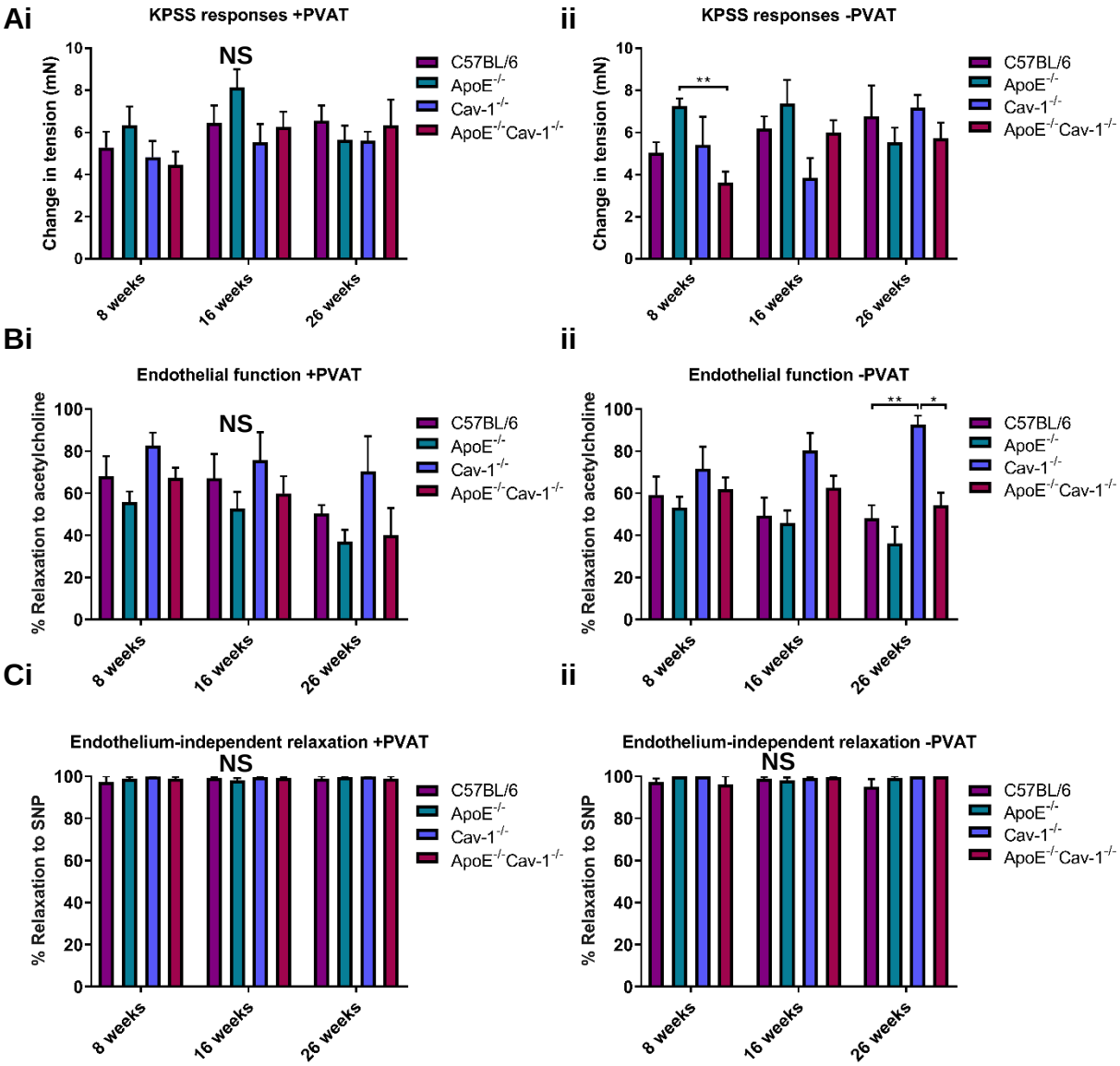

Appendix 2.4 KPSS contraction responses, endothelial function and endothelium-independent relaxations of PVAT-intact or PVAT-denuded isolated aortic rings from C57BL/6, ApoE$^{-/-}$, Cav-1$^{-/-}$ and ApoE$^{-/-}$Cav-1$^{-/-}$ mice fed a normal diet

*Isolated aortic rings, with Ai) PVAT left intact or Aii) PVAT removed, were challenged with 100 mM KPSS and contractile responses measured. Endothelial function was assessed by pre-constricting the aortic preparations with phenylephrine (10 µM) and then exposing them to the endothelium-dependent vasodilator, acetylcholine (10 µM) Bi) in the presence of PVAT or Bii) in the absence of PVAT. Endothelium-independent vasodilation was assessed through pre-constricting the aortic preparations with phenylephrine (10 µM) and then exposure to sodium nitroprusside (10 µM) Ci) in the presence of PVAT or Cii) in the absence of PVAT. PVAT = perivascular adipose tissue. Data are expressed as mean ± S.E.M, KPSS contraction was measured in mN and relaxation was measured as percentage relaxation from maximal contraction. Statistical analysis was carried out by two-way ANOVA, with Bonferroni's post hoc tests, n = 4-8 mice per group, * P < 0.05, ** P < 0.01.*

Appendix 2.5 A comparison of the contractility of PVAT-intact and PVAT-denuded aortic rings from normal diet-fed C57BL/6 and ApoE$^{-/-}$ mice in response to cumulative doses of phenylephrine

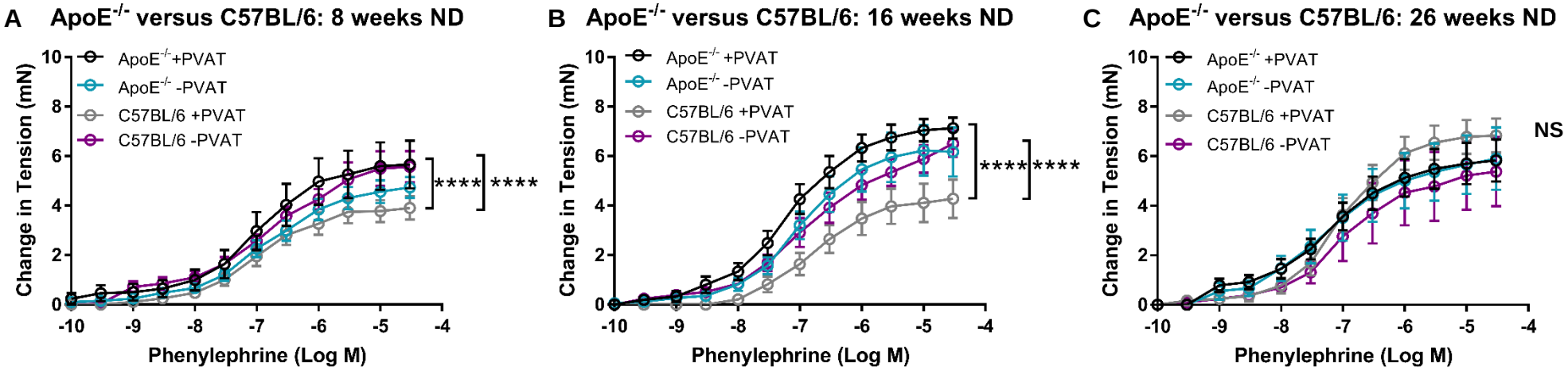

Appendix 2.5 A comparison of the contractility of PVAT-intact and PVAT-denuded aortic rings from normal diet-fed C57BL/6 and ApoE$^{-/-}$ mice in response to cumulative doses of phenylephrine

*Aortic preparations were challenged with cumulative doses of phenylephrine (1 x 10^{-10} - 3 x 10^{-5} mol/L). A) The contractions of aortic rings from ApoE$^{-/-}$ and C57BL/6 mice were compared after 8 weeks on a ND, post weaning. The PVAT-intact aortic rings of ApoE$^{-/-}$ mice contracted significantly more than those of the C57BL/6 mice whereas, no differences in contraction were observed between PVAT-denuded aortic rings of ApoE$^{-/-}$ and C57BL/6 mice. These findings were replicated in the 16-week ND-fed groups B) PVAT-intact aortic rings from ApoE$^{-/-}$ mice contracted significantly more than those of the C57BL/6 strain although, no differences were observed between PVAT-denuded aortic preparations. However, after 26 weeks on a ND, post weaning, C) the contractions of aortic rings from ApoE$^{-/-}$ and C57BL/6 mice were similar in the presence or absence of PVAT. ND = normal diet. PVAT = perivascular adipose tissue. Dose response data are reported as absolute change in tension and expressed as mean ± S.E.M., n = 6-8 mice per group, **** P < 0.0001, two-way ANOVA with Bonferroni's post hoc tests.*

Appendix 2.6 A comparison of the contractility of PVAT-intact and PVAT-denuded aortic rings from normal diet-fed C57BL/6 and Cav-1$^{-/-}$ mice in response to cumulative doses of phenylephrine

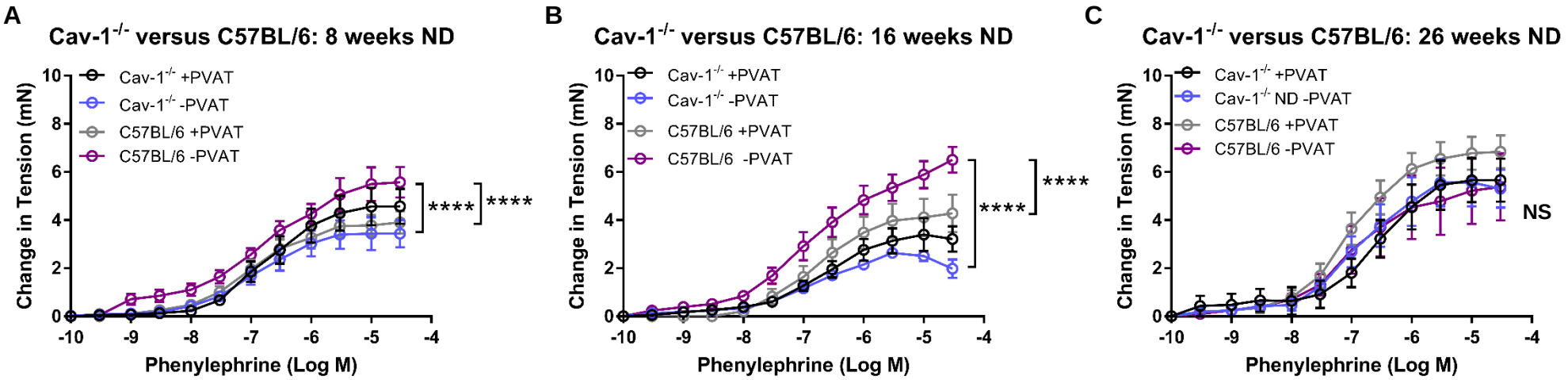

Appendix 2.6 A comparison of the contractility of PVAT-intact and PVAT-denuded aortic rings from normal diet-fed C57BL/6 and Cav-1$^{-/-}$ mice in response to cumulative doses of phenylephrine

*Aortic preparations were exposed to cumulative doses of phenylephrine (1 x 10^{-10} - 3 x 10^{-5} mol/L). A) The contractions of aortic rings from Cav-1$^{-/-}$ and C57BL/6 mice were compared after 8 weeks on a ND, post weaning. In the absence of PVAT, the aortic rings of Cav-1$^{-/-}$ mice exhibited lower vasoconstrictor responses to phenylephrine than C57BL/6 mice however, no differences in response were observed between PVAT-intact aortic rings. Similar findings were observed in the 16 week ND-fed Cav-1$^{-/-}$ mice B) PVAT-denuded aortic rings from Cav-1$^{-/-}$ mice contracted significantly less than those of the C57BL/6 strain although the contractions of PVAT-intact artic rings were similar. After 26 weeks on a ND, post weaning, C) the contractions of PVAT-intact and PVAT-denuded aortic rings from Cav-1$^{-/-}$ and C57BL/6 mice were similar. ND = normal diet. PVAT = perivascular adipose tissue. Dose response data are reported as absolute change in tension and expressed as mean ± S.E.M., n = 4-9 mice per group, **** P < 0.0001, two-way ANOVA with Bonferroni's post hoc tests.*

Appendix 2.7 A comparison of the contractility of PVAT-denuded and PVAT-intact aortic rings from normal diet-fed ApoE$^{-/-}$Cav-1$^{-/-}$ double knockout, ApoE$^{-/-}$ and Cav-1$^{-/-}$ mice in response to cumulative doses of phenylephrine

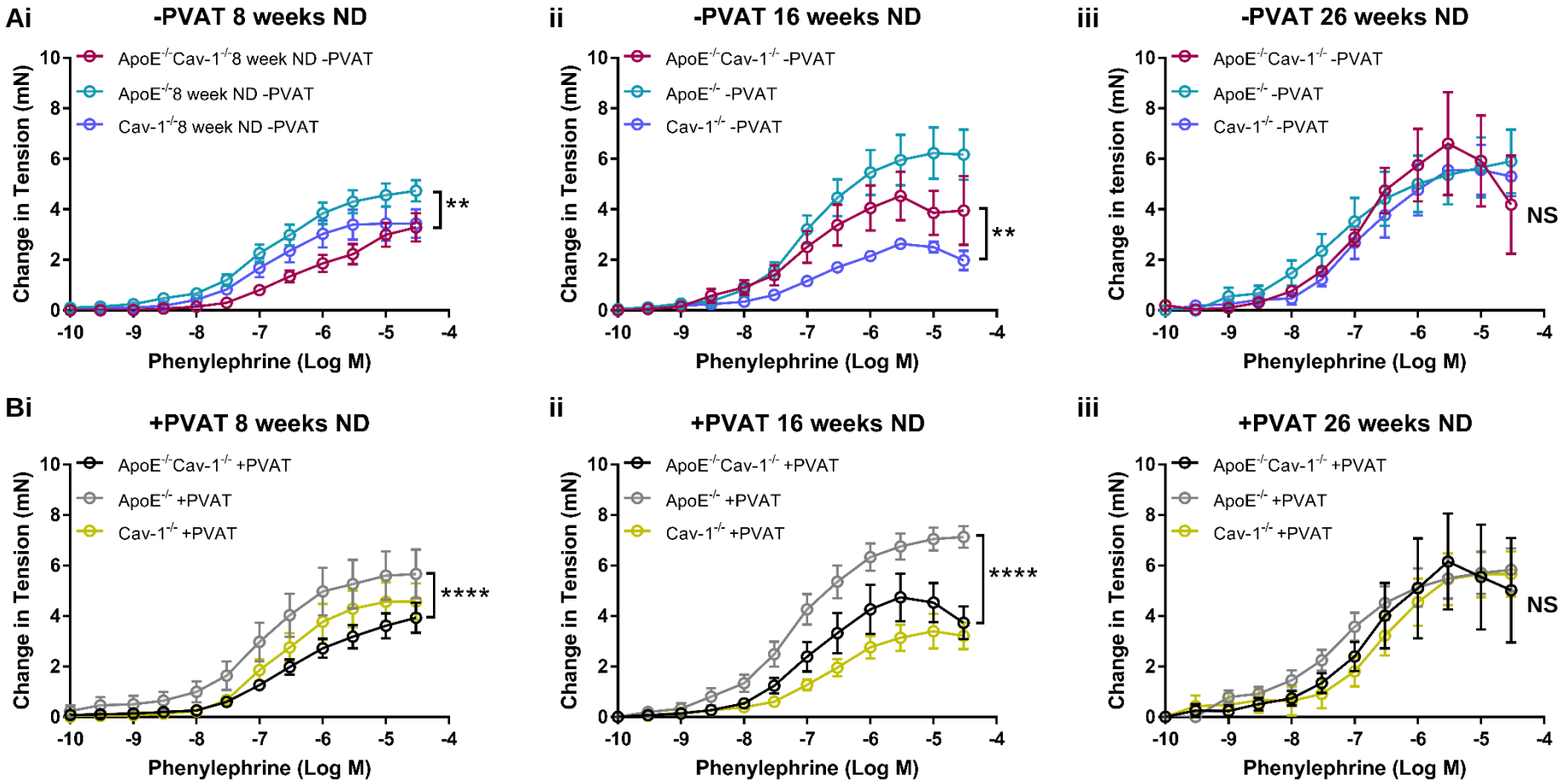

Appendix 2.7 A comparison of the contractility of PVAT-denuded and PVAT-intact aortic rings from normal diet-fed ApoE$^{-/-}$Cav-1$^{-/-}$ double knockout, ApoE$^{-/-}$ and Cav-1$^{-/-}$ mice in response to cumulative doses of phenylephrine

*Aortic rings were exposed to cumulative doses of phenylephrine (1 x 10^{-10} - 3 x 10^{-5} mol/L). The contractile responses of aortic rings from ApoE$^{-/-}$Cav-1$^{-/-}$ double knockout mice were compared to the background strains (ApoE$^{-/-}$ and Cav-1$^{-/-}$ mice). A) The contractions of PVAT-denuded aortic rings were assessed at each feeding time-point. Ai) The contractions of PVAT-denuded aortic rings from ApoE$^{-/-}$Cav-1$^{-/-}$ double knockout mice were similar to Cav-1$^{-/-}$ responses. However, the responses of the ApoE$^{-/-}$Cav-1$^{-/-}$ double knockout mice were significantly attenuated compared to the aortic ring contractions of ApoE$^{-/-}$ mice. Aii) After 16 weeks on a ND, post weaning, PVAT-denuded aortic rings from ApoE$^{-/-}$Cav-1$^{-/-}$ double knockout mice exhibited greater contractile responses than those observed from the Cav-1$^{-/-}$ mice whereas, no significant differences in contractile response were observed between the ApoE$^{-/-}$Cav-1$^{-/-}$ double knockout mice and the ApoE$^{-/-}$ strain. Aiii) After 26 weeks on a ND, the contractions of PVAT-denuded aortic rings from ApoE$^{-/-}$Cav-1$^{-/-}$ double knockout mice were similar to the responses of both the ApoE$^{-/-}$ and Cav-1$^{-/-}$ mice. Bi) The contractions of PVAT-intact aortic rings from ApoE$^{-/-}$Cav-1$^{-/-}$ double knockout mice were comparable to the responses of the Cav-1$^{-/-}$ aortic rings although, this contraction was significantly dampened in comparison to the aortic preparations from ApoE$^{-/-}$ mice. Bii) A similar pattern was observed after 16 weeks on a ND, with no differences between the contractions of Cav-1$^{-/-}$ and ApoE$^{-/-}$Cav-1$^{-/-}$ double knockout mice. On the contrary, vasoconstriction of PVAT-intact aortic rings from ApoE$^{-/-}$ mice was significantly enhanced compared to the ApoE$^{-/-}$Cav-1$^{-/-}$ double knockout mice. Biii) After 26 weeks on a ND, the contractile responses of PVAT-intact aortic rings from ApoE$^{-/-}$Cav-1$^{-/-}$ double knockout mice were similar to the responses observed in the ApoE$^{-/-}$ and Cav-1$^{-/-}$ mice. ND = normal diet. PVAT = perivascular adipose tissue Dose response data are reported as absolute change in tension and expressed as mean ± S.E.M., n = 4-10 mice per group, two-way ANOVA with Bonferroni's post hoc tests ** P < 0.01, **** P < 0.0001.*

Appendix 2.8 Assessment of aortic PVAT weight and composition in normal diet-fed ApoE$^{-/-}$Cav-1$^{-/-}$ double knockout, ApoE$^{-/-}$ and Cav-1$^{-/-}$ mice

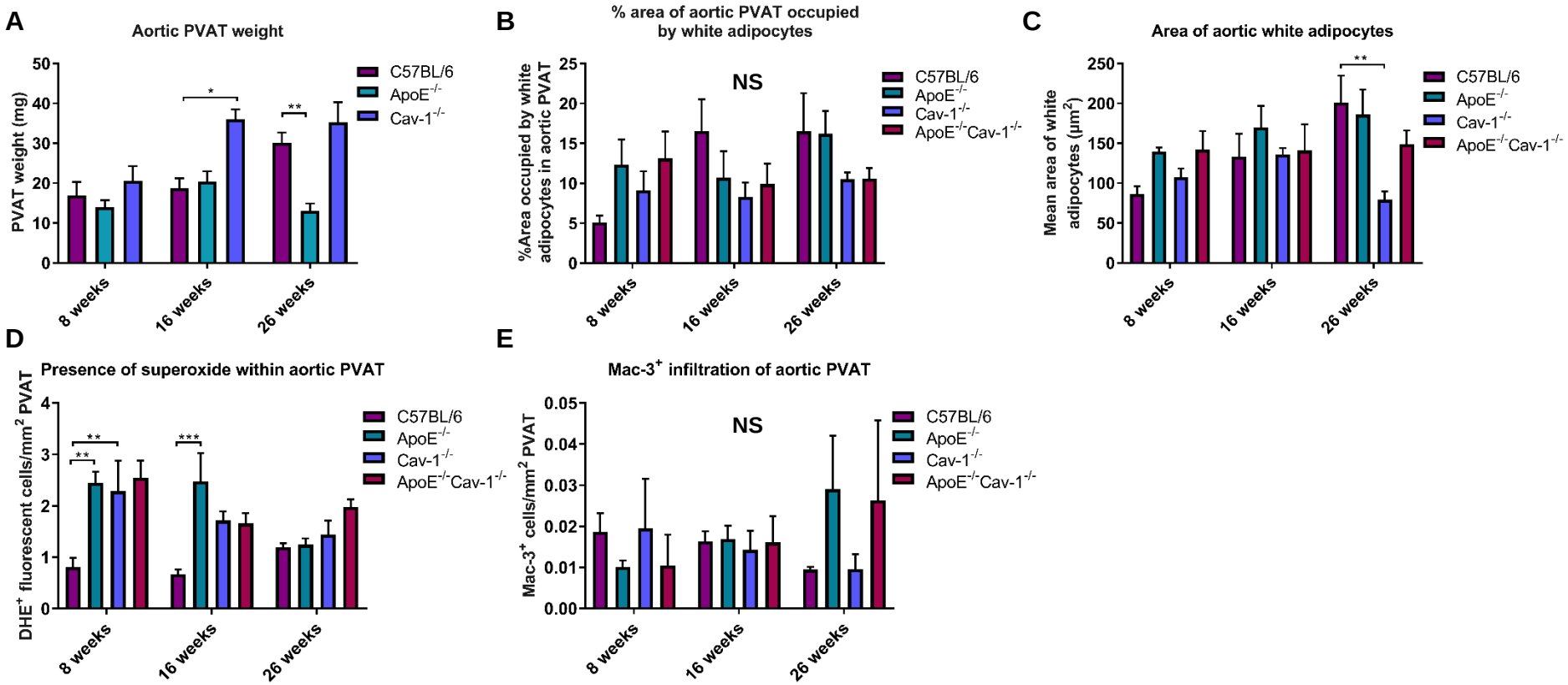

Appendix 2.8 Assessment of aortic PVAT weight and composition in normal diet-fed ApoE$^{-/-}$Cav-1$^{-/-}$ double knockout, ApoE$^{-/-}$ and Cav-1$^{-/-}$ mice

*A) Aortic PVAT from C57BL/6, ApoE$^{-/-}$ and Cav-1$^{-/-}$ mice was dissected away from the aorta and weighed n = 3-8 mice per group. B) Haematoxylin and eosin staining was used to visualise PVAT morphology. The total area occupied of aortic PVAT occupied by white adipocytes was measured. C) White adipocyte area was measured by drawing around the adipocyte outlines. D) Superoxide within aortic PVAT was detected using dihydroethidium (DHE) staining. E) Macrophage infiltration within the PVAT was assessed using a Mac-3 marker. PVAT = perivascular adipose tissue Data are expressed as mean ± S.E.M. DHE^{+} and Mac-3^{+} staining are presented as cells/mm^2 PVAT. Statistical analysis was carried out by two-way ANOVA, with Bonferroni's post hoc tests, n = 3-4 mice per group, * P < 0.05, ** P < 0.01, *** P < 0.001*

~References~

Adebiyi, A., G. Zhao, S. Y. Cheranov, A. Ahmed, et al. (2007). "Caveolin-1 abolishment attenuates the myogenic response in murine cerebral arteries." Am J Physiol Heart Circ Physiol 292(3): 10.

Agarwal, A., M. G. Winner, S. D. Sithu and S. Srivastava (2014). Quantification and Characterization of Atherosclerotic Lesions in Mice. Manual of Research Techniques in Cardiovascular Medicine, John Wiley & Sons, Ltd: 320-331.

Aghamohammadzadeh, R., A. S. Greenstein, R. Yadav, M. Jeziorska, et al. (2013). "Effects of bariatric surgery on human small artery function: evidence for reduction in perivascular adipocyte inflammation, and the restoration of normal anticontractile activity despite persistent obesity." J Am Coll Cardiol 62(2): 128-135.

Ait-Oufella, H., S. Taleb, Z. Mallat and A. Tedgui (2011). "Recent Advances on the Role of Cytokines in Atherosclerosis." Arteriosclerosis, Thrombosis, and Vascular Biology 31(5): 969-979.

Aktan, F. (2004). "iNOS-mediated nitric oxide production and its regulation." Life Sciences 75(6): 639-653.

Alp, N. J., M. A. McAteer, J. Khoo, R. P. Choudhury, et al. (2004). "Increased endothelial tetrahydrobiopterin synthesis by targeted transgenic GTP-cyclohydrolase I overexpression reduces endothelial dysfunction and atherosclerosis in ApoE-knockout mice." Arterioscler Thromb Vasc Biol 24(3): 445-450.

Ang, L. S., R. P. Cruz, A. Hendel and D. J. Granville (2008). "Apolipoprotein E, an important player in longevity and age-related diseases." Exp Gerontol 43(7): 615-622.

Ararat, E. and F. V. Brozovich (2009). "Losartan Decreases p42/44 MAPK Signaling and Preserves LZ+ MYPT1 Expression." PLoS ONE 4(4): e5144.

Araujo, H. N., C. P. Valgas da Silva, A. C. Sponton, S. P. Clerici, et al. (2015). "Perivascular adipose tissue and vascular responses in healthy trained rats." Life Sci 125: 79-87.

Ardanaz, N., W. H. Beierwaltes and P. J. Pagano (2008). "Distinct hydrogen peroxide-induced constriction in multiple mouse arteries: potential influence of vascular polarization." Pharmacol Rep 60(1): 61-67.

Ardanaz, N. and P. J. Pagano (2006). "Hydrogen peroxide as a paracrine vascular mediator: regulation and signaling leading to dysfunction." Exp Biol Med (Maywood) 231.

Bach, M. E., M. Barad, H. Son, M. Zhuo, et al. (1999). "Age-related defects in spatial memory are correlated with defects in the late phase of hippocampal long-term potentiation in vitro and are attenuated by drugs that enhance the cAMP signaling pathway." Proc Natl Acad Sci U S A 96(9): 5280-5285.

Bai, L., G. Shi, L. Zhang, F. Guan, et al. (2014). "Cav-1 deletion impaired hematopoietic stem cell function." Cell Death & Disease 5(3): e1140.

Bailey-Downs, L. C., Z. Tucsek, P. Toth, D. Sosnowska, et al. (2013). "Aging Exacerbates Obesity-Induced Oxidative Stress and Inflammation in Perivascular Adipose Tissue in Mice: A Paracrine Mechanism Contributing to Vascular Redox Dysregulation and Inflammation." The Journals of Gerontology Series A: Biological Sciences and Medical Sciences 68(7): 780-792.

Ballinger, S. W., C. Patterson, C. A. Knight-Lozano, D. L. Burow, et al. (2002). "Mitochondrial Integrity and Function in Atherogenesis." Circulation 106(5): 544.

Barham, D. and P. Trinder (1972). "An improved colour reagent for the determination of blood glucose by the oxidase system." Analyst 97(1151): 142-145.

Barton, M. (2011). "The discovery of endothelium-dependent contraction: The legacy of Paul M. Vanhoutte." Pharmacological Research 63(6): 455-462.

Barton, M., C. C. Haudenschild, L. V. d'Uscio, S. Shaw, et al. (1998). "Endothelin ET(A) receptor blockade restores NO-mediated endothelial function and inhibits atherosclerosis in apolipoprotein E-deficient mice." Proc Natl Acad Sci U S A 95(24): 14367-14372.

Bazzoni, G. and E. Dejana (2004). "Endothelial cell-to-cell junctions: molecular organization and role in vascular homeostasis." Physiol Rev 84(3): 869-901.

Bentzon, J. F. and E. Falk (2010). "Atherosclerotic lesions in mouse and man: is it the same disease?" Curr Opin Lipidol 21(5): 434-440.

Beny, J. L., M. N. Nguyen, M. Marino and M. Matsui (2008). "Muscarinic receptor knockout mice confirm involvement of M3 receptor in endothelium-dependent vasodilatation in mouse arteries." J Cardiovasc Pharmacol 51(5): 505-512.

Berthoud, H. R., E. A. Fox and W. L. Neuhuber (2006). "Vagaries of adipose tissue innervation." Am J Physiol Regul Integr Comp Physiol 291(5): R1240-1242.

Bhatia, M. (2005). "Hydrogen sulfide as a vasodilator." IUBMB Life 57(9): 603-606.

Bjorndal, B., L. Burri, V. Staalesen, J. Skorve, et al. (2011). "Different adipose depots: their role in the development of metabolic syndrome and mitochondrial response to hypolipidemic agents." J Obes 2011: 490650.

Blackwell, B. N., T. J. Bucci, R. W. Hart and A. Turturro (1995). "Longevity, body weight, and neoplasia in ad libitum-fed and diet-restricted C57BL6 mice fed NIH-31 open formula diet." Toxicol Pathol 23(5): 570-582.

Blackwell, K. A., J. P. Sorenson, D. M. Richardson, L. A. Smith, et al. (2004). "Mechanisms of aging-induced impairment of endothelium-dependent relaxation: role of tetrahydrobiopterin." American Journal of Physiology - Heart and Circulatory Physiology 287(6): H2448-H2453.

Blankenberg, S., S. Barbaux and L. Tiret (2003). "Adhesion molecules and atherosclerosis." Atherosclerosis 170(2): 191-203.

Blough, E. R., K. M. Rice, D. H. Desai, P. Wehner, et al. (2007). "Aging alters mechanical and contractile properties of the Fisher 344/Nnia X Norway/Binia rat aorta." Biogerontology 8(3): 303-313.

Boguski, M. S. Comparative genomics: the mouse that roared, Nature. 2002 Dec 5;420(6915):515-6.

Bonaventura, D., C. N. Lunardi, G. J. Rodrigues, M. A. Neto, et al. (2008). "A novel mechanism of vascular relaxation induced by sodium nitroprusside in the isolated rat aorta." Nitric Oxide 18(4): 287-295.

Bond, A. R. and C. L. Jackson (2011). "The fat-fed apolipoprotein E knockout mouse brachiocephalic artery in the study of atherosclerotic plaque rupture." J Biomed Biotechnol 2011: 379069.

Bonomini, F., F. Filippini, T. Hayek, M. Aviram, et al. (2010). "Apolipoprotein E and its role in aging and survival." Experimental Gerontology 45(2): 149-157.

Bonthu, S., D. D. Heistad, D. A. Chappell, K. G. Lamping, et al. (1997). "Atherosclerosis, vascular remodeling, and impairment of endothelium-dependent relaxation in genetically altered hyperlipidemic mice." Arterioscler Thromb Vasc Biol 17(11): 2333-2340.

Bostrom, P., J. Wu, M. P. Jedrychowski, A. Korde, et al. (2012). "A PGC1-[agr]-dependent myokine that drives brown-fat-like development of white fat and thermogenesis." Nature 481(7382): 463-468.

Bournat, J. C. and C. W. Brown (2010). "Mitochondrial dysfunction in obesity." Curr Opin Endocrinol Diabetes Obes 17(5): 446-452.

Boydens, C., N. Maenhaut, B. Pauwels, K. Decaluwe, et al. (2012). "Adipose tissue as regulator of vascular tone." Curr Hypertens Rep 14(3): 270-278.

Brandes, R. P. (2007). "The fatter the better? Perivascular adipose tissue attenuates vascular contraction through different mechanisms." Br J Pharmacol 151(3): 303-304.

Brandes, R. P., I. Fleming and R. Busse (2005). "Endothelial aging." Cardiovascular Research 66(2): 286-294.

Brandes, R. P., F. H. Schmitz-Winnenthal, M. Félétou, A. Gödecke, et al. (2000). "An endothelium-derived hyperpolarizing factor distinct from NO and prostacyclin is a major endothelium-dependent vasodilator in resistance vessels of wild-type and endothelial NO synthase knockout mice." Proc Natl Acad Sci USA 97.

Brayton, C. F., P. M. Treuting and J. M. Ward (2012). "Pathobiology of Aging Mice and GEM: Background Strains and Experimental Design." Veterinary Pathology Online 49(1): 85-105.

Briand, N., S. Le Lay, W. C. Sessa, P. Ferre, et al. (2011). "Distinct roles of endothelial and adipocyte caveolin-1 in macrophage infiltration and adipose tissue metabolic activity." Diabetes 60(2): 448-453.

Brinkmann, O., K. Schmerbach, U. J. Tietge, T. Dietrich, et al. (2014). "Changes in arterial function in a mouse model of human familial hypercholesterolaemia." Acta Physiol 211(1): 61-72.

Britton, K. A. and C. S. Fox (2011). "Perivascular adipose tissue and vascular disease." Clinical lipidology 6(1): 79-91.

Britton, K. A., A. Pedley, J. M. Massaro, E. M. Corsini, et al. (2012). "Prevalence, distribution, and risk factor correlates of high thoracic periaortic fat in the Framingham Heart Study." J Am Heart Assoc 1(6): e004200.

Brown, A. J., Z. Teng, P. C. Evans, J. H. Gillard, et al. (2016). "Role of biomechanical forces in the natural history of coronary atherosclerosis." Nat Rev Cardiol 13(4): 210-220.

Brown, N. K., Z. Zhou, J. Zhang, R. Zeng, et al. (2014). "Perivascular adipose tissue in vascular function and disease: a review of current research and animal models." Arterioscler Thromb Vasc Biol 34(8): 1621-1630.

Brozovich, F. V., C. J. Nicholson, C. V. Degen, Y. Z. Gao, et al. (2016). "Mechanisms of Vascular Smooth Muscle Contraction and the Basis for Pharmacologic Treatment of Smooth Muscle Disorders." Pharmacological Reviews 68(2): 476-532.

Bryan, N. S. and M. B. Grisham (2007). "Methods to Detect Nitric Oxide and its Metabolites in Biological Samples." Free radical biology & medicine 43(5): 645-657.

Buchwalow, I. B., T. Podzuweit, W. Böcker, V. E. Samoilova, et al. (2002). "Vascular smooth muscle and nitric oxide synthase." The FASEB Journal 16(6): 500-508.

Bucolo, G. and H. David (1973). "Quantitative determination of serum triglycerides by the use of enzymes." Clin Chem 19(5): 476-482.

Bunker, A. K. and M. H. Laughlin (2010). "Influence of exercise and perivascular adipose tissue on coronary artery vasomotor function in a familial hypercholesterolemic porcine atherosclerosis model." J Appl Physiol (1985) 108(3): 490-497.

Busse, R., G. Edwards, M. Feletou, I. Fleming, et al. (2002). "EDHF: bringing the concepts together." Trends Pharmacol Sci 23(8): 374-380.

Bussey, C. E., S. B. Withers, R. G. Aldous, G. Edwards, et al. (2016). "Obesity-Related Perivascular Adipose Tissue Damage Is Reversed by Sustained Weight Loss in the Rat." Arteriosclerosis, Thrombosis, and Vascular Biology 36(7): 1377-1385.

Calabro, P., I. Samudio, J. T. Willerson and E. T. Yeh (2004). "Resistin promotes smooth muscle cell proliferation through activation of extracellular signal-regulated kinase 1/2 and phosphatidylinositol 3-kinase pathways." Circulation 110(21): 3335-3340.

Caligioni, C. (2009). "Assessing Reproductive Status/Stages in Mice." Current protocols in neuroscience / editorial board, Jacqueline N. Crawley ... [et al.] APPENDIX: Appendix-4I.

Campos, H., C. Khoo and F. M. Sacks (2005). "Diurnal and acute patterns of postprandial apolipoprotein B-48 in VLDL, IDL, and LDL from normolipidemic humans." Atherosclerosis 181(2): 345-351.

Cannon, R. O., 3rd (1998). "Role of nitric oxide in cardiovascular disease: focus on the endothelium." Clin Chem 44(8 Pt 2): 1809-1819.

Caro, C. G., J. M. Fitz-Gerald and R. C. Schroter (1969). "Arterial wall shear and distribution of early atheroma in man." Nature 223(5211): 1159-1160.

Carvajal, J. A., A. M. Germain, J. P. Huidobro-Toro and C. P. Weiner (2000). "Molecular mechanism of cGMP-mediated smooth muscle relaxation." J Cell Physiol 184(3): 409-420.

Catapano, A. L., Ž. Reiner, G. De Backer, I. Graham, et al. (2011). "ESC/EAS Guidelines for the management of dyslipidaemias: The Task Force for the management of dyslipidaemias of the European Society of Cardiology (ESC) and the European Atherosclerosis Society (EAS)." Atherosclerosis 217(1): 3-46.

Celermajer, D. S., K. E. Sorensen, D. J. Spiegelhalter, D. Georgakopoulos, et al. (1994). "Aging is associated with endothelial dysfunction in healthy men years before the age-related decline in women." Journal of the American College of Cardiology 24(2): 471-476.

Chamley-Campbell, J., G. R. Campbell and R. Ross (1979). "The smooth muscle cell in culture." Physiol Rev 59(1): 1-61.

Chang, L., L. Villacorta, R. Li, M. Hamblin, et al. (2012a). "Loss of perivascular adipose tissue on peroxisome proliferator-activated receptor-gamma deletion in smooth muscle cells impairs intravascular thermoregulation and enhances atherosclerosis." Circulation 126(9): 1067-1078.

Chang, L., L. Villacota, C. Dou, E. Chen, et al. (2012b). "Abstract 662: Perivascular Adipose Tissue-derived Prostaglandins Constrict Vessel." Hypertension 60(Suppl 1): A662-A662.

Chatterjee, T. K., L. L. Stoll, G. M. Denning, A. Harrelson, et al. (2009). "Proinflammatory phenotype of perivascular adipocytes: influence of high-fat feeding." Circ Res 104(4): 541-549.

Chen, G. and H. Suzuki (1989). "Some electrical properties of the endothelium-dependent hyperpolarization recorded from rat arterial smooth muscle cells." J Physiol 410: 91-106.

Chen, Y., X. Wang, J. Mai, X. Zhao, et al. (2013). "C-reactive protein promotes vascular endothelial dysfunction partly via activating adipose tissue inflammation in hyperlipidemic rabbits." Int J Cardiol 168(3): 2397-2403.

Chidlow, J. H., Jr. and W. C. Sessa (2010). "Caveolae, caveolins, and cavins: complex control of cellular signalling and inflammation." Cardiovasc Res 86(2): 219-225.

Chiu, J. J. and S. Chien (2011). "Effects of disturbed flow on vascular endothelium: pathophysiological basis and clinical perspectives." Physiol Rev 91(1): 327-387.

Cho, K. A. and S. C. Park (2005). "Caveolin-1 as a prime modulator of aging: a new modality for phenotypic restoration?" Mech Ageing Dev 126(1): 105-110.

Cinti, S. (2005). "The adipose organ." Prostaglandins Leukot Essent Fatty Acids 73(1): 9-15.

Cobb C., W. R., Farrell K., Eisner D., Austin C., Holt C. (2013). Abstract Endothelial-dependent relaxation in the murine thoracic aorta is transiently increased after high fat feeding. International Union of Physiological Sciences Meeting 2013, University of Manchester.

Cobb, C. J. (2013). Vascular Function Prior to the Development of Overt Atherosclerosis. Doctor of Philosophy, University of Manchester.

Cohen, A. W., R. Hnasko, W. Schubert and M. P. Lisanti (2004a). "Role of caveolae and caveolins in health and disease." Physiol Rev 84(4): 1341-1379.

Cohen, A. W., D. S. Park, S. E. Woodman, T. M. Williams, et al. (2003a). "Caveolin-1 null mice develop cardiac hypertrophy with hyperactivation of p42/44 MAP kinase in cardiac fibroblasts." American Journal of Physiology - Cell Physiology 284(2): C457-C474.

Cohen, A. W., B. Razani, W. Schubert, T. M. Williams, et al. (2004b). "Role of Caveolin-1 in the Modulation of Lipolysis and Lipid Droplet Formation." Diabetes 53(5): 1261-1270.

Cohen, A. W., B. Razani, X. B. Wang, T. P. Combs, et al. (2003b). "Caveolin-1-deficient mice show insulin resistance and defective insulin receptor protein expression in adipose tissue." Am J Physiol Cell Physiol 285(1): 26.

Cohen, A. W., W. Schubert, D. L. Brasaemle, P. E. Scherer, et al. (2005). "Caveolin-1 expression is essential for proper nonshivering thermogenesis in brown adipose tissue." Diabetes 54(3): 679-686.

Cohen , J. C., E. Boerwinkle , T. H. J. Mosley and H. H. Hobbs (2006). "Sequence Variations in PCSK9, Low LDL, and Protection against Coronary Heart Disease." New England Journal of Medicine 354(12): 1264-1272.

Coleman, R., T. Hayek, S. Keidar and M. Aviram (2006). "A mouse model for human atherosclerosis: Long-term histopathological study of lesion development in the aortic arch of apolipoprotein E-deficient (E0) mice." Acta Histochemica 108(6): 415-424.

Conti, M. A. and R. S. Adelstein (1981). "The relationship between calmodulin binding and phosphorylation of smooth muscle myosin kinase by the catalytic subunit of 3':5' cAMP-dependent protein kinase." J Biol Chem 256(7): 3178-3181.

Cooper, A. and A. M. Heagerty (1998). "Endothelial dysfunction in human intramyocardial small arteries in atherosclerosis and hypercholesterolemia." American Journal of Physiology - Heart and Circulatory Physiology 275(4): H1482-H1488.

Cordain, L., S. B. Eaton, A. Sebastian, N. Mann, et al. (2005). "Origins and evolution of the Western diet: health implications for the 21st century." The American Journal of Clinical Nutrition 81(2): 341-354.

Corriu, C., M. Feletou, E. Canet and P. M. Vanhoutte (1996). "Endothelium-derived factors and hyperpolarization of the carotid artery of the guinea-pig." Br J Pharmacol 119(5): 959-964.

Costa, R. M., F. P. Filgueira, R. C. Tostes, M. H. Carvalho, et al. (2016). "H2O2 generated from mitochondrial electron transport chain in thoracic perivascular adipose tissue is crucial for modulation of vascular smooth muscle contraction." Vascul Pharmacol.

Crauwels, H. M., C. E. Van Hove, A. G. Herman and H. Bult (2000). "Heterogeneity in relaxation mechanisms in the carotid and the femoral artery of the mouse." Eur J Pharmacol 404(3): 341-351.

Crauwels, H. M., C. E. Van Hove, P. Holvoet, A. G. Herman, et al. (2003). "Plaque-associated endothelial dysfunction in apolipoprotein E-deficient mice on a regular diet. Effect of human apolipoprotein AI." Cardiovasc Res 59(1): 189-199.

Cypess, A. M., Y. C. Chen, C. Sze, K. Wang, et al. (2012). "Cold but not sympathomimetics activates human brown adipose tissue in vivo." Proc Natl Acad Sci U S A 109(25): 10001-10005.

d'Uscio, L. V., T. A. Baker, C. B. Mantilla, L. Smith, et al. (2001a). "Mechanism of endothelial dysfunction in apolipoprotein E-deficient mice." Arterioscler Thromb Vasc Biol 21(6): 1017-1022.

d'Uscio, L. V., L. A. Smith and Z. S. Katusic (2001b). "Hypercholesterolemia impairs endothelium-dependent relaxations in common carotid arteries of apolipoprotein E-deficient mice." Stroke 32.

Dashwood, M. R., A. Dooley, X. Shi-Wen, D. J. Abraham, et al. (2007). "Does periadventitial fat-derived nitric oxide play a role in improved saphenous vein graft patency in patients undergoing coronary artery bypass surgery?" J Vasc Res 44(3): 175-181.

Deckert, V., G. Lizard, N. Duverger, A. Athias, et al. (1999). "Impairment of endothelium-dependent arterial relaxation by high-fat feeding in ApoE-deficient mice: toward normalization by human ApoA-I expression." Circulation 100(11): 1230-1235.

Deeg, R. and J. Ziegenhorn (1983). "Kinetic enzymic method for automated determination of total cholesterol in serum." Clin Chem 29(10): 1798-1802.

Derbyshire, E. R. and M. A. Marletta (2012). "Structure and regulation of soluble guanylate cyclase." Annu Rev Biochem 81: 533-559.

DeSouza, C. A., L. F. Shapiro, C. M. Clevenger, F. A. Dinenno, et al. (2000). "Regular aerobic exercise prevents and restores age-related declines in endothelium-dependent vasodilation in healthy men." Circulation 102(12): 1351-1357.

Després, J.-P. (2012). "Body Fat Distribution and Risk of Cardiovascular Disease: An Update." Circulation 126(10): 1301-1313.

DeVallance, E., K. Branyan, K. Lemaster, R. Skinner, et al. (2016). "Exercise Training in the Metabolic Syndrome Improves Perivascular Adipose Gene Expression." The FASEB Journal 30(1 Supplement): 771.779.

Dominiczak, A. F., M. McIntyre, D. Rees, C. A. Hamilton, et al. (1997). "Estrogen effects on nitric oxide release." Hypertension 29(6): 1357.

Donato, A. J., L. B. Gano, I. Eskurza, A. E. Silver, et al. (2009). "Vascular endothelial dysfunction with aging: endothelin-1 and endothelial nitric oxide synthase." Am J Physiol Heart Circ Physiol 297(1): 22.

Drab, M., P. Verkade, M. Elger, M. Kasper, et al. (2001). "Loss of caveolae, vascular dysfunction, and pulmonary defects in caveolin-1 gene-disrupted mice." Science 293(5539): 2449-2452.

Du Clos, T. W. (2013). "Pentraxins: structure, function, and role in inflammation." ISRN Inflamm 14(379040): 379040.

Dudzinski, D. M. and T. Michel (2007). "Life history of eNOS: partners and pathways." Cardiovasc Res 75(2): 247-260.

Duffy, S. J., B. T. Tran, G. New, R. N. Tudball, et al. (1998). "Continuous release of vasodilator prostanoids contributes to regulation of resting forearm blood flow in humans." Am J Physiol 274(4 Pt 2): H1174-1183.

Egan, K. M., J. A. Lawson, S. Fries, B. Koller, et al. (2004). "COX-2-derived prostacyclin confers atheroprotection on female mice." Science 306(5703): 1954-1957.

Eichhorn, B. and D. Dobrev (2007). "Vascular large conductance calcium-activated potassium channels: Functional role and therapeutic potential." Naunyn-Schmiedeberg's Archives of Pharmacology 376(3): 145-155.

Elahi, M. M., Y. X. Kong and B. M. Matata (2009). "Oxidative stress as a mediator of cardiovascular disease." Oxidative Medicine and Cellular Longevity 2(5): 259-269.

Engel, D., L. Beckers, E. Wijnands, T. Seijkens, et al. (2011). "Caveolin-1 deficiency decreases atherosclerosis by hampering leukocyte influx into the arterial wall and generating a regulatory T-cell response." FASEB J 25(11): 3838-3848.

Eriksson, J. W. (2007). "Metabolic stress in insulin's target cells leads to ROS accumulation – A hypothetical common pathway causing insulin resistance." FEBS Letters 581(19): 3734-3742.

Everson, W. V. and E. J. Smart (2001). "Influence of caveolin, cholesterol, and lipoproteins on nitric oxide synthase: implications for vascular disease." Trends Cardiovasc Med 11(6): 246-250.

Ewart, M. A., S. Kennedy, D. Macmillan, A. L. Raja, et al. (2014). "Altered vascular smooth muscle function in the ApoE knockout mouse during the progression of atherosclerosis." Atherosclerosis 234(1): 154-161.

Falk, E., P. K. Shah and V. Fuster (1995). "Coronary Plaque Disruption." Circulation 92(3): 657-671.

Farrell, K. A. (2008). C-Myb in the pathogenesis of atherosclerosis. Doctor of Philosophy, University of Manchester.

Fazio, S., V. R. Babaev, M. E. Burleigh, A. S. Major, et al. (2002). "Physiological expression of macrophage apoE in the artery wall reduces atherosclerosis in severely hyperlipidemic mice." J Lipid Res 43(10): 1602-1609.

Fazio, S., V. R. Babaev, A. B. Murray, A. H. Hasty, et al. (1997). "Increased atherosclerosis in mice reconstituted with apolipoprotein E null macrophages." Proc Natl Acad Sci U S A 94(9): 4647-4652.

Fedorenko, A., P. V. Lishko and Y. Kirichok (2012). "Mechanism of fatty-acid-dependent UCP1 uncoupling in brown fat mitochondria." Cell 151(2): 400-413.

Feletou, M. (2011). Integrated Systems Physiology: from Molecule to Function to Disease. The Endothelium: Part 1: Multiple Functions of the Endothelial Cells-Focus on Endothelium-Derived Vasoactive Mediators. San Rafael (CA), Morgan & Claypool Life Sciences

Copyright (c) 2011 by Morgan & Claypool Life Sciences Publishers.

Feletou, M. and P. M. Vanhoutte (2006). "Endothelium-derived hyperpolarizing factor: where are we now?" Arterioscler Thromb Vasc Biol 26(6): 1215-1225.

Fenton, J. I., N. P. Nunez, S. Yakar, S. N. Perkins, et al. (2009). "Diet-induced adiposity alters the serum profile of inflammation in C57BL/6N mice as measured by antibody array." Diabetes Obes Metab 11(4): 343-354.

Ferla, R., M. Bonomi, L. Otvos and E. Surmacz (2011). "Glioblastoma-derived Leptin Induces Tube Formation and Growth of Endothelial Cells: Comparison with VEGF Effects." BMC Cancer 11(1): 1-11.

Fernández-Alfonso, M. S., M. Gil-Ortega, C. F. García-Prieto, I. Aranguez, et al. (2013). "Mechanisms of Perivascular Adipose Tissue Dysfunction in Obesity." International Journal of Endocrinology 2013: 402053.

Fernandez-Hernando, C., J. Yu, A. Davalos, J. Prendergast, et al. (2010). "Endothelial-specific overexpression of caveolin-1 accelerates atherosclerosis in apolipoprotein E-deficient mice." Am J Pathol 177(2): 998-1003.

Fernandez-Hernando, C., J. Yu, Y. Suarez, C. Rahner, et al. (2009). "Genetic evidence supporting a critical role of endothelial caveolin-1 during the progression of atherosclerosis." Cell Metab 10(1): 48-54.

Feron, O., C. Dessy, S. Moniotte, J. P. Desager, et al. (1999). "Hypercholesterolemia decreases nitric oxide production by promoting the interaction of caveolin and endothelial nitric oxide synthase." J Clin Invest 103(6): 897-905.

Fesus, G., G. Dubrovska, K. Gorzelniak, R. Kluge, et al. (2007). "Adiponectin is a novel humoral vasodilator." Cardiovasc Res 75(4): 719-727.

Fielding, C. J. and P. E. Fielding (2000). "Cholesterol and caveolae: structural and functional relationships." Biochim Biophys Acta 1529(1-3): 210-222.

Fischer, A., D. E. Gutstein, Z. A. Fayad and V. Fuster (2000). "Predicting plaque rupture: enhancing diagnosis and clinical decision-making in coronary artery disease." Vasc Med 5(3): 163-172.

Fitzgibbons, T. P. and M. P. Czech (2014). "Epicardial and Perivascular Adipose Tissues and Their Influence on Cardiovascular Disease: Basic Mechanisms and Clinical Associations." Journal of the American Heart Association 3(2).

Fitzgibbons, T. P., S. Kogan, M. Aouadi, G. M. Hendricks, et al. (2011). "Similarity of mouse perivascular and brown adipose tissues and their resistance to diet-induced inflammation." Am J Physiol Heart Circ Physiol 301(4): H1425-1437.

Flammer, A. J. and T. F. Luscher (2010). "Human endothelial dysfunction: EDRFs." Pflugers Arch 459(6): 1005-1013.

Fleming, I. and R. Busse (1999). "NO: the Primary EDRF." Journal of Molecular and Cellular Cardiology 31(1): 5-14.

Flurkey, K., J. M. Currer and D. E. Harrison (2007). Chapter 20 - Mouse Models in Aging Research A2 - Fox, James G. The Mouse in Biomedical Research (Second Edition). M. T. Davisson, F. W. Quimby, S. W. Barthold, C. E. Newcomer and A. L. Smith. Burlington, Academic Press: 637-672.

Forrester, J. S. (2010). "Redefining Normal Low-Density Lipoprotein Cholesterol: A Strategy to Unseat Coronary Disease as the Nation's Leading Killer." J Am Coll Cardiol 56(8): 630-636.

Forstermann, U. and T. Munzel (2006). "Endothelial nitric oxide synthase in vascular disease: from marvel to menace." Circulation 113(13): 1708-1714.

Forte, P., B. J. Kneale, E. Milne, P. J. Chowienczyk, et al. (1998). "Evidence for a difference in nitric oxide biosynthesis between healthy women and men." Hypertension 32(4): 730-734.

Fournet-Bourguignon, M.-P., M. Castedo-Delrieu, J.-P. Bidouard, S. Leonce, et al. (2000). "Phenotypic and Functional Changes in Regenerated Porcine Coronary Endothelial Cells." Increased Uptake of Modified LDL and Reduced Production of NO 86(8): 854-861.

Frank, P. G. (2010). "Endothelial caveolae and caveolin-1 as key regulators of atherosclerosis." Am J Pathol 177(2): 544-546.

Frank, P. G., M. W. Cheung, S. Pavlides, G. Llaverias, et al. (2006). "Caveolin-1 and regulation of cellular cholesterol homeostasis." Am J Physiol Heart Circ Physiol 291(2): H677-686.

Frank, P. G., H. Lee, D. S. Park, N. N. Tandon, et al. (2004a). "Genetic ablation of caveolin-1 confers protection against atherosclerosis." Arterioscler Thromb Vasc Biol 24(1): 98-105.

Frank, P. G. and M. P. Lisanti (2004b). "Caveolin-1 and caveolae in atherosclerosis: differential roles in fatty streak formation and neointimal hyperplasia." Curr Opin Lipidol 15(5): 523-529.

Frank, P. G., S. Pavlides, M. W. Cheung, K. Daumer, et al. (2008). "Role of caveolin-1 in the regulation of lipoprotein metabolism." Am J Physiol Cell Physiol 295(1): C242-248.

Frank, P. G., S. Pavlides and M. P. Lisanti (2009). "Caveolae and transcytosis in endothelial cells: role in atherosclerosis." Cell Tissue Res 335(1): 41-47.

Frank, P. G., S. E. Woodman, D. S. Park and M. P. Lisanti (2003). "Caveolin, caveolae, and endothelial cell function." Arterioscler Thromb Vasc Biol 23(7): 1161-1168.

Fransen, P., T. Van Assche, P. J. Guns, C. E. Van Hove, et al. (2008). "Endothelial function in aorta segments of apolipoprotein E-deficient mice before development of atherosclerotic lesions." Pflugers Arch 455.

Fridez, P., A. Makino, D. Kakoi, H. Miyazaki, et al. (2002). "Adaptation of conduit artery vascular smooth muscle tone to induced hypertension." Ann Biomed Eng 30(7): 905-916.

Frith, C. H., B. Highman, G. Burger and W. D. Sheldon (1983). "Spontaneous lesions in virgin and retired breeder BALB/c and C57BL/6 mice." Lab Anim Sci 33(3): 273-286.

Fu, C., J. He, C. Li, J. Y. Shyy, et al. (2010). "Cholesterol increases adhesion of monocytes to endothelium by moving adhesion molecules out of caveolae." Biochim Biophys Acta 1801(7): 702-710.

Fu, Y., X. L. Moore, M. K. Lee, M. A. Fernandez-Rojo, et al. (2012). "Caveolin-1 plays a critical role in the differentiation of monocytes into macrophages." Arterioscler Thromb Vasc Biol 32(9): e117-125.

Fukami, K., S. Yamagishi and S. Okuda (2014). "Role of AGEs-RAGE system in cardiovascular disease." Curr Pharm Des 20(14): 2395-2402.

Furchgott, R. F. (1996). "THe discovery of endothelium-derived relaxing factor and its importance in the identification of nitric oxide." JAMA 276(14): 1186-1188.

Furchgott, R. F. and P. M. Vanhoutte (1989). "Endothelium-derived relaxing and contracting factors." Faseb j 3(9): 2007-2018.

Furchgott, R. F. and J. V. Zawadzki (1980). "The obligatory role of endothelial cells in the relaxation of arterial smooth muscle by acetylcholine." Nature 288(5789): 373-376.

Furfine, E. S., M. F. Harmon, J. E. Paith and E. P. Garvey (1993). "Selective inhibition of constitutive nitric oxide synthase by L-NG-nitroarginine." Biochemistry 32(33): 8512-8517.

Furfine, E. S., M. F. Harmon, J. E. Paith, R. G. Knowles, et al. (1994). "Potent and selective inhibition of human nitric oxide synthases. Selective inhibition of neuronal nitric oxide synthase by S-methyl-L-thiocitrulline and S-ethyl-L-thiocitrulline." J Biol Chem 269(43): 26677-26683.

Galvez-Prieto, B., B. Somoza, M. Gil-Ortega, C. F. Garcia-Prieto, et al. (2012). "Anticontractile Effect of Perivascular Adipose Tissue and Leptin are Reduced in Hypertension." Front Pharmacol 3: 103.

Gao, J., H. Katagiri, Y. Ishigaki, T. Yamada, et al. (2007a). "Involvement of Apolipoprotein E in Excess Fat Accumulation and Insulin Resistance." Diabetes 56(1): 24-33.

Gao, Y. J. (2007). "Dual modulation of vascular function by perivascular adipose tissue and its potential correlation with adiposity/lipoatrophy-related vascular dysfunction." Curr Pharm Des 13(21): 2185-2192.

Gao, Y. J., C. Lu, L. Y. Su, A. M. Sharma, et al. (2007b). "Modulation of vascular function by perivascular adipose tissue: the role of endothelium and hydrogen peroxide." Br J Pharmacol 151(3): 323-331.

Gao, Y. J., K. Takemori, L. Y. Su, W. S. An, et al. (2006). "Perivascular adipose tissue promotes vasoconstriction: the role of superoxide anion." Cardiovasc Res 71(2): 363-373.

Gao, Y. J., Z. H. Zeng, K. Teoh, A. M. Sharma, et al. (2005). "Perivascular adipose tissue modulates vascular function in the human internal thoracic artery." J Thorac Cardiovasc Surg 130(4): 1130-1136.

Garcia-Cardena, G., P. Oh, J. Liu, J. E. Schnitzer, et al. (1996). "Targeting of nitric oxide synthase to endothelial cell caveolae via palmitoylation: implications for nitric oxide signaling." Proc Natl Acad Sci U S A 93(13): 6448-6453.

Gasparrini, M., D. Rivas, A. Elbaz and G. Duque (2009). "Differential expression of cytokines in subcutaneous and marrow fat of aging C57BL/6J mice." Exp Gerontol 44(9): 613-618.

Georgeon-Chartier, C., C. Menguy, A. Prevot and J. L. Morel (2013). "Effect of aging on calcium signaling in C57Bl6J mouse cerebral arteries." Pflugers Arch 465(6): 829-838.

Gerhard, M., M. A. Roddy, S. J. Creager and M. A. Creager (1996). "Aging progressively impairs endothelium-dependent vasodilation in forearm resistance vessels of humans." Hypertension 27(4): 849-853.

Getz, G. S. and C. A. Reardon (2012). "Animal models of atherosclerosis." Arterioscler Thromb Vasc Biol 32(5): 1104-1115.

Ghitescu, L., A. Fixman, M. Simionescu and N. Simionescu (1986). "Specific binding sites for albumin restricted to plasmalemmal vesicles of continuous capillary endothelium: receptor-mediated transcytosis." J Cell Biol 102(4): 1304-1311.

Gil-Ortega, M., P. Stucchi, R. Guzmán-Ruiz, V. Cano, et al. (2010). "Adaptative Nitric Oxide Overproduction in Perivascular Adipose Tissue during Early Diet-Induced Obesity." Endocrinology 151(7): 3299-3306.

Giordano, A., C. Tonello, A. Bulbarelli, V. Cozzi, et al. (2002). "Evidence for a functional nitric oxide synthase system in brown adipocyte nucleus." FEBS Lett 514(2-3): 135-140.

Gollasch, M. (2012). "Vasodilator signals from perivascular adipose tissue." Br J Pharmacol 165(3): 633-642.

Gollasch, M. and G. Dubrovska (2004a). "Paracrine role for periadventitial adipose tissue in the regulation of arterial tone." Trends in Pharmacological Sciences 25(12): 647-653.

Gollasch, M. and G. Dubrovska (2004b). "Paracrine role for periadventitial adipose tissue in the regulation of arterial tone." Trends Pharmacol Sci 25(12): 647-653.

Gomez, D. and G. K. Owens (2012). "Smooth muscle cell phenotypic switching in atherosclerosis." Cardiovasc Res 95(2): 156-164.

Goode, G. K. and A. M. Heagerty (1995). "In Vitro Responses of Human Peripheral Small Arteries in Hypercholesterolemia and Effects of Therapy." Circulation 91(12): 2898-2903.

Goodwin, D. C., L. M. Landino and L. J. Marnett (1999). "Effects of nitric oxide and nitric oxide-derived species on prostaglandin endoperoxide synthase and prostaglandin biosynthesis." Faseb j 13(10): 1121-1136.

Gotsman, I., R. Gupta and A. H. Lichtman (2007). "The influence of the regulatory T lymphocytes on atherosclerosis." Arterioscler Thromb Vasc Biol 27(12): 2493-2495.

Graja, A. and T. J. Schulz (2015). "Mechanisms of Aging-Related Impairment of Brown Adipocyte Development and Function." Gerontology 61(3): 211-217.

Grayson, T. H., P. S. Chadha, P. P. Bertrand, H. Chen, et al. (2013). "Increased caveolae density and caveolin-1 expression accompany impaired NO-mediated vasorelaxation in diet-induced obesity." Histochem Cell Biol 139(2): 309-321.

Greenstein, A. S. (2012). "New Targets and Opportunities at the Level of the Endothelium." Hypertension 60(4): 896-897.

Greenstein, A. S., K. Khavandi, S. B. Withers, K. Sonoyama, et al. (2009). "Local inflammation and hypoxia abolish the protective anticontractile properties of perivascular fat in obese patients." Circulation 119(12): 1661-1670.

Greif, M., A. Becker, F. von Ziegler, C. Lebherz, et al. (2009). "Pericardial adipose tissue determined by dual source CT is a risk factor for coronary atherosclerosis." Arterioscler Thromb Vasc Biol 29(5): 781-786.

Gros, R., R. Van Wert, X. You, E. Thorin, et al. (2002). "Effects of age, gender, and blood pressure on myogenic responses of mesenteric arteries from C57BL/6 mice." American Journal of Physiology - Heart and Circulatory Physiology 282(1): H380-H388.

Guzik, T. J., N. E. West, R. Pillai, D. P. Taggart, et al. (2002). "Nitric oxide modulates superoxide release and peroxynitrite formation in human blood vessels." Hypertension 39(6): 1088-1094.

Harrison, D. G. (1997). "Endothelial function and oxidant stress." Clin Cardiol 20(11 Suppl 2): Ii-11-17.

Hashimoto, Y. and T. R. Soderling (1990). "Phosphorylation of smooth muscle myosin light chain kinase by Ca2+/calmodulin-dependent protein kinase II: comparative study of the phosphorylation sites." Arch Biochem Biophys 278(1): 41-45.

Hausman, N., J. Martin, M. J. Taggart and C. Austin (2012). "Age-related changes in the contractile and passive arterial properties of murine mesenteric small arteries are altered by caveolin-1 knockout." J Cell Mol Med 16(8): 1720-1730.

Head, B. P., J. N. Peart, M. Panneerselvam, T. Yokoyama, et al. (2010). "Loss of Caveolin-1 Accelerates Neurodegeneration and Aging." PLoS One 5(12): e15697.

Heimerl, S., G. Liebisch, S. L. Lay, A. Böttcher, et al. (2008). "Caveolin-1 deficiency alters plasma lipid and lipoprotein profiles in mice." Biochemical and Biophysical Research Communications 367(4): 826-833.

Hemmeryckx, B., D. Loeckx, T. Dresselaers, U. Himmelreich, et al. (2010). "Age-associated adaptations in murine adipose tissues." Endocr J 57(10): 925-930.

Henrichot, E., C. E. Juge-Aubry, A. Pernin, J. C. Pache, et al. (2005). "Production of chemokines by perivascular adipose tissue: a role in the pathogenesis of atherosclerosis?" Arterioscler Thromb Vasc Biol 25(12): 2594-2599.

Henrion, D. (2005). "Pressure and flow-dependent tone in resistance arteries. Role of myogenic tone." Arch Mal Coeur Vaiss 98(9): 913-921.

Herman, A. G. and S. Moncada (2005). "Therapeutic potential of nitric oxide donors in the prevention and treatment of atherosclerosis." Eur Heart J 26(19): 1945-1955.

Hermenegildo, C., P. J. Oviedo, M. A. García-Pérez, J. J. Tarín, et al. (2005). "Effects of Phytoestrogens Genistein and Daidzein on Prostacyclin Production by Human Endothelial Cells." Journal of Pharmacology and Experimental Therapeutics 315(2): 722-728.

Hofmann, S. M., D. Perez-Tilve, T. M. Greer, B. A. Coburn, et al. (2008). "Defective Lipid Delivery Modulates Glucose Tolerance and Metabolic Response to Diet in Apolipoprotein E–Deficient Mice." Diabetes 57(1): 5-12.

Holguin, N., R. Aguilar, R. A. Harland, B. A. Bomar, et al. (1985). "The aging mouse partially models the aging human spine: lumbar and coccygeal disc height, composition, mechanical properties, and Wnt signaling in young and old mice." J Appl Physiol 116(12): 1551-1560.

Hosogai, N., A. Fukuhara, K. Oshima, Y. Miyata, et al. (2007). "Adipose tissue hypoxia in obesity and its impact on adipocytokine dysregulation." Diabetes 56(4): 901-911.

Houtkooper, R. H., C. Argmann, S. M. Houten, C. Cantó, et al. (2011). "The metabolic footprint of aging in mice." Scientific Reports 1: 134.

Huang, Z. H., C. A. Reardon and T. Mazzone (2006). "Endogenous ApoE Expression Modulates Adipocyte Triglyceride Content and Turnover." Diabetes 55(12): 3394-3402.

Huo, Y. and K. Ley (2001). "Adhesion molecules and atherogenesis." Acta Physiol Scand 173(1): 35-43.

Iacobellis, G., N. Singh, S. Wharton and A. M. Sharma (2008). "Substantial Changes in Epicardial Fat Thickness After Weight Loss in Severely Obese Subjects." Obesity 16(7): 1693-1697.

Ignarro, L. J., R. E. Byrns, G. M. Buga, K. S. Wood, et al. (1988). "Pharmacological evidence that endothelium-derived relaxing factor is nitric oxide: use of pyrogallol and superoxide dismutase to study endothelium-dependent and nitric oxide-elicited vascular smooth muscle relaxation." J Pharmacol Exp Ther 244(1): 181-189.

Intengan, H. D. and E. L. Schiffrin (2000). "Structure and Mechanical Properties of Resistance Arteries in Hypertension." Role of Adhesion Molecules and Extracellular Matrix Determinants 36(3): 312-318.

Ishida, I., H. Kubo, S. Suzuki, T. Suzuki, et al. (2002). "Hypoxia diminishes toll-like receptor 4 expression through reactive oxygen species generated by mitochondria in endothelial cells." J Immunol 169(4): 2069-2075.

Iwabu, M., T. Yamauchi, M. Okada-Iwabu, K. Sato, et al. (2010). "Adiponectin and AdipoR1 regulate PGC-1alpha and mitochondria by Ca(2+) and AMPK/SIRT1." Nature 464(7293): 1313-1319.

Jawien, J., P. Nastalek and R. Korbut (2004). "Mouse models of experimental atherosclerosis." J Physiol Pharmacol 55(3): 503-517.

Jespersen, N. Z., T. J. Larsen, L. Peijs, S. Daugaard, et al. (2013). "A classical brown adipose tissue mRNA signature partly overlaps with brite in the supraclavicular region of adult humans." Cell Metab 17(5): 798-805.

Johansson, M. E., U. Hagg, J. Wikstrom, A. Wickman, et al. (2005). "Haemodynamically significant plaque formation and regional endothelial dysfunction in cholesterol-fed ApoE$^{-/-}$ mice." Clin Sci (Lond) 108(6): 531-538.

Johns, A., P. Leijten, H. Yamamoto, K. Hwang, et al. (1987). "Calcium regulation in vascular smooth muscle contractility." Am J Cardiol 59(2): 18a-23a.

Johnson-Leger, C. A., M. Aurrand-Lions, N. Beltraminelli, N. Fasel, et al. (2002). "Junctional adhesion molecule-2 (JAM-2) promotes lymphocyte transendothelial migration." Blood 100(7): 2479-2486.

Johnson, J. L. and C. L. Jackson (2001). "Atherosclerotic plaque rupture in the apolipoprotein E knockout mouse." Atherosclerosis 154(2): 399-406.

Jonker, J. W., J. M. Suh, A. R. Atkins, M. Ahmadian, et al. (2012). "A PPAR[ggr]-FGF1 axis is required for adaptive adipose remodelling and metabolic homeostasis." Nature 485(7398): 391-394.

Joshi, S., V. Sedivy, D. Hodyc, J. Herget, et al. (2009). "KCNQ Modulators Reveal a Key Role for KCNQ Potassium Channels in Regulating the Tone of Rat Pulmonary Artery Smooth Muscle." The Journal of Pharmacology and Experimental Therapeutics 329(1): 368-376.

Judkins, C. P., C. G. Sobey, T. T. Dang, A. A. Miller, et al. (2006). "NADPH-induced contractions of mouse aorta do not involve NADPH oxidase: a role for P2X receptors." J Pharmacol Exp Ther 317(2): 644-650.

Kalinowski, L. and T. Malinski (2004). "Endothelial NADH/NADPH-dependent enzymatic sources of superoxide production: relationship to endothelial dysfunction." Acta Biochim Pol 51(2): 459-469.

Karagiannides, I., R. Abdou, A. Tzortzopoulou, P. J. Voshol, et al. (2008). "Apolipoprotein E predisposes to obesity and related metabolic dysfunctions in mice." FEBS Journal 275(19): 4796-4809.

Karavia, E. A., D. J. Papachristou, I. Kotsikogianni, I. Giopanou, et al. (2011). "Deficiency in apolipoprotein E has a protective effect on diet-induced nonalcoholic fatty liver disease in mice." FEBS Journal 278(17): 3119-3129.

Kauser, K., V. da Cunha, R. Fitch, C. Mallari, et al. (2000). "Role of endogenous nitric oxide in progression of atherosclerosis in apolipoprotein E-deficient mice." American Journal of Physiology - Heart and Circulatory Physiology 278(5): H1679-H1685.

Kawahito, H., H. Yamada, D. Irie, T. Kato, et al. (2013). "Periaortic adipose tissue-specific activation of the renin-angiotensin system contributes to atherosclerosis development in uninephrectomized apoE$^{-/-}$ mice." Am J Physiol Heart Circ Physiol 305(5): H667-675.

Kawashima, S., T. Yamashita, M. Ozaki, Y. Ohashi, et al. (2001). "Endothelial NO synthase overexpression inhibits lesion formation in mouse model of vascular remodeling." Arterioscler Thromb Vasc Biol 21(2): 201-207.

Ketonen, J., J. Shi, E. Martonen and E. Mervaala (2010). "Periadventitial adipose tissue promotes endothelial dysfunction via oxidative stress in diet-induced obese C57Bl/6 mice." Circ J 74(7): 1479-1487.

Kiefer, F. W., P. Cohen and J. Plutzky (2012). "Fifty shades of brown: perivascular fat, thermogenesis, and atherosclerosis." Circulation 126(9): 1012-1015.

Kim, M.-K., T. Tomita, M.-J. Kim, H. Sasai, et al. (2009). "Aerobic exercise training reduces epicardial fat in obese men." Journal of Applied Physiology 106(1): 5-11.

Kim, M. J., J. Dawes and W. Jessup (1994). "Transendothelial transport of modified low-density lipoproteins." Atherosclerosis 108(1): 5-17.

Kimura, K., K. Tsuda, A. Baba, T. Kawabe, et al. (2000). "Involvement of nitric oxide in endothelium-dependent arterial relaxation by leptin." Biochem Biophys Res Commun 273(2): 745-749.

Knot, H. J. and M. T. Nelson (1998). "Regulation of arterial diameter and wall [Ca2+] in cerebral arteries of rat by membrane potential and intravascular pressure." J Physiol 508 (Pt 1): 199-209.

Ko, E. A., M. Y. Song, R. Donthamsetty, A. Makino, et al. (2010). "Tension Measurement in Isolated Rat and Mouse Pulmonary Artery." Drug discovery today. Disease models 7(3-4): 123-130.

Köhn, C., J. Schleifenbaum, I. A. Szijártó, L. Markó, et al. (2012). "Differential Effects of Cystathionine-γ-lyase–Dependent Vasodilatory H(2)S in Periadventitial Vasoregulation of Rat and Mouse Aortas." PLoS ONE 7(8): e41951.

Koller, A., D. Sun and G. Kaley (1993). "Role of shear stress and endothelial prostaglandins in flow- and viscosity-induced dilation of arterioles in vitro." Circ Res 72(6): 1276-1284.

Kurtel, H., S. F. Rodrigues, C. E. Yilmaz, A. Yildirim, et al. (2013). "Impaired vasomotor function induced by the combination of hypertension and hypercholesterolemia." Journal of the American Society of Hypertension : JASH 7(1): 14-23.

Kwak, B. R., M. Bäck, M.-L. Bochaton-Piallat, G. Caligiuri, et al. (2014). "Biomechanical factors in atherosclerosis: mechanisms and clinical implications()." European Heart Journal 35(43): 3013-3020.

Kypreos, K. E., S. Zafirovic, P.-I. Petropoulou, P. Bjelogrlic, et al. (2014). "Regulation of Endothelial Nitric Oxide Synthase and High-Density Lipoprotein Quality by Estradiol in Cardiovascular Pathology." Journal of Cardiovascular Pharmacology and Therapeutics 19(3): 256-268.

Lakatta, E. G. (2002). "Age-associated cardiovascular changes in health: impact on cardiovascular disease in older persons." Heart Fail Rev 7(1): 29-49.

Lampe, P. D. and A. F. Lau (2000). "Regulation of gap junctions by phosphorylation of connexins." Arch Biochem Biophys 384(2): 205-215.

Lampe, P. D. and A. F. Lau (2004). "The effects of connexin phosphorylation on gap junctional communication." Int J Biochem Cell Biol 36(7): 1171-1186.

Lamping, K. G. and F. M. Faraci (2001). "Role of Sex Differences and Effects of Endothelial NO Synthase Deficiency in Responses of Carotid Arteries to Serotonin." Arterioscler Thromb Vasc Biol 21(4): 523-528.

Landmesser, U., B. Hornig and H. Drexler (2004). "Endothelial function: a critical determinant in atherosclerosis?" Circulation 109.

Laursen, J. B., M. Somers, S. Kurz, L. McCann, et al. (2001). "Endothelial regulation of vasomotion in apoE-deficient mice: implications for interactions between peroxynitrite and tetrahydrobiopterin." Circulation 103(9): 1282-1288.

Lavie, C. J., R. V. Milani and H. O. Ventura (2009). "Obesity and Cardiovascular Disease: Risk Factor, Paradox, and Impact of Weight Loss." J Am Coll Cardiol 53(21): 1925-1932.

Le Blanc, C., C. Mironneau, C. Barbot, M. Henaff, et al. (2004). "Regulation of vascular L-type Ca2+ channels by phosphatidylinositol 3,4,5-trisphosphate." Circ Res 95(3): 300-307.

Le Lay, S. and T. V. Kurzchalia (2005). "Getting rid of caveolins: phenotypes of caveolin-deficient animals." Biochim Biophys Acta 1746(3): 322-333.

Leal, C. M., S. L. Pereira, A. E. Kümmerle, D. M. Leal, et al. (2012a). "Antihypertensive profile of 2-thienyl-3,4-methylenedioxybenzoylhydrazone is mediated by activation of the A2A adenosine receptor." European Journal of Medicinal Chemistry 55: 49-57.

Leal, J., R. Luengo-Fernandez, A. Gray and T. N. in Nichols M, Scarborough P, Rayner M et al. (2012b). Economic Costs. European Cardiovascular Disease Statistics 2012. S. E. H. N. O. K. Løgstrup, S. (European Society of Cardiology). Brussels, European Heart Network: 116-123.

Lee, M. Y. K., H.-F. Tse, C.-W. Siu, S.-G. Zhu, et al. (2007). "Genomic Changes in Regenerated Porcine Coronary Arterial Endothelial Cells." Arteriosclerosis, Thrombosis, and Vascular Biology 27(11): 2443-2449.

Lee, R. M., C. Lu, L. Y. Su and Y. J. Gao (2009). "Endothelium-dependent relaxation factor released by perivascular adipose tissue." J Hypertens 27(4): 782-790.

Lee, S. E. and H. S. Kim (2012). "Human resistin in cardiovascular disease." J Smooth Muscle Res 48(1): 27-35.

Lee, Y.-H., E. P. Mottillo and J. G. Granneman (2014). "Adipose tissue plasticity from WAT to BAT and in between." Biochimica et Biophysica Acta (BBA) - Molecular Basis of Disease 1842(3): 358-369.

Lee, Y. C., H. H. Chang, C. L. Chiang, C. H. Liu, et al. (2011). "Role of perivascular adipose tissue-derived methyl palmitate in vascular tone regulation and pathogenesis of hypertension." Circulation 124(10): 1160-1171.

Lehman, S. J., J. M. Massaro, C. L. Schlett, C. J. O'Donnell, et al. (2010). "Peri-aortic fat, cardiovascular disease risk factors, and aortic calcification: the Framingham Heart Study." Atherosclerosis 210(2): 656-661.

Leiter, E. H., F. Premdas, D. E. Harrison and L. G. Lipson (1988). "Aging and glucose homeostasis in C57BL/6J male mice." FASEB J 2(12): 2807-2811.

Leloup, A. J., C. E. Van Hove, G. R. De Meyer, D. M. Schrijvers, et al. (2015). "Basal activity of voltage-gated Ca(2+) channels controls the IP3-mediated contraction by alpha(1)-adrenoceptor stimulation of mouse aorta segments." Eur J Pharmacol 760: 163-171.

Lembo, G., C. Vecchione, L. Fratta, G. Marino, et al. (2000). "Leptin induces direct vasodilation through distinct endothelial mechanisms." Diabetes 49(2): 293-297.

Leong, X.-F., C.-Y. Ng and K. Jaarin (2015). "Animal Models in Cardiovascular Research: Hypertension and Atherosclerosis." BioMed Research International 2015: 11.

Lessard-Beaudoin, M., M. Laroche, M.-J. Demers, G. Grenier, et al. (2015). "Characterization of age-associated changes in peripheral organ and brain region weights in C57BL/6 mice." Experimental Gerontology 63: 27-34.

Li, L., J. C. Mamputu, N. Wiernsperger and G. Renier (2005). "Signaling pathways involved in human vascular smooth muscle cell proliferation and matrix metalloproteinase-2 expression induced by leptin: inhibitory effect of metformin." Diabetes 54(7): 2227-2234.

Li, M. and N. K. Fukagawa (2010). "Age-related changes in redox signaling and VSMC function." Antioxid Redox Signal 12(5): 641-655.

Li, S., F. Galbiati, D. Volonte, M. Sargiacomo, et al. (1998). "Mutational analysis of caveolin-induced vesicle formation. Expression of caveolin-1 recruits caveolin-2 to caveolae membranes." FEBS Lett 434(1-2): 127-134.

Li, Y., K. Mihara, M. Saifeddine, A. Krawetz, et al. (2011). "Perivascular adipose tissue-derived relaxing factors: release by peptide agonists via proteinase-activated receptor-2 (PAR2) and non-PAR2 mechanisms." Br J Pharmacol 164(8): 1990-2002.

Libby, P., (2001). "Current Concepts of the Pathogenesis of the Acute Coronary Syndromes." Circulation 104(3): 365-372.

Libby, P., P. M. Ridker and G. K. Hansson (2011). "Progress and challenges in translating the biology of atherosclerosis." Nature 473(7347): 317-325.

Lidell, M. E., M. J. Betz, O. Dahlqvist Leinhard, M. Heglind, et al. (2013). "Evidence for two types of brown adipose tissue in humans." Nat Med 19(5): 631-634.

Lin, Y., L. Bai, Y. Chen, N. Zhu, et al. (2015). "Practical assessment of the quantification of atherosclerotic lesions in apoE(-)/(-) mice." Mol Med Rep 12(4): 5298-5306.

Lipman, R. D., R. T. Bronson, D. Wu, D. E. Smith, et al. (1998). "Disease incidence and longevity are unaltered by dietary antioxidant supplementation initiated during middle age in C57BL/6 mice." Mechanisms of Ageing and Development 103(3): 269-284.

Lizcano, F. and D. Vargas (2016). "Biology of Beige Adipocyte and Possible Therapy for Type 2 Diabetes and Obesity." Int J Endocrinol 2016: 9542061.

Lloyd-Jones, D. M., P. F. Wilson, M. G. Larson and et al. (2003). "LIfetime risk of coronary heart disease by cholesterol levels at selected ages." Archives of Internal Medicine 163(16): 1966-1972.

Lohmann, C., N. Schafer, T. von Lukowicz, M. A. Sokrates Stein, et al. (2009). "Atherosclerotic mice exhibit systemic inflammation in periadventitial and visceral adipose tissue, liver, and pancreatic islets." Atherosclerosis 207(2): 360-367.

Lohn, M., G. Dubrovska, B. Lauterbach, F. C. Luft, et al. (2002). "Periadventitial fat releases a vascular relaxing factor." FASEB J 16(9): 1057-1063.

Lu, C., L. Y. Su, R. M. Lee and Y. J. Gao (2011a). "Alterations in perivascular adipose tissue structure and function in hypertension." Eur J Pharmacol 656(1-3): 68-73.

Lu, C., A. X. Zhao, Y. J. Gao and R. M. Lee (2011b). "Modulation of vein function by perivascular adipose tissue." Eur J Pharmacol 657(1-3): 111-116.

Lu, S., S. Purohit, A. Sharma, W. Zhi, et al. (2012). "Serum insulin-like growth factor binding protein 6 (IGFBP6) is increased in patients with type 1 diabetes and its complications." International Journal of Clinical and Experimental Medicine 5(3): 229-237.

Lucchesi, P. A., S. Belmadani and K. Matrougui (2005). "Hydrogen peroxide acts as both vasodilator and vasoconstrictor in the control of perfused mouse mesenteric resistance arteries." J Hypertens 23(3): 571-579.

Lundberg, J. O., M. T. Gladwin and E. Weitzberg (2015). "Strategies to increase nitric oxide signalling in cardiovascular disease." Nat Rev Drug Discov 14(9): 623-641.

Luo, S., H. Lei, H. Qin and Y. Xia (2014). "Molecular mechanisms of endothelial NO synthase uncoupling." Curr Pharm Des 20(22): 3548-3553.

Lusis, A. J. (2000). "Atherosclerosis." Nature 407(6801): 233-241.

Lynch, F. M., S. B. Withers, Z. Yao, M. E. Werner, et al. (2013). "Perivascular adipose tissue-derived adiponectin activates BK(Ca) channels to induce anticontractile responses." Am J Physiol Heart Circ Physiol 304(6): H786-795.

Lyons, D., S. Roy, M. Patel, N. Benjamin, et al. (1997). "Impaired nitric oxide-mediated vasodilatation and total body nitric oxide production in healthy old age." Clin Sci (Lond) 93(6): 519-525.

Ma, L., S. Ma, H. He, D. Yang, et al. (2010). "Perivascular fat-mediated vascular dysfunction and remodeling through the AMPK/mTOR pathway in high-fat diet-induced obese rats." Hypertens Res 33(5): 446-453.

Madamanchi N.R., Vendrov A., Runge M.S., "Oxidative Stress and Vascular Disease" Arterioscler Thromb Vasc Biol 25(1): 29-38.

Maenhaut, N., C. Boydens and J. Van de Voorde (2010). "Hypoxia enhances the relaxing influence of perivascular adipose tissue in isolated mice aorta." Eur J Pharmacol 641(2-3): 207-212.

Maenhaut, N. and J. Van de Voorde (2011). "Regulation of vascular tone by adipocytes." BMC Med 9(25): 1741-7015.

Mahabadi, A. A., N. Reinsch, N. Lehmann, J. Altenbernd, et al. (2010). "Association of pericoronary fat volume with atherosclerotic plaque burden in the underlying coronary artery: a segment analysis." Atherosclerosis 211(1): 195-199.

Maiellaro, K. and W. R. Taylor (2007). "The role of the adventitia in vascular inflammation." Cardiovasc Res 75(4): 640-648.

Malek, A. M., S. L. Alper and S. Izumo (1999). "Hemodynamic shear stress and its role in atherosclerosis." Jama 282(21): 2035-2042.

Malinowski, M., M. A. Deja, K. S. Golba, T. Roleder, et al. (2008). "Perivascular tissue of internal thoracic artery releases potent nitric oxide and prostacyclin-independent anticontractile factor." Eur J Cardiothorac Surg 33(2): 225-231.

Marchesi, C., T. Ebrahimian, O. Angulo, P. Paradis, et al. (2009). "Endothelial nitric oxide synthase uncoupling and perivascular adipose oxidative stress and inflammation contribute to vascular dysfunction in a rodent model of metabolic syndrome." Hypertension 54(6): 1384-1392.

Martin, S., M. A. Fernandez-Rojo, A. C. Stanley, M. Bastiani, et al. (2012). "Caveolin-1 deficiency leads to increased susceptibility to cell death and fibrosis in white adipose tissue: characterization of a lipodystrophic model." PLoS One 7(9): 26.

Martin, W., R. F. Furchgott, G. M. Villani and D. Jothianandan (1986). "Depression of contractile responses in rat aorta by spontaneously released endothelium-derived relaxing factor." J Pharmacol Exp Ther 237(2): 529-538.

Martinet, W., M. W. M. Knaapen, G. R. Y. De Meyer, A. G. Herman, et al. (2002). "Elevated Levels of Oxidative DNA Damage and DNA Repair Enzymes in Human Atherosclerotic Plaques." Circulation 106(8): 927-932.

Marungruang, N., F. Fak and E. Tareke (2016). "Heat-treated high-fat diet modifies gut microbiota and metabolic markers in apoe$^{-/-}$ mice." Nutr Metab 13(22): 016-0083.

Mattu, H. S. and H. S. Randeva (2013). "Role of adipokines in cardiovascular disease." Journal of Endocrinology 216(1): T17-T36.

Matz, R. L., M. Alvarez de Sotomayor, C. Schott and R. Andriantsitohaina (2003). "Preservation of vascular contraction during ageing: dual effect on calcium handling and sensitization." Br J Pharmacol 138(5): 745-750.

Mayr, M., Y. L. Chung, U. Mayr, X. Yin, et al. (2005). "Proteomic and metabolomic analyses of atherosclerotic vessels from apolipoprotein E-deficient mice reveal alterations in inflammation, oxidative stress, and energy metabolism." Arterioscler Thromb Vasc Biol 25(10): 2135-2142.

McGill, H. C., Jr., C. A. McMahan, E. E. Herderick, G. T. Malcom, et al. (2000). "Origin of atherosclerosis in childhood and adolescence." Am J Clin Nutr 72(5 Suppl): 1307S-1315S.

Meijer, R. I., W. Bakker, C. L. Alta, P. Sipkema, et al. (2013). "Perivascular adipose tissue control of insulin-induced vasoreactivity in muscle is impaired in db/db mice." Diabetes 62(2): 590-598.

Meir, K. S. and E. Leitersdorf (2004). "Atherosclerosis in the apolipoprotein-E-deficient mouse: a decade of progress." Arterioscler Thromb Vasc Biol 24(6): 1006-1014.

Melrose, H., G. Edwards, A. H. Heagerty and C. Austin (2015). "LB03.05: THE ANTI-CONTRACTILE EFFECTS OF PVAT ARE MODULATED BY AGE. THE ROLE OF NITRIC OXIDE." J Hypertens 33 Suppl 1: e127.

Menazza, S. and E. Murphy (2016). "The Expanding Complexity of Estrogen Receptor Signaling in the Cardiovascular System." Circulation Research 118(6): 994-1007.

Meyer, M. R., N. C. Fredette, M. Barton and E. R. Prossnitz (2013). "Regulation of vascular smooth muscle tone by adipose-derived contracting factor." PLoS One 8(11): e79245.

Meyer, M. R., N. C. Fredette, M. Barton and E. R. Prossnitz (2014). "Endothelin-1 but not Angiotensin II Contributes to Functional Aging in Murine Carotid Arteries." Life sciences 118(2): 213-218.

Meyrelles, S. S., V. A. Peotta, T. M. Pereira and E. C. Vasquez (2011). "Endothelial Dysfunction in the Apolipoprotein E-deficient Mouse: insights into the influence of diet, gender and aging." Lipids in Health and Disease 10(1): 1-18.

Miao, C. Y. and Z. Y. Li (2012). "The role of perivascular adipose tissue in vascular smooth muscle cell growth." Br J Pharmacol 165(3): 643-658.

Miller, N. E. (1982). "Coronary atherosclerosis and plasma lipoproteins: epidemiology and pathophysiologic considerations." J Cardiovasc Pharmacol 4 Suppl 2: S190-195.

Min, S. Y., J. Kady, M. Nam, R. Rojas-Rodriguez, et al. (2016). "Human 'brite/beige' adipocytes develop from capillary networks, and their implantation improves metabolic homeostasis in mice." Nat Med 22(3): 312-318.

Mineo, C. and P. W. Shaul (2012). "Regulation of eNOS in caveolae." Adv Exp Med Biol 729: 51-62.

Moghadasian, M. H., B. M. Mcmanus, L. B. Nguyen, S. Shefer, et al. (2001). "Pathophysiology of apolipoprotein E deficiency in mice: relevance to apo E-related disorders in humans." The FASEB Journal 15(14): 2623-2630.

Monk, B. A. and S. J. George (2015). "The Effect of Ageing on Vascular Smooth Muscle Cell Behaviour - A Mini-Review." Gerontology 61(5): 416-426.

Montani, J. P., J. F. Carroll, T. M. Dwyer, V. Antic, et al. (2004). "Ectopic fat storage in heart, blood vessels and kidneys in the pathogenesis of cardiovascular diseases." Int J Obes Relat Metab Disord 28 Suppl 4: S58-65.

Moon, S. K., L. J. Thompson, N. Madamanchi, S. Ballinger, et al. (2001). "Aging, oxidative responses, and proliferative capacity in cultured mouse aortic smooth muscle cells." Am J Physiol Heart Circ Physiol 280(6): H2779-2788.

Moore, P. K., O. A. al-Swayeh, N. W. Chong, R. A. Evans, et al. (1990). "L-NG-nitro arginine (L-NOARG), a novel, L-arginine-reversible inhibitor of endothelium-dependent vasodilatation in vitro." Br J Pharmacol 99(2): 408-412.

Muller-Delp, J., S. A. Spier, M. W. Ramsey, L. A. Lesniewski, et al. (2002). "Effects of aging on vasoconstrictor and mechanical properties of rat skeletal muscle arterioles." Am J Physiol Heart Circ Physiol 282(5): H1843-1854.

Muller, W. A. (2003). "Leukocyte-endothelial-cell interactions in leukocyte transmigration and the inflammatory response." Trends Immunol 24(6): 327-334.

Mulvany, M. J. and W. Halpern (1977). "Contractile properties of small arterial resistance vessels in spontaneously hypertensive and normotensive rats." Circ Res 41(1): 19-26.

Murphy, J. G. and R. A. Khalil (2000). "Gender-specific reduction in contractility and [Ca(2+)](i) in vascular smooth muscle cells of female rat." Am J Physiol Cell Physiol 278(4): C834-844.

Murray, P. J. and T. A. Wynn (2011). "Protective and pathogenic functions of macrophage subsets." Nat Rev Immunol 11(11): 723-737.

Nakamura, K., J. J. Fuster and K. Walsh (2014). "Adipokines: a link between obesity and cardiovascular disease." J Cardiol 63(4): 250-259.

Nakashima, Y., A. S. Plump, E. W. Raines, J. L. Breslow, et al. (1994). "ApoE-deficient mice develop lesions of all phases of atherosclerosis throughout the arterial tree." Arterioscler Thromb 14(1): 133-140.

Napoli, C., F. P. D'Armiento, F. P. Mancini, A. Postiglione, et al. (1997). "Fatty streak formation occurs in human fetal aortas and is greatly enhanced by maternal hypercholesterolemia. Intimal accumulation of low density lipoprotein and its oxidation precede monocyte recruitment into early atherosclerotic lesions." J Clin Invest 100(11): 2680-2690.

Neves, K. B., Nguyen Dinh Cat, A., Alves-Lopes, R., Hood, K. Y., da Costa, R. M., Mestriner, F. L., Lobato, N. S., Montezano, A. C., Touyz, R. M., Oliveira, A. M., and Tostes, R. C. (in press 2016). "Chemerin receptor blockade improves vascular insulin signaling in diabetic obese mice." Diabetes.

Nichols, M., N. Townsend, P. Scarborough and M. Rayner (2012). European Cardiovascular Disease Statistics 2012. Brussels, Belgium and France, The European Heart Network, the European Society of Cardiology and the British Heart Foundation Health Promotion Research Group.

Nicoletti, A., G. Caligiuri, I. Tornberg, T. Kodama, et al. (1999). "The macrophage scavenger receptor type A directs modified proteins to antigen presentation." Eur J Immunol 29(2): 512-521.

Nisoli, E., C. Tonello, L. Briscini and M. O. Carruba (1997). "Inducible nitric oxide synthase in rat brown adipocytes: implications for blood flow to brown adipose tissue." Endocrinology 138(2): 676-682.

Nissen, S. E., E. Tuzcu, P. Schoenhagen and et al. (2004). "Effect of intensive compared with moderate lipid-lowering therapy on progression of coronary atherosclerosis: A randomized controlled trial." JAMA 291(9): 1071-1080.

Nordestgaard, B. G., M. Benn, P. Schnohr and A. Tybjærg-Hansen (2007). "NOnfasting triglycerides and risk of myocardial infarction, ischemic heart disease, and death in men and women." JAMA 298(3): 299-308.

North, B. J. and D. A. Sinclair (2012). "The intersection between aging and cardiovascular disease." Circ Res 110(8): 1097-1108.

Nunes-Souza, V., C. J. Cesar-Gomes, L. J. Da Fonseca, S. Guedes Gda, et al. (2016). "Aging Increases Susceptibility to High Fat Diet-Induced Metabolic Syndrome in C57BL/6 Mice: Improvement in Glycemic and Lipid Profile after Antioxidant Therapy." Oxid Med Cell Longev 2016: 1987960.

Nystrom, F. H., H. Chen, L.-N. Cong, Y. Li, et al. (1999). "Caveolin-1 Interacts with the Insulin Receptor and Can Differentially Modulate Insulin Signaling in Transfected Cos-7 Cells and Rat Adipose Cells." Molecular Endocrinology 13(12): 2013-2024.

Oelkrug, R., M. Kutschke, C. W. Meyer, G. Heldmaier, et al. (2010). "Uncoupling Protein 1 Decreases Superoxide Production in Brown Adipose Tissue Mitochondria." The Journal of Biological Chemistry 285(29): 21961-21968.

Office for National Statistics. (2015, 23.06.16). "Population Estimates for UK, England and Wales, Scotland and Northern Ireland: mid-2015." from

http://www.ons.gov.uk/peoplepopulationandcommunity/populationandmigration/populationestimates/bulletins/annualmidyearpopulationestimates/mid2015#uk-population-continues-to-age.

Ogami, M., Y. Ikura, M. Ohsawa, T. Matsuo, et al. (2004). "Telomere Shortening in Human Coronary Artery Diseases." Arterioscler Thromb Vasc Biol 24(3): 546-550.

Ohashi, K., M. Nishimura, A. G. Terasaki and H. Nakagawa (1994). "A 36-kDa protein of the dense bodies of smooth muscle cells." J Biochem 116(6): 1354-1359.

Ohashi, Y., S. Kawashima, K. i. Hirata, T. Yamashita, et al. (1998). "Hypotension and reduced nitric oxide-elicited vasorelaxation in transgenic mice overexpressing endothelial nitric oxide synthase." Journal of Clinical Investigation 102(12): 2061-2071.

Öhman, M. K., W. Luo, H. Wang, C. Guo, et al. (2011). "Perivascular visceral adipose tissue induces atherosclerosis in apolipoprotein E deficient mice." Atherosclerosis 219(1): 33-39.

Otter, D. and C. Austin (1999). "Mechanisms of hypoxic vasodilatation of isolated rat mesenteric arteries: a comparison with metabolic inhibition." The Journal of Physiology 516(1): 249-259.

Ouwens, D. M., H. Sell, S. Greulich and J. Eckel (2010). "The role of epicardial and perivascular adipose tissue in the pathophysiology of cardiovascular disease." Journal of Cellular and Molecular Medicine 14(9): 2223-2234.

Owen, M. K., F. A. Witzmann, M. L. McKenney, X. Lai, et al. (2013). "Perivascular adipose tissue potentiates contraction of coronary vascular smooth muscle: influence of obesity." Circulation 128(1): 9-18.

Owens, G. K., M. S. Kumar and B. R. Wamhoff (2004). "Molecular regulation of vascular smooth muscle cell differentiation in development and disease." Physiol Rev 84(3): 767-801.

Ozen, G., A. Daci, X. Norel and G. Topal (2015). "Human perivascular adipose tissue dysfunction as a cause of vascular disease: Focus on vascular tone and wall remodeling." European Journal of Pharmacology 766: 16-24.

Pacher, P., A. Vaslin, R. Benkő, J. G. Mabley, et al. (2004). "A New, Potent Poly(ADP-ribose) Polymerase Inhibitor Improves Cardiac and Vascular Dysfunction Associated with Advanced Aging." Journal of Pharmacology and Experimental Therapeutics 311(2): 485-491.

Paigen, B., B. Y. Ishida, J. Verstuyft, R. B. Winters, et al. (1990). "Atherosclerosis susceptibility differences among progenitors of recombinant inbred strains of mice." Arteriosclerosis 10(2): 316-323.

Paigen, K. (1995). "A miracle enough: the power of mice." Nat Med 1(3): 215-220.

Palmer, R. M., A. G. Ferrige and S. Moncada (1987). "Nitric oxide release accounts for the biological activity of endothelium-derived relaxing factor." Nature 327(6122): 524-526.

Park, A., W. K. Kim and K.-H. Bae (2014). "Distinction of white, beige and brown adipocytes derived from mesenchymal stem cells." World Journal of Stem Cells 6(1): 33-42.

Park, D. S., A. W. Cohen, P. G. Frank, B. Razani, et al. (2003). "Caveolin-1 null ($^{-/-}$) mice show dramatic reductions in life span." Biochemistry 42(51): 15124-15131.

Park, J., J.-J. Chung and J. B. Kim (2007). "New evaluations of redox regulating system in adipose tissue of obesity." Diabetes Research and Clinical Practice 77(3, Supplement): S11-S16.

Park, S. C. (2002). "Functional recovery of senescent cells through restoration of receptor-mediated endocytosis." Mech Ageing Dev 123(8): 917-926.

Park, W. Y., J. S. Park, K. A. Cho, D. I. Kim, et al. (2000). "Up-regulation of caveolin attenuates epidermal growth factor signaling in senescent cells." J Biol Chem 275(27): 20847-20852.

Parolini, I., M. Sargiacomo, F. Galbiati, G. Rizzo, et al. (1999). "Expression of caveolin-1 is required for the transport of caveolin-2 to the plasma membrane. Retention of caveolin-2 at the level of the golgi complex." J Biol Chem 274(36): 25718-25725.

Pavlides, S., J. L. Gutierrez-Pajares, C. Danilo, M. P. Lisanti, et al. (2012). "Atherosclerosis, caveolae and caveolin-1." Adv Exp Med Biol 729: 127-144.

Pavlides, S., J. L. Gutierrez-Pajares, S. Katiyar, J.-F. Jasmin, et al. (2014). "Caveolin-1 regulates the anti-atherogenic properties of macrophages." Cell and Tissue Research 358(3): 821-831.

Payne, B. A. I. and P. F. Chinnery (2015). "Mitochondrial dysfunction in aging: Much progress but many unresolved questions." Biochimica et Biophysica Acta (BBA) - Bioenergetics 1847(11): 1347-1353.

Payne, G. A., H. G. Bohlen, U. D. Dincer, L. Borbouse, et al. (2009). "Periadventitial adipose tissue impairs coronary endothelial function via PKC-beta-dependent phosphorylation of nitric oxide synthase." Am J Physiol Heart Circ Physiol 297(1): H460-465.

Payne, G. A., L. Borbouse, S. Kumar, Z. Neeb, et al. (2010). "Epicardial perivascular adipose-derived leptin exacerbates coronary endothelial dysfunction in metabolic syndrome via a protein kinase C-beta pathway." Arterioscler Thromb Vasc Biol 30(9): 1711-1717.

Payne, G. A., M. C. Kohr and J. D. Tune (2012). "Epicardial perivascular adipose tissue as a therapeutic target in obesity-related coronary artery disease." British Journal of Pharmacology 165(3): 659-669.

Pearson, K. J., J. A. Baur, K. N. Lewis, L. Peshkin, et al. (2008). "Resveratrol delays age-related deterioration and mimics transcriptional aspects of dietary restriction without extending lifespan." Cell metabolism 8(2): 157-168.

Pendse, A. A., J. M. Arbones-Mainar, L. A. Johnson, M. K. Altenburg, et al. (2009). "Apolipoprotein E knock-out and knock-in mice: atherosclerosis, metabolic syndrome, and beyond." J Lipid Res 50 Suppl: S178-182.

Percy, D. H. and S. W. Barthold (2008). Chapter 1. Mouse, Pathology of Laboratory Rodents and Rabbits. Pathology of Laboratory Rodents and Rabbits, Blackwell Publishing Professional: 3-124.

Pereira, S. S., L. G. Teixeira, E. C. Aguilar, R. O. Matoso, et al. (2012). "Differences in adipose tissue inflammation and oxidative status in C57BL/6 and ApoE$^{-/-}$ mice fed high fat diet." Anim Sci J 83(7): 549-555.

Perez-Lopez, F. R., L. Larrad-Mur, A. Kallen, P. Chedraui, et al. (2010). "Gender differences in cardiovascular disease: hormonal and biochemical influences." Reprod Sci 17(6): 511-531.

Perreault, M. and A. Marette (2001). "Targeted disruption of inducible nitric oxide synthase protects against obesity-linked insulin resistance in muscle." Nat Med 7(10): 1138-1143.

Perrotta, I. (2013). "Ultrastructural features of human atherosclerosis." Ultrastruct Pathol 37(1): 43-51.

Peters, L. L., R. F. Robledo, C. J. Bult, G. A. Churchill, et al. (2007). "The mouse as a model for human biology: a resource guide for complex trait analysis." Nat Rev Genet 8(1): 58-69.

Peterson, T. E., L. V. d'Uscio, S. Cao, X. L. Wang, et al. (2009). "Guanosine triphosphate cyclohydrolase I expression and enzymatic activity are present in caveolae of endothelial cells." Hypertension 53(2): 189-195.

Piepoli, M. F., A. W. Hoes, S. Agewall, C. Albus, et al. (2016). "2016 European Guidelines on cardiovascular disease prevention in clinical practice." The Sixth Joint Task Force of the European Society of Cardiology and Other Societies on Cardiovascular Disease Prevention in Clinical Practice (constituted by representatives of 10 societies and by invited experts)Developed with the special contribution of the European Association for Cardiovascular Prevention & Rehabilitation (EACPR) .

Pletcher, M. J., K. Bibbins-Domingo, K. Liu, S. Sidney, et al. (2010). "Nonoptimal Lipids Commonly Present in Young Adults and Coronary Calcium Later in Life: The CARDIA (Coronary Artery Risk Development in Young Adults) Study." Annals of Internal Medicine 153(3): 137-146.

Pletcher, M. J., E. Vittinghoff, A. Thanataveerat, K. Bibbins-Domingo, et al. (2016). "Young Adult Exposure to Cardiovascular Risk Factors and Risk of Events Later in Life: The Framingham Offspring Study." PLoS One 11(5).

Plump, A. S., J. D. Smith, T. Hayek, K. Aalto-Setala, et al. (1992). "Severe hypercholesterolemia and atherosclerosis in apolipoprotein E-deficient mice created by homologous recombination in ES cells." Cell 71(2): 343-353.

Pojoga, L. H., T. M. Yao, L. A. Opsasnick, A. E. Garza, et al. (2014). "Dissociation of Hyperglycemia from Altered Vascular Contraction and Relaxation Mechanisms in Caveolin-1 Null Mice." The Journal of Pharmacology and Experimental Therapeutics 348(2): 260-270.

Pojoga, L. H., T. M. Yao, S. Sinha, R. L. Ross, et al. (2008). "Effect of dietary sodium on vasoconstriction and eNOS-mediated vascular relaxation in caveolin-1-deficient mice." Am J Physiol Heart Circ Physiol 294(3): 4.

Putney, J. W. and T. Tomita (2012). "Phospholipase C Signaling and Calcium Influx." Advances in biological regulation 52(1): 152-164.

Qin, Y. W., P. Ye, J. Q. He, L. Sheng, et al. (2010). "Simvastatin inhibited cardiac hypertrophy and fibrosis in apolipoprotein E-deficient mice fed a "Western-style diet" by increasing PPAR alpha and gamma expression and reducing TC, MMP-9, and Cat S levels." Acta Pharmacol Sin 31(10): 1350-1358.

Rahman, A. and K. Sward (2009). "The role of caveolin-1 in cardiovascular regulation." Acta Physiol 195(2): 231-245.

Rajendran, P., T. Rengarajan, J. Thangavel, Y. Nishigaki, et al. (2013). "The vascular endothelium and human diseases." Int J Biol Sci 9(10): 1057-1069.

Rajsheker, S., D. Manka, A. L. Blomkalns, T. K. Chatterjee, et al. (2010). "Crosstalk between perivascular adipose tissue and blood vessels." Curr Opin Pharmacol 10(2): 191-196.

Ralph, P., M. K. Ho, P. B. Litcofsky and T. A. Springer (1983). "Expression and induction in vitro of macrophage differentiation antigens on murine cell lines." J Immunol 130(1): 108-114.

Raman, K. G., R. E. Gandley, J. Rohland, M. S. Zenati, et al. (2011). "Early hypercholesterolemia contributes to vasomotor dysfunction and injury associated atherogenesis that can be inhibited by nitric oxide." J Vasc Surg 53.

Rammos, C., U. B. Hendgen-Cotta, R. Deenen, J. Pohl, et al. (2014). "Age-related vascular gene expression profiling in mice." Mech Ageing Dev 135: 15-23.

Randriamboavonjy, V. and I. Fleming (2005). "Endothelial nitric oxide synthase (eNOS) in platelets: how is it regulated and what is it doing there?" Pharmacol Rep 57 Suppl: 59-65.

Rapoport, R. M., M. B. Draznin and F. Murad (1983). "Endothelium-dependent relaxation in rat aorta may be mediated through cyclic GMP-dependent protein phosphorylation." Nature 306(5939): 174-176.

Rath, G., C. Dessy and O. Feron (2009). "Caveolae, caveolin and control of vascular tone: nitric oxide (NO) and endothelium derived hyperpolarizing factor (EDHF) regulation." J Physiol Pharmacol 4: 105-109.

Razani, B., T. P. Combs, X. B. Wang, P. G. Frank, et al. (2002a). "Caveolin-1-deficient mice are lean, resistant to diet-induced obesity, and show hypertriglyceridemia with adipocyte abnormalities." J Biol Chem 277(10): 8635-8647.

Razani, B., J. A. Engelman, X. B. Wang, W. Schubert, et al. (2001). "Caveolin-1 null mice are viable but show evidence of hyperproliferative and vascular abnormalities." J Biol Chem 276(41): 38121-38138.

Razani, B., X. B. Wang, J. A. Engelman, M. Battista, et al. (2002b). "Caveolin-2-Deficient Mice Show Evidence of Severe Pulmonary Dysfunction without Disruption of Caveolae." Molecular and Cellular Biology 22(7): 2329-2344.

Rebiger, L., S. Lenzen and I. Mehmeti (2016). "Susceptibility of brown adipocytes to pro-inflammatory cytokine toxicity and reactive oxygen species." Bioscience Reports 36(2): e00306.

Reddick, R. L., S. H. Zhang and N. Maeda (1994). "Atherosclerosis in mice lacking apo E. Evaluation of lesional development and progression." Arterioscler Thromb Vasc Biol 14(1): 141-147.

Rees, D. D., R. M. Palmer, R. Schulz, H. F. Hodson, et al. (1990). "Characterization of three inhibitors of endothelial nitric oxide synthase in vitro and in vivo." Br J Pharmacol 101(3): 746-752.

Reuter, H. (1986). "Voltage-dependent mechanisms for raising intracellular free calcium concentration: calcium channels." Ciba Found Symp 122: 5-22.

Richard, D., A. C. Carpentier, G. Dore, V. Ouellet, et al. (2010). "Determinants of brown adipocyte development and thermogenesis." Int J Obes (Lond) 34 Suppl 2: S59-66.

Richardson, P. D., M. J. Davies and G. V. Born (1989). "Influence of plaque configuration and stress distribution on fissuring of coronary atherosclerotic plaques." Lancet 2(8669): 941-944.

Rizvi, A. A. (2009). "Cytokine biomarkers, endothelial inflammation, and atherosclerosis in the metabolic syndrome: emerging concepts." Am J Med Sci 338(4): 310-318.

Rizzo, V., D. P. McIntosh, P. Oh and J. E. Schnitzer (1998). "In situ flow activates endothelial nitric oxide synthase in luminal caveolae of endothelium with rapid caveolin dissociation and calmodulin association." J Biol Chem 273(52): 34724-34729.

Ross, R. (1993). "The pathogenesis of atherosclerosis: a perspective for the 1990s." Nature 362(6423): 801-809.

Ross, R. (1999a). "Atherosclerosis--an inflammatory disease." N Engl J Med 340(2): 115-126.

Ross, R. (1999b). "Atherosclerosis is an inflammatory disease." Am Heart J 138(5 Pt 2): S419-420.

Rowlatt, C., F. C. Chesterman and M. U. Sheriff (1976). "Lifespan, age changes and tumour incidence in an ageing C57BL mouse colony." Lab Anim 10(10): 419-442.

Russell, A. and S. Watts (2000). "Vascular reactivity of isolated thoracic aorta of the C57BL/6J mouse." J Pharmacol Exp Ther 294(2): 598-604.

Rutkowski, J. M., J. H. Stern and P. E. Scherer (2015). "The cell biology of fat expansion." The Journal of Cell Biology 208(5): 501-512.

Sacks, H. S. and J. N. Fain (2007). "Human epicardial adipose tissue: a review." Am Heart J 153(6): 907-917.

Sacks, H. S., J. N. Fain, B. Holman, P. Cheema, et al. (2009). "Uncoupling protein-1 and related messenger ribonucleic acids in human epicardial and other adipose tissues: epicardial fat functioning as brown fat." J Clin Endocrinol Metab 94(9): 3611-3615.

Sansbury, B. E., T. D. Cummins, Y. Tang, J. Hellmann, et al. (2012). "Overexpression of endothelial nitric oxide synthase prevents diet-induced obesity and regulates adipocyte phenotype." Circ Res 111(9): 1176-1189.

Sarin, S., C. Wenger, A. Marwaha, A. Qureshi, et al. (2008). "Clinical significance of epicardial fat measured using cardiac multislice computed tomography." Am J Cardiol 102(6): 767-771.

Sato, I., I. Morita, K. Kaji, M. Ikeda, et al. (1993). "Reduction of Nitric Oxide Producing Activity Associated with in Vitro Aging in Cultured Human Umbilical Vein Endothelial Cell." Biochemical and Biophysical Research Communications 195(2): 1070-1076.

Schaefer, E. J., R. E. Gregg, G. Ghiselli, T. M. Forte, et al. (1986). "Familial apolipoprotein E deficiency." J Clin Invest 78(5): 1206-1219.

Schildknecht, S. and V. Ullrich (2009). "Peroxynitrite as regulator of vascular prostanoid synthesis." Arch Biochem Biophys 484(2): 183-189.

Schleifenbaum, J., C. Kohn, N. Voblova, G. Dubrovska, et al. (2010). "Systemic peripheral artery relaxation by KCNQ channel openers and hydrogen sulfide." J Hypertens 28(9): 1875-1882.

Schubert, W., P. G. Frank, B. Razani, D. S. Park, et al. (2001). "Caveolae-deficient endothelial cells show defects in the uptake and transport of albumin in vivo." J Biol Chem 276(52): 48619-48622.

Seals, D. R., K. L. Jablonski and A. J. Donato (2011). "Aging and vascular endothelial function in humans." Clinical science (London, England : 1979) 120(9): 357-375.

Sedding, D. G. and R. C. Braun-Dullaeus (2006). "Caveolin-1: dual role for proliferation of vascular smooth muscle cells." Trends Cardiovasc Med 16(2): 50-55.

Sell, H., M. Bluher, N. Kloting, R. Schlich, et al. (2013). "Adipose dipeptidyl peptidase-4 and obesity: correlation with insulin resistance and depot-specific release from adipose tissue in vivo and in vitro." Diabetes Care 36(12): 4083-4090.

Sellers, J. R., M. D. Pato and R. S. Adelstein (1981). "Reversible phosphorylation of smooth muscle myosin, heavy meromyosin, and platelet myosin." J Biol Chem 256(24): 13137-13142.

Seo, H. S., D. M. Lombardi, P. Polinsky, L. Powell-Braxton, et al. (1997). "Peripheral vascular stenosis in apolipoprotein E-deficient mice. Potential roles of lipid deposition, medial atrophy, and adventitial inflammation." Arterioscler Thromb Vasc Biol 17(12): 3593-3601.

Sessa, W. C. (2005). "Regulation of endothelial derived nitric oxide in health and disease." Mem Inst Oswaldo Cruz 1: 15-18.

Seto, S. W., S. M. Krishna, H. Yu, D. Liu, et al. (2013). "Impaired acetylcholine-induced endothelium-dependent aortic relaxation by caveolin-1 in angiotensin II-infused apolipoprotein-E ($ApoE^{-/-}$) knockout mice." PLoS One 8(3): e58481.

Shahid, M. and E. S. Buys (2013). "Assessing Murine Resistance Artery Function Using Pressure Myography." Journal of Visualized Experiments : JoVE(76): 50328.

Shakirova, Y., J. Bonnevier, S. Albinsson, M. Adner, et al. (2006). "Increased Rho activation and PKC-mediated smooth muscle contractility in the absence of caveolin-1." Am J Physiol Cell Physiol 291(6): C1326-1335.

Sharp, L. Z., K. Shinoda, H. Ohno, D. W. Scheel, et al. (2012). "Human BAT possesses molecular signatures that resemble beige/brite cells." PLoS One 7(11): 16.

Shaul, P. W. (2003). "Endothelial nitric oxide synthase, caveolae and the development of atherosclerosis." J Physiol 547(Pt 1): 21-33.

Shaw, L., M. Taggart and C. Austin (2001). "Effects of the oestrous cycle and gender on acute vasodilatory responses of isolated pressurized rat mesenteric arteries to 17 beta-oestradiol." Br J Pharmacol 132(5): 1055-1062.

Shen, W., C. Tian, H. Chen, Y. Yang, et al. (2013). "Oxidative stress mediates chemerin-induced autophagy in endothelial cells." Free Radic Biol Med 55: 73-82.

Shi, W., X. Wang, N. J. Wang, W. H. McBride, et al. (2000). "Effect of macrophage-derived apolipoprotein E on established atherosclerosis in apolipoprotein E-deficient mice." Arterioscler Thromb Vasc Biol 20(10): 2261-2266.

Shibata, R., N. Ouchi and T. Murohara (2009). "Adiponectin and Cardiovascular Disease." Circulation Journal 73(4): 608-614.

Shimokawa, H., H. Yasutake, K. Fujii, M. K. Owada, et al. (1996). "The importance of the hyperpolarizing mechanism increases as the vessel size decreases in endothelium-dependent relaxations in rat mesenteric circulation." J Cardiovasc Pharmacol 28(5): 703-711.

Shin, K., V. C. Fogg and B. Margolis (2006). "Tight junctions and cell polarity." Annu Rev Cell Dev Biol 22: 207-235.

Shipley, R. D. and J. M. Muller-Delp (2005). "Aging decreases vasoconstrictor responses of coronary resistance arterioles through endothelium-dependent mechanisms." Cardiovascular Research 66(2): 374-383.

Shoji, H., K. Takao, S. Hattori and T. Miyakawa (2016). "Age-related changes in behavior in C57BL/6J mice from young adulthood to middle age." Mol Brain 9(11): 016-0191.

Siest, G., T. Pillot, A. Regis-Bailly, B. Leininger-Muller, et al. (1995). "Apolipoprotein E: an important gene and protein to follow in laboratory medicine." Clin Chem 41(8 Pt 1): 1068-1086.

Simionescu, M. and A. Sima (2012). Morphology of Atherosclerotic Lesions. Inflammation and Atherosclerosis. G. Wick and C. Grundtman, Springer Vienna: 19-37.

Sindler, A. L., M. D. Delp, R. Reyes, G. Wu, et al. (2009). "Effects of ageing and exercise training on eNOS uncoupling in skeletal muscle resistance arterioles." The Journal of Physiology 587(15): 3885-3897.

Sindler, A. L., B. S. Fleenor, J. W. Calvert, K. D. Marshall, et al. (2011). "Nitrite supplementation reverses vascular endothelial dysfunction and large elastic artery stiffness with aging." Aging Cell 10(3): 429-437.

Singh, R. B., S. A. Mengi, Y.-J. Xu, A. S. Arneja, et al. (2002). "Pathogenesis of atherosclerosis: A multifactorial process." Experimental & Clinical Cardiology 7(1): 40-53.

Skold, B. H., R. Getty and F. K. Ramsey (1966). "Spontaneous atherosclerosis in the arterial system of aging swine." Am J Vet Res 27(116): 257-273.

Smilde, T. J., S. van Wissen, H. Awollersheim, M. D. Trip, et al. (2001). "Effect of aggressive versus conventional lipid lowering on atherosclerosis progression in familial hypercholesterolemia (ASAP): a prospective, randomised, double-blind trial." The Lancet 357(9256): 577-581.

Smith, J. D. (2002). "Apolipoproteins and aging: emerging mechanisms." Ageing Res Rev 1(3): 345-365.

Sobue, K., K. Hayashi and W. Nishida (1999). "Expressional regulation of smooth muscle cell-specific genes in association with phenotypic modulation." Mol Cell Biochem 190(1-2): 105-118.

Soltis, E. E. and L. A. Cassis (1991). "Influence of perivascular adipose tissue on rat aortic smooth muscle responsiveness." Clin Exp Hypertens A 13(2): 277-296.

Somlyo, A. V. and A. P. Somlyo (1993). "Intracellular signaling in vascular smooth muscle." Adv Exp Med Biol 346: 31-38.

Son, J. W. and S. Kim (2015). "Dipeptidyl Peptidase 4 Inhibitors and the Risk of Cardiovascular Disease in Patients with Type 2 Diabetes: A Tale of Three Studies." Diabetes Metab J 39(5): 373-383.

Song, Y., H. Shen, D. Schenten, P. Shan, et al. (2012). "Aging enhances the basal production of IL-6 and CCL2 in vascular smooth muscle cells." Arterioscler Thromb Vasc Biol 32(1): 103-109.

Stampfli, S. F., A. Akhmedov, C. Gebhard, C. Lohmann, et al. (2010). "Aging induces endothelial dysfunction while sparing arterial thrombosis." Arterioscler Thromb Vasc Biol 30(10): 1960-1967.

Stapleton, P. A., A. G. Goodwill, M. E. James, R. W. Brock, et al. (2010). "Hypercholesterolemia and microvascular dysfunction: interventional strategies." Journal of Inflammation 7(1): 1-10.

Steegenga, W. T., N. J. de Wit, M. V. Boekschoten, N. Ijssennagger, et al. (2012). "Structural, functional and molecular analysis of the effects of aging in the small intestine and colon of C57BL/6J mice." BMC Med Genomics 5(38): 1755-8794.

Stefan, N. and H. U. Haring (2013). "The role of hepatokines in metabolism." Nat Rev Endocrinol 9(3): 144-152.

Steinberg, D. (2010). "Earlier Intervention in the Management of Hypercholesterolemia: What Are We Waiting For?" J Am Coll Cardiol 56(8): 627-629.

Stemme, S., B. Faber, J. Holm, O. Wiklund, et al. (1995). "T lymphocytes from human atherosclerotic plaques recognize oxidized low density lipoprotein." Proc Natl Acad Sci U S A 92(9): 3893-3897.

Stroes, E., M. Hijmering, M. van Zandvoort, R. Wever, et al. (1998). "Origin of superoxide production by endothelial nitric oxide synthase." FEBS Lett 438(3): 161-164.

Strong, J. P., G. T. Malcom, C. McMahan and et al. (1999). "Prevalence and extent of atherosclerosis in adolescents and young adults: Implications for prevention from the pathobiological determinants of atherosclerosis in youth study." JAMA 281(8): 727-735.

Strong, J. P., G. T. Malcom, W. P. Newman, 3rd and M. C. Oalmann (1992). "Early lesions of atherosclerosis in childhood and youth: natural history and risk factors." J Am Coll Nutr 11: 51S-54S.

Sun, S.-w., X.-y. Zu, Q.-h. Tuo, L.-x. Chen, et al. (2010). "Caveolae and caveolin-1 mediate endocytosis and transcytosis of oxidized low density lipoprotein in endothelial cells." Acta Pharmacol Sin 31(10): 1336-1342.

Sundberg, J. P., A. Berndt, B. A. Sundberg, K. A. Silva, et al. (2011). "The mouse as a model for understanding chronic diseases of aging: the histopathologic basis of aging in inbred mice." 2011.

Sverdlov, A. L., D. T. M. Ngo, W. P. A. Chan, Y. Y. Chirkov, et al. (2014). "Aging of the Nitric Oxide System: Are We as Old as Our NO?" Journal of the American Heart Association 3(4).

Swoap, S. J. (2001). "Altered leptin signaling is sufficient, but not required, for hypotension associated with caloric restriction." American Journal of Physiology - Heart and Circulatory Physiology 281(6): H2473-H2479.

Szasz, T., G. F. Bomfim and R. C. Webb (2013). "The influence of perivascular adipose tissue on vascular homeostasis." Vascular Health and Risk Management 9: 105-116.

Szasz, T. and R. C. Webb (2012). "Perivascular adipose tissue: more than just structural support." Clin Sci 122(1): 1-12.

Szasz, T. C.-S., M.A; Webb, R.C (2012). "Abstract 260: Aging Decreases the Anticontractile Effect of Perivascular Adipose Tissue in the Mouse Aorta " Hypertension 60(Georgia Health Sciences Univ, Augusta, GA).

Szerafin, T., N. Erdei, T. Fülöp, E. T. Pasztor, et al. (2006). "Increased Cyclooxygenase-2 Expression and Prostaglandin-Mediated Dilation in Coronary Arterioles of Patients With Diabetes Mellitus." Circulation Research 99(5): e12-317.

Tacke, F. and G. J. Randolph (2006). "Migratory fate and differentiation of blood monocyte subsets." Immunobiology 211(6-8): 609-618.

Taddei, S., A. Virdis, L. Ghiadoni, G. Salvetti, et al. (2001). "Age-related reduction of NO availability and oxidative stress in humans." Hypertension 38(2): 274-279.

Taddei, S., A. Virdis, P. Mattei, L. Ghiadoni, et al. (1995). "Aging and Endothelial Function in Normotensive Subjects and Patients With Essential Hypertension." Circulation 91(7): 1981-1987.

Takaoka, M., D. Nagata, S. Kihara, I. Shimomura, et al. (2009). "Periadventitial adipose tissue plays a critical role in vascular remodeling." Circ Res 105(9): 906-911.

Tanner, J. M., D. T. Kearns, B. J. Kim, C. Sloan, et al. (2010). "Fasting-induced reductions in cardiovascular and metabolic variables occur sooner in obese vs. lean mice." Exp Biol Med (Maywood) 235(12): 1489-1497.

Tarnus, E., H. Wassef, J. F. Carmel, P. Rondeau, et al. (2009). "Apolipoprotein E limits oxidative stress-induced cell dysfunctions in human adipocytes." FEBS Lett 583(12): 2042-2048.

Taylor, A. J., L. E. Sullenberger, H. J. Lee, J. K. Lee, et al. (2004). "Arterial Biology for the Investigation of the Treatment Effects of Reducing Cholesterol (ARBITER) 2: a double-blind, placebo-controlled study of extended-release niacin on atherosclerosis progression in secondary prevention patients treated with statins." Circulation 110(23): 3512-3517.

The Emerging Risk Factors, C. (2010). "C-reactive protein concentration and risk of coronary heart disease, stroke, and mortality: an individual participant meta-analysis." Lancet 375(9709): 132-140.

Thomas, C. M. and E. J. Smart (2007). "Gender as a regulator of atherosclerosis in murine models." Curr Drug Targets 8.

Thorin, E. (2011). "Vascular disease risk in patients with hypertriglyceridemia: endothelial progenitor cells, oxidative stress, accelerated senescence, and impaired vascular repair." Can J Cardiol 27(5): 538-540.

Tomioka, H., Y. Hattori, M. Fukao, A. Sato, et al. (1999). "Relaxation in different-sized rat blood vessels mediated by endothelium-derived hyperpolarizing factor: importance of processes mediating precontractions." J Vasc Res 36(4): 311-320.

Toth, P. P. (2008). "Subclinical atherosclerosis: what it is, what it means and what we can do about it." International Journal of Clinical Practice 62(8): 1246-1254.

Townsend N, B. P., Wilkins E, Wickramasinghe K, Rayner M (2015). "Cardiovascular disease statistics, 2015."

Trayhurn, P., B. Wang and I. S. Wood (2008). "Hypoxia in adipose tissue: a basis for the dysregulation of tissue function in obesity?" Br J Nutr 100(2): 227-235.

Treuting, P. M., N. J. Linford, S. E. Knoblaugh, M. J. Emond, et al. (2008). "Reduction of Age-Associated Pathology in Old Mice by Overexpression of Catalase in Mitochondria." The Journals of Gerontology Series A: Biological Sciences and Medical Sciences 63(8): 813-822.

Trifunovic, A. and N. G. Larsson (2008). "Mitochondrial dysfunction as a cause of ageing." J Intern Med 263(2): 167-178.

Triggle, C. R., S. M. Samuel, S. Ravishankar, I. Marei, et al. (2012). "The endothelium: influencing vascular smooth muscle in many ways." Canadian Journal of Physiology and Pharmacology 90(6): 713-738.

Trushina, E., J. Du Charme, J. Parisi and C. T. McMurray (2006). "Neurological abnormalities in caveolin-1 knock out mice." Behav Brain Res 172(1): 24-32.

Ungvari, Z., G. Kaley, R. de Cabo, W. E. Sonntag, et al. (2010). "Mechanisms of vascular aging: new perspectives." J Gerontol A Biol Sci Med Sci 65(10): 1028-1041.

Uryga, A. K. and M. R. Bennett (2016). "Ageing induced vascular smooth muscle cell senescence in atherosclerosis." J Physiol 594(8): 2115-2124.

Utermann, G., I. Kindermann, H. Kaffarnik and A. Steinmetz (1984). "Apolipoprotein E phenotypes and hyperlipidemia." Human Genetics 65(3): 232-236.

Van Assche, T., P. Fransen, P. J. Guns, A. G. Herman, et al. (2007). "Altered Ca2+ handling of smooth muscle cells in aorta of apolipoprotein E-deficient mice before development of atherosclerotic lesions." Cell Calcium 41(3): 295-302.

Van Hove, C. E., C. Van der Donckt, A. G. Herman, H. Bult, et al. (2009). "Vasodilator efficacy of nitric oxide depends on mechanisms of intracellular calcium mobilization in mouse aortic smooth muscle cells." Br J Pharmacol 158(3): 920-930.

VanderLaan, P. A., C. A. Reardon and G. S. Getz (2004). "Site specificity of atherosclerosis: site-selective responses to atherosclerotic modulators." Arterioscler Thromb Vasc Biol 24(1): 12-22.

Vanhoutte, P. M. (2010). "Regeneration of the Endothelium in Vascular Injury." Cardiovascular Drugs and Therapy 24(4): 299-303.

Varol, C., S. Yona and S. Jung (2009). "Origins and tissue-context-dependent fates of blood monocytes." Immunol Cell Biol 87(1): 30-38.

Vasile, E., M. Simionescu and N. Simionescu (1983). "Visualization of the binding, endocytosis, and transcytosis of low-density lipoprotein in the arterial endothelium in situ." J Cell Biol 96(6): 1677-1689.

Vasquez, E. C., V. A. Peotta, A. L. Gava, T. M. Pereira, et al. (2012). "Cardiac and vascular phenotypes in the apolipoprotein E-deficient mouse." J Biomed Sci 19(22): 1423-0127.

Vazquez-Padron, R. I., D. Lasko, S. Li, L. Louis, et al. (2004). "Aging exacerbates neointimal formation, and increases proliferation and reduces susceptibility to apoptosis of vascular smooth muscle cells in mice." J Vasc Surg 40(6): 1199-1207.

Vecchione, C., A. Maffei, S. Colella, A. Aretini, et al. (2002). "Leptin effect on endothelial nitric oxide is mediated through Akt-endothelial nitric oxide synthase phosphorylation pathway." Diabetes 51(1): 168-173.

Venegas-Pino, D. E., N. Banko, M. I. Khan, Y. Shi, et al. (2013). "Quantitative Analysis and Characterization of Atherosclerotic Lesions in the Murine Aortic Sinus." Journal of Visualized Experiments : JoVE(82): 50933.

Verhagen, S. N., A. Vink, Y. van der Graaf and F. L. Visseren (2012). "Coronary perivascular adipose tissue characteristics are related to atherosclerotic plaque size and composition. A post-mortem study." Atherosclerosis 225(1): 99-104.

Verhagen, S. N. and F. L. Visseren (2011). "Perivascular adipose tissue as a cause of atherosclerosis." Atherosclerosis 214(1): 3-10.

Verlohren, S., G. Dubrovska, S. Y. Tsang, K. Essin, et al. (2004). "Visceral periadventitial adipose tissue regulates arterial tone of mesenteric arteries." Hypertension 44(3): 271-276.

Versari, D., E. Daghini, A. Virdis, L. Ghiadoni, et al. (2009). "Endothelial Dysfunction as a Target for Prevention of Cardiovascular Disease." Diabetes Care 32(Suppl 2): S314-S321.

Victorio, J. A., M. T. Fontes, L. V. Rossoni and A. P. Davel (2016). "Different Anti-Contractile Function and Nitric Oxide Production of Thoracic and Abdominal Perivascular Adipose Tissues." Frontiers in Physiology 7: 295.

Villacorta, L. and L. Chang (2015). "The role of perivascular adipose tissue in vasoconstriction, arterial stiffness, and aneurysm." Hormone molecular biology and clinical investigation 21(2): 137-147.

Vincent, H. K., K. E. Innes and K. R. Vincent (2007). "Oxidative stress and potential interventions to reduce oxidative stress in overweight and obesity." Diabetes Obes Metab 9(6): 813-839.

Virdis, A., A. Bacca, R. Colucci, E. Duranti, et al. (2013). "Endothelial dysfunction in small arteries of essential hypertensive patients: role of cyclooxygenase-2 in oxidative stress generation." Hypertension 62(2): 337-344.

Vogel, R. A. (1997). "Coronary risk factors, endothelial function, and atherosclerosis: a review." Clin Cardiol 20(5): 426-432.

Voghel, G., N. Thorin-Trescases, N. Farhat, A. Nguyen, et al. (2007). "Cellular senescence in endothelial cells from atherosclerotic patients is accelerated by oxidative stress associated with cardiovascular risk factors." Mechanisms of Ageing and Development 128(11–12): 662-671.

Volonte, D., K. Zhang, M. P. Lisanti and F. Galbiati (2002). "Expression of caveolin-1 induces premature cellular senescence in primary cultures of murine fibroblasts." Mol Biol Cell 13(7): 2502-2517.

Walker, M., 3rd, B. R. Campbell, K. Azer, C. Tong, et al. (2009). "A novel 3-dimensional micro-ultrasound approach to automated measurement of carotid arterial plaque volume as a biomarker for experimental atherosclerosis." Atherosclerosis 204(1): 55-65.

Wang, J. C. and M. Bennett (2012). "Aging and atherosclerosis: mechanisms, functional consequences, and potential therapeutics for cellular senescence." Circ Res 111(2): 245-259.

Wang, M., G. Spinetti, R. E. Monticone, J. Zhang, et al. (2011). "A local proinflammatory signalling loop facilitates adverse age-associated arterial remodeling." PLoS One 6(2): e16653.

Wang, M., J. Zhang, L. Q. Jiang, G. Spinetti, et al. (2007a). "Proinflammatory profile within the grossly normal aged human aortic wall." Hypertension 50(1): 219-227.

Wang, P., T. Y. Xu, Y. F. Guan, D. F. Su, et al. (2009). "Perivascular adipose tissue-derived visfatin is a vascular smooth muscle cell growth factor: role of nicotinamide mononucleotide." Cardiovasc Res 81(2): 370-380.

Wang, T. D., W. J. Lee, F. Y. Shih, C. H. Huang, et al. (2010). "Association of epicardial adipose tissue with coronary atherosclerosis is region-specific and independent of conventional risk factors and intra-abdominal adiposity." Atherosclerosis 213(1): 279-287.

Wang, X. M., H. P. Kim, R. Song and A. M. Choi (2006). "Caveolin-1 confers antiinflammatory effects in murine macrophages via the MKK3/p38 MAPK pathway." Am J Respir Cell Mol Biol 34(4): 434-442.

Wang, Y., K. S. Lam, E. W. Kraegen, G. Sweeney, et al. (2007b). "Lipocalin-2 is an inflammatory marker closely associated with obesity, insulin resistance, and hyperglycemia in humans." Clin Chem 53(1): 34-41.

Warboys, C. M., N. Amini, A. de Luca and P. C. Evans (2011). "The role of blood flow in determining the sites of atherosclerotic plaques." F1000 Medicine Reports 3: 5.

Warnick, G. R., M. Nauck and N. Rifai (2001). "Evolution of methods for measurement of HDL-cholesterol: from ultracentrifugation to homogeneous assays." Clin Chem 47(9): 1579-1596.

Watts, S. W., A. M. Dorrance, M. E. Penfold, J. L. Rourke, et al. (2013). "Chemerin connects fat to arterial contraction." Arterioscler Thromb Vasc Biol 33(6): 1320-1328.

Webb, R. C. (2003). "Smooth muscle contraction and relaxation." Advances in Physiology Education 27(4): 201-206.

Weinberg, P. D. (2004). "Rate-limiting steps in the development of atherosclerosis: the response-to-influx theory." J Vasc Res 41(1): 1-17.

Wheeler, J. B., R. Mukherjee, R. E. Stroud, J. A. Jones, et al. (2015). "Relation of murine thoracic aortic structural and cellular changes with aging to passive and active mechanical properties." J Am Heart Assoc 4(3): 001744.

White, R. M., C. O. Rivera and C. A. Davison (2000). "Nitric Oxide-Dependent and -Independent Mechanisms Account for Gender Differences in Vasodilation to Acetylcholine." Journal of Pharmacology and Experimental Therapeutics 292(1): 375-380.

Whitman, S. C. (2004). "A practical approach to using mice in atherosclerosis research." Clin Biochem Rev 25(1): 81-93.

Willens, H. J., P. Byers, J. A. Chirinos, E. Labrador, et al. (2007). "Effects of Weight Loss After Bariatric Surgery on Epicardial Fat Measured Using Echocardiography." The American Journal of Cardiology 99(9): 1242-1245.

Williams, T. D., J. B. Chambers, R. P. Henderson, M. E. Rashotte, et al. (2002). "Cardiovascular responses to caloric restriction and thermoneutrality in C57BL/6J mice." American Journal of Physiology - Regulatory, Integrative and Comparative Physiology 282(5): R1459-R1467.

Withers, S. B., C. Agabiti-Rosei, D. M. Livingstone, M. C. Little, et al. (2011). "Macrophage activation is responsible for loss of anticontractile function in inflamed perivascular fat." Arterioscler Thromb Vasc Biol 31(4): 908-913.

Withers, S. B., L. Simpson, S. Fattah, M. E. Werner, et al. (2014). "cGMP-dependent protein kinase (PKG) mediates the anticontractile capacity of perivascular adipose tissue." Cardiovasc Res 101(1): 130-137.

Wojtala, A., M. Bonora, D. Malinska, P. Pinton, et al. (2014). "Methods to monitor ROS production by fluorescence microscopy and fluorometry." Methods Enzymol 542: 243-262.

Wu, J., P. Bostrom, L. M. Sparks, L. Ye, et al. (2012). "Beige adipocytes are a distinct type of thermogenic fat cell in mouse and human." Cell 150(2): 366-376.

Wunderlich, C., A. Schmeisser, C. Heerwagen, B. Ebner, et al. (2008a). "Chronic NOS inhibition prevents adverse lung remodeling and pulmonary arterial hypertension in caveolin-1 knockout mice." Pulm Pharmacol Ther 21(3): 507-515.

Wunderlich, C., K. Schober, M. Kasper, C. Heerwagen, et al. (2008b). "Nitric oxide synthases are crucially involved in the development of the severe cardiomyopathy of caveolin-1 knockout mice." Biochem Biophys Res Commun 377(3): 769-774.

Wunderlich, C., K. Schober, A. Schmeisser, C. Heerwagen, et al. (2008c). "The adverse cardiopulmonary phenotype of caveolin-1 deficient mice is mediated by a dysfunctional endothelium." J Mol Cell Cardiol 44(5): 938-947.

Xia, N., S. Horke, A. Habermeier, E. I. Closs, et al. (2016). "Uncoupling of Endothelial Nitric Oxide Synthase in Perivascular Adipose Tissue of Diet-Induced Obese Mice." Arterioscler Thromb Vasc Biol 36(1): 78-85.

Xu, H., G. T. Barnes, Q. Yang, G. Tan, et al. (2003). "Chronic inflammation in fat plays a crucial role in the development of obesity-related insulin resistance." J Clin Invest 112(12): 1821-1830.

Xu, X., C. Liu, Z. Xu, K. Tzan, et al. (2012). "Altered adipocyte progenitor population and adipose-related gene profile in adipose tissue by long-term high-fat diet in mice." Life Sciences 90(25–26): 1001-1009.

Xue, B., J.-S. Rim, J. C. Hogan, A. A. Coulter, et al. (2007). "Genetic variability affects the development of brown adipocytes in white fat but not in interscapular brown fat." Journal of lipid research 48(1): 41-51.

Yaghoubi, M., J. Oliver-Krasinski, A. J. Cayatte and R. A. Cohen (2000). "Decreased sensitivity to nitric oxide in the aorta of severely hypercholesterolemic apolipoprotein E-deficient mice." J Cardiovasc Pharmacol 36(6): 751-757.

Yamawaki, H., N. Hara, M. Okada and Y. Hara (2009). "Visfatin causes endothelium-dependent relaxation in isolated blood vessels." Biochem Biophys Res Commun 383(4): 503-508.

Yamawaki, H., N. Tsubaki, M. Mukohda, M. Okada, et al. (2010). "Omentin, a novel adipokine, induces vasodilation in rat isolated blood vessels." Biochem Biophys Res Commun 393(4): 668-672.

Yan, Q. W., Q. Yang, N. Mody, T. E. Graham, et al. (2007). "The adipokine lipocalin 2 is regulated by obesity and promotes insulin resistance." Diabetes 56(10): 2533-2540.

Yanagisawa, M., H. Kurihara, S. Kimura, Y. Tomobe, et al. (1988). "A novel potent vasoconstrictor peptide produced by vascular endothelial cells." Nature 332(6163): 411-415.

Yang, R., L. Powell-Braxton, A. K. Ogaoawara, N. Dybdal, et al. (1999). "Hypertension and endothelial dysfunction in apolipoprotein E knockout mice." Arterioscler Thromb Vasc Biol 19(11): 2762-2768.

Ye, L., J. Wu, P. Cohen, L. Kazak, et al. (2013). "Fat cells directly sense temperature to activate thermogenesis." Proceedings of the National Academy of Sciences 110(30): 12480-12485.

Yuan, R., L. L. Peters and B. Paigen (2011). "Mice as a Mammalian Model for Research on the Genetics of Aging." ILAR journal / National Research Council, Institute of Laboratory Animal Resources 52(1): 4-15.

Yue, L., J. T. Bian, I. Grizelj, A. Cavka, et al. (2012). "Apolipoprotein E enhances endothelial-NO production by modulating caveolin 1 interaction with endothelial NO synthase." Hypertension 60(4): 1040-1046.

Yue, L. and T. Mazzone (2011). "Endogenous adipocyte apolipoprotein E is colocalized with caveolin at the adipocyte plasma membrane." J Lipid Res 52(3): 489-498.

Yue, L., N. Rasouli, G. Ranganathan, P. A. Kern, et al. (2004). "Divergent Effects of Peroxisome Proliferator-activated Receptor γ Agonists and Tumor Necrosis Factor α on Adipocyte ApoE Expression." Journal of Biological Chemistry 279(46): 47626-47632.

Zaborska, K. E., M. Wareing, G. Edwards and C. Austin (2016). "Loss of anti-contractile effect of perivascular adipose tissue in offspring of obese rats." International Journal of Obesity (2005) 40(8): 1205-1214.

Zhang, L. C. L. V. C. D. E. C. J. (2012). Abstract 662: Perivascular Adipose Tissue-derived Prostaglandins Constrict Vessel. Hypertension. 2012; 60: A662, Volume 60, Issue 3 Supplement; September 2012

Zhang, S. H., R. L. Reddick, B. Burkey and N. Maeda (1994). "Diet-induced atherosclerosis in mice heterozygous and homozygous for apolipoprotein E gene disruption." J Clin Invest 94.

Zhang, S. H., R. L. Reddick, J. A. Piedrahita and N. Maeda (1992). "Spontaneous hypercholesterolemia and arterial lesions in mice lacking apolipoprotein E." Science 258(5081): 468-471.

Zhang, W., C. Shu, Q. Li, M. Li, et al. (2015). "Adiponectin affects vascular smooth muscle cell proliferation and apoptosis through modulation of the mitofusin-2-mediated Ras-Raf-Erk1/2 signaling pathway." Mol Med Rep 12(3): 4703-4707.

Zhang, Y., R. Li, Y. Meng, S. Li, et al. (2014). "Irisin Stimulates Browning of White Adipocytes Through Mitogen-Activated Protein Kinase p38 MAP Kinase and ERK MAP Kinase Signaling." Diabetes 63(2): 514-525.

Zhao, Y., P. M. Vanhoutte and S. W. S. Leung (2015). "Vascular nitric oxide: Beyond eNOS." Journal of Pharmacological Sciences 129(2): 83-94.

Zhou, X., B. Teng and S. J. Mustafa (2015). "Sex Difference in Coronary Endothelial Dysfunction in Apolipoprotein E Knockout Mouse: Role of NO and A2A Adenosine Receptor." Microcirculation 22(7): 518-527.

Zielonka, J., J. Vasquez-Vivar and B. Kalyanaraman (2008). "Detection of 2-hydroxyethidium in cellular systems: a unique marker product of superoxide and hydroethidine." Nat Protoc 3(1): 8-21.